DEVELOPMENT OF AN ANALYTICAL MODEL FOR REAL-TIME ASSESSMENT OF TIDAL BARRAGE POWER GENERATION

A Thesis By

MD. RAFIQUL ISLAM KHAN

Submitted in partial fulfillment of the requirement for the degree of

DOCTOR OF PHILOSOPHY

IN

WATER RESOURCES DEVELOPMENT

Institute of Water and Flood Management
BANGLADESH UNIVERSITY OF ENGINEERING AND TECHNOLOGY
March, 2020

CERTIFICATE OF APPROVAL

The thesis titled "**Development of an Analytical Model for Real-Time Assessment of Tidal Barrage Power Generation**" submitted by Md. Rafiqul Islam Khan, Roll No.1009284001P, Session: October 2009, has been accepted as satisfactory in partial fulfillment of the requirement for the degree of Doctor of Philosophy on March 9, 2020.

BOARD OF EXAMINERS

[1]
Dr. Muhammad Shah Alam Khan — **Chairman**
Professor, IWFM, BUET, Dhaka.
(Supervisor)

[2]
Dr. Mohammad Shahjahan Mondal
Professor and Director, IWFM, BUET, Dhaka. — **Member (Ex- officio)**

[3]
Dr. Mohammad Anisul Haque
Professor, IWFM, BUET, Dhaka. — **Member**

[4]
Dr. Mohammad Asad Hussain — **Member**
Professor, IWFM, BUET, Dhaka.

[5]
Dr. Aminul Hoque
Ex-Professor, Department of EEE, BUET, Dhaka
and — **Member**
Vice-Chancellor (Designate)
Eastern University, Dhanmondi, Dhaka.

[6]
Dr. Umme Kulsum Navera — **Member**
Professor,
Department of WRE, BUET, Dhaka

[7]
Professor Dr. Md. Shahid Ullah — **Member External**
Head, Department of Electrical and Electronics Engineering,
Daffodil University, Dhaka.

CANDIDATE'S DECLARATION

This is to certify that this work entitled "**Development of an Analytical Model for Real-Time Assessment of Tidal Barrage Power Generation**" has been done by me under the supervision of Dr. Muhammad Shah Alam Khan, Professor, Institute of Water and Flood Management (IWFM), Bangladesh University of Engineering and Technology (BUET), Dhaka. I do hereby declare that this thesis or any part of it has not been submitted elsewhere for the award of any degree or diploma from any other institution.

……………………………………

Md. Rafiqul Islam Khan

DEDICATED TO

TO MY BELOVED PARENTS, WIFE, SONS AND MY DAUGHTER.

ACKNOWLEDGEMENT

Undertaking this Ph.D. has been a rare experience for me, and it would not have been possible without the support and guidance that I received from many people.

Firstly, I would like to express my heartiest gratitude to my supervisor, Dr. Muhammad Shah Alam Khan, Professor, IWFM, BUET, for providing me an ample opportunity to conduct my Ph.D. under his supervision. He always kept me focused on my research objectives and helped me developing the model. I appreciate Dr. Muhammad Shah Alam Khan for his patience and high efficiency in guiding me in a proper way of conducting this research and continuous supports, encouragement and guidance. It would not be possible for me to complete my research without his valuable contribution.

Sincere thanks go to all members of the Doctoral Committee and Board of examiners- Dr. Mohammad Shahjahan Mondal, Professor, IWFM, BUET; Dr. Mohammad Anisul Haque, Professor, IWFM, BUET; Dr. Mohammad Asad Hussain, Professor, IWFM, BUET and Dr. Aminul Hoque. Former, Professor (Retd.), EEE, BUET, Dr. Umme Kulsum Navera, Professor, WRE, BUET, and Dr. Md. Shahid Ullah Professor and Head of the Department of Electrical and Electronics Engineering, Daffodil International University, Dhaka for their insightful comments, encouragement, and the critical question which encouraged me to widen my research from various perspectives. Special thanks to Dr. Mohammad Asad Hussain, Professor, IWFM, BUET for allowing and helping me to use the nao.99b model and proving me the models results which was used as input in this model. Personally, I am very grateful to him proving me many scientific articles and models.

I would like to thank Commodore M Jahangir Alam, (E), NUP, NDC, PSC, BN, Chairman Payra Port Authority, Commodore Saidur Rahman, ex-Member (Harbor and Marine), Payra Port Authority, Commodore Ashraful Hoq Chowdhury (G), ndc, afwc, psc, BN, Member (Harbor and Marine), Payra Port Authority, Commander Haider Jahan Emon, ex-Chief Hydrographer, Payra Port Authority for their support to allow me to use their Software GeoTide Analyzer 3.0 x2015 for tide analysis.

I would like to thank Ms. Shamsunnaher, Director (Hydrography), Mr. Nayeem Mohammad, Deputy Director (Survey) and Mr. Mohammad Sharfuddin, Assistant Director (Survey) of Hydrography Department, BIWTA.

I would also like to thanks to Mr. Malik Fida A. Khan, Executive Director (In-Charge), CEGIS and Member, National River Conservation Commission, and Mr. ATM Kamal Hossain, Senior Specialist of CEGIS.

This dissertation would not have been possible without the intellectual contribution of my colleagues doing their research works in IWFM.

The author would like to convey special thanks to the authority of the Bangladesh Inland Water Transport Authority (BIWTA) for giving me 20 years tidal data, contour map of Sandwip Channel and allow me to use HYPACK ® Windows ®- based Software for area and volume calculation for the Sandwip channel.

The author would like to convey special thanks to the authority of the Bangladesh Navy for providing me hydrographic chart of Sandwip Channel.

I am indebted to many individuals without whose assistance; this research could not have been completed in time. I want to thank everyone who has helped me along the way.

Finally, I would like to thank my beloved parents, wife, son, and other family members for their endless love and kind support during this journey.

ABSTRACT

The world is focusing on renewable energy especially on solar, wind and tidal energy. However, research on tidal power, more specifically, tidal barrage power, has not yet received due attention. Current approaches and practices for the assessment of tidal barrage power generation do not consider the continuous changes in the head differences between the sea and basin. Rather a static overall estimate using an arbitrary reduction in efficiency and head difference is used. Several equations or formulas based on this assumption are used to assess tidal power. Most of them use a static head rather dynamic head. This study considers the real-time changes in water levels inside and outside the basin to compute the actual power generation potential based on dynamic water head, with the specific objectives of developing an analytical model to assess real-time power and energy, and assessing an optimum basin configuration that generates the maximum tidal power. This study also assesses the tidal barrage power potential in the coastal area of Bangladesh.

A hypothetical model for continuous generation is used as a base case to compute the dynamic head for a tidal barrage. This base model did not consider minimum head for turbine operation to avoid cavitation or provision of gates to increase the efficiency of operation and used a simplified sinusoidal tidal water level variation. However, in reality the observed tide is a superimposition of a series of tidal constituents having different tidal amplitudes, speeds and phase angles. Also, water level at the basin side at any particular time depends on the area of the basin, volume of the basin, basin configuration, water level of the basin, water passing through turbines, etc. In this study, a generalized polynomial equation is developed to calculate water surface area in terms of water level. The real-time analytical model developed in this study, referred to as the 'RTA Model', introduces a set of parameters that more closely represents the actual and real-time water level variations in the basin and the sea. A set of equations represents the discharge through the turbine and gate and computes power generation during different tidal phases. The analytical model has the flexibility to change the turbine capacity (size and number) and gate capacity (size and number). This model is implemented in Excel to test different realistic situations or scenarios of the base case, such as flood-ebb generation and ebb generation. In these cases, the thresholds for power generation and gate operation are considered.

Results from the new RTA Model are compared with those from the hypothetical base model. The maximum peak power from the base model is 654.4 kW compared to 666.6 kW from

the RTA Model. The RTA Model yields 1.86% higher power than that of base model. Similarly, the average peak power from the base model is 261.12 kW against 247.33 kW from the RTA Model. Energy from the RTA Model is 5.60% higher than that from the base model. The RTA Model is tested for three situations - flood-ebb generation with gates, ebb generation with gates and flood generation with gates. Results for 24 hours show that ebb generation with gates gives more energy (9,280 kWh/day) than that for flood-ebb generation with gates (8,125 kWh/day) and flood generation with gates (5,190 kWh/day). Generation time for ebb generation with gates, flood-ebb generation with gates and flood generation with gates are 66%, 48% and 37%, respectively, of the full duration. Ebb generation yields more energy than that of flood-ebb generation, but duration of ebb generation is slightly less than flood-ebb generation. The model is also validated using the data for the Severn tidal barrage, for which the annual energy output was initially 15.09 TWh and was later re-assessed to be 11.12 TWh. Using the present RTA Model (ebb generation), the annual energy output was found to be 10.77 TWh which is only 3.15% less than the latest assessment, and about 28.62% less than the original assessment.

Optimization of the plant capacity is conducted in this study. Generally, the higher the turbine capacity, the higher the extractable energy. However, the cost or investment increases with the capacity. Therefore, capacity optimization is required to make the energy generation cost-effective considering the turbine capacity and its cost. In this study, levelized tariff (cost/kWh) is considered as a basis for plant optimization. Levelized cost of energy (LCOE) is the cost for per unit energy production for the economic life of the plant.

In this study, it is assumed that the water level remains horizontal at the sea and the basin during the tides. However, in reality, the water level in the basin and sea varies non-linearly during each tidal cycle. This non-linearity depends on the aspect ratio (width/length ratio) of the basin and the openings of turbines and gates. To check the sensitivity of the basin aspect ratio, an arbitrarily basin of 10 m depth and 90 km^2 area having aspect ratios of 0.9, 0.625 and 0.4 m were considered with a tidal amplitude of 4 m. Using the two-dimensional NAO.99b model based on non-linear shallow water equations (Matsumoto et al., 2000) the actual non-liner water level variations for this hypothetical basin is determined. It is observed that the higher the aspect ratio the higher the annual energy output. The model was also run to assess the impact of the vertical cross section of the basin on energy generation. It is observed that a trapezoidal basin having a side slope s = 0.5 yields more energy than a trapezoidal basin having a side slope s = 2.0, or a rectangular basin or parabolic basin considering the same tide data (same tidal range) and same area of cross sections (within high tide and low tide) along the length of the basin irrespective of the shape.

In Bangladesh, there are some potential sites for tidal power generation. Generally, at least a 5-meter tidal range is required to generate tidal range power or barrage power. This study reveals that some areas such as Sandwip, Khal No. 10, Mongla and Sadar Ghat (Chattogram) are promising sites for tidal barrage power development. This study applied the analytical RTA Model to a hypothetical case for the Sandwip channel (having a tidal range more than 7 m) to assess the potential of the site.

Using the past 20 years' tidal data, 214 tidal constituents (each of which is considered as a simple harmonic motion with different amplitude, speed and phase) were developed using the 'GeoTide Analyzer (3.0.x, 2015)' software. GeoTide Analyzer converts observed tide gauge data directly into tidal harmonic constants which can then be used to make tidal predictions for any future or past date. Using the bathymetric data of Sandwip channel collected from BIWTA, CEGIS and Bangladesh Navy, an area-elevation curve is drawn which is used in the model to assess the incremental increase or decrease of water level as well as the water level change after a small interval to calculate the head for a given time step. Utilizing the flexibility of the RTA Model to change the number of turbines and gates, as well as their dimensions (diameter and size) and its suitability for flood-ebb generation, ebb generation or flood generation, it is observed that ebb generation yields more energy than that of flood-ebb generation, but duration of ebb generation is slightly shorter than flood-ebb generation. The optimum capacity of the plant is assessed by calculating the LCOE. Model results show that for a basin area of 500 km^2, the average plant capacity for Sandwip channel would be 854 MW and the plant will generate 2,203 GWh annually in ebb generation mode with 400 turbines (each 6 m in diameter) and 800 gates (each 12 m x 8 m in size). The maximum capacity will be 2,757 MW and will supply electricity 29% of the time in a year. The present estimated cost of the plant is BDT 14,763 crore USD 1,678 million (at a conversion rate 1 USD = 88 BDT).

TABLE OF CONTENTS

LIST OF TABLES

LIST OF FIGURES

ACRONYMS AND ABBREVIATIONS

A_b	Area of the impounded basin
bcm	billion cubic metres
BIWTA	Bangladesh Inland Water Transport Authority
BPDB	Bangladesh Power Development Board
Btu	British thermal unit
BUET	Bangladesh University of Engineering and Technology
CD	Chart Datum
CEGIS	Centre for Environmental and Geographic Information Services
Cp	Turbine's power coefficient
CPD	Centre for Policy Dialogue
CO_2	Carbon-di-Oxide
DTP	Dynamic Tidal Power
DoEn	Department of Energy
E	Energy
EEE	Electrical and Electronics Engineering
E_p	Potential energy (kg m^2/s^2 or Joule).
GDP	Gross Domestic Product
GHGs	Greenhouse Gases
GJ	Giga-joule
GOB	Government of Bangladesh
GW	Giga-watt
HAT	Highest Astronomical Tide
HWL	Highest water level
IEA	International Energy Agency
IPP	Independent Power Producers
IPCC	Intergovernmental Panel on Climate Change
IWFM	Institute of Water and Flood Management
IPP	Independent Power Producer
kWh	Kilo-watt hours
LAT	Lowest Astronomical Tide

LWL	Lowest Water Level
M_2	Semi-diurnal lunar tide
MHWN	Mean Higher Water Neap
MHWN	Mean Lower Water neap
MHWS	Mean Higher Water Spring
mkWh	Million Kilo-watt hours
ML	Mean Level
MLWS	Mean Lower Water Spring
MSL	Mean Sea Level
Mt	Metric Ton
Mtoe	Million tonnes of oil equivalent
MW	Mega-watts
P	Power
PJ/yr.	Peta-joule per year=278 million kWh
PSMP	Power System Master Plan
R	Tidal range
RTA Model	Real-Time Analytical Model
S_2	Semi-diurnal solar tide
SDGs	Sustainable Development Goals
SREDA	Sustainable Renewable
SREDA	Sustainable Renewable Energy Development Authority
T	Tidal period (time per cycle)
t/m^3	Ton/m^3
TPES	Total Primary Energy Source
TRACKS	Transforming Climate Knowledge with and for Society
TWh	Tera watt hours
UKAEA	United Kingdom Atomic Energy Authority
UNGA	United Nations' General Assembly
UNDESA	United Nations Department of Economic and Social Affairs
UNFCC	United Nations Framework Convention on Climate Change
WRE	Water Resources Engineering

LIST OF SYMBOLS AND NOTATIONS

As	cross-sectional flow area
τb	bed shear stress
Δh_b	mean tidal range
A	flow area
A_b	area of the basin
B	basin
B=+1	flood tide at basin
B=-1	ebb tide at basin
b	width of the basin
C_{DT}	turbine discharge coefficient
C_{DG}	gate discharge coefficient
E' , G'	diffusive vectors in the x and y direction
E, G	convective flux vectors in the x and y directions respectively
$E_{extractable}$	energy extractable
E_p	potential energy
$E_{p\,(max)}$	maximum potential energy
Fc	centrifugal force
g	acceleration due to earth's gravity
G	gate
H	distance of centre of gravity of the mass from a point of reference in meter
h	water head
a	tidal amplitude
Hd	total water depth
L	length of the basin
m	mass
n	manning's n
Q	discharge
qs	source discharge per unit area
Q_T	turbine flow rate
R	tidal range
ρ	density of sea water
R_e	radius of the earth
s	effects of bed friction, bed slope and the Coriolis force
S	sea
SWE	shallow water equations
Tur	turbine
u	depth-averaged horizontal velocity
U	vector of conversed variables

u, v	depth-averaged horizontal velocities in the x and y directions, respectively
w	width of the basin
Y	water level at sea
Z	water level at basin

CHAPTER 1
INTRODUCTION

1.1 Background

Energy is a key driver of the current unprecedented level of economic growth, prosperity, and globalization, particularly during the past centuries (Simmons, et al., 2014). Throughout this period, a variety of primary energy sources have been used including traditional biomass, coal, oil, and natural gas for energy production. More than 80% of global energy is still produced using fossil fuels causing significant harm to the environment in the form of greenhouse gas emissions and pollution (IEA, 2019). World population, is about 8 billion in 2015, will continue to grow before stabilizing around 10 billion people in 2050 (UNDESA, 2013). Nearly all of this growth will be in the less developed countries. At the same time, urbanization will grow and population will become older. So, global big challenge is how we could supply clean, safe, affordable and scalable energy to the world's growing energy demand.

The Sustainable Development Goals (SDGs), adopted by the United Nations General Assembly (UNGA) in 2015, provide a powerful framework for international cooperation to achieve a sustainable future for the planet (UN, 2015). The 17 SDGs and related 169 targets, at the heart of 'Agenda 2030', define a path to end extreme poverty, fight against inequality and injustice, and protect the planet's environment. Sustainable energy is central to the success of Agenda 2030 (UN, 2015). The global goal on energy (SDG7) encompasses three key targets: (1) ensure affordable, reliable and universal access to modern energy services; (2) increase substantially the share of renewable energy in the global energy mix; and (3) double the global rate of improvement in energy efficiency (UN, 2015). The different targets of the SDG 7 contribute to the achievement of other SDG goals and recently this has been the focus of an increasing number of studies (McCollum, et al., 2018).

Now-a-days world-wide focus is to explore more green energy or renewable energy like hydropower, wind power, solar power, and tidal power in order to achieve the global carbon emission reduction commitments as an attempt to lessen the climate change impacts (Owusu & Asumadu-Sarkodie, 2016).

Earth surface is covered by land (28.89%) and water (71.11%) (USGS, n.d.) Tides on the earth acting on water particles is caused by the gravitational attractions of the moon and the sun. Tidal predictions can therefore be calculated accurately from harmonic analysis of previous recorded data (Parker, 2007). Most coastal areas, with some exceptions, experience two high tides and two low tides every lunar day (Ross, 1995). A solar day is the time (24 hours) that it takes for a specific site on the Earth to rotate from an exact point under the sun to the same point under the sun. Similarly, a lunar day (24 hours and 50 minutes) is the time it takes for a specific site on the Earth to rotate from an exact point under the moon to the same point under the moon. The lunar day is 50 minutes longer than a solar day because the moon revolves around the Earth in the same direction that the Earth rotates around its axis. So, it takes the earth an extra 50 minutes to "catch up" to the moon (Sumich, 1996). There are several periodic cycles which affect the tidal ranges; the most important are the lunar and solar tidal cycles. In 1687, Sir Isaac Newton explained that ocean tides result from the gravitational attraction of the sun and moon on the oceans of the earth (Sumich, 1996). The combined effects of the gravitational forces exerted by the moon and the sun, and the rotation of the Earth create tides which are periodic rise and fall of sea water levels. A tidal barrage is a dam-like structure allows water to flow into a bay or river during high tide, and releases the water during low tide through turbines and gates. The rise and fall of water level creates potential energy stored between two levels and in-stream kinetic energy in the moving water. Power generated from tides either by converting potential energy or by utilizing the in-stream kinetic energy into useful forms of power, mainly electricity is called tidal power (Neil, et al., 2018). Tidal barrage power plants harness the potential energy contained in an impounding basin where a relatively large tidal range exists (Angeloudis, et al., 2018). Tidal power is a permanent source of energy, accurately predictable and free from all types of pollutions.

Bangladesh Government has a constitutional mandate to adopt effective measures to bring about a radical transformation in the rural areas through the promotion of agricultural revolution, rural electrification, development of industries and improvement of education, communication and public health, and removing the disparity between the urban and rural areas (GOB, 1972). Last few decades, Bangladesh power sector faced huge challenges to meet the demand and overcome the load shedding problems both in rural areas as well as urban areas. A recent survey reveals that power outages result in a loss of industrial output worth $1 billion a year which reduces the GDP growth by about half a percentage point in Bangladesh (Independent, 2018). Without adequate power, development is not getting pace in the country. The present Government after taking over charge enacted "The Quick Enhancement of Electricity and Energy Supply (Special Provisions) Act, 2010 to ensuring uninterrupted supply of electricity and energy to the system. Now, Bangladesh Power Sector is moving towards attaining long term goals to ensure energy sustainability (Moazzem, 2019) by establishing capacity of 27,400 MW in 2030 and 51,000 MW in 2041 (PSMP, 2016). The power sector has been able to come out from the period of crisis (SREDA, 2015). Access to electricity (% of total population) in 2008 was 47% which raised to 91.5% in 2018. Maximum peak generation was 4,130 MW in against of maximum demand 5,569 MW in 2008 and these rose to 10958 MW in against of 14,014 MW in 2018. The projected peak electricity demand in coming years (base case) would be 14,500 MW (in 2021), 27,400 MW (in 2030), and 51,000 MW (in 2041) respectively (PSMP, 2016). The power sector has experienced considerable progress in meeting the demand for electricity. Access, coverage, and level of consumption have significantly increased over the years. Daily load shedding has significantly dropped from 1107 mKWh in 2009 to 32 mKWh in 2018. (Moazzem, 2019) However, Bangladesh's coverage (76 per cent) and access are still behind South Asia average (85.6 per cent) in 2016. Besides, energy use efficiency has been improving. As of 2018 total installed capacity of 154 power plants is 15042 MW out of which government owned power plants is 8845 MW, Rental power plants 1745 MW and IPP 4452 MW (PSMP, 2016).

When it comes to generating renewable energy, Bangladesh's past performance has seen a mix of success and failure. According to the "Renewable Energy Policy, 2008", the government was supposed to achieve 5% power generation from renewable sources by 2015, and 10% (supposed to be double) by 2020 (GOB, 2008). The government did not attain its goal of generating five percent of the country's electricity from renewable sources by 2015. Bangladesh is currently generating around 572.63 MW of electricity from renewables out of which 230 MW from hydro, 338.65 MW from solar, 2.9 MW from wind and 1.08 MW from Biogas and Biomass, which is just 2.95% of total power generation (Cell, 2020). Experts reckon generating 2000 MW of power (10% of the total) within one year, will be challenging. The government also plans to generate 2,896MW electricity from the same sources by 2021, but slow growth in this sector is nowhere near the projected target. (Nabi, 2019)

Tidal power is enormous, renewable, green, pollution free, predictable, non-depleted but costly and amount of power changes at every single step of time as tide level vary with respect of time (Salequzzaman, 2014). Tidal barrage power plants harness the potential energy contained in an impounding basin where a bay or estuary experiences a tidal range more than 5 m (Etemadi, et al., 2011).

There is huge potential to develop tidal barrage power in the world and same as in Bangladesh. (Roy, et al., 2015) Although tidal power is reasonably predictable, its magnitude changes periodically at different temporal scales because of the variations in tide-producing gravitational forces caused by the sun and the moon (Shevkar & Otari, 2015). Tidal head difference varies so rapidly due to interactions of sun, moon and earth i.e. variation of water head in a tidal basin (tidal barrage power) is higher than that of hydropower. So real time assessment and monitoring is very important. A suitable barrage power site could produce a large quantity of power.

Tidal power can be generated either by converting potential energy or by utilizing the in-stream kinetic energy into electrical energy. Tidal barrage power plants harness the potential energy contained in an impounding basin where a relatively large tidal range exists. Although tidal power is reasonably predictable, its magnitude changes periodically at different temporal scales because of the variations in tide-producing gravitational forces caused by the sun and the moon. Energy has been extracted from tides for centuries (McErlean, et al., 2007). At present there are five *tidal range* power plants in operation around the world (Shevkar & Otari, 2015) *La Rance* tidal power (240 MW) in France and the *Sihwa Lake* tidal power plant (254 MW) in South Korea are two larger tidal power plants. Other three tidal range power plants, relatively small in size, are: *Kislaya Guba* (1.7 MW) in Russia, *Annapolis Royal* (20 MW) in Canada and *Jiangxia* (3.9 MW) in China.

In Bangladesh, having a long coastline (approximately 710 km) and a relatively medium tidal range of 2-7 m has a large potential to harness tidal power. (Ahmad, et al., 2018). A simple theoretical analysis of the data shows that power generation would vary proportionately with basin area and square of tidal range. An analysis of the coastal tide data of Bangladesh shows that in 2019 the tidal range was the minimum (2.81m) at Barisal and the maximum (7.65m) at Sandwip which indicates there are some potentiality in the coastal area to harness tidal barrage power. Since tidal heights vary with respect to time, real-time assessment and monitoring is very important. Small to large scale power generation plants can be established in the coastal areas like Sandwip, Mongla, Khepupara, Cox's Bazar, Hiron Points, Galachipa, Patuakhali and Barisal. (Halder, et al., 2015) Although the government of Bangladesh emphasizes the need for renewable energy (GOB, 2008) an assessment of the potential for tidal power generation in Bangladesh is yet to be initiated.

In the assessment of tidal power generation, the basic equation relates the mass of water and water head difference with the theoretical potential energy while the energy available from a barrage depends on water surface impounded by the barrage and the corresponding tidal range (McErlean, et al., 2007). However, a minimum water head difference between the sea and the basin is required for tidal power generation (Lamb, 1994). In the current practice for assessing the tidal power potential for a plant, primarily the duration of power generation and hydraulic efficiency are considered. Power generation duration is assumed to be one-third time of the day and the efficiency of the system is assumed to be 90%. Based on these, the design extractable power is 30% of potential energy (Xia, et al., 2012); (Rashid, et al., 2012).

Several methods and numerical approaches have been developed to assess tidal power and energy. Prandle (1984) used tidal amplitude instead of tidal range to assess the maximum tidal power. The actual extractable energy per tidal cycle equals to 0.27 E_{max} (for ebb only) and 0.37 E_{max} (for two-way generation). Lamb (1994) used mean tidal range instead of maximum tidal range whereas Rashid, et al., (2012) used tidal range and 60% conversion factor to calculate power. Tester, et al., (2012) used an average power conversion efficiency of 33% and Xia, et al., (2012) used the mean tidal range for tidal power assessment. Neil, et al., (2018) suggested theoretical and zero dimensional (0D) models with more detailed depth-averaged (2D) equations and hydro-environmental tools for the assessment of tidal power. Alam, *et al*., (2012) developed a method to calculate the required number of turbines based on the impounded water volume and the water flow passing through the turbines.

In a tidal barrage, tidal water level on the sea side is a superimposition of a number of periodically-varying tidal constituents (Parker, 2007), while the water level in the basin depends on the geometric configuration of the basin and operational control of the turbines (Tousif & Taslim, 2011). All previous methods for the assessment of tidal power are based on fixed assumed variables such as duration of power generation, and ignore the actual real-time variability in these variables. Assessment of power generation potential based on real-time water head differences, long-term tidal data and basin configuration will yield a more accurate estimation of power generation. An analytical model based on a set of equations that describe this real-time variability will be instrumental in designing tidal barrage power plants.

This study would attempt to develop a new methodology for calculating real time water head, power and energy and identify appropriate site and possible plant capacity of tidal barrage power. This study would provide an idea for developing a tidal barrage plant in Bangladesh.

1.2 Objectives

The goal of this study was to achieve a better estimation of tidal power generation by establishing a real-time functional relation (i) between water level and basin volume, which in turn relate to turbine discharge and water level changes in the basin, and (ii) among the tidal constituents having different phases and amplitudes in the sea side, expressed as a superimposed function with respect to time. This approach will require formulation of an analytical model employing equations to compute the dynamic water head, power and energy considering water level variations in a tidal barrage.

The main objectives of the study were to:

1) develop an analytical model with equations to compute dynamic water head, power and energy for a tidal barrage with variable water levels at the sea and the basin;
2) determine the optimum basin configuration that yields the maximum tidal power; and

3) assess the tidal power generation potential from a tidal barrage in the coastal area of Bangladesh.

Outcome of the study

An analytical model for computing real-time water head, power and energy potential for a tidal barrage is developed. The model is useful in assessing tidal power potential more accurately.

Original contribution of the study

The previous approaches and practices for the assessment of tidal barrage power generation did not consider the continuous changes in the head differences between the sea and basin, rather a static overall estimate using an arbitrary reduction in efficiency and head difference is used. This study has considered the real-time changes in water levels inside and outside the basin to compute the actual power generation potential based on dynamic water head, and developed a new analytical model to represent the water level variations and basin configuration.

1.3 Research Questions

In order to achieve the objectives, the following research questions have been addressed in the next chapters:

(1) How can we improve the existing approaches to assess tidal barrage power?

There are a few numbers of tidal barrage power in the world. In most of the cases, energy and power were assessed using simple formula of power and energy where some authors used tidal range, some used tidal amplitude, some used average tidal range and some used average head which didn't represent the real water head. None of them used dynamic head to assess tidal barrage power for a particular time. In this study, though the same formulas of power and energy are used but instead of tidal range or amplitude or average head, dynamic head, the real-time water head for a particular time is used to calculate power and energy.

(2) How can we improve the existing formulas to assess real time dynamic water head, energy and power generation?

Instead of using tidal range or tidal amplitude or average range or average head, the dynamic head (real-time water level difference between the basin and sea) is used to assess real-time power. So, in a tidal period, we get a series of dynamic heads and capacities. To compute dynamic head for a tidal barrage, "Isle of Whithorn Model" is modified and equations are improved to assess (i) flood-ebb generation with gate; (ii) only flood generation with gate; and (iii) only ebb generation with gate where the earlier only considered continuous generation (which is impracticable) without gate.

(3) How can we develop an analytical model to assess tidal barrage power?

In this study, capacity of a tidal barrage is assessed by developing an analytical model where real-time water head is used to calculate power and energy. Real-time water head is the difference of water levels between sea side and the basin side at real-time. Water level at sea side depends on various factors: such as tidal constituents, basin configuration, local bathymetry and location on the earth surface. Using past tidal data, different tidal constituents (each of which is considered as a simple harmonic motion with different amplitude, speed and phase) are developed using "GeoTide Analyzer 3.0.x, 2015" Software. GeoTide Analyzer converts observed tide gauge data directly into tidal harmonic constants which can then be used to make tidal predictions for any future or past date. Summing up all constituents of simple harmonic motion, we get the real-time water level at the sea side.

On the other hand, water level at the basin side at any particular time depends on basin configuration, area of the basin, water volume, water passed though turbines etc. In this study a generalized equation is developed to calculate water surface area/volume in terms of water level. But, water level at any particular time depends on basin volume and water passed though the turbines. By calculating difference of water levels, dynamic water head is calculated at any particular time. Using dynamic water head, real-time power and energy are calculated. In this way the study ultimately provides a new analytical model to assess real-time water head, power and energy. The model is flexible for number of turbines and gates and as well as those dimensions (dia. and size). Optimum capacity of the plant is assessed by calculating the least levelized cost of energy (LCOE).

(4) What are the impacts of the basin configuration on power generation?

Real-time capacity of the plant at any time and the corresponding energy production for a small-time interval are largely depend on the dynamic head and the volume of water passed though turbines. Secondly, those depend on the tidal prism in the basin theoretically enclosed between two levels at two sides of the barrage. So, the lager the tidal prism, in general the higher the capacity of the plant. The tidal prism or volume of water depends on the configuration of the basin, its aspect ratio and energy gradient line varies between barrage side and upstream side of the basin. How shape and aspect ratio influence the power and energy is discussed in Chapter 5.

(5) What are the potentials of tidal barrage power in the coastal area of Bangladesh?

By analyzing tidal data from "Tide Table 2020" produced by BIWTA, we have observed that the HAT (the highest astronomical tide) and the LAT (the lowest astronomical tide), MHWS, MLWS, MHWN and MLWN are different for different coastal areas. So, tidal ranges at different coastal areas of Bangladesh are different and different plant capacity could be installed at different places. The study reveals that some areas like Sandwip, Khal No. 10, Mongla and Sadar Ghat are some promising sites for tidal barrage power. The study also considers to apply the analytical model for the most promising site Sandwip (having tidal range more than 7 meter) to assess potentials by which the model is tested also.

1.4 Scope and limitation of the study

1.4.1 Scopes of the study

The current approaches and practices for the assessment of tidal barrage power generation do not consider the continuous changes in the head differences between the sea and basin. Rather a static overall estimate using an arbitrary reduction in efficiency and head difference is used. The study considers the real-time changes in water levels inside and outside the basin to compute the actual power generation potential based on dynamic water head, and develop a new analytical model to represent the water level variations and basin configuration. A major outcome of this study is an analytical model for computing real-time water head, power and energy potential in a tidal barrage. The model is useful in assessing tidal power potential more accurately. The study also suggests which type of basin configuration could give maximum output. Besides, the model is validated with the results found for Severn Barrage of UK and also with the results of the base case. The mode is applied for Sandwip Channel of Bangladesh to identify a possible site and possible plant capacity of tidal barrage power.

1.4.2 Limitations of the study

In this study, water levels at sea and the basin are considered horizontal, but it is not perfectly horizontal. Again, technical, economic, environmental, ecological and social issues are not considered in this study. Besides, rainfall, evaporation, temperature, etc., are not used for the analyses in this study.

1.5 Organization of the Dissertation

This dissertation is organized in seven chapters. Chapter 1 provides the background and rationale of the study. It also contains the objectives, outcomes of the study and research questions to achieve objectives. The study scope, limitations and outline of the thesis are also discussed in Chapter 1.

Chapter 2 contains mainly literature review on energy, renewable energy, tidal characteristics, energy from tides, different methods of tidal power generation, tidal stream power, tidal barrage power, different techniques of tidal power generation such as ebb generation, flood generation, flood-ebb generation, two basin schemes, tidal lagoon, dynamic tidal power, barrage power generation, different theories of tidal power, real-time assessment of tidal barrage power, basin configuration and summary of the chapter.

Chapter 3 describes the real-time analytical model development. It contains conceptual basis for power assessment, theoretical formulations and existing equations of power generation, current practices to assess power generation and analytical approach of power assessment. Chapter 3 also contains analytical model development for continuous generation without gates, flood-ebb generation with gates, ebb generation with gates and flood generation with gates. Finally, chapter 3 contains summary of this chapter.

Chapter 4 contains model validation and optimization. Model validation compares results of the Isle of Whithorn tidal barrage using the original Isle case and new Real-Time Analytical (RTA) model. It also compares results for Severn Barrage from UKAEA (1984) study and from the analytical model developed under this study. It also describes how a tidal barrage power plant can be optimized considering levelized cost of energy.

Chapter 5 describes the optimum basin configuration to generate tidal energy. It contains discussions on tidal water levels at sea and basin, its impact on power generation, theoretical formulation, and empirical equations of tidal barge power generation. It compares results considering both steady and unsteady water levels at sea and basin. This chapter also provides comparative results considering different aspect ratios of the basin. It also compares energy variations of different vertical shape basins' especially from a rectangular basin, a trapezoidal basin and a parabolic basin having equal tidal data and range.

Chapter 6 provides an application of the analytical model to assess energy generation from a hypothetical basin of Sandwip channel in the coastal area of Bangladesh. This chapter also contains the procedure to assess tidal barrage power generation using the analytical model developed under this study. It also contains tidal data at some locations of Bangladesh, tidal data for Sandwip channel, tidal constituents of Sandwip channel, formation an equation of area-elevation curve of a hypothetical basin of the Sandwip study area and results from the basin.

Finally, Chapter 7 draws the conclusions and limitations of the study. It also provides recommendations for further studies.

CHAPTER 2
LITERATURE REVIEW

2.1 Introduction

Tides are periodic rise and fall of sea water levels caused by the combined resultants effects of the gravitational forces exerted by the Sun, Moon and Earth system (CIRIA, 1996). In 1687, Sir Isaac Newton explained that ocean tides result from the gravitational attraction of the sun and moon on the oceans of the earth (Sumich, 1996). Tides create water mass movement which is the resultants of series of harmonic motions with different tidal amplitudes and velocities from which tidal power can be generated. Tidal power is a form of hydropower that converts the energy obtained from tides into useful forms of power, mainly electricity. Tidal power could be a permanent source of energy. The biggest advantage of tidal power is that it is reliable, predictable, pollution free, green, renewable and inexhaustible. Now-a-days, tidal power is considered to be an important source of renewable energy.

Chapter two of this thesis contains literature review on energy situation, renewable energy, tidal characteristics, power and energy assessment process including real-time power assessment.

In the following sections of this chapter literature on tidal power is reviewed specially on energy in Section 2.2, renewable energy in Section 2.3, tidal characteristics in Section 2.4, tidal stream power in Section 2.5, tidal barrage power in Section 2.6, barrage power calculations in Section 2.7, different techniques of tidal power generations in Section 2.8, dynamic tidal power in Section 2.9, procedure for tidal barrage power generation in Section 2.10, tidal barrage power assessment in Section 2.11, different theories of tidal power generation in Section 2.12, real-time assessment of tidal barrage power in Section 2.13, basin configuration and power generation in Section 2.14, and summary in Section 2.15.

2.2 Energy

Between 1971 and 2017, world total primary energy supply (TPES) increased, by more than 2.5 times, from 5519 million tons of oil equivalent (Mtoe) to 13972 million tons of oil equivalent and its structure also changed where dominant fuel oil fell from 44% to 32% and natural gas grew from 16% to 22%. The share of coal is increased from 26% to 27% between 1971 to 2017. Biofuel decreased from 11% to 10%, nuclear power increased from 1 % to 5%, hydropower remains unchanged (2%) and by this time other renewables took about 2% share as shown in Figure 2.1.

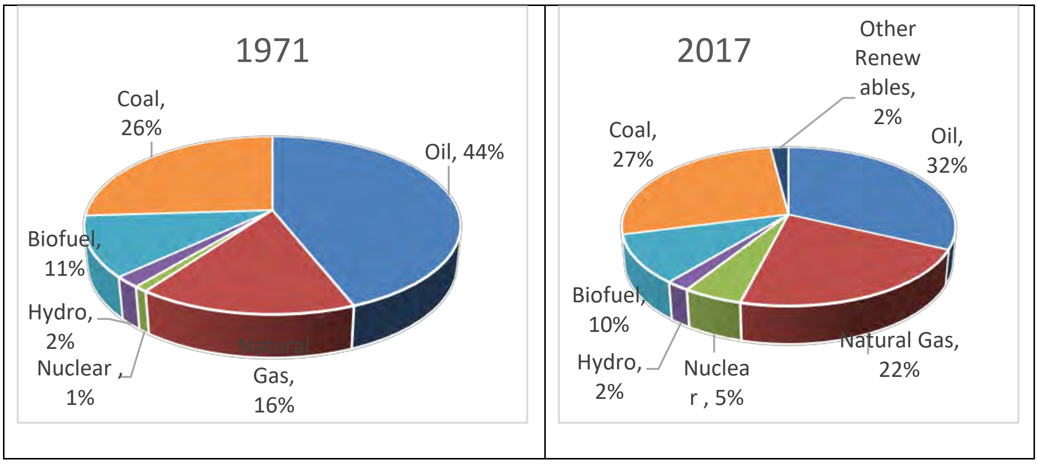

Figure 2. 1: Shares of primary energy sources between year 1971 and 2017. Source: (Looney, 2020)

On the other hand, world total final energy consumption increased manifolds from 4659 Mtoe in 1971 to 9717 Mtoe in 2017. Share of energy consumptions from different sources is listed in the following Table 2.1:

Table 2.1: Share of energy consumptions from different sources.

Sl. No.	Sources	In 1971	In 2017
1	Oil	48.3%,	41%
2	Natural gas	14%	15.5%
3	Electricity	9.4%	18.9%,
4	Biofuels and waste	13%	10.7%,
5	Coal	13.6%	10.5%
6	others	1.7%	3.4%

But electricity consumption was increased from 6131 TWh (1973) to 25606 TWh (2017).

2.3 Renewable Energy

At present, renewable energy is only 800 TWh which is supposed to be more than double over 1800 TWh to protect the environment (World Bank, 2019). Thus, renewable energy sources, especially solar, hydro, wind, biogas, etc. should be harnessed more to protect the environment.

In 1973, CO_2 emissions from fuel combustion were 15,460 Mt that rose to 32,840 Mt in 2017. Outlook for world total primary energy supply (TPES) in 2040 will be 12,581 Mtoe based on new policies scenario and 9958 Mtoe based on sustainable development scenario and corresponding CO_2 emission will be 35881 Mt and 17647 Mt respectively. So, world should adopt sustainable development scenario to keep the CO_2 emission to a minimum level.

Tidal power is enormous, renewable, green, pollution free, predictable, non-depleted but costly and site specific. Tidal barrage power plants harness the potential energy contained in an impounding basin where a relatively large tidal range exists but amount of power changes at every single step of time as head vary with respect to time. Energy has been extracted from tides for centuries (McErlean, 2007). There is huge potential to develop tidal barrage power in the world and the same also in Bangladesh as it has some channels with medium/high tidal ranges. As the magnitude of tides changes periodically at different temporal scales because of the variations in tide-producing gravitational forces caused by the sun and the moon (Shevkar & Otari, 2015), tidal power is intermittent and of different capacities. Tidal head difference varies with respect to time due to interactions of sun, moon and earth. This variation of water head in a tidal basin (tidal barrage power) is rapid than that of hydropower. So real time assessment and monitoring is very much important.

Bangladesh Government has constitutional mandate to adopt effective measures to bring the rural areas in development through the promotion of agricultural revolution, rural electrification, development of industries and improvement of education, communication and public health and removing the disparity between the urban and rural areas (Article 16 of Bangladesh's Constitution, 1972). Last few decades, the country was facing major challenges to meet the power demand

and to overcome the load shedding problems in rural areas as well as urban areas. A recent survey reveals that power outages result in a loss of industrial output worth $1 billion in a year which reduces the GDP growth by about half a percentage point in Bangladesh (ICCB, 2018). The present Government after taking over charge in 2009 enacted "The Quick Enhancement of Electricity and Energy Supply (Special Provisions) Act, 2010 to ensure uninterrupted supply of electricity and energy to the system. At present, Power Sector is moving towards attaining long term goals to ensure energy sustainability (Moazzem & Ali, 2019) by establishing capacity of 24,000 MW in 2021, 30,000 MW in 2030 and 60,000 MW in 2041 respectively (Power Cell, 2020). Bangladesh power sector has been able to come out from the period of crisis (SREDA, 2015). Access to electricity as % of total population in 2008 was 47% which raised to 96% in 2019. The maximum peak generation was 4,130 MW in 2008 and these rose to 12,893 MW W in 2019 (May 29, 2019). As of 2nd December 2019, the total installed capacity of Bangladesh is 22,727 MW out of which government owned power plant is 9740 MW (42.86%), IPP is 6916 MW (30.430%) , SIPP is 350 MW (1.54%), rental is 1404 MW (6.18%) (Private is 8670 MW), import 1160 MW (5.10%), captive power is 2800 MW (12.32%), renewables other than hydro is 357 MW (1.57%) (BPDB, 2019). At present access to electricity 96% (2020) and per capita consumption is 510 kWh. At present, there are as many as 20 quick rental power plants are in operation (BPDB, 2020). This implies that quick rental power plants are still contributing a significant portion of electricity generation (6.18%) in the country and renewables are not getting any pace. According to the "Renewable Energy Policy, 2008" of GOB, the government of Bangladesh was needed to produce 5% energy from renewable resources by 2015 and 10% of the same by 2020. The government has not achieved its target of producing 5% energy from renewable resources by 2015. Bangladesh can currently generate 22,727 MW electricity including captive and renewables from different sources among which 627.92 MW from renewable energy sources which is just 2.76% of total capacity, out of which 230 MW from hydro, 393.99 MW from solar, 2.9 MW from wind and 1.03 MW from Biogas and Biomass (Power Cell, 2020). Experts are saying that generating of 2400 megawatts (10% of total) from renewable resources by 2021 will be a challenging task. The slow growth in the renewable sector is nowhere near the expected target.

2.4 Tidal Characteristics

2.4.1 General characteristics

The principal of tidal forces is generated by the Moon and Sun on the sea of the earth. Sir Isaac Newton, in 1687, explained that ocean tides result from the gravitational attractions of the sun and moon on the oceans of the earth (Sumich, 1996). But the Equilibrium Theory of the Tides" was presented by Darwin in 1898. He described that the tides are water fluctuations apparent to an observer traversing along a constant latitude line (Burstyn, 1962). Tides are the periodic motion of the waters of the sea due to the inter-attractive forces between the celestial bodies. Tides are very long-period waves that move through the oceans in response to the forces exerted by the moon and sun. Tide and current are not the same. Tide is the vertical rise and fall of the water and tidal current is the horizontal flow (Khare, et al., 2018). Tidal water level is a superimposition of a number of periodically-varying tidal constituents. The Moon is the main tide-generating body. Due to its greater distance, the Sun's effect is only 46 per cent of the Moon's (Bowditch, 2002); (Dean, 1966).

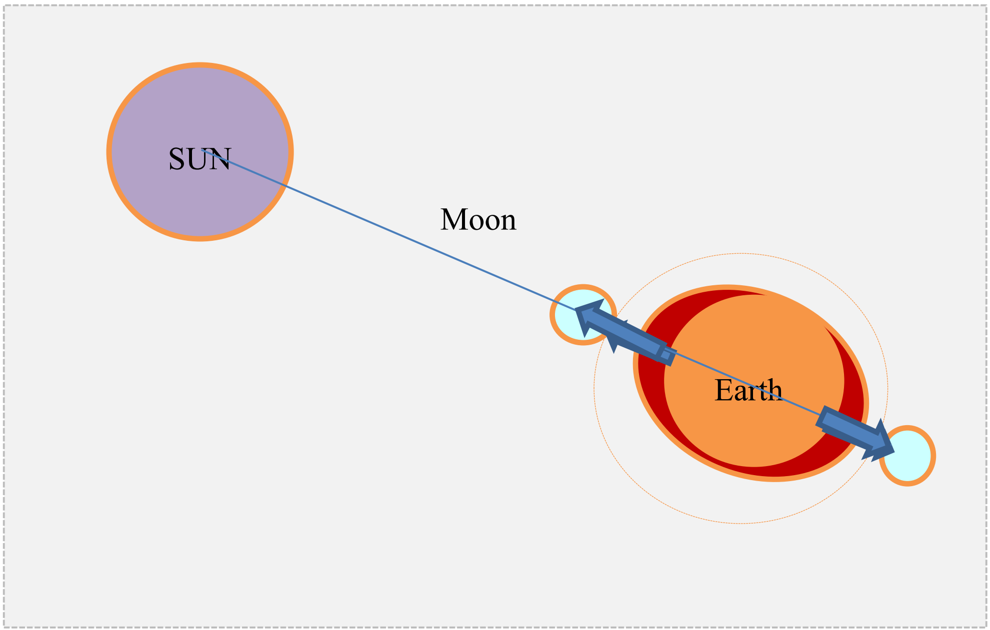

Figure 2. 2: Pull of the Sun and the Moon on the Earth.

The amplitude of water level variations at different points on the earth depends on the latitude and the nature of the shore. Due to the rotation of the earth on its own axis causes two high tides and two low tides daily at any place. The revolution of the moon around the earth increases the time interval between two successive high tides from 12 hours to about 12 hours and 25 minutes. As the moon revolution takes about 28 days, the three bodies, i.e. the sun, the moon and the earth are in alignment every two weeks at new and full moon.

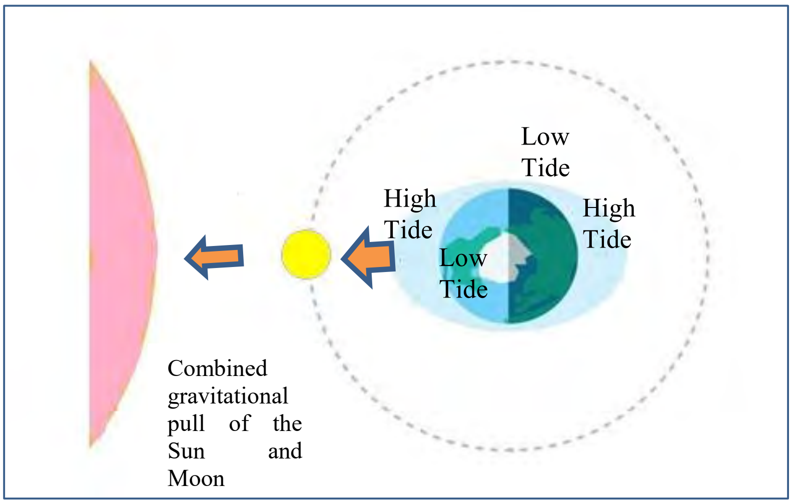

Figure 2.3: Combined gravitational pull of the Sun and the Moon.

A solar day is the time (24 hours) that it takes for a specific site on the Earth to rotate from an exact point under the sun to the same point under the sun. Similarly, a lunar day (24 hours and 50 minutes) is the time it takes for a specific site on the Earth to rotate from an exact point under the moon to the same point under the moon. The lunar day is 50 minutes longer than a solar day because the moon revolves around the Earth in the same direction that the Earth rotates around its axis. So, it takes the earth an extra 50 minutes to "catch up" to the moon (Sumich, 1996), (Thurman, 1994). There are several periodic cycles which effects the tidal ranges, the most important are the lunar and solar tidal cycles. Significant motions of this system include the revolution of the earth around the sun and the revolution of the moon around the earth. In addition, the moon and earth each rotate about their own axes. The plane in which the earth revolves about the sun is called "ecliptic" plane; the axis of the earth is inclined at $66\frac{1}{2}^0$ to the ecliptic plane. The moon's orbit about the earth is inclined at $5^0 9'$ to the ecliptic plane.

The sun and earth both are displaced a small distance from the centres of their respective orbits. The positions of the moon when it is nearest to and farthest from the earth are called the perigee and apogee, respectively. When the moon is at perigee, it has its greatest tide-producing effect on the earth. The terms corresponding to the nearest and farthest positions of the earth from the sun are perihelion and aphelion, respectively. According to Darwin, the tides are the fluctuations in water level observed as one traverse along a line of constant latitude.

The reasons for creating tides are mainly for two factors: (i) gravitational attraction and (ii) centrifugal force. The magnitude of the centrifugal force, F_c is represented by $F_c = \Omega^2$ Re cos φ; where Re is radius of earth, Ω is the rotation of earth, φ is latitude. The earth and moon are revolving about a common axis is called axis of revolution. If T is the period of revolution of the earth and moon about their common axis, the value of T= 27.3 days. As the moon is closer to the earth, the tides caused by the sun are approximately 46% of that produced by the moon. So, during full moon and new moon in the earth-moon-sun system the greatest tides called the spring tides and during the first and last quarters, the lowest tides called the neap tides occur.

During each lunar month, two sets of spring tides and two sets of neap tides occur (Sumich, 1996). Once a month, when the moon is closest to the Earth (at perigee), tide-generating forces are higher than usual, producing above-average ranges in the tides. About two weeks later, when the moon is farthest from the Earth (at apogee), the lunar tide-raising force is smaller, and the tidal ranges are less than average. A similar situation occurs between the Earth and the sun. When the Earth is closest to the sun (perihelion), which occurs about January 2 of each calendar year, the tidal ranges are enhanced. When the Earth is furthest from the sun (aphelion), around July 2, the tidal ranges are reduced (Sumich, 1996) (Thurman, 1994).

2.4.2 Tidal characteristics concerning power generation

The difference in water levels between high tide and low tide is called tidal range which is shown in the Figure 2.4. The rise and fall of water levels in the sea during tides can be represented by a sine curve. One tidal day is of 24 hours and 50 minutes and there are two tidal cycles in one tidal day.

The normal tide is a semi-diurnal tide with a period of 12 hours and 25 minutes. Diurnal tides (24 hours) indicate one high and one low tide created by moon during one rotation of the earth on its axis. The daily tidal cycle follows a sinusoidal pattern.

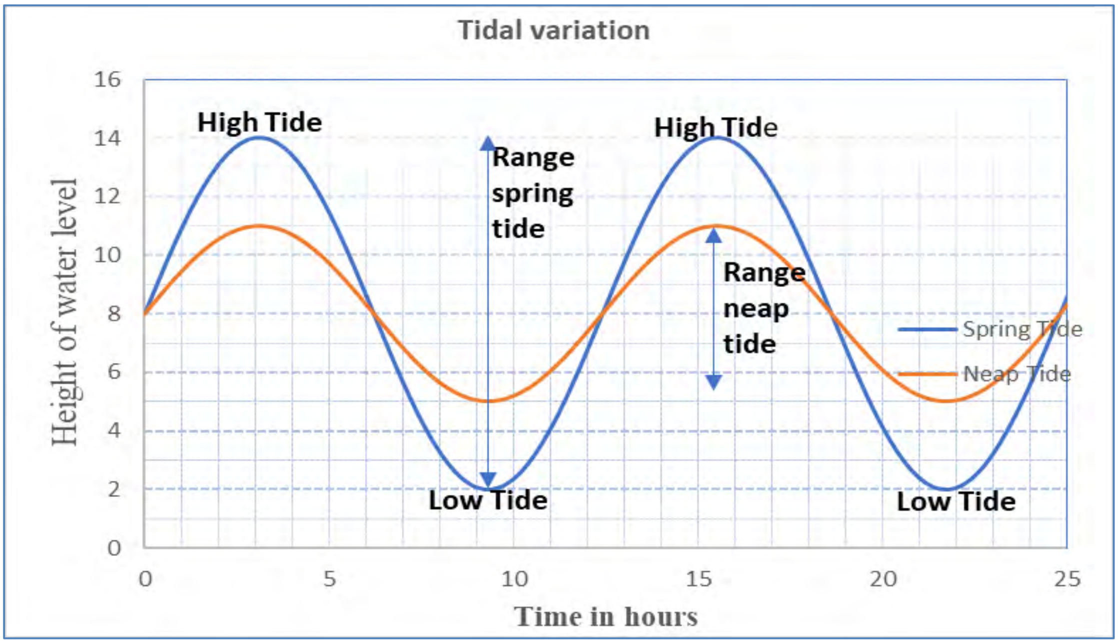

Figure 2.4: Spring and neap tidal range.

Generally, in a rotation (360^0) two maxima and minima are occurred. The relative motions of the earth, moon and sun cause a number of periodic tide-producing forces each represented by a tidal constituent with its own tidal frequency, amplitude and phase angle which are considered as simple harmonic motion and are mutually independent. The resultant tide at any point is composed of a finite number of those constituents. There are three types of tides: diurnal, semidiurnal and mixed (Hagerman, et al., 2006). Tides which have one episode of high water and one episode of low water each day is called diurnal tide. Tides which have two high and two low water episode each day is called semi-diurnal tide. Tides which have two high and two low water episode of different heights each day is called mixed tide.

The dominant tidal constituents are the diurnal constituents, K_1, O_1, P_1, Q_1, and S_1, with periods of 23.93, 25.82, 24.07, 26.87, and 24.00 hours, respectively, and the semidiurnal constituents M_2, S_2, N_2, and S_2, with periods of 12.42, 12.00, 12.66, and

11.97 hours, respectively. Each tidal constituent can be represented as $h(t) = a \cos(\omega t-\varphi)$ where $h(t)$ is the height of the tide at time t, a is the amplitude of the constituent, ω is the angular frequency of the earth and φ is the phase lag.

Tidal power can be generated either by converting potential energy or by utilizing the in-stream kinetic energy into electrical energy (Neil, et al., 2018). Tidal barrage power plants harness the potential energy contained in an impounding basin where a relatively large tidal range exists (Angeloudis, et al., 2018). Most parts of the earth are covered by water surface, so, tidal power can contribute a large portion of global energy need. It also represents a permanent source of energy, accurately predictable and free from all types of pollutions.

Although tidal power is reasonably predictable, its magnitude changes periodically at different temporal scales because of the variations in tide-producing gravitational forces caused by the sun and the moon (Shevkar & Otari, 2015). The amount of tidal energy depends on operating head, basin area and turbine and gate area. In the assessment of tidal energy generation, the basic equation relates the mass of water and water head difference with the theoretical potential energy while the energy available from a barrage depends on water surface impounded by the barrage and the corresponding tidal height (McErlean, 2007).

Mass of water depends on area of the basin. So, higher the basin area, higher would be the power generation. However, a minimum water head between the sea and the basin is required for tidal power generation (Lamb, 1994) to avoid cavitation. Tidal amplitude varies with-respect-to time this is why water head also varies every moment of time. So, real-time assessment is a prerequisite for tidal power assessment.

Locations for tidal range power: around the world that are suitable for tidal range power are relatively limited. Physical constraints are (i) tidal range; (ii) grid connectivity; (iii) geo-morphology; (iv) seabed conditions and (v) available area for an impoundment.

2.4.3 Energy from the tides

Tidal Energy is one of the innovative and evolving technologies, which is commercially not feasible and viable in all cases. It is still in Research & Development (R&D) stage (Shaikh & Shaiyek, 2011). But tidal energy is inexhaustible and is considered as a renewable source. It has an advantage over other sources of energy, because it is less vulnerable to climate change compare to the other sources of energy which change climate randomly (Nicholls-Lee & Turnock, 2008). Potential energy stored between high-tide and low-tide or kinetic energy of fast-moving water is converted to electrical energy. Basically, there are two types of tidal power; namely (i) stream power and (ii) barrage power. Researchers have predicted that UK is capable to produce over 20% of its electrical needs from its tidal resources (Callaghan, 2006). In stream power technology, kinetic energy of moving water is converted into electrical energy is called stream power. Most of the existing technology used for tidal energy conversion is from the wind power industry (Bahaj, et al., 2007) ; (Batten, et al., 2007) (Fraenkel, 2002). Water is 830 times denser than wind and velocity of moving water is used to drive the turbine like wind to generate electricity. The concept of hydropower is used to explore the potential energy into electrical energy as called tidal barrage power where a barrage is constructed to separate the water from sea. The basic principle of tidal barrage power is that a dam/barrage is constructed in such a way that a basin gets separated from the sea and a difference in the water level is obtained between the basin and sea. The constructed basin is filled initially at high tide and emptied when height difference between two sides of the barrage is over a threshold height, 5 ft. (Simeons, 1980) or vice versa passing through sluices and turbine respectively is called barrage power. Due to its greenery and predictability characteristics many countries are trying to explore tidal energy of different forms depending on its availability and feasibility. (Roberts, et al., 2016). Because the earth's tides are ultimately due to gravitational interaction with the moon and sun and the earth's rotation, tidal power is practically inexhaustible and classified as a renewable energy resource.

2.4.4 Different methods of tidal power generation

Tidal power has a long history. Energy has been extracted from the tides for centuries; Strangford Lough Tide Mill, Northern Ireland has been dated to the early 6th Century although the extracted energy was, of course, not used to generate electricity, but to provide mechanical motion.

Different methods have been suggested by different authors for the extraction of tidal energy. There are two primary methods to extract energy from the tides (Khare, et al., 2018). However, the basic principle behind the methods remains same.

Estuaries into which large amounts of ocean water flows due to high tidal range, are captured behind barrages and the turbines are rotated by utilizing the potential energy of the stored water.

The kinetic energy of moving water can be used to extract energy similar to the principle of extraction of wind energy.

Both methods that are mentioned above have been suggested and followed and each has its own advantages and disadvantages (Bryden, et al., 2004). It may also be possible to employ pumping strategies for barrages to obtain better efficiency and to match electricity demand better (MacKay, 2007). Generation of electricity from tidal flow is similar to hydroelectricity generation, except that two-way turbines are utilized to capture the tidal power in both directions of flow.

Different types of tidal power are mentioned below:

Table 2.2: Different types of tidal power.

Tidal Power						
Stream power (Kinetic energy)		**Barrage power** (Potential energy)				
Tidal stream power	Tidal fencing	Ebb power	Flood power	Two-way generation	Dual basin	Pumping

2.5 Tidal Stream Power

2.5.1 Tidal stream generator

A tidal stream generator is a machine that extracts energy from moving masses of water, or tides. These machines function very much like underwater wind turbines, and are sometimes referred to as tidal turbines. Tidal stream generators are the cheapest and the least ecologically damaging among the three main forms of tidal power generation. Since tidal stream generators are an immature technology, no standard technology has yet emerged as the clear winner, but large varieties of designs are being experimented with, some very close to large scale deployment. Several prototypes have shown promise with many companies making bold claims, some of which are yet to be independently verified, but they have not operated commercially for extended periods to establish performances and rates of return on investments.

Various turbine designs have varying efficiencies and therefore varying power output. The available kinetic energy of the stream flow flowing across the cross section with a velocity can be expressed as (Bryden, et al., 2004):

$$P = \frac{\rho A V^3}{2} \cdot C_P \qquad (2.1)$$

where,

P = the power generated (in watts),

C_P = the turbine power coefficient (Betz coefficient 16/27=0.593) (Betz, 1966),

ρ = the density of the water (seawater is 1025 kg/m³),

A = the sweep area of the turbine (in m²), and

V = the velocity of the flow.

Low velocity current (1.2 m/s to 2 m/s) can also be utilized if these currents are available continuously like river current flows (Desmukh & Amitkumar, 2015).

2.5.2 Existing tidal stream power

At present there are many tidal stream power plants are in operation in the world among which some important are cited in Table 2.3.

Table 2.3: Tidal stream power in operations.

Station	Capacity (MW)	Country	Commissioned Year
Race Rocks Tidal Power	0.065	Vancouver Island	September 2006
Strangford Lough SeaGen	1.2	U.K.	2008
Eastern Scheldt Barrier Tidal Power Plant	1.25	Netherland	2015
Bluemull Sound Tidal Stream Array	0.5	UK	2016
Kislaya Guba on the Barents Sea.	0.4 MW/	Soviet Union	2006
Jindo Uldolmok Tidal Power Plant (tidal stream generation)	1 MW	South Korea	2009 (90 MW by 2013)

2.5.3 Advantage of a stream generator

(1) Tidal stream turbines are basically like as wind turbines that can be installed wherever there is strong tidal flow or velocity. Water is about 800 times denser than air which can produce more power than wind.

(2) No extra submerging of land is involved unlike hydropower.

(3) It is free from pollution.

(4) It is renewable, green and predictable.

2.5.4 Disadvantage of a stream generator

(1) The major drawback of tidal stream power is their uneven operation.

(2) Heavy initial costing and long construction period.

(3) Turbine efficiency may significantly reduce total energy generation.

(4) Sea water is corrosive that can cause harm to the turbine.

(5) Sedimentation and siltation of basins may cause serious problems.

(6) Installation as well as its protection against flow may be difficult.

2.6 Tidal Barrage Power

2.6.1 Tidal barrage

A tidal barrage is like a dam used to capture the energy from masses of water moving in and out of a basin due to tide producing forces. Instead of damming water on one side like a conventional dam, a tidal barrage first allows water to flow into the basin during high tide to store water, and then releasing the water back to the sea during low tide. Turbines are placed at sluice gates to capture the energy as the water flows in and out. Water is controlled to create water head to produce power using these sluice gates and turbines at prime times of the tidal cycle.

The barrage method of extracting tidal energy is similar to hydropower method that involves building a barrage across a bay or river that is subject to tidal flow. Turbines installed in the barrage wall generate power as water flows in and out of the estuary basin, bay, or river. These systems are similar to a hydro dam that produces pressure head or static head- a height of water pressure. When the water level outside of the basin or lagoon changes relative to the water level inside the basin or lagoon, the head is able to drive the turbines, the system can produce power. A schematic plan view is shown in Figure 2.5.

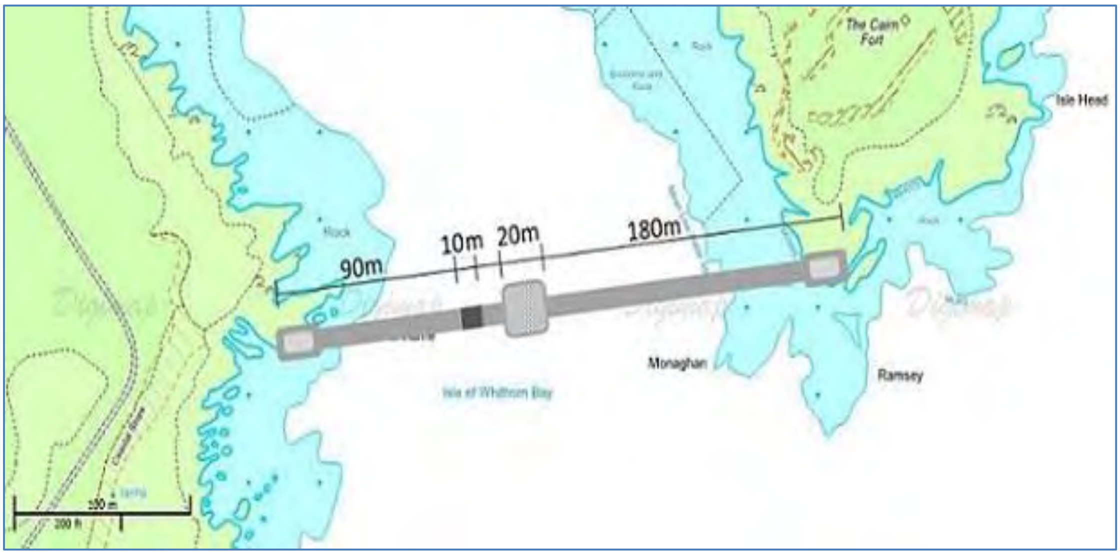

Figure 2.5: A schematic plan view of a tidal barrage.
Source: (University of Strathclyde, 2015).

Generally, the basic elements of a tidal barrage are caissons, embankments, sluices, turbines, generator and ship locks. Location of a barrage is selected in such a place where tidal fluctuation is high i.e. tidal range is higher, can impound a large area and barrage construction cost is low. A schematic side view of a tidal barrage is shown in Figure 2.6.

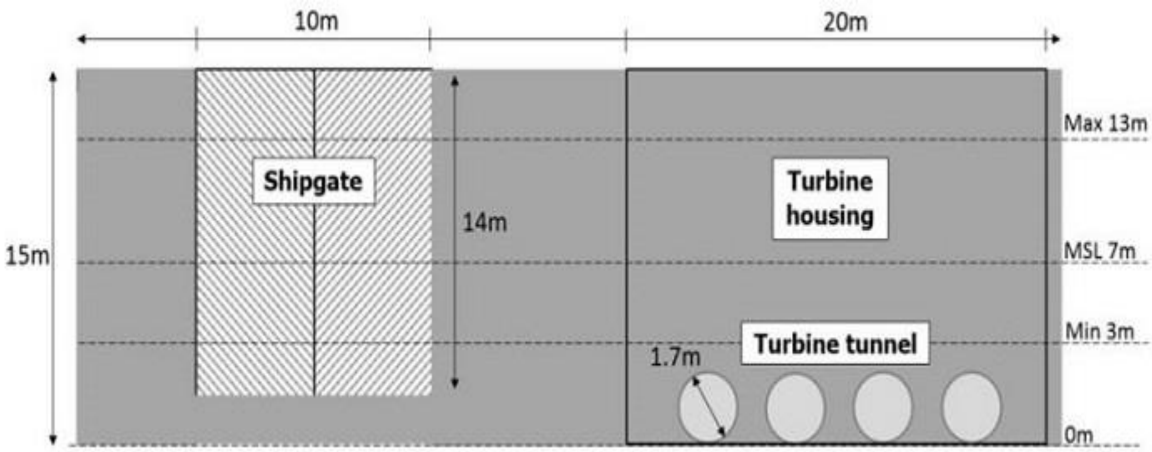

Figure 2.6: A schematic side view of a tidal barrage.
Source: (University of Strathclyde, 2015).

2.6.2 Existing tidal barrage power plants

Several large-scale tidal power generation plants are operating around the globe. *La Rance* tidal barrage power plant, operated by Electricite de France (EDF), having 24 turbines with a peak capacity of 240 MW, is the first tidal power plant in the world commissioned in 1966. On the other hand, 254 MW Sihwa Lake tidal power plant in South Korea is the largest tidal barrage power plant in the world. The Kislaya Guba tidal power plant commissioned in 1968 as a trial project in Russia with the initial capacity of 400 kW has grown to 1.7 MW. The Annapolis Royal Generating Station (20 MW) on the Annapolis River in Nova Scotia, Canada constructed in 1984. The Jiangxia tidal range power plant (3.9 MW) was opened in 1985 in China. Table 2.4 shows major tidal barrage power plants in operation in the world:

Table 2.4: List of tidal barrage power plants in operations in the world.

Station	Capacity (MW)	Country	Commissioned Year
Rance Tidal Power Station	240	France	1966
Kislaya Guba Tidal Power Station	1.7	Russia	1968
Jiangxia Tidal Power Station	3.2	China	1980
Annapolis Royal Generating Station	20	Canada	1984
Sihwa Lake Tidal Power Station	254	South Korea	2011

Source: (Haque & Khatun, 2017).

Several other tidal power stations have been proposed or are under construction. These include Garorim Bay in South Korea (520MW), Severn Barrage at Wales (8640MW), Gulf of Kutch Energy project in India (50MW), and Tugurskaya (3640MW), Mezenskaya (12,000-8,000MW) and Penzhinskaya (87,100MW) in Russia.

2.7 Barrage Power Calculation

Potential energy available in a volume of water can be expressed as:

$$E_p = \mathrm{mg}\frac{h}{2} \qquad (2.2)$$

where,

E_p= potential energy;

m= mass of the volume of water;

g= the acceleration due to the earth's gravity = 9.81 meters per second squared; and

h= height of the water volume from low level.

Putting the value of m= $A_b h\rho$ in Equation (2.2) E_p could be expressed as:

$$E_p = \text{mg}\frac{h}{2} = \frac{1}{2}\rho g A_b h^2 \tag{2.3}$$

A_b is the horizontal area of the basin;

ρ is the density of water = 1025 kg per cubic meter (seawater varies between 1021 and 1030 kg per cubic meter).

The energy available from a barrage depends on the mass of water. If the centre of gravity of a volume of water stored or contained between high tide and low tide, the potential energy (Tousif & Taslim, 2011); (Haque & Khatun, 2017)) could be expressed as:

$$E_p = \frac{1}{2}\rho g A_b R^2 \tag{2.4}$$

where, R is tidal range and R=h; the difference in water levels at high tide and low tide.

Average potential power for one tidal period becomes (Tiwari & Gupta, 2010) as:

$$\bar{P} = \frac{E_p}{T} \tag{2.5}$$

$$\bar{P} = A_b \rho g \frac{R^2}{2T} = \frac{1}{2}\rho g A_b R^2 / T \tag{2.6}$$

where,

$\bar{P}$ is the average power output in watts;

E_p is the energy output in a tidal cycle in hrs.;

R is the vertical tidal range; and

T is the tidal period (time per cycle) in hrs.

The maximum head is only available at the moment of low water, assuming the high-water level is still present in the basin.

2.8 Different Techniques of Tidal Barrage Power Generation

Tidal barrage power can be generated following different techniques such as ebb generation, flood generation, two-ways generation, pumping, two-basin schemes, tidal lagoon and new concept of dynamic tidal power (DTP). Each technique is elaborated below:

2.8.1 Ebb generation

In this technique, power is generated during ebb tide only. A schematic vertical view of a tidal power for ebb-generation is shown in Figure 2.7.

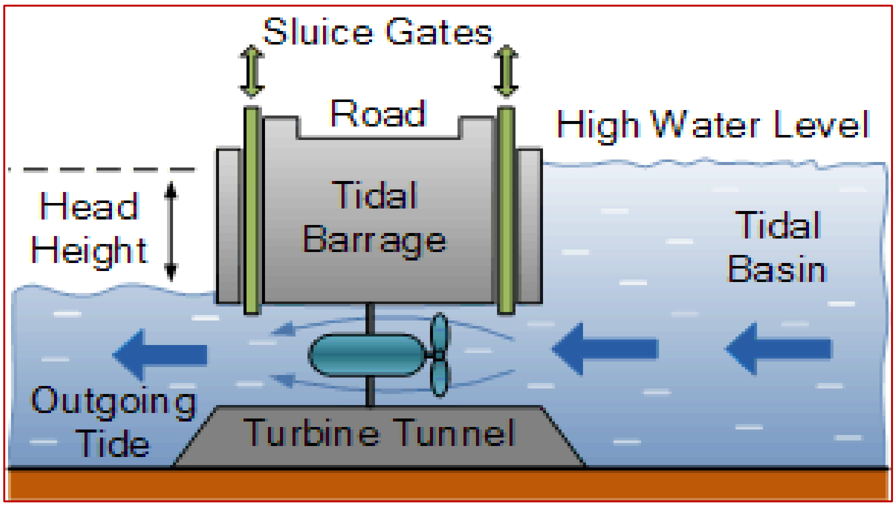

Figure 2.7: Schematic vertical view of a tidal power for ebb-generation.
Source: (Alternative Energy, 2020)**.**

In ebb generation the following techniques are adopted:

- The basin is filled at the high tide and then closed while the tide recedes.
- When there is a significant gap between water levels, generation occurs as the reservoir drains to the sea before incoming tide refills it.
- The basin is filled through the sluices until high tide. Then the sluice gates are closed.
- At this stage there may be "pumping" to raise the level further. The turbine gates are kept closed until the sea level falls to create sufficient head across the barrage, and then turbines are opened, so that the turbines generate until the head is again low. Then the sluices are opened, turbines disconnected and the basin is filled again. The cycle repeats itself.

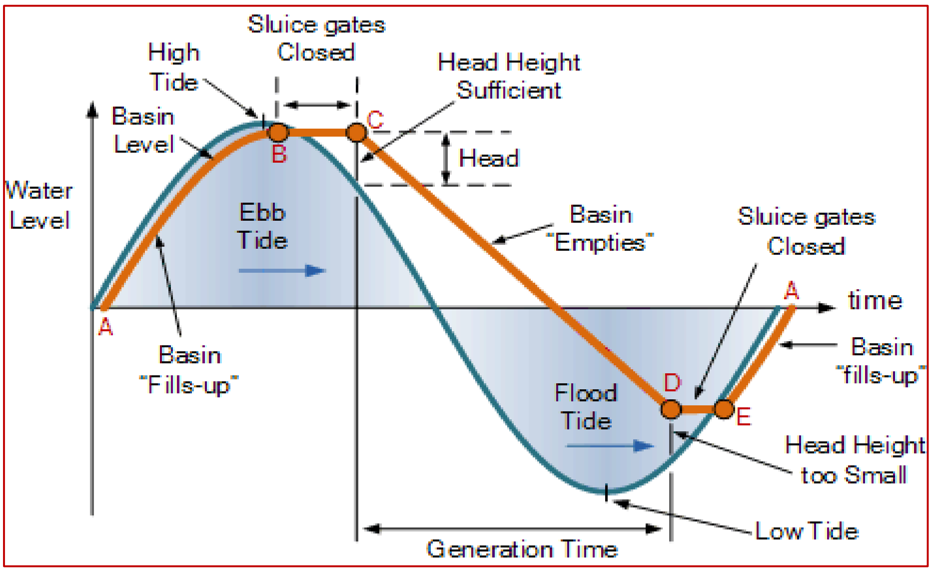

Figure 2.8: Techniques for ebb-power generation.
Source: (Alternative Energy, 2020)

Ebb generation (also known as outflow generation) takes its name because generation occurs as the tide changes tidal direction. Figure 2.7 shows schematic vertical view of a tidal power project for ebb generation and Figure 2.8 shows the techniques for generating ebb power. During flood tide, turbines are kept closed and during ebb tide, turbines are kept opened for power generation in ebb power generation techniques.

2.8.2 Flood generation

In this technique, power is generated during flood tide only. In flood generation the following techniques are adopted:

- The basin is emptied at ebb tide through sluice gates until high tide and then sluices gates are kept closed until there is a significant gap between water levels when generation is started.
- The generation continues until the head drops to a minimum threshold level that requires to stop the turbines. Then turbines and gates are kept closed until water levels are same.
- After that, gates are opened to drain the water from basin to the sea until flood tide occurs.
- The cycle repeats itself. This is generally much less efficient than ebb generation (Shaikh & Shaiyek, 2011). Figure 2.9 shows the techniques for generating tidal barrage flood generation.

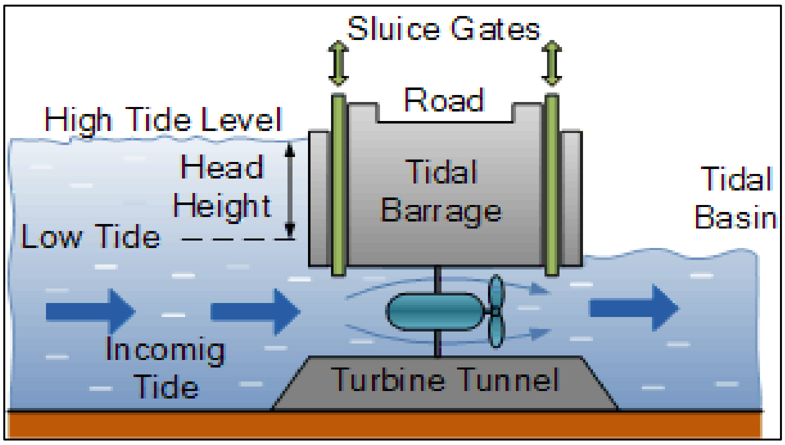

Figure 2.9: Flood-generation Techniques.
Source: (Alternative Energy, 2020).

2.8.3 Two-ways generation

In two ways generation, power is generated at both ebb tide and flood tide. It combines both ebb generation and flood generation. In two-ways generation the following techniques are adopted:

- In one-way ebb generation, the rising tide enters the enclosed basin through sluice gates, turbines remain idle. Once the maximum level in the enclosed basin is achieved, the gates are closed until a sufficient head develops on the falling tide. Power is subsequently generated until a predetermined minimum head (h_{min}) difference is reached. In one-way flood generation, the whole process is reversed.
- In two-way generation, energy is extracted from the ebb phases and the flood phases of the tidal cycle, supplemented with or without pumping water to further increase the water heads. Figure 2.9 shows schematic representation of a two-way-generation technique with filling.

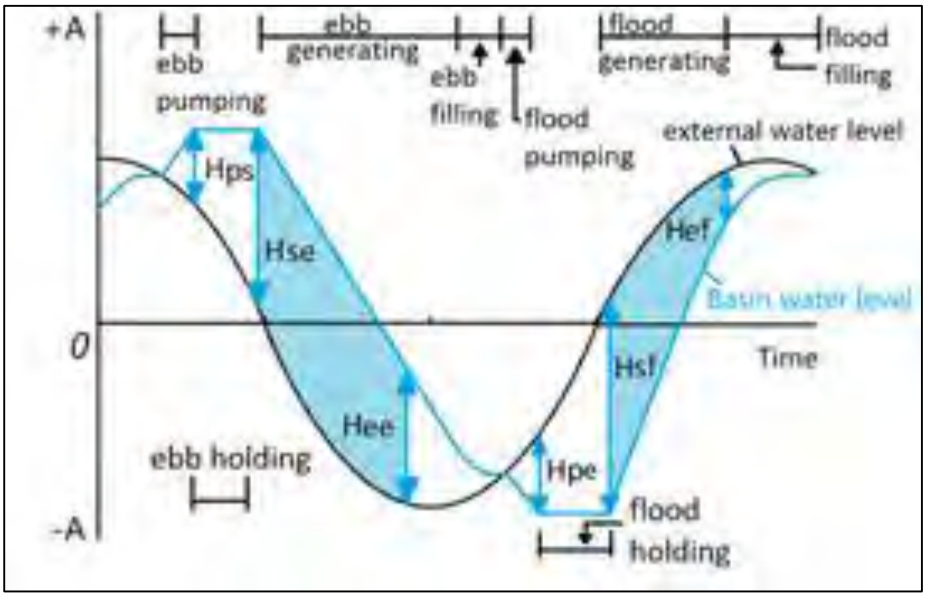

Figure 2.10: Schematic representation of the operational mode (including pumping) of a two-way tidal power generation.
Source: (Xue, et al., 2019)**.**

2.8.4 Pumping

Pumping helps to increase head both at ebb generation and flood generation. The techniques adopted are mentioned below:

- For ebb generation basin is filled through gates until ebb tide, then sluice gates are closed. At this stage water could be pumped to the basin to raise water level further by using excess energy in the grid. This would yield more energy during ebb generation, because power output is not a linear relationship, rather, strongly related to the squared of head.
- For flood generation basin is emptied through gates until flood tide, and then sluice gates are closed. At this stage water could be pumped to the sea from basin to raise water level further. This would yield more energy during flood generation, because power output is not a linear relationship, rather, strongly related to the squared of head.

2.8.5 Two-basin schemes

Another form of tidal barrage is that of the dual basin type. The following techniques are adopted for two-basin schemes:

- With two basins, one is filled at high tide and the other is emptied at low tide. Turbines are placed between the basins.
- Two-basin schemes offer advantages over normal schemes in that generation time can be adjusted with high flexibility and it is also possible to generate almost continuously.
- In normal estuarine situations, however, two basin schemes are very expensive to construct due to the cost of the extra length of barrage.

If there is some favourable geography, where extra barrage is not needed which are well suited to this type of scheme, could be favourable.

2.8.6 Tidal lagoon power

Tidal lagoon is one kind of tidal barrage which can be constructed at any estuary to generate electricity from the natural rise and fall of the tides. Same techniques are adopted like a tidal barrage. In a tidal barrage, normally, three sides are bounded by natural land and other side is bounded by a barrage. But in a tidal lagoon all sides are bounded by a barrage/ barrages. Tidal lagoons are man-made structures work in a similar way like a tidal barrage by capturing a large volume of water and then release to drive turbines that generate electricity. Figure 2.11 shows a schematic plan view of a tidal lagoon power plant.

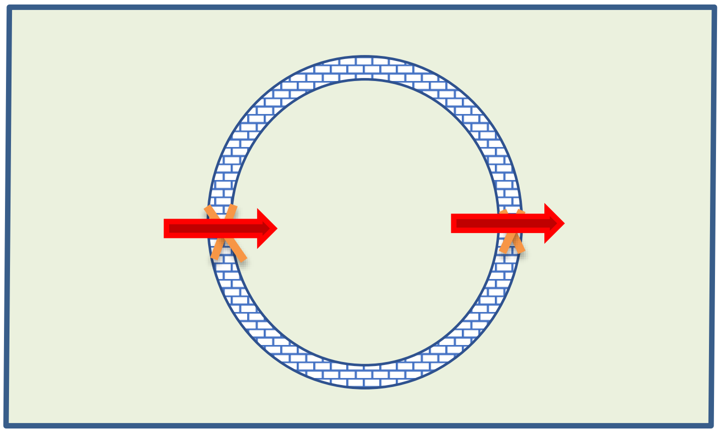

Figure 2. 11: Schematic plan view of a tidal lagoon power plant.

2.9 Dynamic Tidal Power (DTP)

2.9.1 New concept of tidal power

Dynamic tidal power (DTP) is a new concept of tidal power generation where large dam like structure is installed to create water head. Though this method is not tested yet for tidal power generation but it could contribute much towards renewable energy. A large dam is constructed extending from the coast straight to the ocean, with a perpendicular barrier at the far end, forming a large 'T' shape. Normally, a DTP is considered with a long dam of 30 to 60 km which is built perpendicular to the coast, running straight out into the ocean, without enclosing an area. Figure 2.12 shows a schematic plan view of a dynamic tidal power.

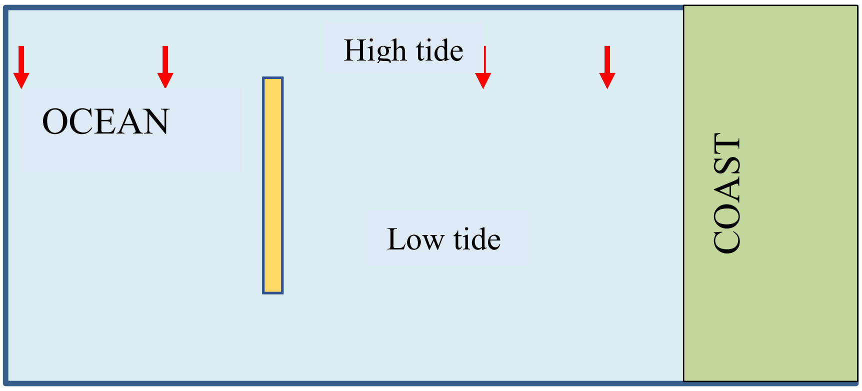

Figure 2.12: A schematic plan view of a dynamic tidal power plant.

This concept is developed to use both potential energy and kinetic energy of tides. Due to restriction of movement of flowing water due to dam, water on one side of the dam is at a higher level than the other side. This water difference drives a series of turbines installed within the dam and generates electricity.

2.9.2 Benefit of a DTP

Major benefit of a DTP is that a single dam can accommodate over 8 GW (8000 MW) of installed capacity, with a capacity factor of about 30%, for an estimated annual power production of each dam of about 23 billion kWh (Shaikh & Shaiyek, 2011). Dynamic tidal power doesn't require a very high natural tidal range, so more sites are available and the total availability of power is very high in countries with suitable conditions, such as Korea, China, and the UK (the total amount of available power in China is estimated at 80-150 GW) (Shaikh & Shaiyek, 2011).

2.9.3 Challenges of a DTP

A major challenge is that the power generation capacity from a DTP increases as the square of the dam length (both head and volume increase in a more or less linear manner for increased dam length). Economic viability of a DTP is estimated to be reached for dam lengths of about 30 km. That's why it is not probably practised yet. Other challenges are shipping routes, marine ecology, sediments, and storm surges.

2.10 Procedure for Tidal Barrage Power Generation

Basic principle of tidal barrage power plant is that a barrage is constructed in such a way that a basin is separated from the sea and a difference in the water levels is obtained between the basin and sea due to tidal fluctuations. A tidal barrage power plant consists of three main parts, namely: (i) the barrage itself, (2) the sluice gate, and (iii) the turbine and generator. The constructed basin is filled during high tide and emptied during low tide passing through sluices and turbine respectively and generate. Both flood-ebb generation or only flood generation or only ebb generation is possible-each has different operation principles those discussed in Chapter 3.

From equations (2.4) and (2.6) it is reveals that the power varies with respect to (i) difference in water levels across the barrage and (ii) the mass of water allowed to flow through the turbines.

2.11 Tidal Barrage Power Assessment

Potential energy contained in a basin between high tide and low tide can be expressed as:

From equation (2.3) we get, $E_p = \frac{1}{2}\rho g A_b h^2$

where;

E_p = potential energy in Jules;

ρ= density of water in kg/m^3;

g = acceleration due to gravity in m/s^2;

A_b = area of the basin in m^2; and

h =water head difference in m.

Every day there are two high tides and two low tides. So, theoretically generation will be 2 times in a day.

So, potential energy per day is:

$$E_P \text{ per day} = \rho g A_b h^2 \text{ Jule/day} \tag{2.7}$$

Power, P (average)= $\frac{1}{86400}\rho g A_b h^2$Jule/sec

$$\overline{P} = \frac{1}{84600}\,\rho g A_b h^2 \text{ watt}$$

Theoretical, $\overline{P} = \frac{1}{86400}\rho g A_b h^2 \text{ X } 10^{-6}$ MW

$$P = \frac{1}{86400}\rho g A_b h^2 \text{ X } 10^{-6} \text{ MW} \tag{2.8}$$

For power generation, there should be some minimum head for turbine starting (Lewis, et al., 2017). So, all the times it is not possible to produce energy.

In the assessment of tidal power, the basic equation relates the mass of water and water head difference with the theoretical potential energy while the energy available from a barrage depends on water surface area impounded by the barrage and the corresponding tidal range (Shevkar & Otari, 2015); (McErlean, 2007). However, a minimum water 3head difference between the sea and the basin is required for tidal power generation (Lamb, 1994). In the current practice for assessing the tidal power potential for a plant, primarily the duration of power generation and hydraulic efficiency are considered. Assuming power conversion of system is 30% of potential energy (Tester, et al., 2012); (Rashid, et al., 2012). Hence, energy:

$$E_{\text{extractable}} = 30\% \text{ of } E_{p.} \tag{2.9}$$

Using above equations (2.8) and (2.9) power and energy are calculated.

In large portion of the world tidal ranges are very low (say, 1 meter) and therefore not suitable for electric power generation. However, at some places having various coastal complexities give good tidal patterns owing to resonant effects of local geography. The tidal range noted 18 to 21 m near the Magellan Strait and the shores of America respectively. In Sandwip channel tidal range varies from 4 to 7 m. Tidal power may be generated in various ways; such as tidal stream power using water velocity, tidal barrage power using potential head differences, wave power using tidal waves, ebb power during low tide, flood power during high tide, pump generation by increasing head by pumping water etc.

2.12 Different Theories of Tidal Power Generation

Different authors suggested different formulas to assess tidal power. These are mentioned below:

Lamp (1994) used mean tidal range to assess the potential energy contained in the water volume impounded in a basin which can be expressed as:

$$E_P=0.5\rho g A_b \Delta h_b^2 \qquad (2.10)$$

where,

E_P=potential energy over a tide cycle (GJ);

ρ= density of sea water (1.027 t/m^3);

g= acceleration due to gravity (9.807 m/s^2);

A_b= horizontal area of the enclosed basin (km^2); and

Δh_b=mean tidal range in the basin (m).

In a coastal area having two flood tides and two ebb tides, with a semi-diurnal period of 12.42 hours. Potential energy per day from the barrage approximates to:

$$E = \frac{24}{12.42} E_P \qquad (2.11)$$

Therefore, $\bar{P}=\frac{24}{12.42} E_P/86400 = 0.11263\ A_b.\Delta h_b^2$ MW

where,

A_b is in km^2 and Δh_b is in m (2.12)

According to **Tester, et al., (2012)** tidal energy projects are characterized by low values of power conversion efficiency of η, usually ranging from 20-40% with an average of 33% often being used. They proposed the following formula for annual energy calculation:

$$E_{yr}=0.987\ A_b.\Delta h_b^2\ \eta \qquad (2.13)$$

where,

E_{yr} = Annual energy (GWh);

A_b= area of the basin (Km^2);

Δh_b=mean tidal range in the basin (m); and

η = efficiency of the system.

Prandle (1984) used tidal amplitude to estimate the maximum potential energy over the course of a tidal period which is expressed as:

$$E_{p\,(max)} = 4\rho g A_b h_a^2 \qquad (2.14)$$

where,

$E_{p\,(max)}$ = maximum potential energy at a tidal period;

h_a =tidal amplitude;

A_b= impounded basin water surface area in m^2;

g = gravitational acceleration (=9.807 m/s^2); and

ρ = density of water (=1025kg/m^3).

(Prandle, 1984) also suggested an initial estimate of the actual extractable energy per tidal cycle both for ebb generation and two ways generation which are as follows:

For ebb generation, $E_{extractable}$= 0.27 $E_{P\,(max)}$ (2.15)

For two-ways generation, $E_{extractable}$= 0.37 $E_{P\,(max)}$ (2.16)

Rashid, *at al*., (2012) used tidal range instead of tidal head and suggested for conversion efficiency 60% to assess power potential. According to him energy content of the water in a basin at high tide is:

E_{max} = ½ × area × density × gravitational acceleration × tidal range squared. (2.17)

There are 2 high tides and 2 low tides every day. Therefore, the total energy potential per day equals to 4 times of energy for a single tide. He cited an example that suppose the tidal range of tide at a particular place is 39 feet = 12 m (approx.), the surface of the tidal energy harnessing plant is 9 km² (9 ×10^6 m^2) and density of sea water = 1025.18 kg/m^3. So, potential energy content of the water in the basin at high tide = ½ × area × density × gravitational acceleration × tidal range squared = ½ × 9 × 10^6 m^2 × 1025 kg/m^3 × 9.81 m/s^2 × (12 m)^2 =6.5 × 10^{12} J (approx.). If we consider 2 high tides and 2 low tides every day, the total energy potential per day will be 4 times of energy for a single tide. = 6.5 × 10^{12} J × 4 = 2.6× 10^{13} J. Therefore, the mean power generation potential = Energy generation potential / time in 1 day = 2.6 × 10^{13} J / 86400 s = 301.6 MW. As they used 60% conversion factor to calculate power, so average power P will be 301.6 MW * 60% = 180.9 MW (approx.)

According to (Shaikh & Shaiyek, 2011) the potential energy is mainly dependent on the tidal prism of the basin. Potential energy obtained due to the stored water can be calculated as:

$$E_p = \frac{1}{2}\rho g A_b h^2 \tag{2.18}$$

where,

h is the vertical tidal range;

A_b is the horizontal area of the barrage basin;

ρ is the density of water = 1025 kg per cubic meter (seawater varies between 1021 and 1030 kg/m^3); and

g is the acceleration due to the Earth's gravity = 9.81 m/s^2.

Xia, *at al.,* (2012) used the mean tidal range for tidal power assessment. According to Xia (2012) coastal regions having two flood and two ebb tides, with a semi-diurnal period of 12.42 hours potential energy per day from a barrage approximates to (Xia, et al., 2012):

$$E_P \text{ (per day)} = \frac{24}{12.42} E_P \tag{2.19}$$

$$\overline{P} = \frac{24}{12.42} E_P/86400 \tag{2.20}$$

where,

E_P (per day) = the energy per day (GJ/day); and

E_P = the energy per tidal cycle (GJ/tidal cycle).

$\overline{P}$ = average power (GJ/s); and

E_P = the energy per tidal cycle (GJ/tidal cycle).

Putting the values of other components of equation (2.18) and (2.20) average power is:

$$\overline{P} = 0.11263\ (A_b.\Delta h_b^2) \tag{2.21}$$

where,

$\overline{P}$ = average power (MW);

A_b= horizontal area of the enclosed basin (km^2); and

Δh_b=mean tidal range in the basin (m).

(Neil, et al., 2018) suggested theoretical and zero dimensional (0D) models with more detailed depth-averaged (2D) equations and hydro-environmental tools for the assessment of tidal power that often require high performing computing capabilities for practical applications. According to (Neil, et al., 2018) for a given the downstream $\eta_{dn,i}$ and upstream $\eta_{up,i}$ water level at any point in time t (indicated by subscript i), the upstream water level at t+αδt (subscript i+1) can be calculated as (Angeloudis, et al., 2018), (Baker and Leach, 2006):

$$\eta_{up,i+1} = \eta_{up,i} + \frac{Q\ (Hi) + Qin,i}{A\ (\eta up,i)} \Delta t \qquad (2.22)$$

where,

Q= the flow volume (m^3/s) through a hydraulic structure can be expressed as:

$$Q = C_D A_s \sqrt{2gh}) \qquad (2.23)$$

C_D = a discharge coefficient;

A_s = the cross-sectional flow area (m^2); and

g = the acceleration due to gravity (m/s^2).

$A\ (\eta up, i)$ = the wetted surface area of the lagoon, assuming a constant water level surface of η_{up}.

Q_{in} corresponds to the sum of inflows/outflows through sources other than the impoundment, e.g. rivers or outflows, h is the water head difference,

$$h = \eta_{up,i} - \eta_{dn,i} \qquad (2.24)$$

The power P produced from a tidal range turbine for a given h can be:

$$P = n\rho g Q_T h \qquad (2.25)$$

where,

P =the power output;

ρ = the fluid density;

Q_T = the turbine flow rate;

n = an overall efficiency factor associated with the turbines; and

h = the water head difference.

Even though a 0D modelling approach is computationally efficient, but limitations of this method are that between the two-time intervals, wetted water level is assumed constant and water levels of two sides are to be measured. This method also neglected the basin configuration/geometry as water surface may vary with respect to water level. Such an assumption can yield over-optimistic results, as reported in Angeloudis *et al.*,

(2016) and Yates *et al.,* (2016). Consequently, the analysis should be expanded to account for the regional hydrodynamic impacts through refined coastal modelling tools tailored to the operation of tidal lagoons.

In 1-D modelling: Neil *et al.* (2018) used Saint-Venant equations, to investigate the interaction of tidal range projects with the regional hydrodynamics:

$$\frac{\partial A}{\partial t} + \frac{\partial (Au)}{\partial x} = 0 \qquad (2.26)$$

and

$$\frac{\partial u}{\partial t} + u\frac{\partial u}{\partial x} + g\frac{\partial \eta}{\partial x} = -\frac{\tau b}{\rho Hd} \qquad (2.27)$$

where,

A = the flow area and is a function of the water elevation, η

η =elevation of water at sea

u = the (scalar) depth-averaged horizontal velocity;

H_d= η + h, the total water depth;

h = the mean water depth; and

τ_b represents bed shear stress effects through a Manning n formulation.

Alam et al., (2012**)** developed a method to calculate the required number of turbines based on the impounded water volume and the water flow passing through the turbines. The number of turbines (N_T) is needed to discharge the large volume of water would be given by the equation (2.28) and power can be calculated using equation (2.29).

where,

$$N_T = (A_b.\ h)/\ (q.t) \qquad (2.28)$$

and

$$P=\eta \rho ghqN_T \qquad (2.29)$$

where,

N_T= no. of turbines.

A_b= area of reservoir basin in m^2;

h = water head in m;

q = flow rate in m^3/s per turbine; and

t = turbine running time in sec.

η = turbine efficiency;

ρ = density of water, kg/m^3;

g = acceleration due to gravity, m/s^2;

According to (Pugh, 1987) the potential energy contained in a basin of surface area A_b, filled at high tide and discharging at low tide into the sea:

Consider a basin of surface of area A, m^2 at the maximum basin level. Let R be the range of the tide and V the volume of water stored from the low level to high tide level. The volume of water contained in an elemental strip of thickness dz; at surface area of A_{bz}, at a depth z above the low tide in the basin, $dV = A_{bz}.dz$

Ocean with single basin tidal project assume that the basin energy assessment through single basin system is empty with its water level, z = 0 and the ocean is at high tide level, z = R. By instantaneously filling the basin, the energy potential available is:
$E= \int \rho. dV. g. z$.

$$\text{So, } E= A\int_0^{2a} \rho gzdz \tag{2.30}$$

where a is the tidal amplitude, ρ is the density of water and g is the gravitational acceleration, which gives:

$$E=A.\rho g\frac{(2a)2}{2}=2A\rho ga^2 \tag{2.31}$$

This process could be repeated by filling the basin again from the low-water level, at the time of high water in the open sea. So, the total energy theoretically available in each tidal cycle is:

$$E=4A\rho ga^2 \tag{2.32}$$

and the mean power generation, P is

$$E=4A\rho ga^2/\text{ (tidal period)} \tag{2.33}$$

A team of Strathclyde University developed a simplified, hypothetical theoretical model to calc ulate water level variation in the basin and power using time stepping method considering continuous bi-directional water flow through the turbines and hence continuous power generation (University of Strathclyde, 2015). They used a single tidal constituent as tide data and a linearly variable curve to represent area-elevation relation of the basin. They developed a theoretical model to see how water level and power vary if turbines are kept open continuously (both inflow and outflow through the turbines) without any control mechanism i.e. no gates and no minimum head requirement for turbine operation to protect. The team did not consider minimum head for turbine operation in-order-to avoid cavitation. Again, the team considered continuous generation irrespective of water heads and did not consider provision of gates. They did not also consider ebb generation or flood generation or two-way generation with minimum head requirement. The simplified tidal barrage system considered continuous, bidirectional flow through turbines. The barrage of Isle is 310 m long and 4 (four) turbines each 1.7 m diameter were housed within 20 m of the barrage length and 10 m ship gate was installed for navigational purpose.

The team calculated theoretical continuous power irrespective of water head which is not realistic in practical cases and also developed a theoretical case of "Tidal Barrage Calculation Spread Sheet" (**shown in Appendix A.1**) to calculate power generation.

2.13 Real-time Assessment of Tidal Barrage Power

In a tidal barrage, tidal water level on the sea side is a superimposition of a number of periodically-varying tidal constituents, while the water level in the basin depends on the geometric configuration of the basin and operational control of the turbines. So, water head difference (h) between the two sides of a barrage will vary every moment. So, every moment power will vary as the head varies every moment. So, real-time power assessment and optimization of the plant are very important to harness maximum energy from a particular barrage and to avoid over capacity which may not be cost effective.

2.14 Basin Configuration and Power Generation

The relative distances and positions of the sun, moon and earth all affect the size and magnitude of the earth's two tidal bulges. The magnitude of tides can be strongly influenced by the shape of the shoreline. When oceanic tidal bulges hit wide continental margins, the height of the tides can be magnified. Conversely, mid-oceanic islands not near continental margins typically experience very small tides of 1 meter or less (Thurman, 1994). The moon is a major influence on the earth's tides, but the sun also generates considerable tidal forces.

Solar tides are about half as large as lunar tides and are expressed as a variation of lunar tidal patterns, not as a separate set of tides (Taylor, 2014) . When the sun, moon, and earth are in alignment (at the time of the new or full moon), the solar tide has an additive effect on the lunar tide, creating extra-high high tides, and very low, low tides-both commonly called spring tides. One week later, when the sun and moon are at right angles to each other, the solar tide partially cancels out the lunar tide and produces moderate tides known as neap tides. During each lunar month, two sets of spring tides and two sets of neap tides occur (Sumich, 1996). The shape of bays and estuaries also can magnify the intensity of tides. Funnel-shaped bays in particular can dramatically alter tidal magnitude. The Bay of Fundy in Nova Scotia is the classic example of this effect, and has the highest tides in the world-over 15 meters (Thurman, 1994). Narrow inlets and shallow water also tend to dissipate incoming tides. Inland bays such as Laguna Madre, Texas, and Pamlico Sound, North Carolina, have areas classified as non-tidal even though they have ocean inlets. In estuaries with strong tidal rivers, such as the Delaware River and Columbia River, powerful seasonal river flows in the spring can severely alter or mask the incoming tide.

Local wind and weather patterns also can affect tides. Strong offshore winds can move water away from coastlines, exaggerating low tide exposures. Onshore winds may act to pile up water onto the shoreline, virtually eliminating low tide exposures. High - pressure systems can depress sea levels, leading to clear sunny days with exceptionally low tides. Conversely, low-pressure systems that contribute to cloudy, rainy conditions typically are associated with tides than are much higher than predicted.

From the equation (2.3), E= $\frac{1}{2}\eta\rho g A_b h^2$, it reveals that energy generation from a tidal barrage depends on the amount of tidal prism (equals to Ah) contained between the water levels at high-tide and low-tide and the distance of the centre of the gravity (h/2) of a tidal prism from the low level of the tidal prism. So, optimum basin will be that on which will yield maximum value of Ah^2. Energy varies due to shape of the basin. For the same tidal range, due shape of the basin, example: rectangular basin or trapezoidal basin or parabolic basin or even circular basin energy varies due to variation of volume of tidal prism and its centre of gravity. Besides, water level in the basin is not exactly horizontal, it is unsteady and depends on the aspect ratio which is omitted most of the cases.

2.15 Summary

Considering global carbon emission reduction commitments, all nations are trying to explore different options to harness renewable energy including tidal energy. Now-a-days, tidal energy is considered as a permanent source of renewable energy, because it is predictable, pollution free, green, inexhaustible and reliable. But tidal energy depends on tidal range (for barrage power) and/or water velocity (for stream power) of tides which again depend on centrifugal forces among sun, moon and earth. Unfortunately, all sites do not qualify above minimum criteria to produce tidal power. The shape of channel can magnify the intensity of tides. Funnel-shaped channels in particular can dramatically alter tidal magnitude. So, some sites are feasible and some sites are not feasible for tidal power.

To assess tidal power, especially for tidal barrage power, several authors used different formulas in assessing tidal energy potential and capacity of the plant. In most cases (as discussed in Section 2.10) potential extractable energy and power is assessed based on tidal range or amplitude and some assumptions (say, η = 30%) which are static in nature. For a tidal barrage, tides are changing continuously with respect to time. Therefore, the head (h) is not static; rather it is dynamic that indicates that there is a gap in assessing capacity of the tidal power plant in designing hydraulic structures and turbines. Capacity of the plant and energy are time series values over the period.

To be more specific, it is mentionable that several authors used different equations/formulas to assess tidal power. Prandle (1984) used tidal amplitude instead of tidal range to assess the tidal power. According to him the actual extractable energy per tidal cycle is 0.27 E_{max} (for ebb only) and 0.37 E_{max} (for two-ways generation). Lamb (1994) used mean tidal range instead of maximum tidal range whereas Rashid *et al.* (2012) used tidal range and 60% conversion factor to calculate power. Tester, et al.(2012) used an average power conversion efficiency of 33% (Tester, et al., 2012) and Xia *at al*. (2012) used the mean tidal range for tidal power assessment (Xia, et al., 2012). Neil *et al.* (2018) suggested theoretical and zero dimensional (0D) models with more detailed depth-averaged (2D) equations and hydro-environmental tools for the assessment of tidal power (Neil, et al., 2018). Alam *et al.* (2015) developed a method to calculate the required number of turbines based on the impounded water volume and the water flow passing through the turbines (Alam, et al., 2012).

All previous methods for the assessment of tidal power are based on fixed assumed variables such as duration of power generation, and ignore the actual real-time variability in these variables. Assessment of power potential based on real-time water head differences, long-term tidal data and basin configuration will yield a more accurate estimation of power generation.

The previous approaches and practices for the assessment of tidal barrage power generation do not consider the continuous changes of head differences between the sea and basin. Rather a static overall estimate using an arbitrary reduction in efficiency and head difference is used. A tool is needed to consider the real-time changes in water levels inside and outside the basin to compute the actual power potential based on dynamic water head to represent the water level variations and basin configuration both shape and aspect ratios.

The study considers the real-time changes in water levels inside and outside the basin to compute the actual power potential based on dynamic water head, and develop a new analytical model to represent the water level variations with multi-tidal constituents and arbitrary basin configuration.

CHAPTER 3
ANALYTICAL MODEL DEVELOPMENT

3.1 Introduction

In a tidal barrage, tidal water level on the sea side is a superimposition of a number of periodically-varying tidal constituents, while the water level in the basin depends on the operational control of the turbines and the geometric configuration of the basin. All previous approaches for the assessment of tidal power are based on some fixed assumed variables such as mean tidal range, duration and ignore the actual real-time variability of these variables. Assessment of power generation potential considering real-time water head differences based on long-term tidal data and also considering basin configuration might yield a more accurate estimation of power generation.

The purpose of this chapter is to develop an analytical model for better estimation of tidal power generation by establishing a real-time functional relation (i) between water level and basin volume, which in turn will relate to turbine discharge and change of water levels in the basin, and (ii) among the tidal constituents having different phases and amplitudes in the sea side, expressed as a superimposed function with respect to time. This approach will require formulation of an analytical model employing equations to compute the dynamic water head, power and energy considering water level variations in a tidal barrage. An analytical model based on a set of equations that describe this real-time variability will be instrumental in designing tidal barrage power plants.

The rest of this chapter describes conceptual basis for power generation assessment in Section 3.2, base case: Isle of Whithorn tidal barrage in Section 3.3, real-time analytical model in Section 3.4, flood-ebb generation without gates in Section 3.4.4, flood-ebb generation with gates in Section 3.4.5, ebb generation with gates in Section 3.4.6, flood generation with gates in Section 3.4.7, comparison between base case and the RTA model in Section 3.5, comparison of results from RTA model for different modes of operation in Section 3.6 and summary in Section 3.7.

3.2 Conceptual Basis for Power Generation Assessment

In assessment of tidal power generation, the basic equation relates the mass of water and water head difference with the theoretical potential energy while the energy available from a barrage depends on water surface impounded by the barrage and the corresponding mean tidal range. In the current practice for assessing the tidal power potential for a plant, primarily the duration of power generation, basin area, tidal range and hydraulic efficiency are considered. Several methods and numerical approaches have been developed to assess tidal power and energy. In most of the cases power generation duration is assumed to be one-third time of the day and the efficiency of the system is assumed to be 90%. Based on these, in most cases the design extractable power is considered 30% of potential energy.

All previous approaches for the assessment of tidal power ignored the real-time variability of water levels at two sides of the barrage. An analytical model based on a set of equations that describe this real-time variability of water levels is developed which will help in designing tidal barrage power plants that will yield a more accurate estimation of power generation.

A schematic plan view of a tidal barrage power is shown in Figure 3.1. Turbines are placed below the turbine housing along the barrage. Ship gates are used to pass the ships from sea to the basin and from basin to sea. A vertical cross section along the barrage is shown in Figure 3.2.

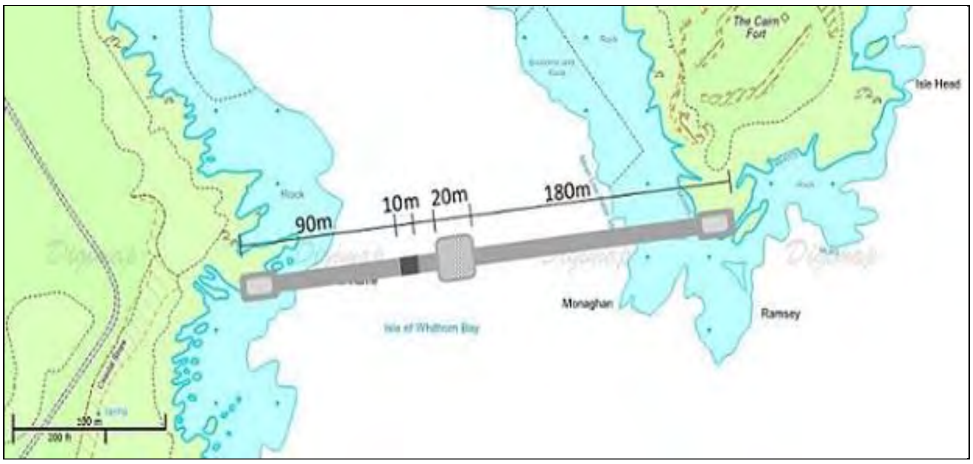

Figure 3.1: Schematic plan view of a tidal barrage.
Source: (University of Strathclyde, 2015).

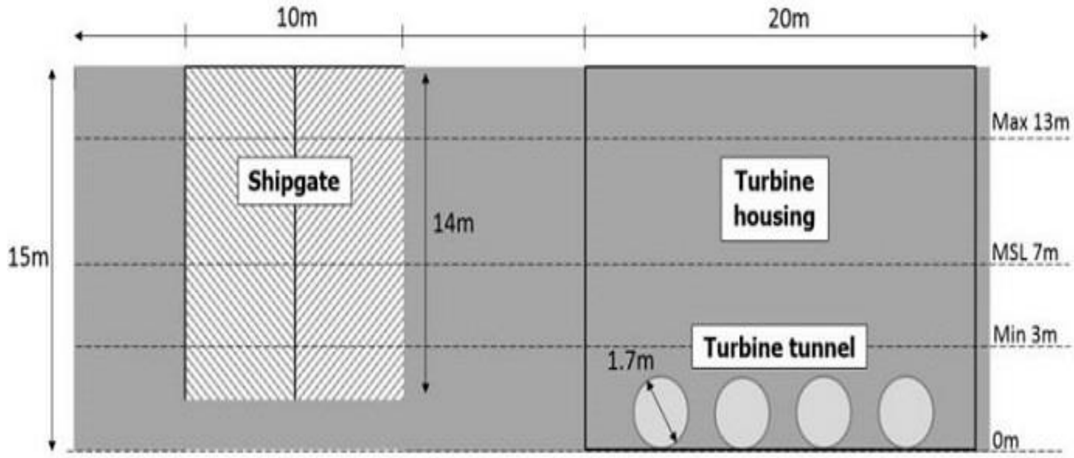

Figure 3. 2: A vertical cross section along Isle of Whithorn barrage.
Source: (University of Strathclyde, 2015).

3.3 Base Case: Isle of Whithorn Tidal Barrage

The "Isle of Whithorn Case" is a simplified, theoretical andhypothetical case fits for continuous flow during both ebb tide and flood tide through turbines is taken as a base (henceforth referred as base case) for this study purpose. In the base case, provision of gates is not considered. So, the base case does not suit for (i) flood-ebb generation with gates; (ii) flood generation only; (iii) ebb generation only; and (iv) flood-ebb generation with gates. The base case is a very simplified, hypothetical and theoretical case.

The first requirement for any tidal power scheme is to consider a minimum gross differential head of about 1.52 m between the basin and the sea or between basins, to permit power generation (Simeons, 2019). The base case did not consider this minimum head requirement in-order-to avoid cavitation for turbine operation.

In the base case, a single tidal constituent and a simple relation of basin's area vs. elevation was considered. But in real cases, observed tide is a superimposition of series of tidal constituents having different tidal amplitudes, speeds and phase angles and basin water surface might be a polynomial equation of multiple orders instead a linear relation with elevation. The base case is a theoretical case of "Tidal Barrage Calculation Spread Sheet" (**shown in Appendix A.1**) is developed to compute continuous power generation irrespective of water heads, which is not realistic in

practical cases. The base case is not suitable for (i) flood generation; or (ii) ebb generation; or even (iii) flood-ebb generation with gates.
This study considered the limitations & constraints of the base case and it is addressed by modifying, improving the base case equations and inserting some new equations. A comparison is discussed in Section 3.5.

3.4 Real-Time Analytical (RTA) Model

The main aim of this study was to develop a real-time analytical model (henceforth referred to RTA model) to assess tidal barrage power generation. In order to make the RTA model more flexible and useable, it is developed in such a way so that it can cope up with any practical complex situations. RTA model is fit for any mode of operation, multiple tidal constituents and complex basin configurations. The RTA model is suitable for ebb generation, flood generation and two-ways generation with or without provision of gates and any inflows through rivers, rainfall, precipitations or by pumping to the basin or outflows by pumping or spill out from the basin with the provision of minimum heads for turbine opening and closing.

RTA model considered real-time power generation that changes at different temporal scales-changes every day, every spring & neap period and every lunar & solar month and every year. The RTA model is developed to cope up with these situations and to assess real time power generation with different temporal scales which depends on tidal characteristics, basin configuration and operational control.

The RTA model is developed to assess real-time power generation considering dynamic water head of a tidal barrage and for this purpose; an analytical model is developed to compute real-time power generation considering variable water levels at the sea and the basin.

This analytical model is developed for different mode of barrage operations, namely: (i) flood-ebb generation without gates (considering minimum head requirement); (ii) flood-ebb generation with gates; (iii) ebb generation and (iv) flood generation are considered.

3.4.1 Develop a relation between water surface area and water level of the basin

The relation of water surface area and elevation can be expressed as Equation (3.1):

$$A_b = a_n Z^n + a_{n-1} Z^{n-1} + a_{n-2} Z^{n-2} + a_{n-3} Z^{n-3} + \cdots + a_1 Z^1 + a_0 \; = f(Z) \qquad \mathbf{(3.1)}$$

where,

A_b= water surface area (m^2) of the basin at level Z;

Z = water level of the basin (m) at any time, t; and

n= polynomial order.

$a_n, a_{n-1}\ a_{n-2}$ …. etc. are the coefficients.

3.4.2 Form an equation to represent water level of tides

Tide at sea is a superimposition of multiple tidal constituents which can be expressed as Equation (3.2):

$$Y(t) = a_0 + \sum_{i=1}^{n} a_i \cos\left(\frac{2\pi t}{T} - \emptyset_i\right) \qquad (3.2)$$

where,

Y(t) = water level at sea due to tidal effect;

a_0 =mean level above chart datum;

n= number of tidal constituents;

a_i= amplitude of i^{th} tidal constituent;

T_i= tidal period of i^{th} tidal constituents; and

$\emptyset_i$= is the phase angle of i^{th} tidal constituent.

3.4.3 Some assumptions for the RTA model

For the basin, flood tide is considered when water level at the sea is higher than the water level at the basin and ebb tide is considered when water level at the sea is lower than the water level at the basin at any time,t_i i.e. flood tide when Y(t_i)>Z(t_i)) and ebb tide when Y(t_i) <Z(t_i) at any time t_i. For analytical expression the water head difference (h) between sea and basin considered positive irrespective of the sign. So, absolute value of h is taken omitting the plus (+) and minus (-) sign, hence h:

Head, h_i = absolute [Y(t_i) -Z(t_i)] (3.3)

Basin flood tide (B= +1) when Y(t_i)>Z(t_i) (3.4)

Basin ebb tide (B= -1) when Y(t_i) < Z (t_i) (3.5)

On the other hand, **for the sea**, flood tide is considered when sea water level Y(t_{i+1}) at $t_{i+1}$is higher than the sea water level Y(t_i) at t_i and ebb tide is considered when sea water level Y(t_{i+1}) at $t_{i+1}$is lower than the sea water level Y(t_i) at t_i

Head, h_{i+1} = absolute [Y(t_{i+1}) -Z(t_{i+1})] (3.6)

Sea flood tide (S= +1) when Y(t_{i+1})>Y(t_i) (3.7)

Sea ebb tide (S= -1) when Y(t_{i+1})<Y(t_i) (3.8)

3.4.4 RTA model for flood-ebb generation without gates

Description of RTA model for flood-ebb generation without gate is mentioned below:

3.4.4.1 Guiding principles for continuous generation without gate

Guiding principle for flood-ebb generation without gate is described below:

(1) At the outset water level of the both sides of the barrage are kept at the same level keeping turbines are open. At t=0 water level of both sides is equal, at this stage, turbines are closed and head difference (h) is equal to zero (0).

(2) For flood-ebb generation without gates, turbines are opened (θ_T=1) when water head is =>h_S (minimum head for turbine starting: say, 2.0 m) and continues until h> h_C (head for closing turbine operation: say, 1.8m). When h=<h_C, turbine is closed (θ_T=0).

(3) Operation rules are expressed in graphical representation in Figure 3.3.

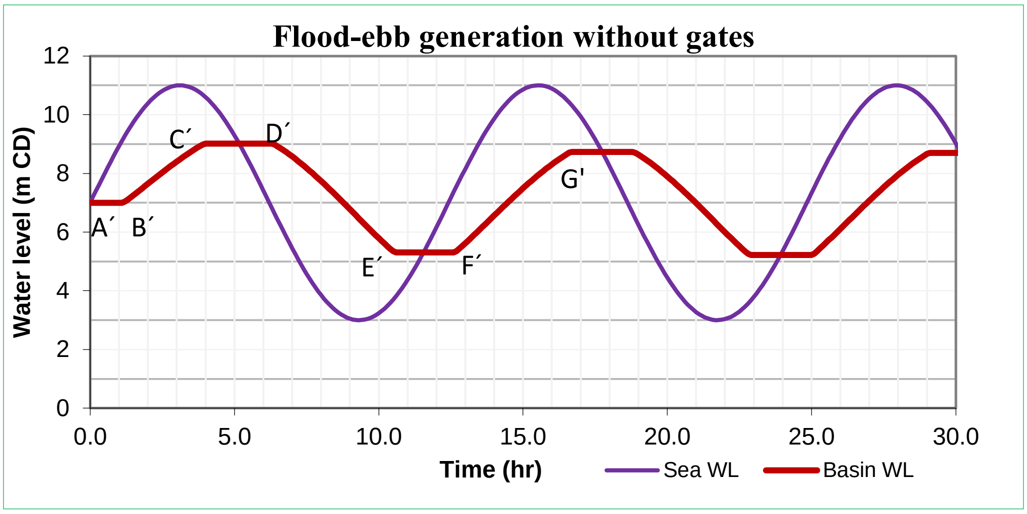

Figure 3. 3: Operational rules for flood-ebb generation without gates.

3.4.4.2 Development of RTA model to assess power for flood-ebb generation without gates

The technique for development of RTA model to assess power for flood-ebb generation without gates is described below:

(a) Estimate dynamic head

Let us think water level at sea is Y(t_i) and water level at the basin is Z(t_i) at any time t_i.

Water head (h) at any time (t_1) between basin and sea will be equal to:

$$h = \text{Absolute } [Y(t_i)-Z(t_i)] \tag{3.9}$$

where,

Y(t_i) = water level at the sea at any time t_i; and

and Z(t_i) = water level at the basin at any time t_i.

(b) Procedure to develop RTA model for flood-ebb generation without gates

During flood tide or ebb tide at the basin, if head, h =>h_S (2.0 m) turbine will open for power generation. Power generation will be stopped when water head becomes to h=<h_C (1.8 m). The detailed procedure is elaborated in Table 3.1.

Table 3.1: Turbine operation criteria for flood-ebb generation without gates.

Point (at Figure 3.3)	Sea (S) water level (Y), Flood tide (1), Ebb tide (-1)	Basin (B) water level (Z), Flood tide (1), Ebb tide (-1)	Head, (h=Y-Z), m	Turbine (Tur): Open=1, Close=0
A	1	1	0	0
B′	1	1	=> h_S (2.0)	1
	1	1	>h_C (1.8)	1
	-1	1	>h_C (1.8)	1
C′	-1	1	=h_C (1.8)	0
	-1	-1	<h_C (1.8)	0
D′	-1	-1	>=h_S (2.0)	1
	-1	-1	>h_C (1.8))	1
	1	-1	>h_C (1.8))	1
E′	1	-1	<=h_C (1.8))	0
	1	-1	<h_C (1.8)	0
	1	1	<h_C (1.8)	0
F′	1	1	>=h_S (2.0)	1
	1	1	>h_C (1.8))	1
	-1	1	>h_C (1.8))	1
G′	-1	1	<=h_C (1.8))	0

(c) Operation rules of turbines for flood-ebb generation without gates

In flood-ebb system without gates, operational procedure of turbines will be different from other systems, no gates are considered. During flood tide or ebb tide at the basin, if head =>h_S (2.0 m) turbine will be opened for power generation and it will be stopped when water head (h) becomes to =<h_C $(1.8\ m)$.

(d) **Velocity of water through turbines**

Velocity of water through turbine will be equals to:

$$V_T = \theta_T\ C_{DT}\ \sqrt{2gh} \tag{3.10}$$

where,

V_T= water velocity through turbine;

θ_T= 0 (zero) when turbine is closed;

θ_T=1 (one) when turbine is opened;

C_{DT} =coefficient of discharge through turbine;

g = acceleration due to gravity; and

h= water head.

(e) Velocity of water through gates

For flood-ebb generation without gates, the technique applied is that gate is considered always closed i.e. θ_G= 0 (zero) is taken.

Velocity of water through gate will be equals to:

$$V_G = \theta_G \, C_{DG} \sqrt{2gh} \quad (3.11)$$

where,

V_G= water velocity through gates;

θ_G= 0 (zero) i.e. gate is closed;

C_{DG} = coefficient of discharge through turbine;

g = acceleration due to gravity; and

h= water head.

(f) Discharge passed through turbine

Discharge trough turbine, $Q_{T=}N_T V_T A_T$ (3.12)

where,

$Q_{T=}$= discharge passed through turbines;

N_T = number of turbines;

V_T = velocity of water through turbines;

A_T= area of a turbine = $\frac{\pi D^2}{4}$; and

D= diameter of turbine.

(g) Discharge passed through gates

For flood-ebb generation without gate the number of turbines is taken as zero (0).

Discharge trough gates, $Q_G = N_G V_G A_G$ (3.13)

where,

$Q_{G=}$= discharge passed through gates;

N_G = number of gates=0

V_G = velocity of water through gates;

A_G= area of a gate = $B_G * H_G$; and

B_G= width of the gate opening; and

H_G= height of the gate openings.

(h) Volume of inflows/outflows

The volume of water inflow to the basin through precipitation, rainfall or river inflow or inflow by pumping or outflow by pumping or spill out from the basin can be expressed as Equation (3.14):

$$V_{i/o}=\theta_{i/o}.Q_{i/o}.\ \Delta t \tag{3.14}$$

where,

$V_{i/o}$ = volume of water inflow/outflow to the basin, m^3

$Q_{i/o}$= discharge inflow or outflow to the basin, m^3/s

Δt = duration of inflow or outflow, seconds= $(t_2 - t_1)$

$\theta_{i/o}$= ±1, for inflow (+) sign and for outflow (-) sign.

(i) **Volume of water change at the basin**

$$\Delta V_w = \frac{(Q_1+Q_2)}{2}(t_2 - t_1) \pm V_{i/o} \tag{3.15}$$

Where,

ΔV_w= Volume of water change at the basin between time period $t_1$and t_2

Q_1= Q_{T1}+Q_{G1}= discharge through turbines and gates at time t_1

Q_2= Q_{T2}+Q_{G2}= discharge through turbines and gates at time t_2

Q_T= discharge through turbine

Q_G = discharge through gates

$V_{i/o} = \theta_{i/o}.Q_{i/o}.\Delta t$= volume of water inflow/outflow to the basin

$Q_{i/o}$= discharge inflow or outflow to the basin

Δt = duration of inflow or outflow = $(t_2 - t_1)$

$\theta_{i/o}$= ±1, for inflow (+) sign and for outflow (-) sign.

(j) **Area of the basin**

The relation of water surface area and elevation is expressed as:

$$A_b = a_n Z^n + a_{n-1} Z^{n-1} + a_{n-2} Z^{n-2} + a_{n-3} Z^{n-3} + \cdots + a_1 Z^1 + a_0 = f(Z) \quad (3.16)$$

where,

A_b= water surface area (m^2) of the basin at level Z;

Z= water level of the basin (m) at any time, t; and

n= polynomial order.

$a_n, a_{n-1}\ a_{n-2}$ etc…are the coefficient.

(k) Calculations of water level at the basin

Suppose, at any time t_1 water level of the basin is Z_1 and area of the water surface of the basin is A_{b1} and at time t_2 water level of the basin is Z_2 and area of the water surface of the basin is A_{b2}. Similarly, at any time t_1 water level of the sea is Y_1 and at time t_2 water level of the basin is Y_2. Water head difference between basin and sea at time t_1 is h_1 and at time t_2 is h_2. Again, discharge at time t_1 is Q_1 and at time t_2 is Q_2.

Then

$$A_{b1} = f(Z_1) \quad (3.17)$$

$$A_{b2} = f(Z_2) \quad (3.18)$$

$$Z_2 = Z_1 \pm \partial Z_2 \quad (3.19)$$

where,

Z_1 =water level at the basin at time t_1

Z_2 =water level at the basin at time t_2

∂Z_2= change in water level at the basin between $time\ t_1$ and t_2

During flood tide at the basin, $Z_2 = Z_1 + \partial Z_2$ (3.20)

During ebb tide at the basin, $Z_2 = Z_1 - \partial Z_2$ (3.21)

∂Z_2 = change in water level at the basin between $time\ t_1$ and t_2 can be calculated using the following matrix Equations (3.22):

$$\begin{bmatrix} V_{T1} = \theta_T\ C_{DT}\sqrt{2gh_1} \\ Q_{T1} = N_T\ V_{T1}\ A_T \\ V_{G1} = \theta_G\ C_{DG}\sqrt{2gh_1} \\ \mathrm{Q_{G1}} = \mathrm{N_G V_{G1} A_G} \\ Q_1 = Q_{T1} + \mathrm{Q_{G1}} \\ V_{T2} = \theta_T\ C_{DT}\sqrt{2gh_2} \\ Q_{T2} = N_T\ V_{T2}\ A_T \\ V_{G2} = \theta_G\ C_{DG}\sqrt{2gh_2} \\ \mathrm{Q_{G2}} = \mathrm{N_G V_{G2} A_G} \\ Q_2 = Q_{T2} + \mathrm{Q_{G2}} \\ \mathrm{V}_{i/o} = \theta_{i/o}\ Q_{i/o}(t_2 - t_1) \\ \Delta V_w = \dfrac{(Q_1 + Q_2)}{2}(t_2 - t_1) \pm \mathrm{V}_{i/o} \\ \partial Z_2 = \dfrac{\Delta V_w}{(A_{b1} + A_{b2})/2} \end{bmatrix} \quad (3.22)$$

where, h_1, V_{T1}, Q_{T1}, V_{G1}, $\mathrm{Q_{G1}}$, Q_1 and A_{b1} are the water head, velocity of water through turbines, discharge through turbines, velocity of water through gates, discharge through gates, total discharge and basin water surface area respectively at time t_1 and h_2, V_{T2}, Q_{T2}, V_{G2} $\mathrm{Q_{G2}}$, Q_2 and A_{b2} are the water head, velocity of water through turbines, discharge through turbines, velocity of water through gates, discharge through gates total discharge and basin water surface area respectively at time t_2. ΔV_w= average incremental volume of water during time interval $t_2\ and\ t_1$. Other symbols are usual notations expressed above.

∂Z_2= change of water level at the basin between time period t_1 and t_2 and new water level at the basin will be Z_2= $Z_1 \pm\ \partial Z_2$.

(I) Power (kW) calculation

Electrical power, P at any time, t

$P\ (kW) = \eta \rho g Q_T h/1000$ (3.23)

where, P =electrical power, in kW;

η =efficiency of turbine=0.4;

ρ =density of water= 1.025 kg/m^3;

Q_T=discharge through turbine in m^3/s; and

h= head difference between the sea and the basin in m.

(m) Energy (kWh) calculation

Energy generation, E (kWh) between time period t_1 and t_2

$$E\ (kWh) = \frac{(P_1+P_2)/2}{(t_2-t_1).3600} \quad (3.24)$$

where, E =electrical energy, in kWh;

P_1 and P_2 are the electrical power at time t_1 and t_2 ; ; and t in hours.

3.4.4.4 Model results for flood-ebb generation without gates

The basic information taken to run the model is shown in Table 3.2**.**

Table 3. 2: Basic data taken to run the RTA model.

Sl No.	Elements	Value	Unit
1	Area of basin, A_b at HWL from equation (3.16)	…	km^2
2	Acceleration of gravity, g	9.807	m/s^2
3	Density sea water, ρ	1025	kg/m^3
4	Threshold h to start turbine, h_S	2.0	m
5	Threshold h to stop turbine, h_C	1.8	m
6	Turbine tunnel dia., D	7.6	m each
7	Turbine discharge coefficient, C_{DT}	0.9	
8	No. of turbines, N_T	1	Nos.
9	Turbine efficiency, η	0.4	
10	Width of single gate, B_G	3.5	m
11	Gate discharge coefficient, C_{DG}	0.65	
12	Number of gates, N_G	1	Nos.
13	Height of the gate opening, H_G	3	m

Above input data is changeable for the RTA model, hence the RTA model is robust and flexible.

The RTA model is run considering a simple basin characteristics of linear relation [a_0=40617.95 and a_1=15864.36 (University of Strathclyde, 2015) and other coefficients equals to zero] and by plotting the linear relation, we get Figure 3.4.

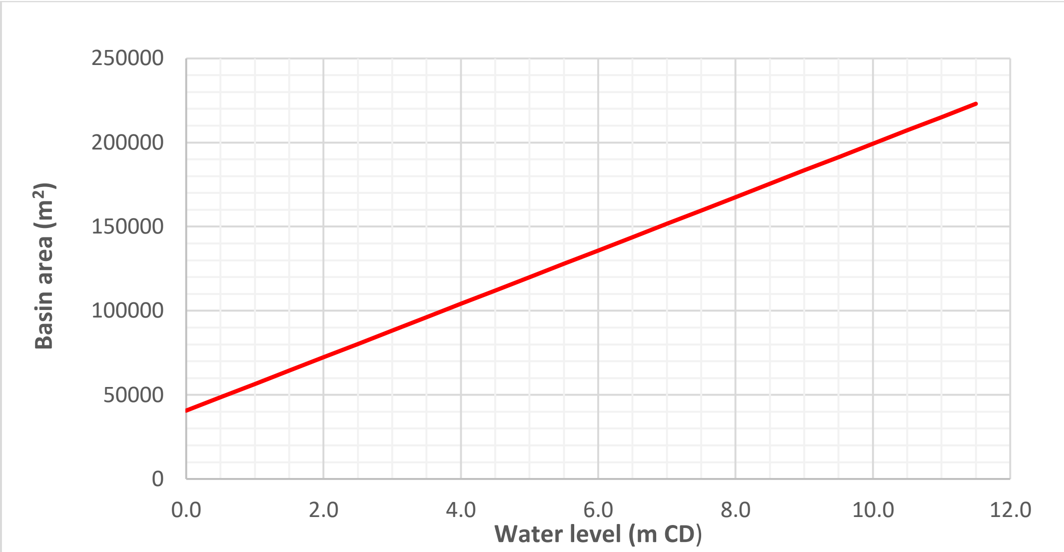

Figure 3. 4: Basin area vs. water level.

Again, taking a simple case having a single constituent with an amplitude, a= 4m; phase angle, δ=0; and tidal period (T) = 12.42 hours and datum at Z_o = 7 m, we get the sea level variation which is shown in Figure 3.5.

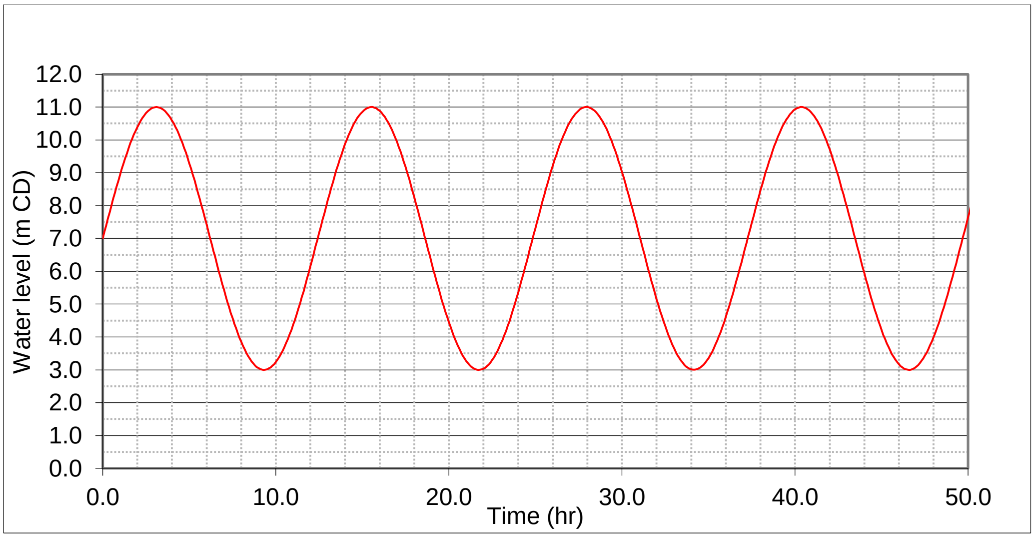

Figure 3. 5: Sea water level variation with respect to time.

Running the RTA model, we get the results which are shown in the Table 3.3.

Table 3.3: Results of RTA model for flood-ebb generation without gates.

Model results	1 Turbine having 2.6 m diameter		
	RTA Model (minimum head 2m)	Base case (no minimum head)	Difference from base case
Power, kW	666.60	654.44	(1.86% increase)
Energy, kWh/day	7404	7013	(5.60% increase)

From Table 3.3, it is observed that for a simple case (such as base case), RTA model yields roughly 5% higher energy than that of from base case. Base case calculates energy even head is close to zero, on the other hand in the RTA model, turbine is not opened until h reaches to h_S (2.0 m) and power is proportional to h^2. So the result is slightly higher.

3.4.5 RTA model for flood-ebb generation with gates

Description of RTA model for flood-ebb generation with gate is mentioned below:

3.4.5.1 Guiding principles for flood-ebb generation with gate

Guiding principle for flood-ebb generation with gate is mentioned below:

(1) At the outset, let think that at t=0, tides at the both sides of the barrage are similar in nature i.e. both are flood tides or ebb tides as per definitions adopted in the Equations from (3.3) to (3.8); water level of the both sides of the barrage are kept at the same level keeping gates are opened and turbine is closed. At t=0 water level of both sides is equal and at that stage head difference (h) is equal to zero (0).

(2) When head reaches to h=0, both turbines and gates are closed (θ_T=0, θ_G=0). Water level of the basin will remain unchanged but water level of the sea will be changing and head difference will also be changing. Turbines will be opened (θ_T=1) when water head reaches to h=>h_S (minimum head for starting turbines: say, 2.0 m) and

continues until h> h_C (head for closing turbine operation: say, 1.8m). When head becomes to h=<h_C, turbine is closed (θ_T=0) to avoid cavitation but gate is opened (θ_G=1) to pour the basin quickly and continue until h reaches to zero i.e. 0<=h=<h_C, Turbines are closed (θ_T=0) and gates are opened (θ_G=1) to pour or empty the basin quickly.

(3) Operation rules are expressed in graphical representation in the Figure 3.6.

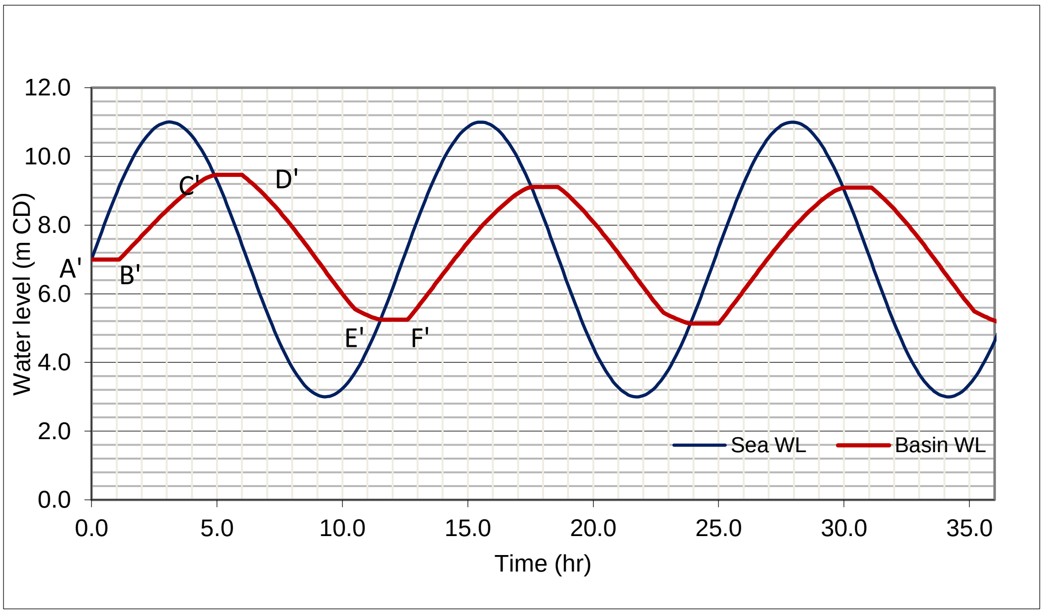

Figure 3. 6: Operational rules for flood-ebb generation with gates.

3.4.5.2 Development of RTA model to assess power for flood-ebb generation with gates

The technique for development of RTA model to assess power for flood-ebb generation with gates is described below:

(a) Estimate dynamic head

Let us think water level at sea is Y(t_i) and water level at the basin is Z(t_i) at any time t_i.

Water head (h) at any time (t_1) between basin and sea will be equal to:

h = Absolute [Y(t_i)-Z(t_i)] (3.25)

where,

Y(t_i) = water level at the sea at any time t_i; and

and Z(t_i) = water level at the basin at any time t_i.

(b) Procedure to develop RTA model for flood-ebb generation with gates

During flood tide or ebb tide at the basin, if head =>h_S (2.0 m) turbine will be opened for power generation. Power generation will be stopped when water head (h) becomes to <=h_C (1.8 m). This is expressed in Table 3.4.

Table 3.4: Turbine/gate operation criteria for flood-ebb with gates system.

Point (at Figure 3.6)	Sea (S) water level (Y), Flood tide (1); Ebb tide (-1)	Basin (B) water level (Z) Flood tide (1); Ebb tide (-1)	Head, (h =Y-Z) m	Turbine (Tur) (Open=1; Close=0)	Gate (G) (Open=1; Close=0)
A'	1	1	0	0	0
B′	1	1	=>h_S (2.0)	1	0
	1	1	>h_C (1.8)	1	0
	-1	1	>h_C (1.8)	1	0
	-1	1	=h_C (1.8)	0	1
	-1	1	<h_C (1.8)	0	1
C′	-1	-1	0	0	0
	-1	-1	<h_S (2.0)	0	0
D′	-1	-1	=>h_S (2.0)	1	0
	-1	-1	>h_C (1.8)	1	0
	1	-1	>h_C (1.8)	1	0
	1	-1	=h_C (1.8)	0	1
	1	-1	<=h_C (1.8)	0	1
E′	1	1	0	0	0

© Operation rules of turbines for flood-ebb generation with gates

During flood tide or ebb tide at the basin and if head >=h_S (2.0 m) turbine will be opened for power generation and it will continue until head (h) is >h_C $(1.8\ m)$. When head (h) is <=h_C $(1.8\ m)$ turbine should be stopped in order to avoid cavitation.

(d) Operation rules of gates for flood-ebb generation with gates

For flood-ebb generation with gates, operational rules of gates are articulated from Figure 3.6 and Table 3.4. It is mentioned below:

(i) When tides are similar in nature (either flood or ebb) at both sides of the barrage and water head is zero (0) or less than h_S (0=h< 2m), both turbines and gates will be remained closed.

(ii) When tides are similar in nature (either flood or ebb) at both sides of the barrage and head is equal to or greater than h_S (2.0 m), turbines are opened and gates are remained closed.

(iii) When turbine is in operation and certainly head falls to <= $h_C\ (1.8\,m)$ at different nature of tides at two sides of the barrage, then turbines will be closed but gate is opened to pour the basin rapidly.

(e) **Velocity of water through turbines**

Velocity of water through turbine will be equals to:

$$V_T = \theta_T\, C_{DT} \sqrt{2gh} \quad (3.26)$$

where,

V_T= water velocity through turbine;

θ_T= 0 (zero) when turbine is closed;

θ_T=1 (one) when turbine is opened;

C_{DT} =coefficient of discharge through turbine;

g = acceleration due to gravity; and

h= water head.

(f) Velocity of water through gates

Velocity of water through gate will be equals to:

$$V_G = \theta_G\, C_{DG} \sqrt{2gh} \quad (3.27)$$

where,

V_G= water velocity through gates;

θ_G= 0 (zero) when gate is closed;

θ_G=1 (one) when gate is opened;

C_{DG} = coefficient of discharge through turbine;

g = acceleration due to gravity; and

h= water head.

.

(g) Discharge passed through turbine

Discharge trough turbine, $Q_{T=}N_T V_T A_T$ (3.28)

where,

$Q_{T=}$= discharge passed through turbines;

N_T = number of turbines;

V_T = velocity of water through turbines;

A_T= area of a turbine = $\frac{\pi D^2}{4}$; and

D= diameter of turbine.

(h) Discharge passed through gates

Discharge trough gates, $Q_G = N_G V_G A_G$ (3.29)

where,

$Q_{G=}$= discharge passed through gates;

N_G = number of gates;

V_G = velocity of water through gates;

A_G= area of a gate = $B_G * H_G$; and

B_G= width of the gate opening; and

H_G= height of the gate openings.

(i) Water volume inflows/outflows

The volume of water inflow to the basin through precipitation, rainfall or river inflow or inflow by pumping or outflow by pumping or spill out from the basin can be expressed as Equation (3.30):

$V_{i/o} = \theta_{i/o} . Q_{i/o} . \Delta t$ (3.30)

where,

$V_{i/o}$ = volume of water inflow/outflow to the basin

$Q_{i/o}$= discharge inflow or outflow to the basin

Δt = duration of inflow or outflow = $(t_2 - t_1)$

$\theta_{i/o}$= ±1, for inflow (+) sign and for outflow (-) sign.

(j) **Volume of water change at the basin**

$$\Delta V_w = \frac{(Q_1+Q_2)}{2}(t_2 - t_1) \pm V_{i/o} \tag{3.31}$$

Where,

ΔV_w= Volume of water change at the basin between time period t_1 and t_2

$Q_1 = Q_{T1}+Q_{G1}$= discharge through turbines and gates at time t_1

$Q_2 = Q_{T2}+Q_{G2}$= discharge through turbines and gates at time t_2

Q_T= discharge through turbine

Q_G = discharge through gates

$V_{i/o}=\theta_{i/o}.Q_{i/o}.\Delta t$= volume of water inflow/outflow to the basin

$Q_{i/o}$= discharge inflow or outflow to the basin

Δt = duration of inflow or outflow = $(t_2 - t_1)$

$\theta_{i/o}$= ±1, for inflow (+) sign and for outflow (-) sign.

(k) **Area of the basin**

The relation of water surface area and elevation is expressed as:

$$A_b = a_n Z^n + a_{n-1}Z^{n-1} + a_{n-2}Z^{n-2} + a_{n-3}Z^{n-3} + \cdots + a_1 Z^1 = f(Z) \tag{3.32}$$

where,

A_b= water surface area (m^2) of the basin at level Z;

Z= water level of the basin (m) at any time, t; and

n= polynomial order.

a_n, a_{n-1} a_{n-2} etc…are the coefficient.

(l) Calculations of water level at the basin

Suppose, at any time t_1 water level of the basin is Z_1 and area of the water surface of the basin is A_{b1} and at time t_2 water level of the basin is Z_2 and area of the water surface of the basin is A_{b2}. Similarly, at any time t_1 water level of the sea is Y_1 and at time

t_2 water level of the basin is Y_2. Water head difference between basin and sea at time t_1 is h_1 and at time t_2 is h_2. Again, discharge at time t_1 is Q_1 and at time t_2 is Q_2.

Then

$$A_{b1} = f(Z_1) \quad (3.33)$$

$$A_{b2} = f(Z_2) \quad (3.34)$$

$$Z_2 = Z_1 \pm \partial Z_2 \quad (3.35)$$

where,

Z_1 =water level at the basin at time t_1

Z_2 =water level at the basin at time t_2

∂Z_2= change in water level at the basin between $time\ t_1$ and t_2

During flood tide at the basin, $Z_2 = Z_1 + \partial Z_2$. (3.36)

During ebb tide at the basin, $Z_2 = Z_1 - \partial Z_2$ (3.37)

∂Z_2 = change in water level at the basin between $time\ t_1$ and t_2 can be calculated using the following matrix Equations (3.38):

where, h_1, V_{T1}, Q_{T1}, V_{G1}, Q_{G1} , Q_1 and $A_{b1}$are the water head, velocity of water through turbines, discharge through turbines, velocity of water through gates, discharge through gates, total discharge and basin water surface area respectively at time t_1 and h_2, V_{T2}, Q_{T2}, V_{G2} Q_{G2} , Q_2 and A_{b2} are the water head, velocity of water through turbines, discharge through turbines, velocity of water through gates, discharge through gates total discharge and basin water surface area respectively at time t_2. ΔV_w= average incremental volume of water during time interval $t_2\ and\ t_1$. Other symbols are usual notations expressed above.

$$\left[\begin{array}{c} V_{T1} = \theta_T\, C_{DT} \sqrt{2gh_1} \\ Q_{T1} = N_T\, V_{T1}\, A_T \\ V_{G1} = \theta_G\, C_{DG} \sqrt{2gh_1} \\ \mathrm{Q_{G1}} = \mathrm{N_G V_{G1} A_G} \\ Q_1 = Q_{T1} + \mathrm{Q_{G1}} \\ V_{T2} = \theta_T\, C_{DT} \sqrt{2gh_2} \\ Q_{T2} = N_T\, V_{T2}\, A_T \\ V_{G2} = \theta_G\, C_{DG} \sqrt{2gh_2} \\ \mathrm{Q_{G2}} = \mathrm{N_G V_{G2} A_G} \\ Q_2 = Q_{T2} + \mathrm{Q_{G2}} \\ \mathrm{V}_{i/o} = \theta_{i/o}\;\; Q_{i/o}(t_2 - t_1) \\ \Delta V_w = \dfrac{(Q_1 + Q_2)}{2}(t_2 - t_1) \pm \mathrm{V}_{i/o} \\ \partial Z_2 = \dfrac{\Delta V_w}{(A_{b1} + A_{b2})/2} \end{array}\right] \tag{3.38}$$

∂Z_2= change of water level at the basin between time period t_1 and t_2 and new water level at the basin will be Z_2= $Z_1 \pm\ \partial Z_2$.

(m) Power (kW) Calculation

Electrical power, P at any time, t

$$\mathrm{P\ (kW)} = \eta\rho g Q_T h/1000 \tag{3.39}$$

where, P =electrical power, in kW;

η =efficiency of turbine=0.4;

ρ =density of water= 1.025 kg/m^3;

Q_T=discharge through turbine in m^3/s; and

h= head difference between the sea and the basin in m.

(n) Energy (kWh) Calculation

Energy generation, E (kWh) between time period t_1 and t_2

$$\mathrm{E\ (kWh)} = \frac{(P_1+P_2)/2}{(t_2-t_1).3600} \tag{3.40}$$

where, E =electrical energy, in kWh;

P_1 and P_2 are the electrical power at time t_1 and t_2; and t in hours.

3.4.5.3 Model results for flood-ebb generation with gates

The basic information taken to run the model is shown in Table 3.5.

Table 3.5: Basic data taken to run the RTA model.

Sl No.	Elements	Value	Unit
1	Area of basin, A_b at HWLfrom equation (3.32)	…	km^2
2	Acceleration of gravity, g	9.807	m/s^2
3	Density sea water, ρ	1025	kg/m^3
4	Threshold h to start turbine, h_S	2.0	m
5	Threshold h to stop turbine, h_C	1.8	m
6	Turbine tunnel dia., D	7.6	m each
7	Turbine discharge coefficient, C_{DT}	0.9	
8	No. of turbines, N_T	1	Nos.
9	Turbine efficiency, η	0.4	
10	Width of single gate, B_G	3.5	m
11	Gate discharge coefficient, C_{DG}	0.65	
12	Number of gates, N_G	1	Nos.
13	Height of the gate opening, H_G	3	m

The RTA model is run considering a simple basin characteristics of linear relation [a_0=40617.95 and a_1=15864.36 (University of Strathclyde, 2015) and other coefficients equals to zero] and by plotting the linear relation, we get Figure 3.7.

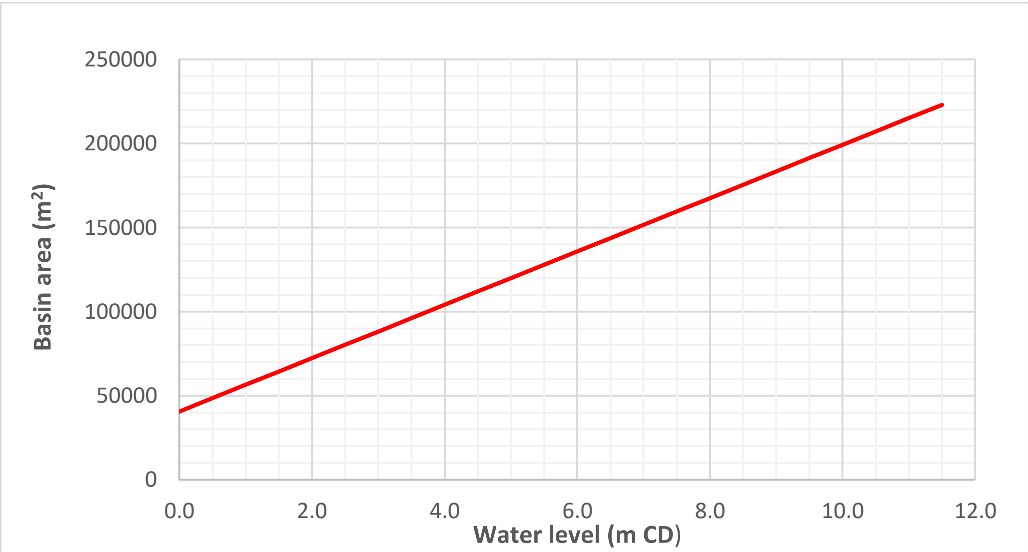

Figure 3.7: Basin area vs. water level for the base case.

Again, taking a simple case having a single constituent with an amplitude, a= 4m; phase angle, δ=0; and tidal period (T) = 12.42 hours and datum at Z_o = 7 m, we get the sea level variation which is shown in Figure 3.8.

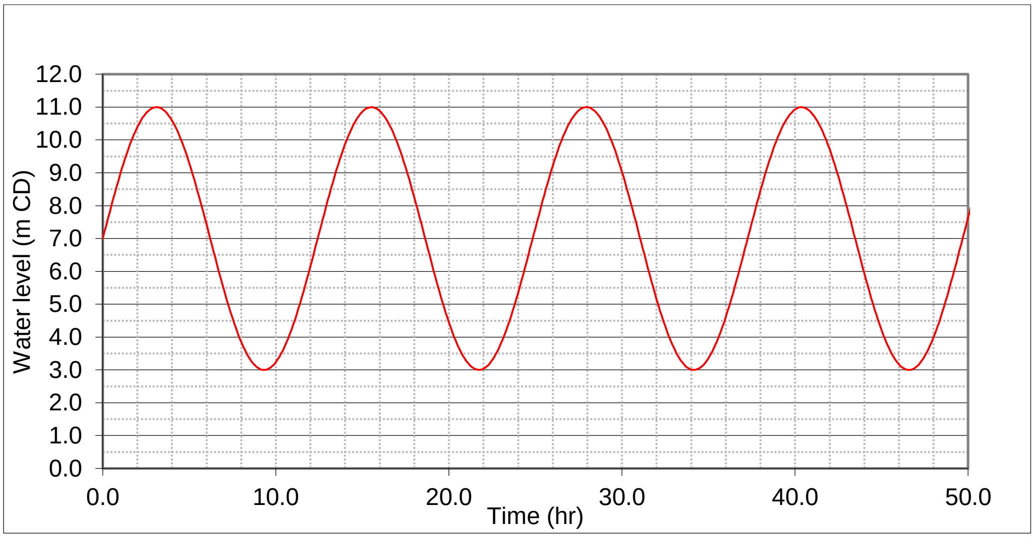

Figure 3. 8: Sea water level variation with respect to time.

Running the RTA model, we get the results which are shown in the Table 3.6.

Table 3.6: Results flood-ebb generation with gates for one turbine and one gate.

Parameter	Criteria	Values
Power output (kW)	Max.	743
	Avg.	478
	Min.	249
Energy, kWh	Per tidal cycle	7403
Basin WL (m CD)	Max.	9.56
	Min.	4.74
Head (m)	Max.	4.24
	Min.	-
	Avg.	2.33
Tidal range, Sea	Max.	8.00
Tidal range, Basin	Max.	4.82
Production period	One tidal day	63%
Non-production period	One tidal day	38%

Table 3.7: Results flood-ebb generation with gates for different number of turbine and one gate.

No. of Turbines (T) + Gates (G)		1T+ 1G	1T+ 2G	1T+ 3G	2T+ 1G	2T+ 2G	2T+ 3G
Power output (kW)	Max.	743	800	841	881	945	985
	Avg.	478	496	513	648	667	683
	Min.	249	246	245	483	485	483
Energy, kWh	Per tidal cycle	7403	8125	8601	7625	8513	8921
Basin WL (m CD)	Max.	9.56	9.91	10.14	9.91	10.31	10.53
	Min.	4.74	4.49	4.39	3.77	3.36	3.21
Head (m)	Max.	4.24	4.45	4.61	2.99	3.14	3.22
	Min.	-	-	-	-	-	-
	Avg.	2.33	2.44	2.52	1.75	1.79	1.83
Tidal range, Sea	Max.	8.00	8.00	8.00	8.00	8.00	8.00
Tidal range, Basin	Max.	4.82	5.42	5.75	6.15	6.95	7.32
Production period		63%	66%	68%	48%	52%	53%
Non-production period		38%	34%	32%	52%	48%	47%

(N.B: 1T means one turbine and 1G means one gate)

3.4.6 RTA model for ebb generation with gates

3.4.6.1 Guiding principles for ebb generation with gates

In ebb generation power is produced during ebb tide only. During flood tide turbines are closed and gates are kept open. During ebb tide turbine starts operating when water head difference (h) becomes equal to or greater than h_S(say, 2.0 m) i.e. h=> h_S(2.0 m) and continue up to h>h_C (say, 1.8 m). When h <=h_C(1.8 m) turbines are closed. During ebb tide gates are remained closed.

Based on tide conditions operational procedure could be divided in the followings two ways:

a) During flood tide at the basin, turbines are closed (θ_T=0) and gates are opened (θ_G=1).

b) During ebb tide at the basin, gates are closed (θ_G=0), turbines are opened (θ_T=1) when h>=h_S (2.0 m) and continue up to h>h_C(1.8 m). When h <=h_C(1.8 m) turbines are closed (θ_T=0).

c)

3.4.6.2 Development of RTA model for ebb generation with gates

The technique for development of RTA model to assess power for ebb generation is described below:

(a) Estimate dynamic head

Let, think water level at sea is $Y(t_i)$ and water level at the basin is $Z(t_i)$ at any time t_i.

Water head (h) at any time (t_1) between basin and sea will be equal to:

$$h = \text{Absolute}\ [Y(t_i)-Z(t_i)] \qquad (3.41)$$

where,

$Y(t_i)$ = water level at the sea at any time t_i; and

and $Z(t_i)$ = water level at the basin at any time t_i.

(b) Procedure to develop the model

For ebb generation the logics for the operation of turbines and gates can be expressed graphically in the following Figure 3.9.

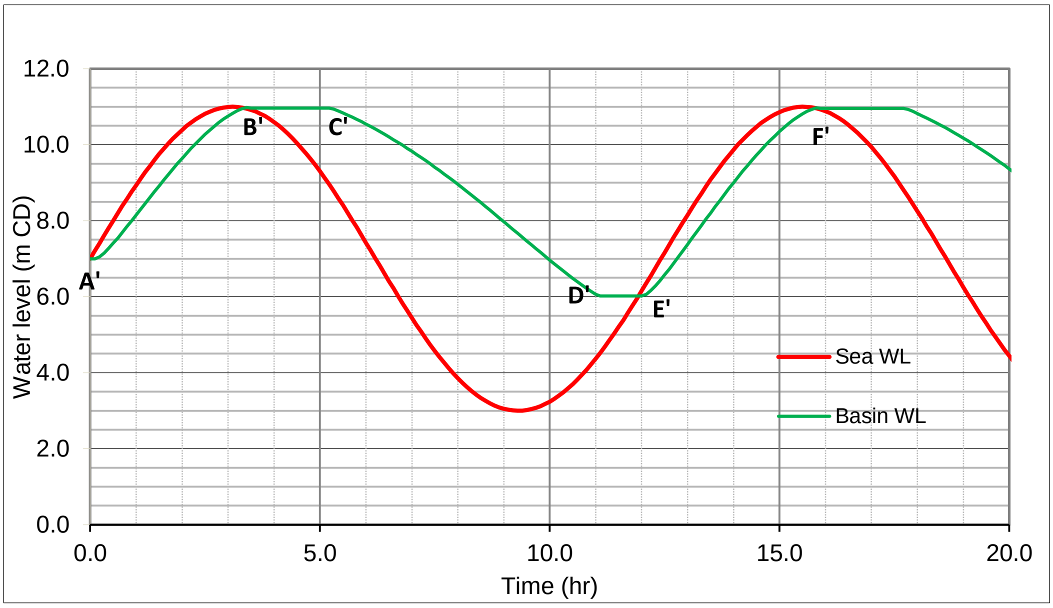

Figure 3.9: Operational rules for ebb generation with gates.

The logics for the operation of turbines and gates for ebb generation is expressed in Table 3.8.

Table 3.8: Turbine/gate operation criteria.

Point (At Figure 3.9)	Sea (S) water level (y), [Flood tide (1), Ebb tide (-1)	Basin (B) water level (z), Flood tide (1), Ebb tide (-1)	Head (h = y-z), m	Turbine (T) (Open=1 Close=0)	Gate (G) (Open=1 Close=0)
A′	1	1	h=0	0	1
	1	1	h<2.0	0	1
	-1	1	h<2.0	0	1
B′	-1	-1	h=0	0	0
	-1	-1	h<2.0	o	0
C′	-1	-1	>=2.0	1	0
	-1	-1	h>1.8	1	0
D′	1	-1	h=1.8	1	0
	1	-1	h<1.8<0	0	0
E′	1	1	h=0	0	1
F′	1	1	h=0	0	1

(c) Operational rules for turbine for ebb generation with gates

For ebb generation at the basin with gates system, during flood tide, turbines are closed (=0) and during ebb tide at the basin, turbines are opened (=1) when h>= 2.0 and continue up to h>1.8. When h <=1.8 m turbines are closed (Tur=0).

(d) Operational rules for gates for ebb generation with gates

For ebb generation at the basin with gates system, during flood tide gates are opened and during ebb tide gates are closed.

(e) Velocity of water through turbines

Velocity of water through turbine will be equals to:

$$V_T = \theta_T \, C_{DT} \sqrt{2gh} \qquad (3.42)$$

where,

V_T= water velocity through turbine;

θ_T= 0 (zero) when turbine is closed;

θ_T=1 (one) when turbine is opened;

C_{DT} =coefficient of discharge through turbine;

g = acceleration due to gravity; and

h= water head.

(f) Velocity of water through gates

Velocity of water through gate will be equals to:

$V_G = \theta_G \; C_{DG} \sqrt{2gh}$ (3.43)

where,

V_G= water velocity through gates;

θ_G= 0 (zero) when gate is closed;

θ_G=1 (one) when gate is opened;

C_{DG} = coefficient of discharge through turbine;

g = acceleration due to gravity; and

h= water head.

.

(g) Discharge passed through turbine

Discharge trough turbine, $Q_{T=}N_T V_T A_T$ (3.44)

where,

$Q_{T=}$= discharge passed through turbines;

N_T = number of turbines;

V_T = velocity of water through turbines;

A_T= area of a turbine = $\frac{\pi D^2}{4}$; and

D= diameter of turbine.

(h) Discharge passed through gates

Discharge trough gates, $Q_G = N_G V_G A_G$ (3.45)

where,

$Q_{G=}$= discharge passed through gates;

N_G = number of gates;

V_G = velocity of water through gates;

A_G= area of a gate = $B_G * H_G$; and

B_G= width of the gate opening; and

H_G= height of the gate openings.

(i) Water volume inflows/outflows

The volume of water inflow to the basin through precipitation, rainfall or river inflow or inflow by pumping or outflow by pumping or spill out from the basin can be expressed as Equation (3.42):

$V_{i/o}=\theta_{i/o}.Q_{i/o}.\ \Delta t$ (3.46)

where,

$V_{i/o}$ = volume of water inflow/outflow to the basin, m^3

$Q_{i/o}$= discharge inflow or outflow to the basin, m^3/s

Δt = duration of inflow or outflow, seconds. = $(t_2 - t_1)$

$\theta_{i/o}$= ±1, for inflow (+) sign and for outflow (-) sign.

(j) **Volume of water change at the basin**

$\Delta V_w = \frac{(Q_1+Q_2)}{2}(t_2 - t_1) \pm V_{i/o}$ (3.47)

Where,

ΔV_w= Volume of water change at the basin between time period $t_1$and t_2

Q_1= Q_{T1}+Q_{G1}= discharge through turbines and gates at time t_1

Q_2= Q_{T2}+Q_{G2}= discharge through turbines and gates at time t_2

Q_T= discharge through turbine

Q_G = discharge through gates

$V_{i/o}=\theta_{i/o}.Q_{i/o}.\ \Delta t$= volume of water inflow/outflow to the basin

$Q_{i/o}$= discharge inflow or outflow to the basin

Δt = duration of inflow or outflow = $(t_2 - t_1)$

$\theta_{i/o}$= ±1, for inflow (+) sign and for outflow (-) sign.

(k) **Area of the basin**

The relation of water surface area and elevation is expressed as:

$$A_b = a_n Z^n + a_{n-1} Z^{n-1} + a_{n-2} Z^{n-2} + a_{n-3} Z^{n-3} + + a_1 Z^1 + a_0 \;\; = f\,(\mathrm{Z}) \quad (3.48)$$

where,

A_b= water surface area (m^2) of the basin at level Z;

Z= water level of the basin (m) at any time, t; and

n= polynomial order.

$a_n, a_{n-1}\; a_{n-2}$ etc…are the coefficient.

(l) Calculations of water level at the basin

Suppose, at any time t_1 water level of the basin is Z_1 and area of the water surface of the basin is A_{b1} and at time t_2 water level of the basin is Z_2 and area of the water surface of the basin is A_{b2}. Similarly, at any time t_1 water level of the sea is Y_1 and at time t_2 water level of the basin is Y_2. Water head difference between basin and sea at time t_1 is h_1 and at time t_2 is h_2. Again, discharge at time t_1 is Q_1 and at time t_2 is Q_2.

Then

$$A_{b1} = f(Z_1) \quad (3.49)$$

$$A_{b2} = f(Z_2) \quad (3.50)$$

$$Z_2 = Z_1 \pm \partial Z_2 \quad (3.51)$$

where,

Z_1 =water level at the basin at time t_1

Z_2 =water level at the basin at time t_2

∂Z_2 = change in water level at the basin between $time\; t_1$ and t_2

During flood tide at the basin, $Z_2 = Z_1 + \partial Z_2$ (3.52)

During ebb tide at the basin, $Z_2 = Z_1 - \partial Z_2$ (3.53)

∂Z_2 = change in water level at the basin between $time\ t_1$ and t_2 can be calculated using the following matrix Equations (3.54):

where, $h_1,\ V_{T1},\ Q_{T1}, V_{G1}$, Q_{G1} , Q_1 and $A_{b1}$are the water head, velocity of water through turbines, discharge through turbines, velocity of water through gates, discharge through gates, total discharge and basin water surface area respectively at time t_1 and $h_2,\ V_{T2}$, Q_{T2}, V_{G2} Q_{G2} , Q_2 and A_{b2} are the water head, velocity of water through turbines, discharge through turbines, velocity of water through gates, discharge through gates total discharge and basin water surface area respectively at time t_2. ΔV_w= average incremental volume of water during time interval $t_2\ and\ t_1$. Other symbols are usual notations expressed above.

$$\begin{bmatrix} V_{T1} = \theta_T\ C_{DT}\ \sqrt{2gh_1} \\ Q_{T1} = N_T\ V_{T1}\ A_T \\ V_{G1} = \theta_G\ C_{DG}\ \sqrt{2gh_1} \\ Q_{G1} = N_G V_{G1} A_G \\ Q_1 = Q_{T1} + Q_{G1} \\ V_{T2} = \theta_T\ C_{DT}\ \sqrt{2gh_2} \\ Q_{T2} = N_T\ V_{T2}\ A_T \\ V_{G2} = \theta_G\ C_{DG}\ \sqrt{2gh_2} \\ Q_{G2} = N_G V_{G2} A_G \\ Q_2 = Q_{T2} + Q_{G2} \\ V_{i/o} = \theta_{i/o}\ Q_{i/o}(t_2 - t_1) \\ \Delta V_w = \dfrac{(Q_1 + Q_2)}{2}(t_2 - t_1) \pm V_{i/o} \\ \partial Z_2 = \dfrac{\Delta V_w}{(A_{b1} + A_{b2})/2} \end{bmatrix} \tag{3.54}$$

∂Z_2= change of water level at the basin between time period t_1 and t_2 and new water level at the basin will be Z_2= $Z_1 \pm\ \partial Z_2$.

(m) Power (kW) Calculation

Electrical Power,

$$P\ (kW) = \eta \rho g Q_T h/1000 \tag{3.55}$$

where, P =electrical power, in kW;

η =efficiency of turbine=0.4;

ρ =density of water= 1.025 kg/m^3;

Q_T=discharge through turbine in m^3/s; and h= head difference between the sea and the basin in m.

(n) Energy (kWh) Calculation

Energy generation, E (kWh) between time period t_1 and t_2

$$E\ (kWh) = \frac{(P_1+P_2)/2}{(t_2-t_1).3600} \tag{3.56}$$

where, E = eelectrical energy, in kWh;

P_1 and P_2 are the electrical power at time t_1 and t_2; and t in hours.

3.4.6.3 Model results for ebb generation

The basic information taken to run the model is shown in Table 3.9.

Table 3.9: Basic data taken to run the RTA model.

Sl No.	Elements	Value	Unit
1	Area of basin, A_b at HWL from equation (3.48)	…	km^2
2	Acceleration of gravity, g	9.807	m/s^2
3	Density sea water, ρ	1025	kg/m^3
4	Threshold h to start turbine, h_S	2.0	m
5	Threshold h to stop turbine, h_C	1.8	m
6	Turbine tunnel dia., D	7.6	m each
7	Turbine discharge coefficient, C_{DT}	0.9	
8	No. of turbines, N_T	1	Nos.
9	Turbine efficiency, η	0.4	
10	Width of single gate, B_G	3.5	m
11	Gate discharge coefficient, C_{DG}	0.65	
12	Number of gates, N_G	1	Nos.
13	Height of the gate opening, H_G	3	m

The RTA model is run considering a simple basin characteristics of linear relation [a_0=40617.95 and a_1=15864.36 (University of Strathclyde, 2015) and other coefficients equals to zero] and by plotting the linear relation, we get Figure 3.10.

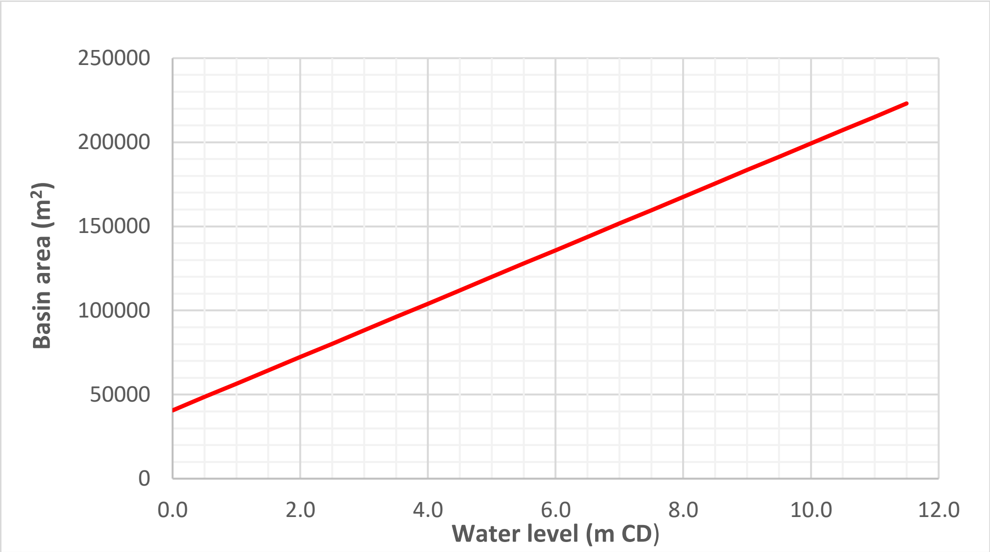

Figure 3. 10: Basin area vs. water level for ebb generation.

Again, taking a simple case having a single constituent with an amplitude, a= 4m; phase angle, δ=0; and tidal period (T) = 12.42 hours and datum at Z_o = 7 m, we get the sea level variation which is shown in Figure 3.11.

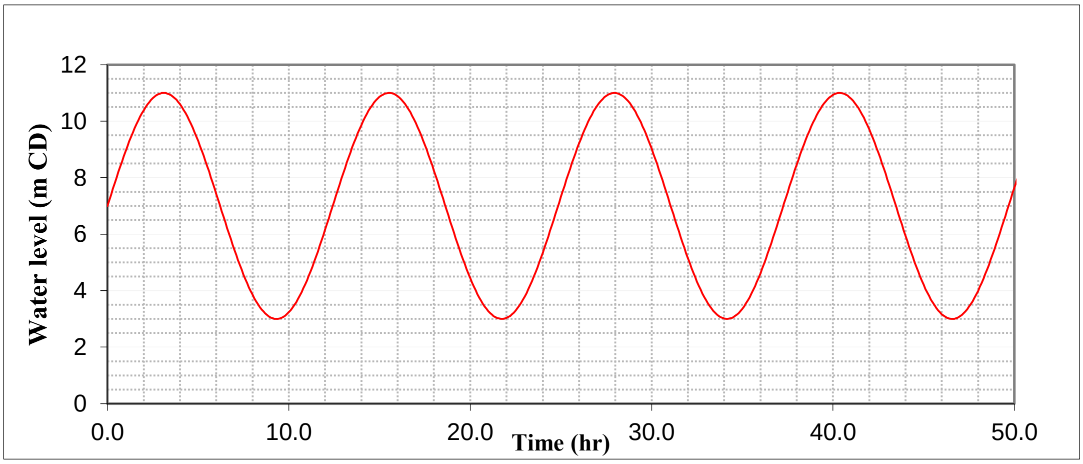

Figure 3.11: Sea water level variation with respect to time for ebb generation.

Running the RTA model, we get the results which are shown in the Table 3.10.

Table 3. 10: Results for one turbine and one gate for ebb generation.

Parameters	Criteria	Values
Power output (kW)	Max.	905
	Min.	206
	Avg.	262
Energy	kWh/day	6485
Head (m)	Max.	4.84
	Min.	-
Head (m)	Avg.	2.61
Basin WL (m CD)	Max.	8.40
	Min.	7.00
TR Sea	Max.	8.00
TR Basin	Max.	1.40
Production period		41%
Non-production period		59%

Results for different number of turbines and gates are shown in Table 3.11.

Table 3.11: Results for different number of turbines and gates for ebb generation.

Turbine (T)+ Gate (G)		1T+ 1G	1T+ 2G	1T+ 3G	1T+ 4G	2T+ 1G	2T+ 2G	3T+ 3G
Power output (kW)	Max	905	1187	1352	1453	1495	1863	2139
	Min	206	210	224	222	443	415	414
	Avg.	262	374	452	507	370	551	683
Energy, kWh/day		6485	9280	11211	12582	9186	13665	16943
Head (m)	Max	4.84	5.80	6.32	6.63	4.26	4.93	5.41
	Min	-	-	-	-	-	-	-
	Avg.	2.61	2.83	2.99	3.11	2.41	2.53	2.64
Basin WL (m CD)	Max	8.40	9.45	10.03	10.38	8.30	9.13	9.72
	Min	7.00	7.00	7.00	7.00	6.02	6.77	7.00
Tidal range sea (m)	m	8.00	8.00	8.00	8.00	8.00	8.00	8.00
Tidal range basin (m)	m	1.40	2.45	3.03	3.38	2.28	2.36	2.72
Production	136	41%	48%	52%	55%	35%	42%	0.47
Non-production	112	59%	52%	48%	45%	65%	58%	0.53

Note: 1T mean one turbine; 1G means one gate etc.

3.4.7 RTA model for flood generation with gates

3.4.7.1 Guiding principle for flood generation with gates

In flood generation power is produced during flood tide only. During ebb tide turbines are closed and gates are kept open. During flood tide turbine starts operating when water head difference (h) becomes equal to or greater than h_S (2.0 m) i.e. h=>h_S (2.0 m) and continue up to h>h_C (1.8 m). When h <=h_C (1.8 m) turbines are closed. During flood tide gates are remained closed.

Based on tide conditions operational procedure could be divided in the followings two ways:

1 During ebb tide at the basin, turbines are closed (θ_T=0) and gates are opened (θ_G=1).
2 During flood tide at the basin, gates and turbines are closed (θ_T=0, θ_G=0) until h<h_S (2.0 m). When h=> h_S (2.0 m), turbines are opened (θ_T=1) and continue up to h>h_C (1.8 m). When h <=h_C (1.8 m) turbines are closed (θ_T=0).

3.4.7.2 Development RTA model to assess power for flood generation

The technique for development of RTA model to assess power for flood generation is described below:

(a) Estimate dynamic head

Let us think water level at sea is Y(t_i) and water level at the basin is Z(t_i) at any time t_i.

Water head (h) at any time (t_1) between basin and sea will be equal to:

$$h = \text{Absolute } [Y(t_i)-Z(t_i)] \tag{3.57}$$

where,

$Y(t_i)$ = water level at the sea at any time t_i; and

and $Z(t_i)$ = water level at the basin at any time t_i.

(b) Procedure to develop the model

During flood tide gates are kept closed and during ebb tide gates are kept open. On the other hand, during ebb tide turbines are kept closed and during flood tide turbines start operating when water head difference (h) reaches equal to or greater than h_S (2.0 m) i.e. h=> h_S (2.0 m) and operation continues up to head greater than h_C (1.8 m) i.e. h>h_C (1.8 m). When h <=h_C (1.8 m) turbines are closed. The procedure is shown in Figure 3.12.

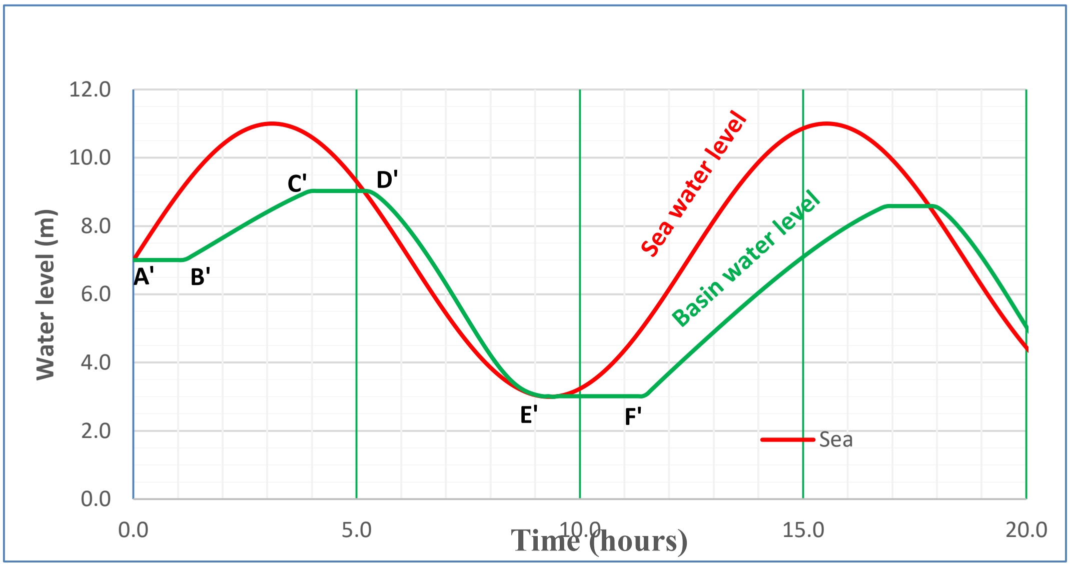

Figure 3.12: Operational rules for flood generation with gates.

During flood tide at the basin, gates are kept closed and turbines start operating when water head difference (h) reaches to => h_S (2.0 m) and continue up to h>h_C (1.8 m). When h <=h_C (1.8 m) turbines are closed. During ebb tide at the basin gates are opened and turbines are closed. This is expressed in the Table 3.12.

Table 3. 12: Turbine/gate operation criteria for flood generation with gates.

Point (at Figure 3.12)	Sea (S) water level (Y), flood tide (1); ebb tide (-1)	Basin (B) water level (Z), flood tide (1); ebb tide (-1)	Head (h=Y-Z), (m)	Turbine (Tur) (Open=1 Close=0)	Gate (G) (Open=1 Close=0)
A′	1	1	h=0	0	0
	1	1	$<h_S$ (2.0 m)	0	0
B′	1	1	$=>h_S$ (2.0 m)	1	0
	1	1	$>h_C$ (1.8 m)	1	0
	-1	1	$>h_C$ (1.8 m)	1	0
C′	-1	1	$=h_C$ (1.8 m)	0	0
	-1	1	$<h_C$ (1.8 m)	0	0
D′	-1	-1	h=0	0	1
	-1	-1	$<h_S$ (2.0 m)	0	1
E′	1	1	h=0	0	1
	1	1	$<h_S$ (2.0 m)	0	0
F′	1	1	$=>h_S$ (2.0 m)	1	0

(c) Operation of turbines and gates for flood generation

From Figure 3.12 and Table 3.13, it is evident that during flood tide at the basin, gates are kept closed and turbines start operating when water head difference (h) reaches to $=>h_S$ (2.0 m) and continue up to h$>h_C$ (1.8 m). When h $<=h_C$ (1.8 m) turbines are closed. During ebb tide at the basin gates are opened and turbines are closed.

(d) Velocity of water through turbines

Velocity of water through turbine will be equals to:

$$V_T = \theta_T \, C_{DT} \sqrt{2gh} \qquad (3.58)$$

where,

V_T= water velocity through turbine;

θ_T= 0 (zero) when turbine is closed;

θ_T=1 (one) when turbine is opened;

C_{DT} =coefficient of discharge through turbine;

g = acceleration due to gravity; and

h= water head.

(e) Velocity of water through gates

Velocity of water through gate will be equals to:

$$V_G = \theta_G \ C_{DG} \sqrt{2gh} \quad (3.59)$$

where,

V_G= water velocity through gates;

θ_G= 0 (zero) when gate is closed;

θ_G=1 (one) when gate is opened;

C_{DG} = coefficient of discharge through turbine;

g = acceleration due to gravity; and

h= water head.

.

(f) Discharge passed through turbine

Discharge trough turbine, $Q_{T=} N_T V_T A_T$ (3.60)

where,

$Q_{T=}$= discharge passed through turbines;

N_T = number of turbines;

V_T = velocity of water through turbines;

A_T= area of a turbine = $\frac{\pi D^2}{4}$; and

D= diameter of turbine.

(g) Discharge passed through gates

Discharge trough gates, $Q_G = N_G V_G A_G$ (3.61)

where,

$Q_{G=}$= discharge passed through gates;

N_G = number of gates;

V_G = velocity of water through gates;

A_G= area of a gate = $B_G.H_G$; and

B_G= width of the gate opening; and

H_G= height of the gate openings.

(h) Water volume inflows/outflows

The volume of water inflow to the basin through precipitation, rainfall or river inflow or inflow by pumping or outflow by pumping or spill out from the basin can be expressed as Equation (3.57):

$$V_{i/o}=\theta_{i/o}.Q_{i/o}.\ \Delta t \quad (3.62)$$

where,

$V_{i/o}$ = volume of water inflow/outflow to the basin, m^3

$Q_{i/o}$= discharge inflow or outflow to the basin, m^3/s

Δt = duration of inflow or outflow, seconds.= $(t_2 - t_1)$

$\theta_{i/o}$= ±1, for inflow (+) sign and for outflow (-) sign.

(i) **Volume of water change at the basin**

$$\Delta V_w = \frac{(Q_1+Q_2)}{2}(t_2 - t_1) \pm V_{i/o} \quad (3.63)$$

Where,

ΔV_w= Volume of water change at the basin between time period t_1 and t_2

Q_1= Q_{T1}+Q_{G1}= discharge through turbines and gates at time t_1

Q_2= Q_{T2}+Q_{G2}= discharge through turbines and gates at time t_2

Q_T= discharge through turbine

Q_G = discharge through gates

$V_{i/o}$=$\theta_{i/o}$.$Q_{i/o}$. Δt= volume of water inflow/outflow to the basin

$Q_{i/o}$= discharge inflow or outflow to the basin

Δt = duration of inflow or outflow = $(t_2 - t_1)$

$\theta_{i/o}$= ±1, for inflow (+) sign and for outflow (-) sign.

(j) **Area of the basin**

The relation of water surface area and elevation is expressed as:

$$A_b = a_n Z^n + a_{n-1}Z^{n-1} + a_{n-2}Z^{n-2} + a_{n-3}Z^{n-3} + \cdots + a_1 Z^1 + a_0 \;\; = f(Z) \quad (3.64)$$

where,

A_b= water surface area (m^2) of the basin at level Z;

Z= water level of the basin (m) at any time, t; and

n= polynomial order.

$a_n, a_{n-1}\ a_{n-2}$ etc…are the coefficient.

(k) Calculations of water level at the basin

Suppose, at any time t_1 water level of the basin is Z_1 and area of the water surface of the basin is A_{b1} and at time t_2 water level of the basin is Z_2 and area of the water surface of the basin is A_{b2}. Similarly, at any time t_1 water level of the sea is Y_1 and at time t_2 water level of the basin is Y_2. Water head difference between basin and sea at time t_1 is h_1 and at time t_2 is h_2. Again, discharge at time t_1 is Q_1 and at time t_2 is Q_2.

Then

$$A_{b1} = f(Z_1) \quad (3.65)$$

$$A_{b2} = f(Z_2) \quad (3.66)$$

$$Z_2 = Z_1 \pm \partial Z_2 \quad (3.67)$$

where,

Z_1 =water level at the basin at time t_1

Z_2 =water level at the basin at time t_2

∂Z_2= change in water level at the basin between $time\ t_1$ and t_2

During flood tide at the basin, $Z_2 = Z_1 + \partial Z_2$ (3.68)

During ebb tide at the basin, $Z_2 = Z_1 - \partial Z_2$ (3.69)

∂Z_2 = change in water level at the basin between $time\ t_1$ and t_2 can be calculated using the following matrix Equations (3.70):

where, $h_1,\ V_{T1},\ Q_{T1}, V_{G1}, Q_{G1}$, Q_1 and $A_{b1}$are the water head, velocity of water through turbines, discharge through turbines, velocity of water through gates, discharge through gates, total discharge and basin water surface area respectively at time t_1 and $h_2,\ V_{T2},\ Q_{T2},\ V_{G2}$ Q_{G2} , Q_2 and A_{b2} are the water head, velocity of water through turbines, discharge through turbines, velocity of water through gates, discharge through gates total discharge and basin water surface area respectively at time t_2. ΔV_w= average incremental volume of water during time interval $t_2\ and\ t_1$. Other symbols are usual notations expressed above.

$$\begin{bmatrix} V_{T1} = \theta_T\ C_{DT}\ \sqrt{2gh_1} \\ Q_{T1} = N_T\ V_{T1}\ A_T \\ V_{G1} = \theta_G\ C_{DG}\ \sqrt{2gh_1} \\ Q_{G1} = N_G V_{G1} A_G \\ Q_1 = Q_{T1} + Q_{G1} \\ V_{T2} = \theta_T\ C_{DT}\ \sqrt{2gh_2} \\ Q_{T2} = N_T\ V_{T2}\ A_T \\ V_{G2} = \theta_G\ C_{DG}\ \sqrt{2gh_2} \\ Q_{G2} = N_G V_{G2} A_G \\ Q_2 = Q_{T2} + Q_{G2} \\ V_{i/o} = \theta_{i/o}\ \ Q_{i/o}(t_2 - t_1) \\ \Delta V_w = \dfrac{(Q_1 + Q_2)}{2}(t_2 - t_1) \pm V_{i/o} \\ \partial Z_2 = \dfrac{\Delta V_w}{(A_{b1} + A_{b2})/2} \end{bmatrix} \tag{3.70}$$

∂Z_2= change of water level at the basin between time period t_1 and t_2 and new water level at the basin will be Z_2= $Z_1 \pm\ \partial Z_2$.

(l) Power (kW) Calculation

Electrical Pwoer,

$$P\ (kW) = \eta\rho g Q_T h/1000 \tag{3.71}$$

where, P =electrical power, in kW;

η = efficiency of turbine=0.4;

ρ =density of water= 1.025 kg/m^3;

Q_T=discharge through turbine in m^3/s; and

h= head difference between the sea and the basin in m.

(m) Energy (kWh) Calculation

Energy generation, E (kWh) between time period t_1 and t_2

$$E\ (kWh) = \frac{(P_1+P_2)/2}{(t_2-t_1).3600} \tag{3.72}$$

where, E =electrical energy, in kWh;

P_1 and P_2 are the electrical power at time t_1 and t_2; and t in hours.

3.4.7.3 Model results for flood generation

The basic information taken to run the model is shown in Table 3.13.

Table 3.13: Basic data used to run the RTA model.

Sl No.	Elements	Value	Unit
1	Area of basin, A_b at HWLfrom equation (3.64)	…	km^2
2	Acceleration of gravity, g	9.807	m/s^2
3	Density sea water, ρ	1025	kg/m^3
4	Threshold h to start turbine, h_S	2.0	m
5	Threshold h to stop turbine, h_C	1.8	m
6	Turbine tunnel dia., D	7.6	m each
7	Turbine discharge coefficient, C_{DT}	0.9	
8	No. of turbines, N_T	1	Nos.
9	Turbine efficiency, η	0.4	
10	Width of single gate, B_G	3.5	m
11	Gate discharge coefficient, C_{DG}	0.65	
12	Number of gates, N_G	1	Nos.
13	Height of the gate opening, H_G	3	m

The RTA model is run considering a simple basin characteristics of linear relation [a_0=40617.95 and a_1=15864.36 (University of Strathclyde, 2015) and other coefficients equals to zero] and by plotting the linear relation, we get Figure 3.13.

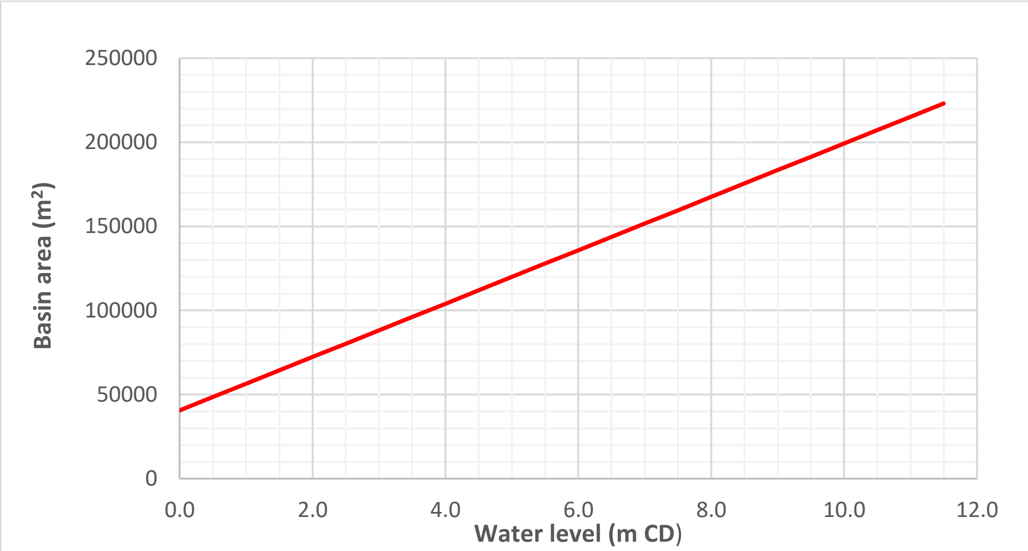

Figure 3.13: Basin area vs. water level for base case.

Again, taking a simple case having a single constituent with an amplitude, a= 4m; phase angle, δ=0; and tidal period (T) = 12.42 hours and datum at Z_o = 7 m, we get the sea level variation which is shown in Figure 3.14.

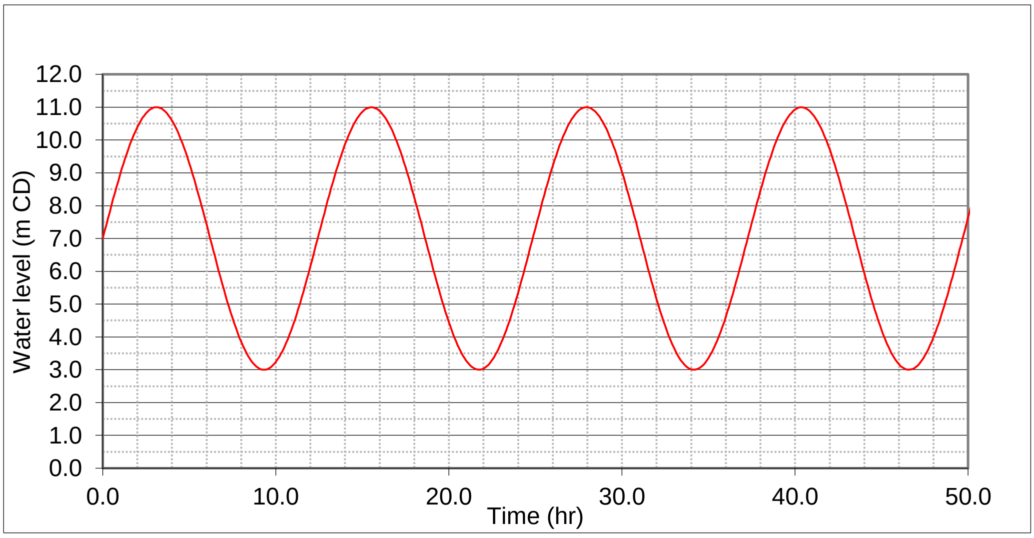

Figure 3. 14: Sea water level variation with respect to time for base case.

Running the RTA model, we get the results which are shown in the Table 3.14.

Table 3.14: Results for one turbine and one gate for flood generation.

Parameters	Criteria	Values
Power output (kW)	Max	646
	Min	206
	Average	376
Energy,	kWh /cycle	4493
Basin WL (m CD)	Max	9.02
	Min	3.33
Head (m) Head (m)	Average	6.30
	Max	3.86
	Min	0.00
Tidal range basin (m)	Max	5.70
Tidal range sea (m)	Max	8.00

Results for different number of turbines and gates are shown in Table 3.15.

Table 3.15: Results for different number of turbines and gates.

Turbine (T)+ Gate (G)		1T+ 1G	1T + 2G	1 T+ 3G	2T+ 1G	2T+ 2G	2t+ 3G	3T+ 3G
Power output (kW)	Max	646	653	654	603	592	576	817
	Min	206	208	208	414	418	418	623
	Average	376	419	420	526	520	512	717
Energy, kWh	/cycle	4493	3838	3846	4130	3360	3303	3084
Basin WL (m CD)	Max	9.02	9.02	9.02	9.30	9.26	9.26	9.16
	Min	3.33	2.99	2.99	3.41	2.96	2.99	2.99
	Average	6.30	6.00	5.84	6.71	6.40	6.24	6.26
Head (m)	Max	3.86	3.89	3.89	2.32	2.30	2.25	2.17
	Min	0.00	0.00	0.00	0.00	0.00	0.00	0.00
Tidal range basin (m)	Max	5.70	6.03	6.03	5.89	6.30	6.27	6.17
Tidal range sea (m)	Max	8.00	8.00	8.00	8.00	8.00	8.00	8.00
Production	43	48%	37%	37%	32%	26%	26%	17%
Non-production	205	52%	63%	63%	68%	74%	74%	83%

(Notations: 1T means one turbine and 1G means one gate).

3.5 Comparison of Base Case and the RTA Model

The base case is a simplified, theoretical and hypothetical case fits for continuous flow through turbines without provision of gates and minimum head requirements for turbines to avoid cavitation. So, the base case does not suit for (i) flood-ebb generation with minimum head requirements without gates; (ii) flood-ebb generation with gates; (iii) ebb generation with gates; and (iv) flood generation with gates. RTA model addressed those constraints and limitations and prepared to make the model robust and flexible by modifying and developing equations. A comparison is listed in the Table 3.16.

Table 3. 16: Comparison of notations and equations between the base case and the RTA model.

Sl No.	Description	Notations and equations used in base case	Notations and equations used in RTA model
1	Water level at sea	$Z_1(t)$	Y(t)
2	Water level at basin	$Z_2(t)$	Z(t)
3.	Nature of tide at basin	(i) Use (+ 1) for flood tide when $Z_1(t)>Z_2(t)$ and (ii) Use (-1) ebb tide when $Z_1(t)<Z_2(t)$	i. Flood tide when Y(t)>Z(t) and expressed as B= (+1) and i. Ebb tide when Y(t)<Z(t) and expressed as B= (-1).
4	Nature of tide at sea	-----	(i) Flood tide when Y(t+1)>Y (t) and expressed as S= (+1) and (ii) Ebb tide when Y(t+1) <Y (t) and expressed as S= (-1).
5	Operation of turbines and gates.	Turbines are continuously opened irrespective of water head, h= Absolute value of Y(t)-Z(t). Minimum head requirement is not considered. There is no provision of gates.	**<u>A. For Flood-ebb generation without gates</u>** (i) During flood tide or ebb tide at both sides of the barrage (i.e. sea side or basin side) and h=absolute value of Y(t)-Z(t) <2.0m, turbine remained closed (θ_T=0). When h=>2.0m, turbine is opened (θ_T=1). (ii) When nature of tides is different (i.e. flood tide at one side and ebb tide

Sl No.	Description	Notations and equations used in base case	Notations and equations used in RTA model
			at another side) and h=absolute value of Y(t)-Z(t) >1.8, turbines continue in operation. But, when h<=1.8m, turbine is closed (θ_T=0). **<u>B. For flood-ebb generation with gates</u>** (i) During flood tide or ebb tide at both sides (i.e. sea side and basin side) and head, h=absolute value of Y(t)-Z(t) <2.0m, both turbines and gates remains closed (θ_T=0) and θ_G=0 are taken. When h=>2.0 m turbine starts operation (θ_T=1), but gate remains closed (θ_G=0) until h reaches to 1.8m. (ii) When nature of tides is different (i.e. flood tide at one side and ebb tide at another side) and h=absolute value of Y(t)-Z(t) >1.8, turbines continue in operation (θ_T=1). But, when h<=1.8m, turbine is closed (θ_T=0) but gates are opened (θ_G=1) to pour or empty the basin quickly. **<u>C. For ebb generation with gates</u>** (i) During flood tide at the basin, turbines remained closed (θ_T=0) and gates are opened (θ_G=1). (ii) During ebb tide at the basin gates are closed (θ_G =0). Turbines are also

Sl No .	Description	Notations and equations used in base case	Notations and equations used in RTA model
			kept closed (θ_T =0) until head, h = <2.0m. Turbines are opened (θ_T=1) when h=>2.0m. (iii) When ebb at the basin but flood tide at the sea and head, h<=1.8m turbines are closed (θ_T=0) but gates are remained closed (θ_G =0). **<u>D. For flood generation with gates</u>** (i) During flood tide at the basin, gates are remained closed (θ_G=0). (ii) During flood tide at the basin and head, h<2.0m turbines remained closed (θ_T=0). But when h=>2.0 m turbines are opened for operation (θ_T=1). (iii) But when flood tide at the basin side and ebb tide at the sea and head, h <=1.8m turbines are closed (θ_T=0).
6	Velocity of water through turbines	$V = C_D\sqrt{2gh}$	$V = \theta_T . C_{DT}\sqrt{2gh}$
7	Velocity of water through gates	……	$V = \theta_G . C_{DG}\sqrt{2gh}$
8	Discharge through turbines	Q_T=N. $C_D\sqrt{2gh}.\pi\frac{D^2}{4}$	$Q_T = N_T . \theta_T . C_{DT}\sqrt{2gh}.\pi\frac{D^2}{4}$
9	Discharge through gates	…..	$Q_G = N_G . \theta_G . C_{DG}\sqrt{2gh}. W_g H_g$

Sl No.	Description	Notations and equations used in base case	Notations and equations used in RTA model
10	Total discharge through openings	Q_T=N. $C_D\sqrt{2gh_t}.\pi\frac{D^2}{4}$	Q = $Q_T + Q_G$
11.	Inflow or outflow	---	$V_{i/o} = \theta_{i/o}\ Q_{i/o}(t_2 - t_1)$
12	dZ (incremental rise or fall of basin water level)	dZ = $(\pm1).Q_T.(T_{t+1} - T_t)/A_b$	$A_{b1} = f(Z_1)$ $A_{b2} = f(Z_2)$ $Z_2 = Z_1 \pm \partial Z_2$ $\Delta V_w = \frac{(Q_1 + Q_2)}{2}(t_2 - t_1) \pm V_{i/o}$ $\partial Z_2 = (\pm1)\frac{\Delta V_w}{(A_{b1}+A_{b2})/2}$
13	Power, P(t)	$P_t = N_T.\eta\rho g.C_D.A_s\sqrt{2gh_t}$	$P_t = \eta\rho g Q_T.h_t$
14	Energy, E	$E = \sum_{t=1}^{n} P_t\ .\Delta t$	$E = \sum_{t=1}^{n} E_t$ $E_t=\frac{1}{2}(P_t + P_{t-1}).(T_t - T_{t-1})$

3.6 Comparison of Results from RTA Model for Different Modes of Operation

3.6.1 Data input taken for RTA Model for different modes

Data input taken for RTA Model for different modes is mentioned in Table 3.17.

Table 3.17: Data input taken for RTA Model for different modes.

Inputs for the system	Value	Unit
Acceleration due to gravity, g	9.807	m/s^2
Density of sea water, ρ	1025	kg/m^3
Threshold h to start turbine, h_S	2.0	m
Threshold h to stop turbine, h_C	1.8	m
Turbine tunnel dia., D	2.6	m
Turbine discharge coefficient, C_{DT}	0.9	
No. of turbines N_T	1	
Turbine efficiency, η	0.4	
Width of single gate, B_G	3.5	m
Gate discharge coeff. C_{DG}	0.65	
Number of gates, N_G	2	
Gate Opening height, H_G	3	m

3.6.2 Tidal characteristics taken for different modes

Tidal characteristics taken for different modes are mentioned in Table 3.18.

Table 3.18 : Tidal characteristics taken for different modes.

Parameters for tide with units	**Value**
Tidal period, T (hr)	12.42
Amplitude, a (m)	4
Phase angle, σ (degree)	0
Datum shift from MSL, a_o (m)	7

3.6.3 Basin characteristics taken for different modes

Basin characteristics taken for different modes are mentioned in Equation (3.73)

$$A_b = 15864.355\ Z + 40617.952 \tag{3.73}$$

where,

A_b= Area of the basin water surface at level Z, m^2

Z= Basin water level, m

3.6.4 Water level, head, power and energy at different modes from RTA model

3.6.4.1 Time series water level of sea and basin at different mode of operations.

Water level of sea and basin at different mode of operations is shown in **Appendix A.2.**

Water level variations of different modes are shown in Figure 3.15.

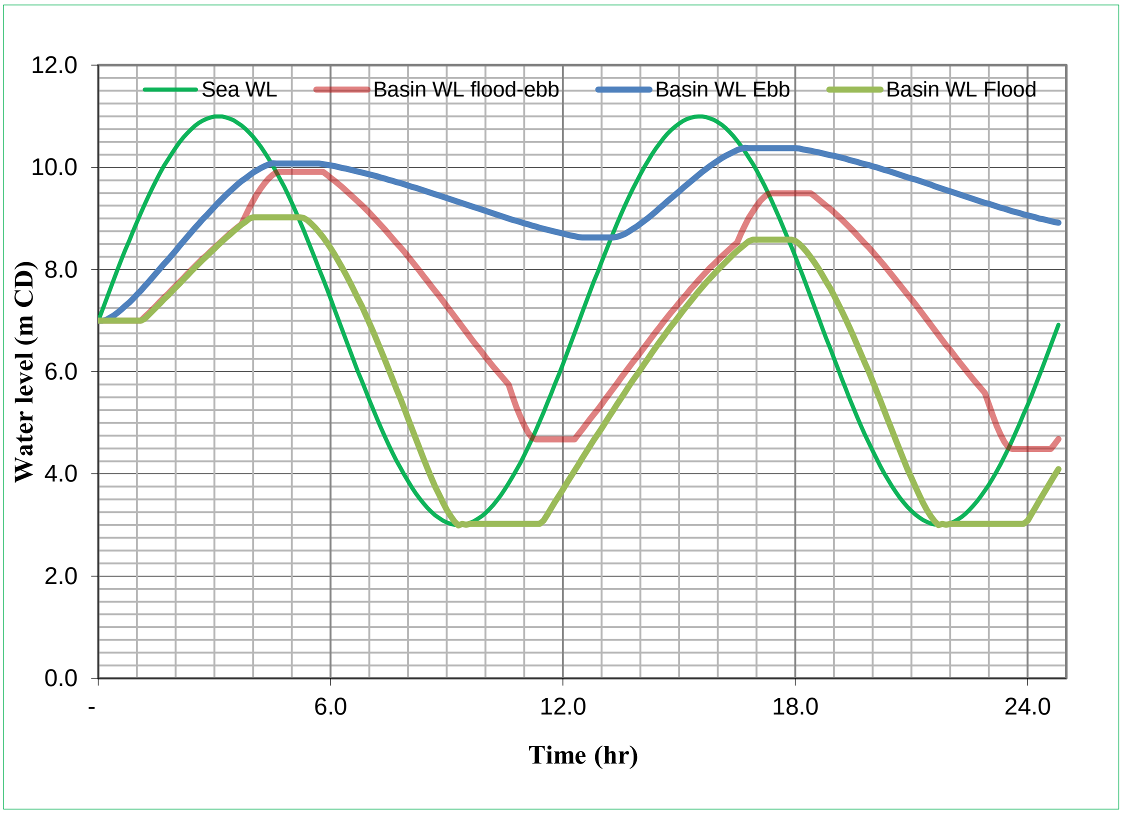

Figure 3.15: Water level variations for different modes of the RTA model.

From Figure 3.15, it is seen that basin water remains at higher level for ebb mode than that of flood-ebb mode and flood mode. Again, basin water remains at higher level for flood-ebb mode than that of flood mode.

3.6.4.2 Time series water head difference between sea and basin at different mode of operation from RTA model.

Water head difference between sea and basin at different mode of operation is shown in **Appendix A.2.**

Time series water head difference between sea and basin at different mode of operation from RTA model is shown in Figure 3.16.

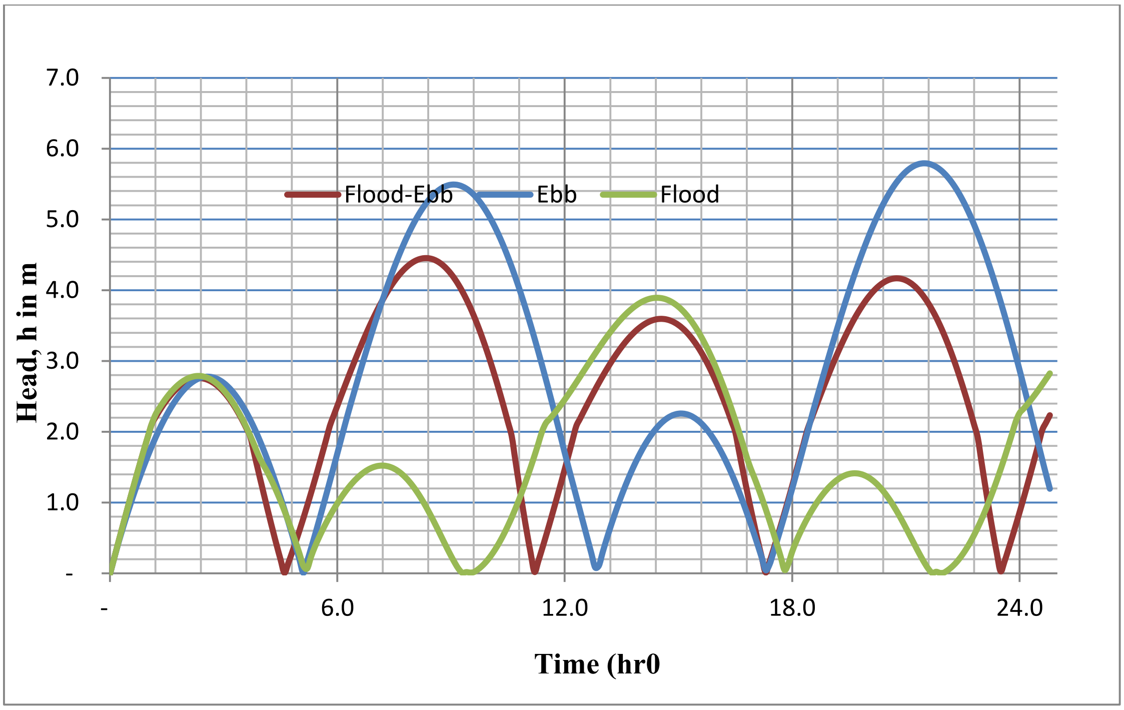

Figure 3.16: Time series of water head difference between sea and basin at different mode of operation from RTA mode.

From Figure 3.16, it is clear that water head difference is higher at flood-ebb mode than that of flood mode. Again, water head difference is higher at ebb mode than that of flood-ebb mode, i.e. ebb mode has higher water heads than that of other modes. If minimum head for turbine operation is considered (model results are obtained considering 2 m for turbine starting head and 1.8 m for turbine closing head), then ebb mode will generate higher power than other modes.

3.6.4.3 Time series power generation for different mode of operation from RTA model

Time series power generation for different mode of operation from RTA model (**See Appendix A.2**) is shown Figure 3.17. In Figure 3.17, sea water level is shown in Primary Axis and time series power for different modes is shown in Secondary Axis respectively.

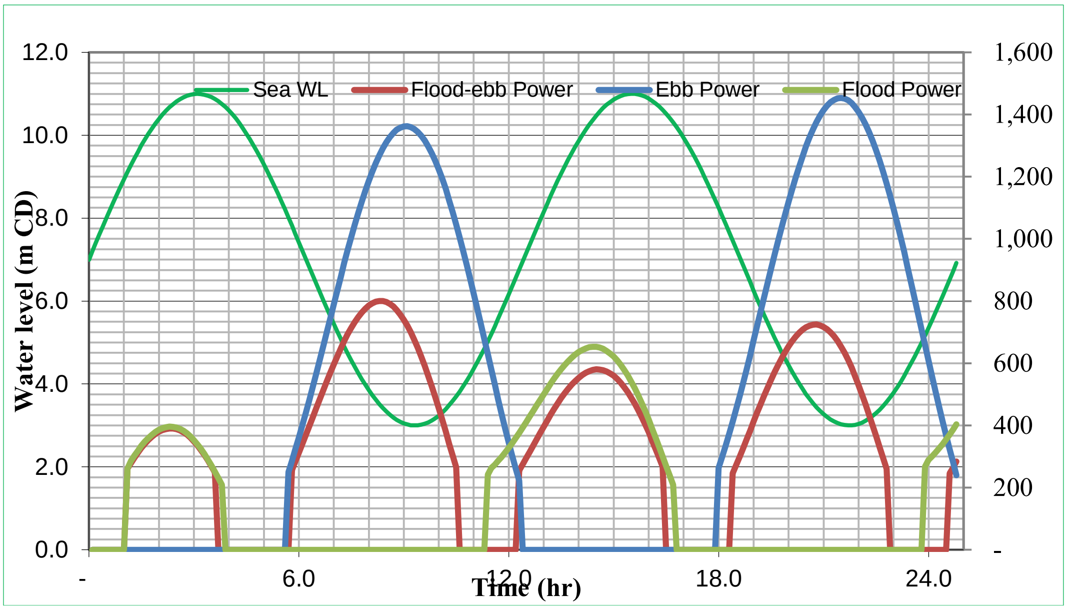

Figure 3.17: Time series of power generation for different mode of operation from RTA model.

From Figure 3.17, it clear that maximum and minimum power for ebb mode only is 1187 kW and 210 kw respectively, whereas maximum & minimum power for flood-ebb mode and flood mode only are 800 kW & 246 kW and 661 kW and 209 kW respectively. From Figure 3.17, it is also clear that within 24.8 hours ebb mode generates power two times, roughly 6 hours each time, for this particular case. But flood-ebb mode generates power three times, roughly 5 hours each time, for this case. So, overall generation period for a tidal day (24.8 hrs.) for flood-ebb mode is higher than that of ebb mode. But, we are more interested for total energy (kWh) generation. So, we have to look into which mode would generate total energy generation. It is discussed in the sub-section 3.6.5.

3.6.5 Comparison of results for different mode of operation from RTA model

The comparison of results for different mode of operation is mentioned Table 3.19

Table 3.19: The comparison of results for different mode of operation.

Elements	Criteria (for a tidal day, 24.8 hrs.)	Flood-ebb mode	Ebb only mode	Flood only mode
Energy (kWh)		8125	9280	5190
Power output (kW)	Max.	800	1187	661
	Avg.>0	496	780	485
	Min. (>0)	246	210	209
Basin WL (m CD)	Max.	9.91	9.45	9.02
	Min.	4.49	7.00	2.99
Head (m)	Max.	4.45	5.80	3.89
	Min.	0.00	0.00	0.00
	Avg.	2.44	2.83	1.61
Tidal range basin (m)	Max.	5.42	5.80	6.03
Tidal range sea (m)	Max.	8.00	8.00	8.00
Production period	%	66%	48%	37%
Non-production period	%	34%	52%	63%

Table 3.19 compares the results for different modes using same data input from RTA model. Table 3.19 provides results for flood-ebb generation, ebb generation and flood generation for 24.8 hours for 1 turbine (2.6 m dia.) and 2 gates (each 3m x 3 m). The energy generation in different modes is shown in Figure 3.18.

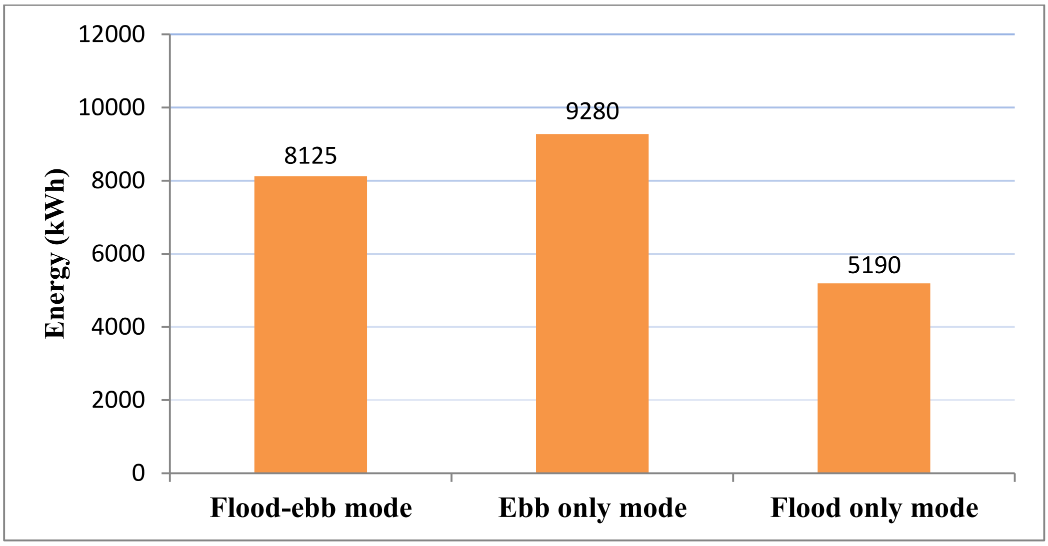

Figure 3.18: Energy generation in different modes using RTA model.

From Table 3.19 and Figure 3.18, it is observed that ebb generation gives more energy (9280 kWh) than that of flood-ebb generation (8125 kWh) and flood generation (5190 kWh). On the other hand, duration of generation for flood-ebb generation, ebb generation and flood generation are 66%, 48%, and 37% respectively. So, it is concluded that ebb generation yields more energy (kWh) than that of flood-ebb generation, but duration of ebb generation is shorter than flood-ebb generation.

3.7 Summary

All previous approaches for the assessment of tidal power are based on some fixed assumed variables such as tidal range, mean tidal range, mean head, duration and ignore the actual real-time variability of these variables. Based on these, in most cases the extractable power is considered certain percentage of potential energy.

A team of University of Strathclyde (2015) developed an excel sheet to calculate power for tidal barrage considering a very simple, theoretical and hypothetical case for continuous generation through turbines where they did not consider minimum head requirement for turbine operation to avoid cavitation and also did not consider provision of gates to improve efficiency. Hence the said case is not suitable for (i) flood-ebb generation without gates with minimum head requirement; (ii) flood-ebb generation with gates; (iii) flood generation with gate; or (iv) ebb generation with gate.

Again, the base case was developed using a single tidal constituent and a simple relation of basin's area and elevation. But in real cases, observed tide is a superimposition of series of multiple tidal constituents having different tidal amplitudes, speeds and phase angles and basin water surface might be a polynomial equation of multiple orders instead a linear relation with elevation. However, the said case is used as a base case for the RTA model development.

Assessment of power potential considering real-time water head differences based on long-term data might yield a more accurate estimation of power generation. For this reason, an analytical model has developed for better estimation of tidal power generation by establishing a real-time functional relation (i) between water level and basin area, which in turn will relate to turbine discharge and change of water levels in the basin, and (ii) among the tidal constituents having different phases and amplitudes in the sea side, expressed as a superimposed function with respect to time. The general equations for potential power and energy are used and modified and improved to adopt different modes of operations such as (i) flood-ebb generation without gates with minimum head requirement; (ii) flood-ebb generation with gates; (iii) flood generation with gates; or (iv) ebb generation with gates.

In real cases observed tide is a superimposition of series of tidal constituents having different tidal amplitudes, speeds and phase angles. Again, the basin water surface is not always a linear relation with elevation rather it could be a polynomial equation of multiple orders. So, RTA model is developed in such a way so that it can adopt multiple tidal constituents forming a generalized equation of tides and any shape of basin configuration forming a polynomial equation of multiple orders for area-elevation. The RTA model could also be used for a series of observed tide data.

The RTA model is run for flood-ebb generation, ebb generation and flood generation using same data input. Comparing the results for 24.8 hours for 1 turbine (2.6 m dia.) and 2 gates (each 3.5 m x 3 m), it is observed that ebb generation gives more energy (9280 kWh) than that of flood-ebb generation (8125 kWh) and flood generation (5190 kWh). On the other hand, duration of generation for flood-ebb generation, ebb generation and flood generation are 66%, 48%, and 37% respectively. So, it is concluded that ebb generation yields more energy than that of flood-ebb generation, but duration of ebb generation is shorter than flood-ebb generation.

The model is verified taking data for Severn barrage and compared the results with other studies on Severn barrage in Chapter 4. The RTA model gives similar results with slight variations of Severn's results from which it could be concluded that RTA model is acceptable and reliable.

CHAPTER 4
MODEL VALIDATION AND OPTIMIZATION

4.1 Introduction

Validation is important to test the accuracy of the model. In this chapter the real-time analytical model developed in Chapter 3 is verified to test whether the model is usable, reliable and acceptable for assessing the tidal barrage power and energy. On the other hand, optimization is necessary to find out the optimum solutions or least cost solution for the desired output.

In the following sections of this chapter described the processes how the model is validated and how the capacity is optimized. Section 4.2 of this chapter described about model validation, Section 4.3 described about optimum plant capacity and summary in Section 4.4.

4.2 Model Validation

4.2.1 Comparison of results of RTA model with base case

Necessary information and data of the model is put in the base case for continuous generation and peak power 654.44 kW is the out-put of the project (1 turbine with 2.6 m diameter) for 12.5 hrs. The RTA model for same turbine diameter with starting minimum head of 2.0 m and turbine closing head 1.8 m results the peak power 666.60 kW. The other parameters of the model are mentioned in Table 4.1. The comparison of the results with the base is shown in Table 4.2.

Table 4.1: Parameters used for the base case and RTA model for power generation.

Parameters	Symbol	Value
Threshold h to start turbine	h_1	2.0
Threshold h to stop turbine	h_2	1.8
Turbine tunnel diameter	D	2.6
Turbine discharge coefficient	Cdt	0.9
No. of turbines	N_T	1
Turbine efficiency	η	0.4
Width of single gate	B_G	4.0
Gate discharge coefficient	Cdg	0.65
Number of gates	N_G	1
Gate Opening depth	d	3

Table 4.2: Comparison of results between base case and RTA model for a tidal cycle.

1 turbine having 2.6 m dia.	Results from base case data	Results from RTA Model	Difference
Max. Peak [kW]	654.44	666.6	+1.86%
Avg. [kW]	261.12	247.33	**-5.28%**
Energy for a tidal cycle	3285.78	3066.88	-6.66%

From Table 4.2 it is evident that the results from the RTA model and base case are more-or-less similar (from -6.66% to +1.86%). The real time analytical model fits for the base case.

4.2.2 Comparison of results of RTA model with Severn tidal barrage

The Severn Barrage is a proposed tidal power station to be built across the Bristol Channel (Severn Estuary). The River Severn has a tidal range of 14 metres-the second highest in the world – making it perfect for tidal power generation (Knight & Hill, 2007). The barrage will be about 10-mile-long between Lavernock Point south of Cardiff, Wales and Brean Down in Somerset, England. The barrage would act as a bridge between England and Wales and will have an operational lifetime of up to 200 years. It would be the world's largest ever renewable energy project, and the UK's largest engineering project since the Channel Tunnel. A total of 214x40MW turbines would be built into the barrage through which the trapped water would return at high pressure when the tide turns generating electricity. In order to permit shipping to pass through the barrage an enormous set of shipping locks would be constructed.

Different studies on Severn barrage suggested different models and results. The basin was assumed a flat bottom and constant water surface area of 480km^2. Three percent (3%) reduction is applied for tidal elevation due to impact of the barrage which was taken M_2=3.15m and S_2=0.95m (Burrows, et al., 2009). The RTA model is run for Severn Barrage for ebb mode considering 216 turbines each 9m diameter (40MW) and 184 sluice gates each 12X12 meter in size.

The total annual energy output of Severn barrage using different approach in different studies are shown in Table 4.3.

Table 4.3: Annual energy (TWh) generation (Ebb) from Severn barrage.

Sl. No.	Different approaches for Severn data	Annual energy output per year (TWh)
1.	RTA model [considering h_{min} (turbine starting) =2.0m and h_{min} (turbine stopping) =1.8m. (Max. power output 6.274GW, minimum power output 1.124GW]	10.77
2.	Turgency/Generation [0D approach] 2006-2008: considering H_{min}=1.0m.]	11.12
3.	RTA Model considering H_{min}=1.0m for turbine operation. (Max. power output 5.585GW, minimum power output 1.629GW]	10.50
4.	DoEn reports [UKAEA, 1980, 1984; DoEn, 1989]	15.09

Source: (Burrows, et al., 2009)

From Table 4.3, it is evident that the annual energy output for Severn barrage using Turgency/Generation 0D approach (2006-2008) considering minimum head of 1.0 m for turbine operation was 11.12 TWh (Burrows, et al., 2009). The difference between the original DoEn (1980s) study and Turgency/Generation 0D approach (2006-2008) is very high. This is due to the impact of the barrage on the tidal characteristics which was not considered earlier DoEn studies (1980s). The annual output from RTA model for Severn barrage considering minimum head of 1.0 m for turbine operation was 10.50 TWh which is 5.58% lower than that of Turgency/Generation model. Considering minimum starting head of 2.0 m for turbine operation and turbine closing head of 1.8 m, the RTA model for Severn barrage results annual energy output 10.77 TWh which is 3.15% lower than that of Turgency/Generation model. Though the results are closer each other, but RTA model is more analytical and provides time series power and energy. The Turgency program calculates the power output and outflow relationship through the use of a turbine hill chart given by (Baker, 1991); (Burrows, et al., 2009). It is more generic and accurate model than Turgency/Generation model. So, it can be concluded that the real time analytical model also fits for the Severn barrage.

4.3 Optimization of Plant Capacity

4.3.1 General discussion

The main purpose of optimization of a tidal barrage power plant is to set optimum number of turbines and gates to get as much as possible maximum energy with cost effective solution. So, there are at least three issues to be considered during optimization; namely (1) to get maximum energy; (2) set optimum number of turbines and gates so that unit price of the energy will be cost effective compare to other available solutions; and (3) turbines and gates could be housed within the barrage and embankment length.

4.3.2 Optimization based on energy generation

Energy generation (ebb power) for Severn barrage with different number of turbines and gates are calculated using the RTA model and is shown in Table 4.4**.**

Table 4.4: Results (Ebb mode) of RTA model using Severn Barrage data.

Sl. No.	No. of turbines	No. of gates	Maximum power (MW)	Annual energy output (TWh)
1.	150	150	5005	8.146
2.	200		6000	9.777
3.	250		6793	10.927
4.	300		7444	11.617
5.	150	200	5005	8.730
6.	200		6000	10.517
7.	250		6793	11.795
8.	300		7444	12.562
9.	150	250	5005	9.133
10.	200		6000	11.029
11.	250		6793	12.393
12.	300		7444	13.212
13.	150	300	5005	9.409
14.	200		6000	11.378
15.	250		6793	12.809
16.	300		7444	13.651
17.	216	184	6274	10.772

Source: (Burrows, et al., 2009).

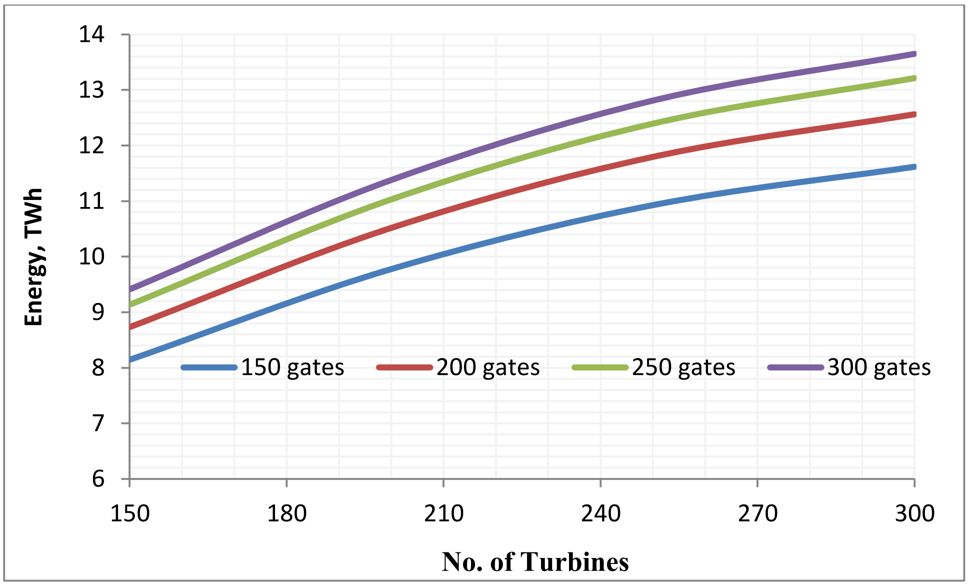

Figure 4.1: Energy generation as a function of turbines for Severn barrage.

From Table 4.4, it is seen that as the turbine and gate increase, the energy generation is also increases. For 300 turbines each 9 m diameter (40 MW) and 300 sluice gates each 12 m X 12 m yield maximum energy 13.651 TWh annually. By increasing the number of turbines for a particular number of gates we can increase energy generation.

Similarly, for a particular number of turbines we can increase energy by increasing nos. of gates. Question may arise to what extent it would continue. To answer this question, we can calculate energy cost per unit.

4.3.3 Optimization based on levelized cost of energy

4.3.3.1 Levelized cost of energy

Regarding optimization there are many tools to optimise a tidal barrage power plant. Levelized cost of energy (LCOE) is one of the tools of optimization. It calculates per unit energy production cost for the economic life of the plant to find out the optimum solutions or least cost solution for desired output.

Levelized cost of energy (LCOE) is the cost for per unit energy production for the economic life of the plant. It compares per unit energy production cost for different capacities. The levelized cost can be calculated using the formula mentioned in the Equation. 4.1 (Department of Indian Energy and US Department of Energy, 2013).

$$LCOE=\frac{\sum_{t=1}^{n}\frac{(I_t+O\&M_t+F_t}{(1+i)^t}}{\sum_{t=1}^{n}\frac{E_t}{(1+i)^t}} \qquad (4.1)$$

where,

LCOE= Levelized cost of energy (€/kWh);

I_t= Investment made in year t (€);

$O\&M_t$= Operation and maintenance in year t (€);

F_t= Fuel cost in year t (€);

E_t= Energy produced in year t (€);

i= Discount rate; and

n= economic life of the plant in yrs.

From Figure 4.1, it is seen that, higher the turbine and gate capacity, higher would be extractable energy. But higher the capacity, higher would be the cost of investment. So, capacity optimization is required to make the energy generation cost-effective considering turbine capacity and its cost. In most of the cases levelized tariff (€/kWh) is considered for plant optimization. Since cost data available is in euros, tariff is calculated in euros.

4.3.3.2 Cost breakdown of tidal barrage power plant

From a report (Burrows, et al., 2009) cost breakdown for 216 turbines and 184 gates for Severn tidal barrage are taken which is shown in Table 4.5**.**

Table 4.5 Cost-breakdown of Severn tidal barrage for 216 turbines and 184 gates.

Sl No.	Items	Symbol	€M (1988 figures)
1.	Civil works		
	Caisson Construction	Cc	
	Construction yards	C_y	339
	Turbine-generator caissons (4.3 km, 54 Nos.) (4 turbines in 1 caisson each 80 m)	Ctgc	1,082
	Sluice Caissons (4.1 km, 46 Nos.) (4 sluices in 1 caisson each 90 m)	Csc	326
	Plain caissons (3.9 km)	C_{pc}	270
	Lock caissons (lump-sum)	C_{lc}	81
	Break water caissons (lump-sum)	C_D	86
	Steel works and installations	Csw	580
	Dredging	Cd	380
	Foundations	Cf	377
	Caissons installations	C_{ci}	148
	Embankments (3.6 km) and breakwaters	C_{eb}	382
	Substations	C_s	65
	Service roads	Csr	141
	Contingencies (15% above costs)	$C_{con.cl}$	639
	Total Civil Works	C_{CL}	4,896
2.	Turbines, generators and ancillary plant		
	Turbines, generators and ancillary plant	Ctgp	2302
	Contingencies	Ccon.tg	115
	Total	Ctg	2,417
3.	TOTAL (15.9 km barrage)		7,313

Source: (Burrows, et al., 2009)

The total cost of the Severn barrage for 216 turbines each 40MW and 184 sluice gates each 12m X 12m with 15.9 km barrage is €M 7,313 (in 1988 figures). Total cost of the Severn barrage for different number of turbines and gates is shown in **Appendix B1**.

4.3.3.3 Calculation of levelized cost of energy (LCOE)

Let assumed economic life of the tidal barrage power is 50 years, plant cost (from Table 4.5) is €M 7,313 (1988 figures), maintenance cost 5% of the plant cost and discount rate 4%, the levelized tariff (Table 4.6) is per unit kWh is 6.62p. Using similar cost breakdown, cost and levelized cost of energy for different sets of turbines and gates are calculated which is shown in Table 4.6.

Table 4. 6: Cost of levelized energy for Severn Barrage.

No. of turbines	No. of gates	Annual energy output (TWh)	Cost of the plant (€M)	Levelized Tariff (p/kWh)
150	150	8.146	6184	7.40
200		9.777	6993	6.97
250		10.927	7803	6.96
300		11.617	8613	7.23
150	200	8.730	6272	7.01
200		10.517	7082	6.57
250		11.795	7892	6.52
300		12.562	8702	6.75
150	250	9.133	6361	6.79
200		11.029	7171	6.34
250		12.393	7981	6.28
300		13.212	8790	6.49
150	300	9.409	6449	6.68
200		11.378	7259	6.22
250		12.809	8069	6.14
300		13.651	8879	6.34
216	184	10.772	7313	6.62

4.3.3.4 Optimization of the plant capacity based on levelized cost of energy.

Using the information from the Table 4.6, the cost of levelized energy for different combination of turbine sets is shown in the Figure 4.2.

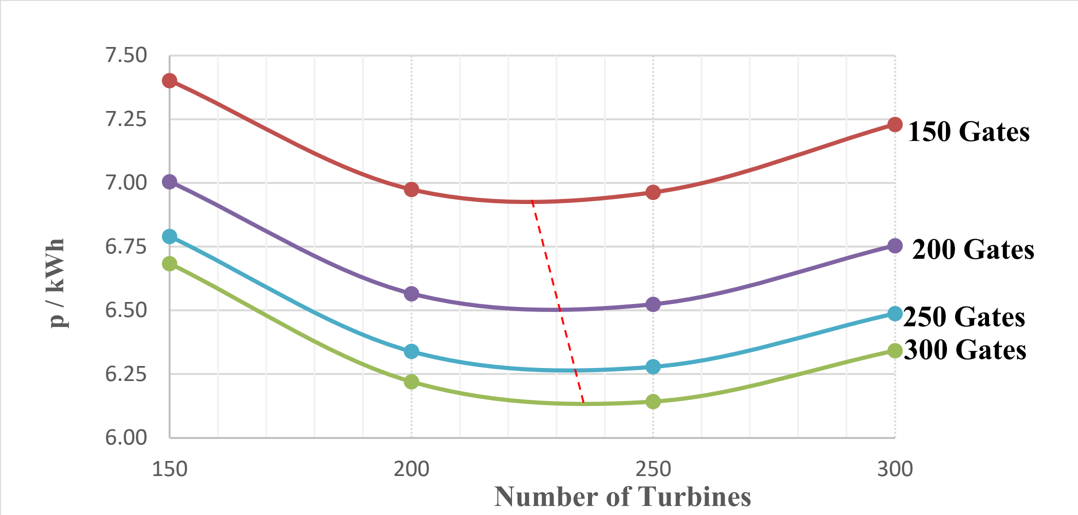

Figure 4. 2 Levelized cost of energy for different combination of turbines and gates.

A dotted line is plotted through minima of curves for different numbers of gates. Figure 4.2 reveals that the levelized cost of energy is minimum for the turbines (9m each) between 225 to 235 in number. Between the turbines 225 to 235, levelized cost of energy again decreases as the number of sluice gates (each 12m X 12m) increases.

Let us take an optimum number of turbines say, 232 in number. The model is run for 232 turbines (9m each) with different numbers of sluice gates ranging from 300 to 500 (12m X 12m) and presented in the Table 4.7 and Figure 4.3.

Table 4.7: Levelized cost of energy (LCOE) for optimum number of turbines (232 turbines) with different number of sluice gates.

Nos. of turbines (9m dia.)	232	232	232	232	232	232	232
No. of gates (12mX12m)	300	350	400	420	430	450	500
Maximum power (MW)	6528	6528	6539	6536	6534	6560	6536
Cost the plant (€M)	7778	7870	7955	7990	8008	8044	8132
Annual energy (TWh)	12.364	12.644	12.850	12.916	12.946	12.9958	13.113
LCOE (€/kWh)	0.0613	0.0607	0.0604	0.06032	0.06031	0.06035	0.0605
LCOE (p/kWh)	6.13	6.07	6.04	6.032	6.031	6.035	6.05

Optimum number of gates for optimum number of turbine (232 turbines) can be found from Figure 4.3.

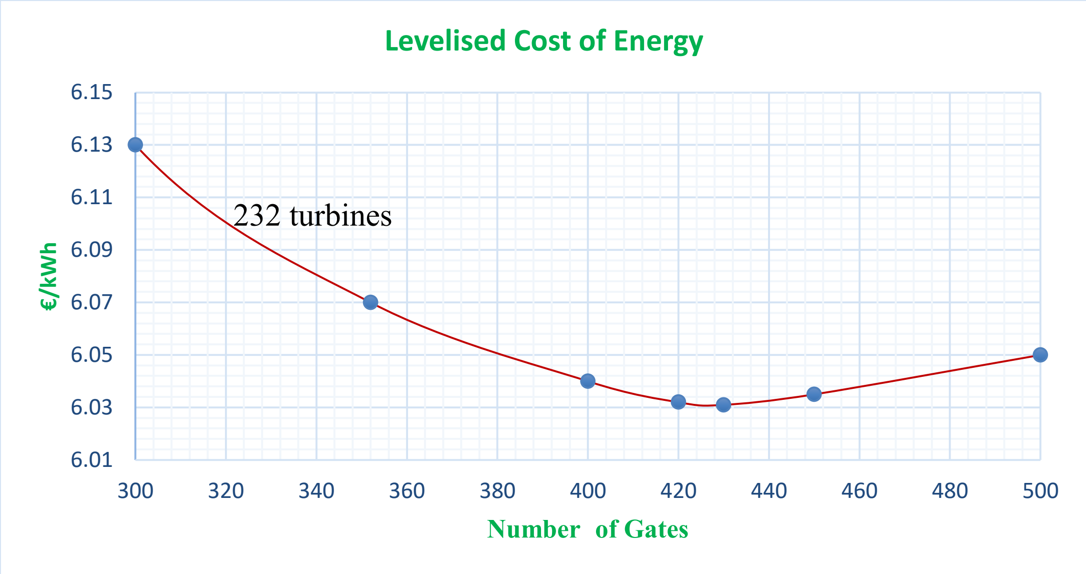

Figure 4.3: Optimum number of gates for optimum number of turbines.

It is evident from Figure 4.3 that the levelized cost of energy for 232 turbines will be minimum for 430 sluice gates which is 6.031 p/kWh.

So, based on levelized cost of energy (6,032 p/kWh), number of turbines and number of sluice gates can be selected. It is observed that 232 turbines (each 9m 40 MW) and 430 gates (12m X12m) is an optimum combination of turbines-gates for the Severn barrage which will provide annual energy output of 12.946 TWh and minimum levelized cost of energy (6.031p/kWh).

4.3.4 Optimization based on barrage length

Figure 4.3, it is seen that 232 turbines 430 gates will yield 12.946 TWh and minimum levelized cost of energy (6.031p/kWh). We had to check whether 430 gates and 232 turbines could be housed within the 16.3 km barrage length.

Table 4.8: Minimum length requirement.

Description	Caisson no.	Length
Turbine-generator caissons (4 turbines in 1 caisson each 80 m) For 232 turbines (4.6 km, 58 Nos.)	9.55	4.6 km
(4 gates in 1 caisson each 90 m) For 420 sluice gates (9.4 km, 105 Nos.)	107	9.4 km
Plain caissons (2.3 km)	-	2.3 km
Total length requirement		16.3 km

So, the barrage can house 232 turbines and 420 gates easily.

4.4 Summary

The main purpose of this chapter was to test the reliability and acceptability of RTA model developed in Chapter 3 and to optimize the plant capacity of a tidal barrage power plant. The RTA model is tested in this chapter comparing (i) the results obtained from RTA model using the data of the Severn tidal barrage with the results of that barrage in the published report (Burrows, et al., 2009) and (ii) the results obtained from RTA model using the data of the base case with the results from the base case. In both cases the results are very closer and found acceptable.

The results obtained from RTA model using Severn barrage data and considering minimum head of 1.0 m for turbine operation was 10.50 TWh which is 5.58% lower than that of the result (11.12 TWh) published using Turgency/Generation model (Burrows, et al., 2009). Again, considering minimum head of 2.0 m for turbine operation and 1.8m for turbine closing, the RTA model for Severn barrage results annual energy output 10.77 TWh which is 3.15% lower than that of Turgency/Generation model. The results for the above two cases are very closer and could consider acceptable. The RTA model is a real time analytical tool where as Turgency/Generation 0D approach used the hill chart given by Baker (1991). On the other hand, RTA model is flexible for all input data. So, it could be commented that RTA model is more robust, reliable and more accurate than other models. The results from RTA model is also compared with the base case and observed that results from the RTA model and the results from base case are more-or-less similar (only 1.23% variation). The real time analytical (RTA) model fits the base case also. So, it could be concluded that RTA model is reliable and acceptable for accessing the tidal barrage power and energy.

Three issues were considered to optimise the plant capacity, namely (i) energy generation; (ii) levelized cost of energy (LCOE); and (iii) length of the barrage. Our aim is to produce maximum energy, as much as possible, but that should be cost effective and the required number of turbines and gates should be accommodated within the barge length. Optimization based on energy generation, it seen that energy generation increases with increase of number of turbines and also increases with increase of number of gates. For 300 turbines each 9 m diameter (40 MW) and 300 sluice gates each 12 m X 12 m yield maximum energy 13.651 TWh annually. Optimisation based on LCOE was also considered. Considering economic life of the Severn tidal barrage of 50 years, maintenance cost 5% of the plant cost and discount rate 4%, the levelized cost of energy is calculated which is 6.34 p/kWh for 300 turbines and 300 gates and 6.62 p/kWh for 216 turbines and 184 gates (See **Appendix B2**). Plotting the minima of curves for different gates (**Figure 4.2)** it is seen that the levelized cost of energy is minimum for the turbines in between 225 to 235. Figure 4.2 also reveals that for the turbines in between 225 to 235, the levelized cost of energy again decreases as the number of sluice gates (each 12m X 12m) increases. So, taking turbine number 232 (in between 225 and 235), RTA model is run again for the gates between 250 to 500 and the levelized cost is again calculated which is plotted in Figure 4.3. It reveals that 232 turbines and 420 gates yield minimum cost-effective energy which is 6.032p/kWh. Considering minimum cost of energy power plant can be optimised. The length of the Severn barrage is 16.3 km which can easily accommodate 232 turbine and 420 gates.

So, considering (i) energy generation (ii) levelized cost of energy and (iii) barrage length, 232 turbines (each 9 m dia.) and 430 gates (each 12 m x12 m) are optimum capacity of the Severn Tidal Barrage which will yield 12.946 TWh annually with a maximum capacity of 6534 MW.

CHAPTER 5
OPTIMUM BASIN CONFIGURATION

5.1 Introduction

The magnitude of tides can be strongly influenced by the shape of the shoreline. The shape of channel also can magnify the intensity of tides. Funnel-shaped bays in particular can dramatically alter tidal magnitude. The Bay of Fundy in Nova Scotia has large effect and has the highest tides in the world, over 15 meters (Thurman, 1994). Equation (2.3), E= $\frac{1}{2}\eta\rho g A_b h^2$ reveals that energy generation from a tidal barrage depends on the amount of tidal prism (volume equals to A_bh; where "A_b" is the water surface area of the basin and "h" is the head difference between the water levels at high-tide and low-tide and the centre of the gravity of tidal prism (h/2) from low level of the tidal prism. Again, volume of tidal prism at any time depends on (i) difference between two water levels (h); (ii) size of the basin (aspect ratio); (iii) area of the basin and (iv) shape of the basin. Theoretically, optimum basin is that one, which results maximum value of $A_b h^2$; where A_b is the water surface area of the basin and h is the water head between the water levels.

In a tidal barrage, tidal water level on the sea side is a superimposition of a number of periodically-varying tidal constituents, while the water level in the basin depends on the geometric configuration of the basin and operational control of the turbines. So, water head is dynamic and capacity of the plant is variable with time. From Equation (2.25), we get power, $P_t = \eta\rho g Q_T h$; where h is dynamic head and Q_T is real time discharge through turbine.

This chapter provides some ideas about the type of basin that yields maximum energy output considering (a) different aspect ratios (width/length ratio) and (b) different shapes (such rectangular, trapezoidal and parabolic cross-section etc.). More specifically, which type of size (width/length) and shape (cross-section) will yield maximum energy considering equal basin area or equal volume of water or equal cross-sectional area of different sizes and shapes of basins having same tidal range.

In the following sections of this chapter discussed about theoretical formulation of energy generation in Section 5.2, power generation from a tidal barrage of different basin configurations in Section 5.3, tidal barrages of different vertical shapes in Section 5.4, energy generation from a rectangular basin in Section 5.4.1, energy generation from a trapezoidal basin in Section 5.4.2, energy generation from a parabolic basin in Section 5.4.3 and summary in Section 5.5.

5.2 Theoretical Formulation

5.4.1 Formation of empirical equation of a basin water surface area

All previous methods for the assessment of tidal power are based on fixed assumed variables such as tidal range, duration of power generation, and ignore the actual real-time variability in these variables. So, dynamic water head and basin configuration or shape (rectangular, trapezoidal or parabolic etc.) is important to assess real-time variability of tidal barrage power plants. The objective of this chapter is to know the energy production variation due to size and shape of the basin.

Let, we consider an empirical equation of the relation between water surface area (A_b) of the impounded tidal basin and water elevation (Z) of the basin is:

$$A_b = a_0 + a_1.Z^1 + a_2.Z^2 + a_3.Z^3 + a_4.Z^4 + a_5.Z^5 + \cdots \quad (5.1)$$

where,
A_b= water surface area of the impounded tidal basin by a barrage at water level, Z.
a_0, a_1, a_2, a_3, a_4, a_5……. are the coefficients of the equation depending on the shape and length of the basin.

5.2.2 Form an equation to represent water level of tides

Tide at sea is a superimposition of multiple tidal constituents which can be expressed as Equation (5.2):

$$Y(t) = a_0 + \sum_{i=1}^{n} a_i \cos(\frac{2\pi t}{T} - \emptyset_i) \quad (5.2)$$

where,

Y(t) = water level at sea due to tidal effect;

a_0 =mean level above chart datum;

n= number of tidal constituents;

a_i= amplitude of i^{th} tidal constituent;

T_i= tidal period of i^{th} tidal constituents; and

$\emptyset_i$= is the phase angle of i^{th} tidal constituent.

5.2.3 Tidal power assessment

The values of the coefficients of equation (5.1) would be derived from actual basin bathymetry. So, taking the (1) bathymetry data and (2) tidal data, either observed data or predicted data (for this study using GeoTide Analyzer 3.0 x 2015) for a particular basin, real time power and energy can be calculated using the RTA model described in Chapter 3.

5.3 Power Generation from A Tidal Barrage of Different Basin Configuration

In calculating power, water levels at both sides of the barrage i.e. at sea side and basin side are assumed horizontal. But in reality, it is not purely horizontal. It depends on hydraulic gradient line (HGL). In a flowing channel, total head is a constant horizontal line. Due to flow volume of water through turbines and gates of a tidal barrage, hydraulic gradient line must varies along the length of the basin or channel. How hydraulic gradient line varies depends on volume of water and length of the basin if other parameters remain same. The terms: energy grade line and hydraulic grade line are frequently used by hydraulic engineers. Let us express each of the terms of the Bernoulli's equation as a head is shown in Figure 5.1.

where,

$$\Delta Z + d_1 + \frac{V_1^2}{2g} = d_2 + \frac{V_2^2}{2g} + h_L \quad (5.3)$$

$$h_L = S_f.\Delta L = \frac{n^2V^2}{R_h^{4/3}}\Delta \mathrm{L} \quad (5.4)$$

where,

ΔZ = Elevation of channel bed;

d_1= depth of the water surface;

V_1= velocity of water at point 1;

d_2= depth of the water surface;

V_2= velocity of water at point 2.

S_o =slope of the bed;

S_f= slope of the energy gradient line;

ΔL= length of the channel

V= velocity of moving water

n= Manning's co-efficient

R= hydraulic radius

EGL= energy gradient line

HGL= hydraulic gradient line= WSL

h_L= head loss due to friction.

In the RTA model it is assumed that tide levels at the sea and the basin are horizontal with respect to time and basin configuration. But in practical it is not horizontal; it varies gradually with respect to time and distance from the turbine/gate openings.

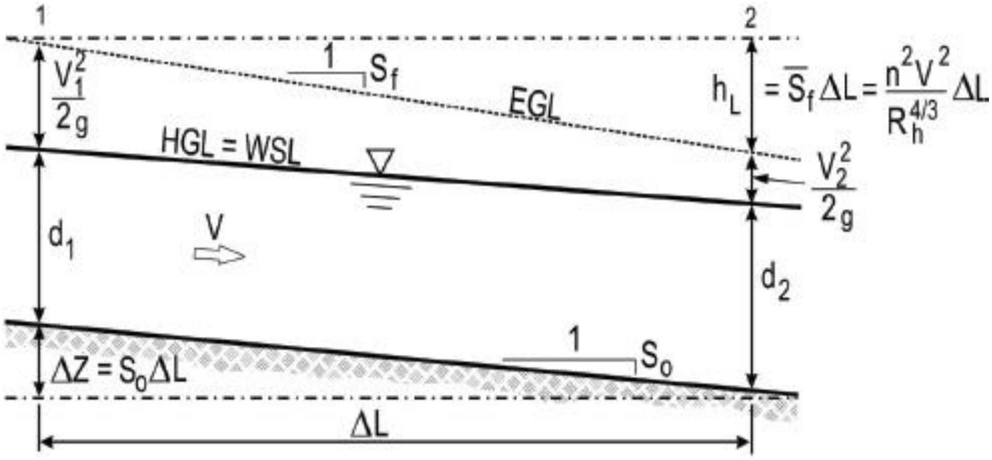

Figure 5.1: Hydraulic gradient lines (HGL) which corresponds to the water surface line (WSL) in a channel. Source: (U.S. Department of Energy, 2013).

In this section, hypothetical basins having area of 90 km^2 with different aspect ratios (w/l ratio) are taken to assess the impact (power generation variations) on tidal power generation using the NAO.99b model (Matsumoto, et al., 2000) .

5.3.1 Configuration/size of the basin

The main aims of this section are to see the impact of basin size on power generation. Let, consider three basins of different aspect ratios (ration of width and length) of (i) 0.9 (width 9 km x length 10 km); (ii) 0.625 (7.5km x length 12km) and 0.4 (width 6 km x 15 km) respectively each of constant water surface area, say, 90km^2. Let the size of openings of three basins be assumed fixed, considered 1/3rd of the least width ≈1/3th of the width of 6 km≈ 2km (say, 5 openings each 0.4 km). Plan view of basins having different aspect ratios with equal plan area of 90 km^2 is shown in Table 5.1.

Table 5.1: Schematic plan view (not in scale) of basins having equal basin area (90 km^2) with different aspect ratios.

Description	Basin area =90 km^2	Basin area =90 km^2	Basin area =90 km^2
Aspect ratio	0.9	0.625	0.4
Basin	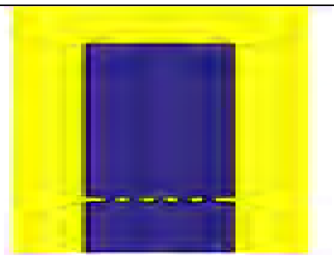	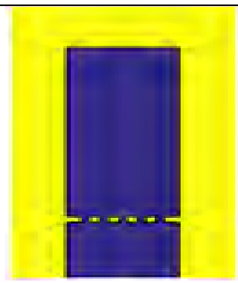	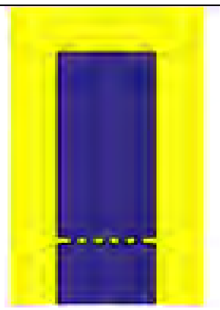
Size	Width=9 km Length=10 km	Width=7.5 km Length=12 km	Width=6 km Length=15 km

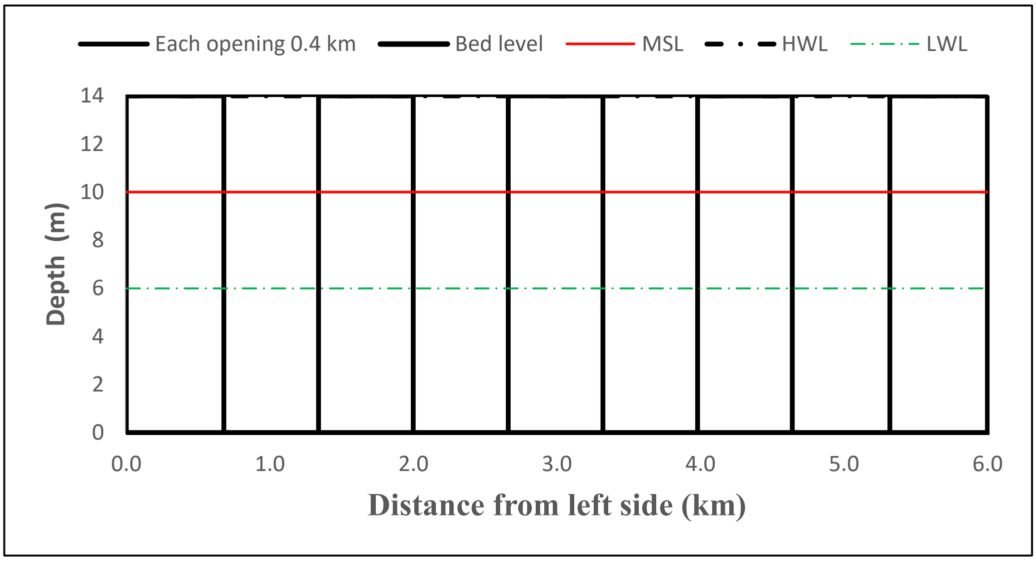

Figure 5. 2: Vertical cross-section of the basin (6 km X 15 km) along openings.

5.3.2 Power generation from a rectangular basin considering horizontal water level at basin and sea.

Let, consider a tide having 4 m tidal amplitude, depth of the basin is 10 m from mean sea level and a constant area 90 km^2. Opening of the basin is 5x0.4 km=2 km.

Let, consider basin openings area same as to turbine effective area which is equivalent to 2 km X water height from bed. So, in this case, turbine opening area is variable with water level due to tidal fluctuations.

Running the RTA model considering continuous generation without gates and ignoring minimum water head requirements for turbine operation, turbine effective area is taken equivalent to openings of the basin openings, we get time series basin's water level which is shown in Figure 5.3.

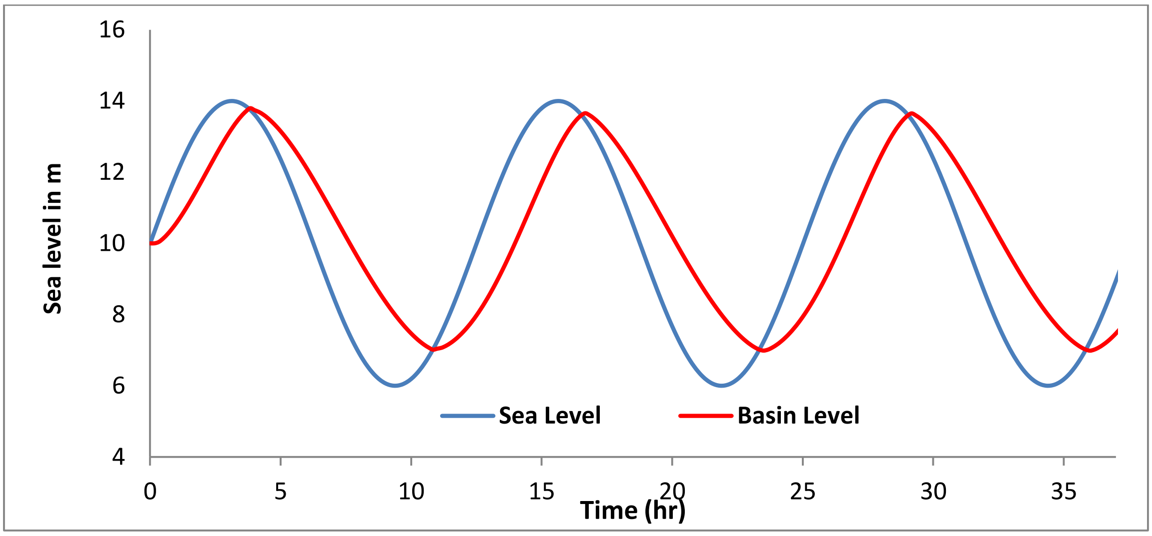

Figure 5. 3: Water levels at sea side and basin side considering water levels are horizontal.

Sea water is considered a sinusoidal curve having tidal period of 12.5 hours with phase angle δ=0. From RTA model the results are shown in Table 5.2.

Table 5. 2: Tidal power for a rectangular basin considering water levels horizontal at sea and the basin.

Serial Number	Parameters	Considering water levels are horizontal	
			Results
1	Power, P	Mean P (MW)	782
2		Max P (MW)	1815
3		Min P (MW)	0.07
4	Energy, E	(GWh) for 4 tidal cycles	32.60
5	Flow rate, Q	Mean Q (m^3/s)	105734
6		Max Q (m^3/s)	169355
7		Min Q (m^3/s)	3706
8	Head, h	Mean h (m)	1.59
9		Max h (m)	2.72
10		Min h (m)	0.00
11	Tidal range of the basin R (m)		6.81

5.3.3 Power generation from a rectangular basin having aspect ratio 0.9

For comparison purpose, let us consider same (i) tide (4 m amplitude), (ii) depth of the basin (10 m from mean sea level) and (iii) basin area (90 km^2). Opening of the basin is 5@ 0.4 km=2 km. Let, assume turbine effective area is equivalent to 2 km X water height from bed. Time series water level inside and outside the barrage for a basin having aspect ratio 0.9 are computed using the NAO.99b model (Matsumoto, et al., 2000) is shown in Figure 5.4.

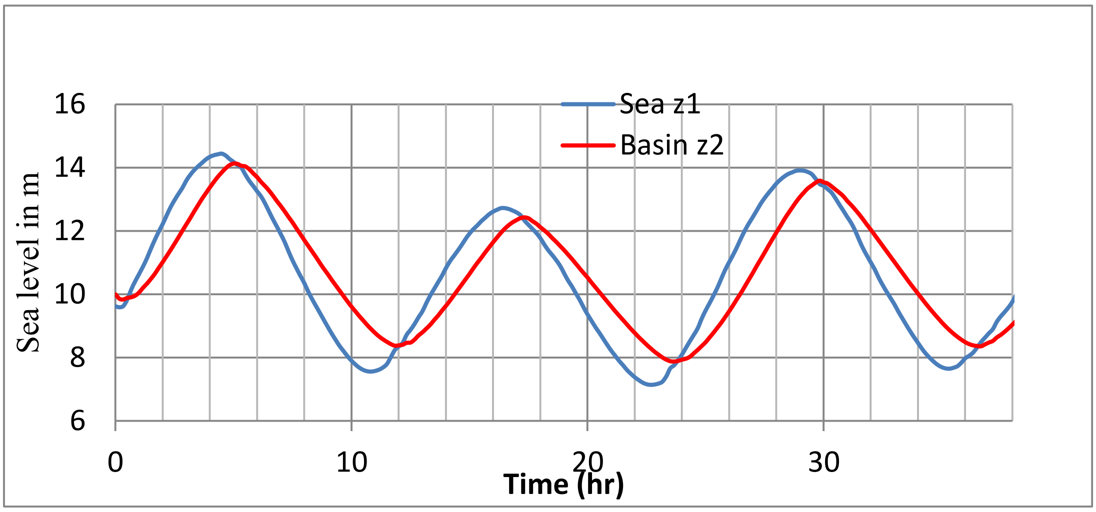

Figure 5. 4 Time series water levels inside and outside the barrage openings for aspect ratio 0.9.

Time series water head is also calculated taking the computed water levels based on which power and energy are calculated using the RTA model. It is assumed that generation is continuous without gates and basin openings area is considered as turbine effective area (omitting minimum water head for turbine operation). The results are shown in Table 5.3.

Table 5. 3: Tidal power for a rectangular basin having aspect ratio 0.9 and taking water levels computed from NAO.99b model.

Serial Number	Parameters	Considering water levels are horizontal	
			Results
1	Power	Mean P (MW)	356
2		Max P (MW)	955
3		Min P (MW)	0.72
4	Energy	For 4 tidal cycles (GWh)	14.82
5	Flow rate Q	Mean Q (m^3/s)	81723
6		Max Q (m^3/s)	136353
7		Min Q (m^3/s)	8930
8	Head H	Mean h (m)	0.94
9		Max h (m)	1.77
10		Min h (m)	0.02
11	Tidal range basin R (m)		6.81

5.3.4 Power generation from a rectangular basin having aspect ratio 0.625

For comparison purpose, let us consider same (i) tide (4 m amplitude), (ii) depth of the basin (10 m from mean sea level) and (iii) basin area (90 km^2). Opening of the basin is 5@ 0.4 km=2 km. Let, assume turbine effective area is equivalent to 2 km X water height from bed. Time series water level inside and outside the barrage for a basin having aspect ratio 0.625 are computed using the NAO.99b model (Matsumoto, et al., 2000) is shown in Figure 5.5.

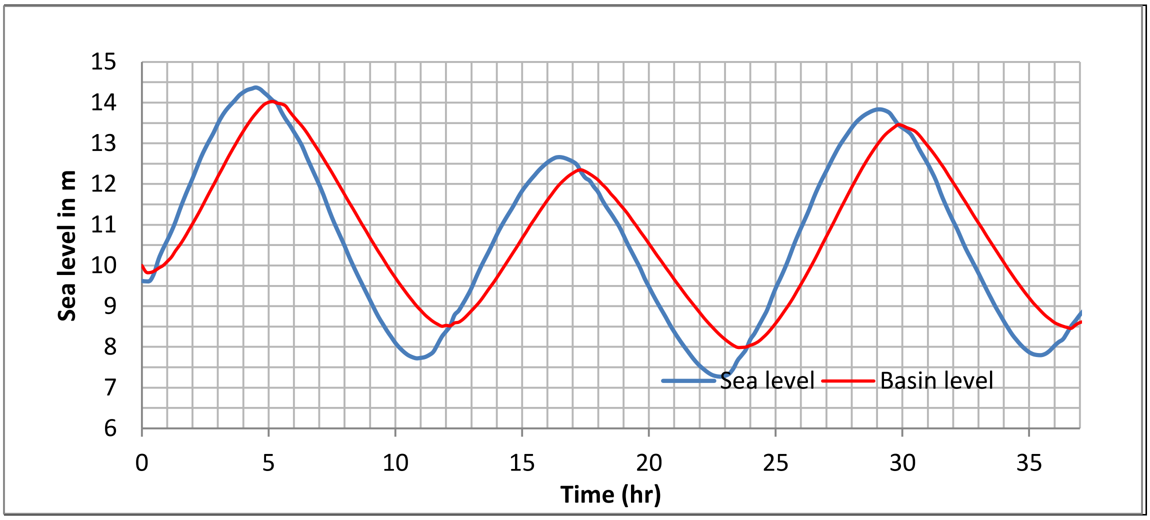

Figure 5. 5: Time series water levels inside and outside the barrage openings for aspect ratio 0.625.

Time series water head is also calculated taking the computed water levels based on which power and energy are calculated using the RTA model. It is assumed that generation is continuous without gates and basin openings area is considered as turbine effective area (omitting minimum water head for turbine operation). The results are shown in Table 5.4.

Table 5. 4: Tidal power for a rectangular basin having aspect ratio 0.625 and taking water levels computed from NAO.99b model.

Serial Number	Parameters	Considering water levels are horizontal	
			Results
1	Power	Mean P (MW)	318
2		Max P (MW)	842
3		Min P (MW)	-
4		Energy for 4 tidal cycles (GWh)	13.251
5	Flow rate Q	Mean Q (m^3/s)	78532
6		Max Q (m^3/s)	130300
7		Min Q (m^3/s)	-
8	Head H	Mean h (m)	0.87
9		Max h (m)	1.62
10		Min h (m)	0.00
11	Tidal range basin R (m)		6.81

5.3.5 Power generation from a rectangular basin having aspect ratio 0.40

For comparison purpose, let us consider same (i) tide (4 m amplitude), (ii) depth of the basin (10 m from mean sea level) and (iii) basin area (90 km^2). Opening of the basin is 5@ 0.4 km=2 km. Let, assume turbine effective area is equivalent to 2 km X water height from bed. Time series water level inside and outside the barrage for a basin having aspect ratio 0.40 are computed using the NAO.99b model (Matsumoto, et al., 2000) is shown in Figure 5.6.

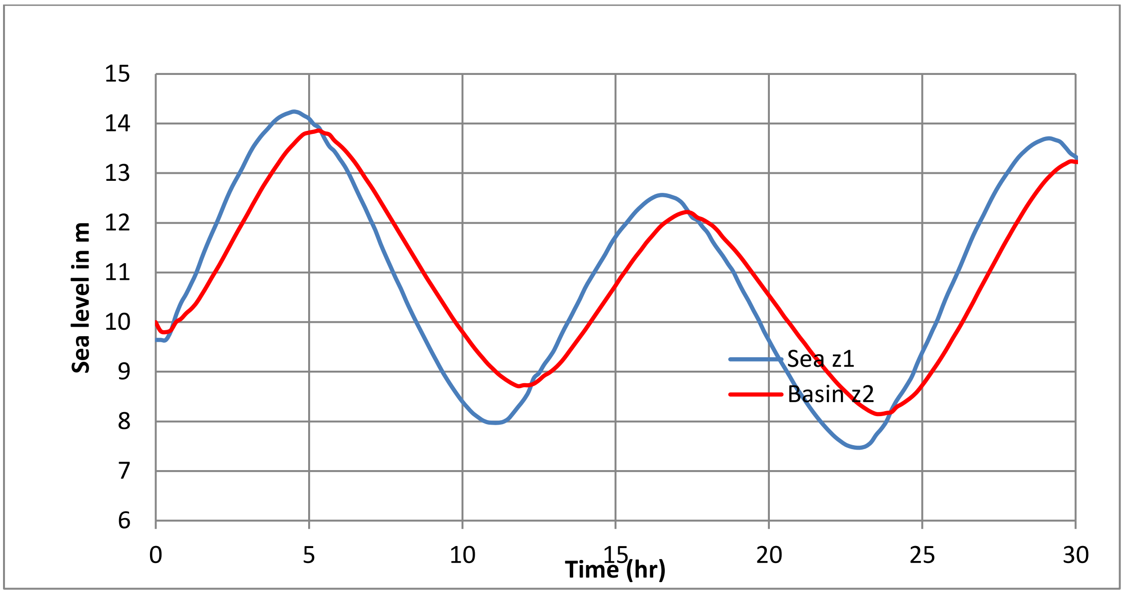

Figure 5. 6: Time series water levels at basin and sea side having aspect ratio 0.40.

Time series water head is also calculated taking the computed water levels based on which power and energy are calculated using the RTA model. It is assumed that generation is continuous without gates and basin openings area is considered as turbine effective area (omitting minimum water head for turbine operation). The results are shown in Table 5.5.

Table 5. 5: Results for a rectangular basin having aspect ratio 0.4 and taking water levels computed from NAO.99b model.

Serial Number	Parameters	Considering water levels are horizontal	
			Results
1	Power	Mean P (MW)	257
2		Max P (MW)	663
3		Min P (MW)	0.42
4	Energy	For 4 tidal cycles (GWh)	10.720
5	Flow rate Q	Mean Q (m^3/s)	73161
6		Max Q (m^3/s)	119633
7		Min Q (m^3/s)	10524
8	Head H	Mean h (m)	0.76
9		Max h (m)	1.41
10		Min h (m)	0.01
11	Tidal range basin R (m)		6.81

5.3.6 Comparison of results considering horizontal and non-horizontal shallow water levels

The results obtained from section 5.3.2 to 5.3.5 for a tidal basin having same basin area of 90 km^2 and same tidal amplitude of 4 m for a rectangular basin (a) considering water level horizontal both at the basin and the sea: no variation irrespective of aspect ratio; and (b) considering non-horizontal shallow water levels using the NAO.99b model (Matsumoto, et al., 2000) for different aspect ratios such as (i) aspect ratio 0.9, (ii) aspect ratio 0.625 and aspect ratio 0.4 respectively.

The comparative time series water heads are shown in Figure 5.7.

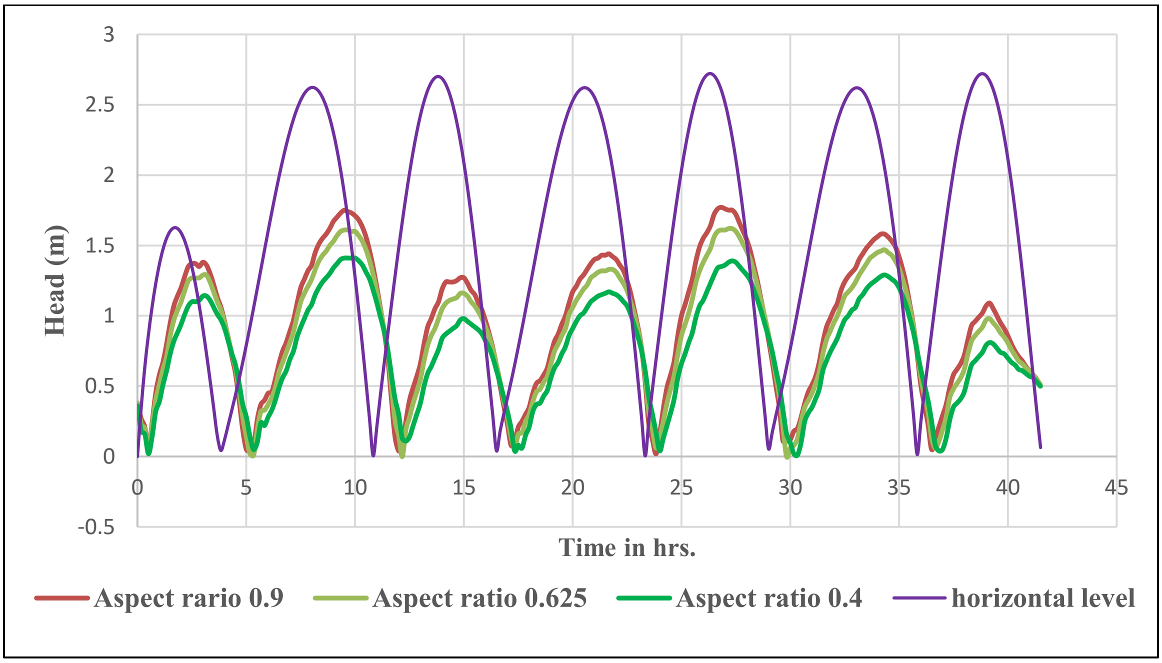

Figure 5. 7: Time series water head variations considering horizontal and non-horizontal shallow water levels with different aspect ratios.

From Figure 5.7, it is evident that time series water head calculated considering water level horizontal at sea and the basin is higher than water head computed for different aspect ratios (0.9, 0.625 and 0.40 respectively) from NAO.99b model. Since power is proportionately varies with head squared (h^2), so power calculated considering horizontal water level would be higher than power generation for different basin configurations.

Table 5. 6: Comparison of results (i) considering water level horizontal at sea and the basin and (ii) considering non-horizontal shallow water level at sea and the basin computed from NAO.99b model for different aspect ratios.

Basin size	90 km^2	9X10	7.5X12	6X15
Basin area	90 km^2	90 km^2	90 km^2	90 km^2
Aspect ratio	irrespective	0.9	0.625	0.4
Mean Power, MW	782	356	318	257
	100%	45%	41%	33%
Energy per Cycle, GWh	32.603	14.816	13.251	10.720
	100%	45%	41%	33%
Max. head, (m)	2.72	1.77	1.62	1.41
	100%	65%	60%	52%
Tidal range basin (m)	6.81	6.25	6.04	5.71
	100%	92%	89%	84%

From Table 5.6 it is observed that mean power and energy reduces with the decrease of aspect ratios. If we consider horizontal water level at both sides of the barrage, both mean power and energy are higher than that of non-horizontal shallow water levels for different aspect ratios. If we consider horizontal water levels at sea and basin, energy output is 32.603 GWh where as it decreases to 14.816 GWh (45%), 13.251GWh (41%) and 10.720 GWh (33%) respectively for aspect ratio of 0.9, 0.625 and 0.40. Mean power variations and energy generation variations are shown in Figure 5.8 and Figure 5.9 respectively.

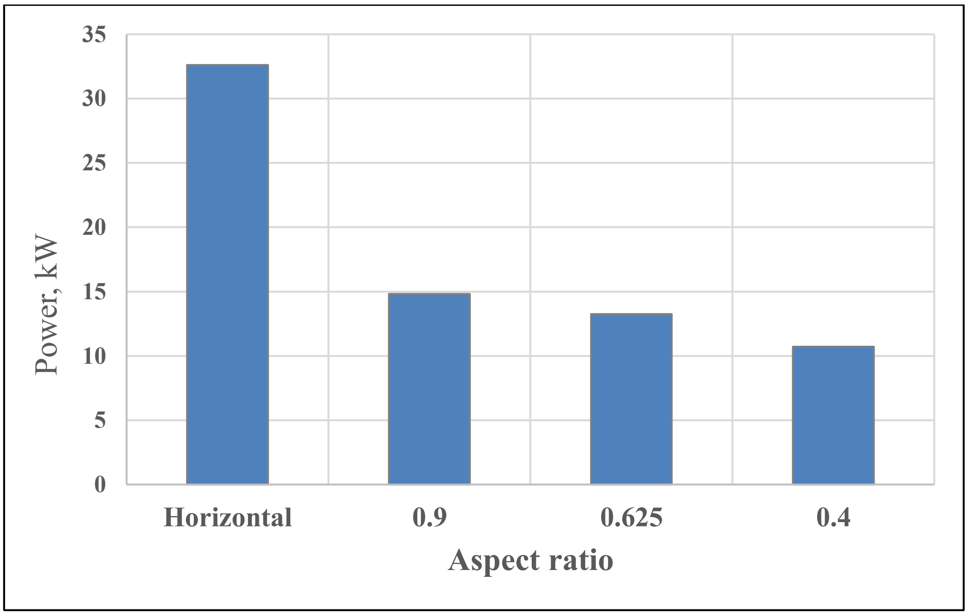

Figure 5. 8: Power generation variations considering (i) water level horizontal and (ii) non-linear water level with different aspect ratios.

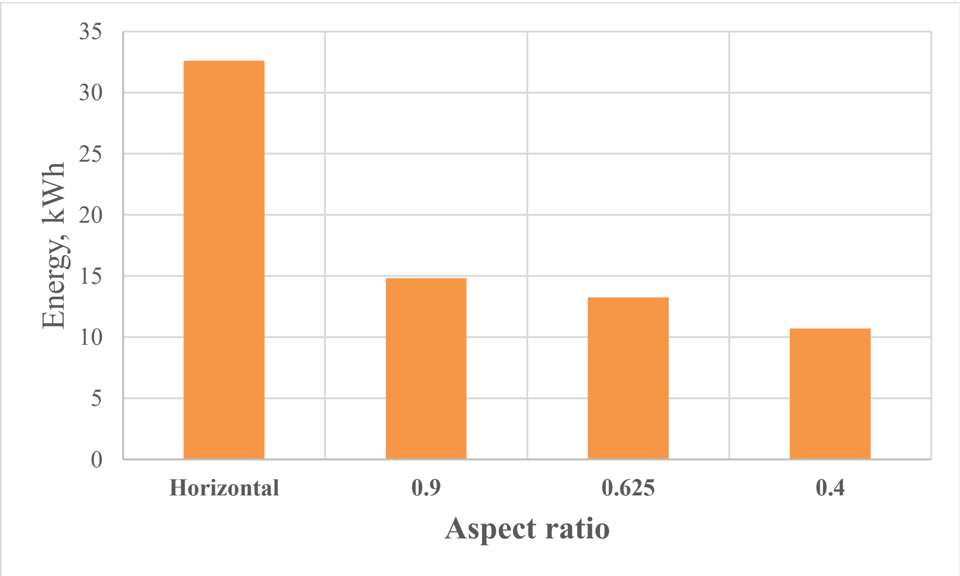

Figure 5. 9: **Energy generation variations considering (i) water level horizontal and (ii) non-linear water level with different aspect ratio**s.

From Figure 5.8 and Figure 5.9, it is clear that power and energy decreases as aspect ratio decreases and it is lower compare to that of we calculates considering horizontal water levels.

Again, one thing should be clear that water levels computed using NAO.99b model where flow is continuous, openings are vertically open and water opening heights are variable with changing water levels, whereas water levels computed from RTA model where turbines are kept submerged, turbine position is fixed, effective area is fixed and minimum head requirements are opted to protect the turbines- which is not exactly similar condition for water flow considered in the NAO.99b model. It would be better if NAO.99b model is applied for a barrage system to see the water level variations. If it would have done then we could get the clear idea about water level variations at sea and the basin for a tidal barrage system which is absent and is not considered in this study.

So, running the RTA model taking the water levels from the NAO.99b model for different aspect rations, the results we get, might be, to some extent, indicative and qualitative. Actual variation will be lesser than what we get from NAO.99b model as water flowing condition in the NAO.99b model and water flowing system in a tidal barrage system is different.

But, it could be concluded that water levels at sea and the basin are not exactly horizontal, it varies with aspect ratios. Higher the aspect ratio, higher is the water head for power generation. So, in selecting a tidal basin or a tidal barrage it is always important to remember that basin with higher aspect ratio will yield higher energy output.

5.4 Power Generation from Tidal Barrages of Different Vertical Shapes.

In this section, the attempt is focused on the impact of different vertical shapes of the basins on power generation. Emphasis is given on vertical section of rectangular shape, trapezoidal shape and parabolic shape.

5.4.1 Power generation from a vertical shape rectangular basin considering horizontal water levels at the basin and sea

Let, width of the basin = b; water elevation of the basin at any time (t) = Z; and length of the basin = L

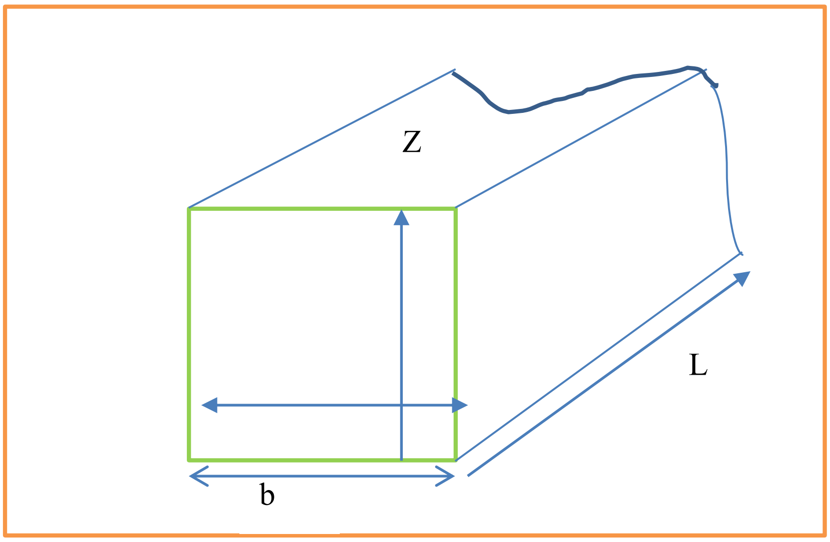

Figure 5. 10: Sketch of a rectangular basin.

So, water surface area of the basin is constant,

A_b= bL (5.5)

Since the values of b and L of a rectangular basin is constant, so, Equation. (5.2) will be expressed as A_b= b.L=constant; which can be expressed as Equation. (5.3)

A_b= Constant ≈ a_0 (5.6)

If we put the values of coefficients a_1, a_2, a_3, a_4, a_5……of the Eqn. (5.1) as zero (0) and b=1 km and L=5 km, then Equation. (5.1) will turn into

$A_b = a_0$ i.e.

$A_b = a_0$ =5 X 10^6. m^2 (5.7)

If the volume of water of the rectangular basin is V_{Rb} , then

V_{Rb}= bLZ (5.8)

5.4.1.1 Input tidal data for RTA model for a tidal basin having vertical section of rectangular shape

The following data (Table 5.7) are assumed to be the input tidal data.

Table 5.7: Input tidal data for a rectangular basin.

Sl. No.	Parameters	Semi-diurnal Lunar Tide	Semi-diurnal Solar Tide
1.	Symbol	M_2	S_2
2.	Tidal Period, T	12.42	12.00
3.	Speed (rad/hr)	0.5059	0.5236
4.	Amplitude, a (m)	3.15	0.95
5.	Phase angle, δ (degree)	0	0
6.	Datum shift from MSL, a_o (m)	0	0

5.4.1.2 Input parameters for a tidal basin having vertical section of rectangular shape for RTA model

Let, assume tidal range, R=2a= =2x (3.15+0.95) =2 x 4.1=8.2 m. So, area of the basin, A_b= b.L=5 km^2= 5,000,000 m^2. Volume of the basin (water enters during high tide) =5,000,000 m^2 x 8.2 m =41,000,000m^3.

5.4.1.3 Power generation for a tidal basin having vertical section of rectangular shape using RTA model

Putting the input tidal data and basin parameters in the RTA model, we get the results which is shown in Table 5.8. The turbine diameter is taken 4m each (2.25 MW) and sluice gates each 12m x12m size is taken.

Table 5. 8: Energy from the rectangular basin (ebb generation).

Nos. of turbine	Nos. gates	Power (MW)	Energy (GWh)	Nos. of turbine	Nos. gates	Power (MW)	Energy (GWh)
10	10	61.00	121.62	20	25	87.08	163.64
10	15	60.87	125.89	20	30	86.90	165.49
10	25	60.69	130.35	20	35	86.88	164.02
10	30	60.56	130.10	25	10	98.00	150.93
10	35	60.95	134.04	25	15	98.09	154.82
15	10	76.00	148.71	25	25	98.03	155.93
15	15	76.08	153.36	25	30	98.03	162.29
15	25	75.89	158.92	25	35	98.11	155.81
15	30	76.02	158.53	30	10	115.00	141.82
15	35	75.81	160.13	30	15	114.98	145.24
20	10	87.00	155.84	30	25	114.96	145.76
20	15	87.22	160.90	30	30	114.96	151.36
20	25	87.08	163.64	30	35	115.13	145.79

The results are plotted in Figure 5.11 and Figure 5.12.

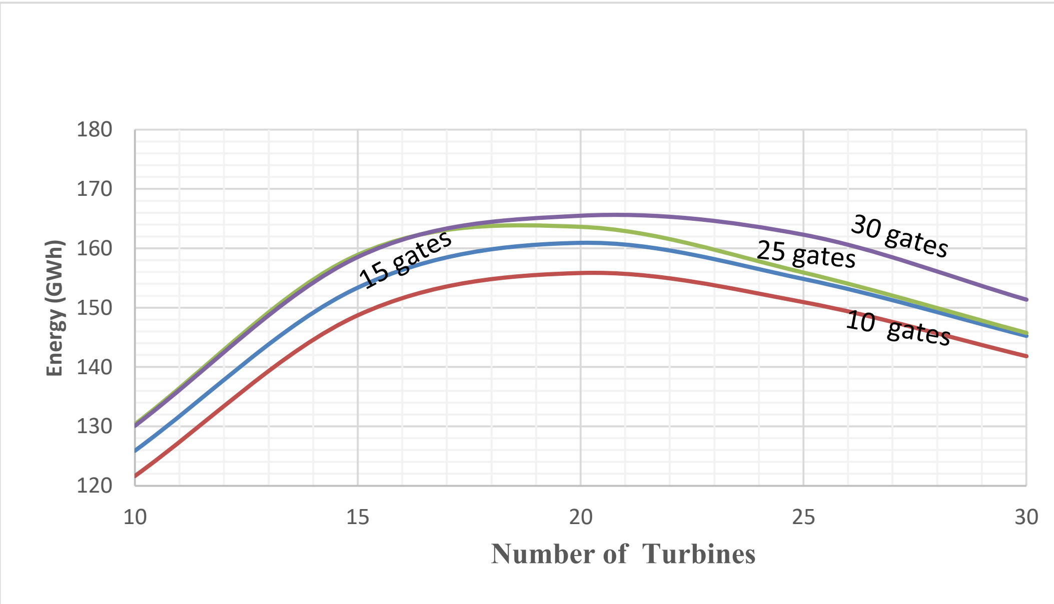

Figure 5. 11: Energy generation from a vertical shape rectangular basin considering horizontal water level.

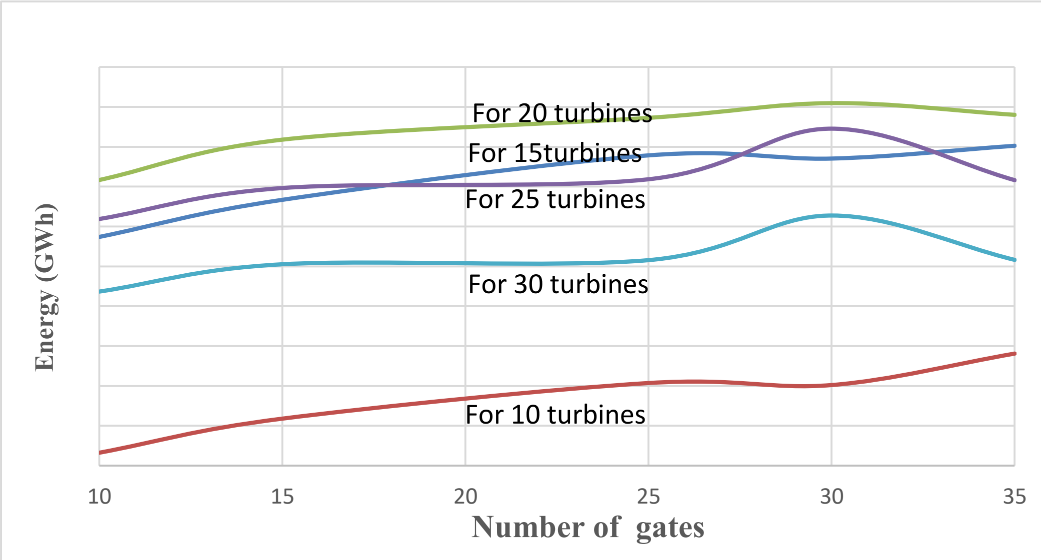

Figure 5. 12: Energy generation from a vertical shape rectangular basin considering water level horizontal.

From Figure 5.11 and Figure 5.12, it is evident that 20 nos. turbines each 4 m dia. (2.25 MW) and 30 nos. sluice gates (each 12m x12m) will yield maximum annual energy output 165.49 GWh with a maximum capacity of 86.90 MW for the rectangular basin with inputs mentioned in Article 5.4.1.1 and 5.4.1.2.

5.4.2 Power generation from vertical shape trapezoidal basin considering horizontal water levels at the basin and sea

5.4.2.1 Parameters of the trapezoidal basin

Figure 5. 13: Sketch of a vertical shape trapezoidal basin.

Let, assume that the trapezoidal basin with similar tidal range R=2a, width of the basin at lowest water level is b_1 and slope of the side is 1: **s** and length of the basin is L.

Let, consider a trapezoidal basin having same water volume between LWL and HWL as like as a rectangular basin within the same tidal range.

If the volume of the of the trapezoidal basin between LWL and HWL is V_{Tb}, then

$$V_{Tb} = [b_1 + (b_1 + 2sZ)]/2.\ ZL \quad (5.9)$$

Since volume of the rectangular basin and volume of trapezoidal basin are considered equal, so from eqn. (5.3) and (5.4) we get,

$$bZL = [b_1 + (b_1 + 2sZ)] /2\ ZL \quad (5.10)$$

where Z =R=tidal range

From Eqn. (5.5) we get,

$$b = b_1 + sR \quad (5.11)$$

$$\text{Or, } b_1 = b - sR \quad (5.12)$$

In article 5.4.1, it is assumed b=1 km= 1000m, L=5 km =5000m and tidal range R=8.2 m.

$$\text{So, } b_1 = 1000 - 8.2s \quad (5.13)$$

Taking different values for slope (s), we will get different types of trapezoidal shape of equal volume of water.

Table 5. 9: Water surface area for of the trapezoidal basin for different side slopes (s).

Side Slope, s	Width ($b1 = b-8.2s$) (m)	Water level Z (m)	Equation of surface area, A_{tb} (km^2) w.r.t. water level (Z in m)	Water surface area of trapezoidal basin $A_{tb}=(b1+2sZ)L$ (km^2) (L in km).
0.5	995.9	2	$A_{tb}= 0.005Z + 4.9795$ **Equation (5.14)**	4.9895
0.5	995.9	4.1		5.0000
0.5	995.9	6		5.0095
0.5	995.9	8		5.0195
0.5	995.9	10		5.0295
1.0	991.8	2	$A = 0.01Z + 4.959$ **Equation (5.15)**	4.9790
1.0	991.8	4.1		5.0000
1.0	991.8	6		5.0190
1.0	991.8	8		5.0390
1.0	991.8	10		5.0590
1.5	987.7	2	$A = 0.015Z + 4.9385$ **Equation (5.16)**	4.9685
1.5	987.7	4.1		5.0000
1.5	987.7	6		5.0285
1.5	987.7	8		5.0585
1.5	987.7	10		5.0885
2.0	983.6	2	$A = 0.02Z + 4.918$ **Equation (5.17)**	4.9580
2.0	983.6	4.1		5.0000
2.0	983.6	6		5.0380
2.0	983.6	8		5.0780
2.0	983.6	10		5.1180

From Table 5.9, it is observed that water surface area at different water level (Z) varies depending on side slope of the trapezoidal section.

5.4.2.2 Input parameters for a vertical shape trapezoidal basin for RTA model

Let, assume input tidal data as shown in Table 5.10.

Table 5. 10: Input tidal data for trapezoidal basin.

Sl. No.	Parameters	Semi-diurnal Lunar Tide	Semi-diurnal Solar Tide
1.	Symbol	M_2	S_2
2.	Tidal Period, T	12.42	12.00
3.	Speed (rad/hr)	0.5059	0.5236
4.	Amplitude, a (m)	3.15	0.95
5.	Phase angle, δ (degree)	0	0
6.	Datum shift from MSL, a_o (m)	0	0

5.4.2.3 Power generation from a vertical shape trapezoidal basin (slope, s=0.5).

Putting the input tidal data and basin parameters in the RTA model, we get the results shown in the Table 5.11. The turbine diameter is taken 4 m each (2.25 MW) and sluice gates 12 m x12 m each.

Table 5. 11: Energy from a vertical shape trapezoidal basin (slope, s=0.5) (ebb generation).

Sl. No.	Nos. Turbine	No. Sluice	Capacity (MW)	Energy (GWh)	Nos. Turbine	No. Sluice	Capacity (MW)	Energy (GWh)
1	15	20	76	155.11	25	40	98	160.90
2	15	30	76	158.26	25	50	98	164.71
3	15	40	76	166.73	25	60	98	150.39
4	15	50	76	157.16	30	20	115	145.16
5	15	60	77	155.32	30	30	115	150.84
6	20	20	87	162.26	30	40	115	**150.13**
7	20	30	87	164.86	30	50	115	154.35
8	20	40	87	170.13	30	60	116	141.11
9	20	50	87	166.96	35	20	133	138.48
10	20	60	86	158.82	35	30	133	143.64
11	25	20	98	155.32	35	40	133	142.83
12	25	30	98	161.47	35	50	134	145.88
13	25	40	98	160.90	35	60	135	135.023

The results are plotted in Figure 5.14 and Figure 5.15

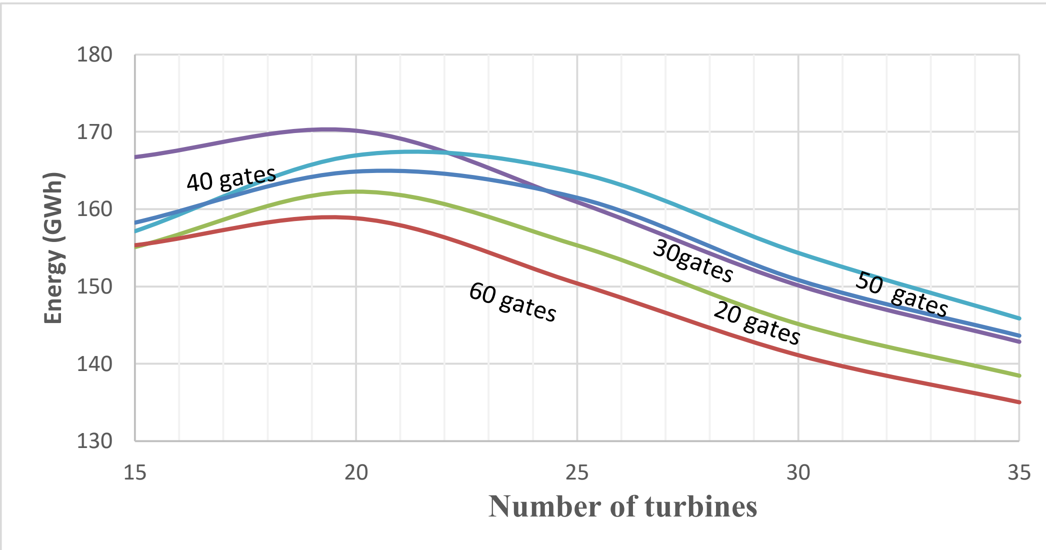

Figure 5. 14: Energy generation from a vertical shape trapezoidal basin (s=0.5) as a function of turbines with different gates.

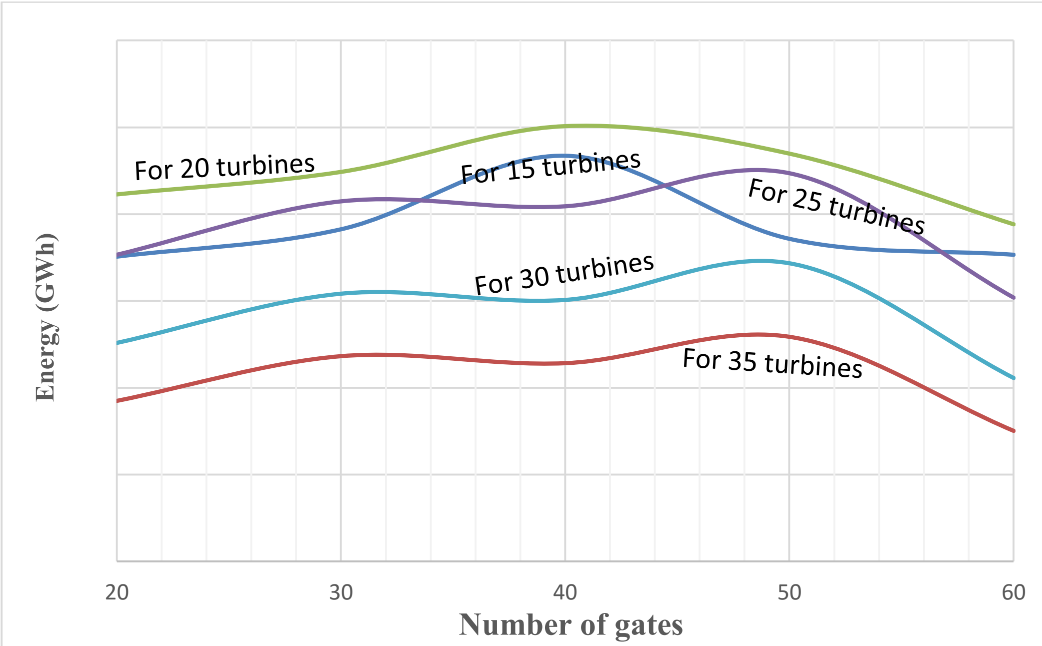

Figure 5. 15: Energy generation from a vertical shape trapezoidal basin (s=0.5) as a function of gates with different turbines.

From Figure 5.14 and Figure 5.15 it is evident that 20 nos. turbines each 4m dia. (2.25 MW) and 40 nos. sluice gates (each 12m x12m) will yield maximum annual energy output 170 GWh with a maximum capacity of 87MW for a trapezoidal basin (s=0.5) with inputs mentioned in Table 5.9 and Table 5.10.

5.4.2.4 Power generation from a vertical shape trapezoidal basin (side slope, s=2.0) considering water level horizontal.

Putting the input tidal data and basin parameters of a trapezoidal basin having side slope s=2.0 in the real time analytical model, we get the results shown in the Table 5.12. The turbine diameter is taken each 4m (2.25 MW) and sluice gates each 12m x12m and other parameters similar that taken for the rectangular basin.

Table 5. 12: **Energy from the trapezoidal basin for slope, s=2.0 (ebb generation).**

Sl. No.	Nos. Turbine	No. Sluice	Energy (GWh)	Capacity (MW)	Nos. Turbine	No. Sluice	Energy (GWh)	Capacity (MW)
1	15	20	129.73	76.38	25	20	135.05	98.55
2	15	30	129.30	76.51	25	30	134.84	98.56
3	15	40	129.27	76.38	25	40	134.57	98.60
4	15	50	127.11	76.36	25	50	133.55	98.69
5	20	20	135.06	87.66	30	20	132.52	115.06
6	20	30	134.77	87.67	30	30	132.34	115.08
7	20	40	134.66	87.82	30	40	132.07	115.46
8	20	50	133.68	87.77	30	50	130.95	115.26

The results are plotted in Figure 5.16 and Figure 5.17

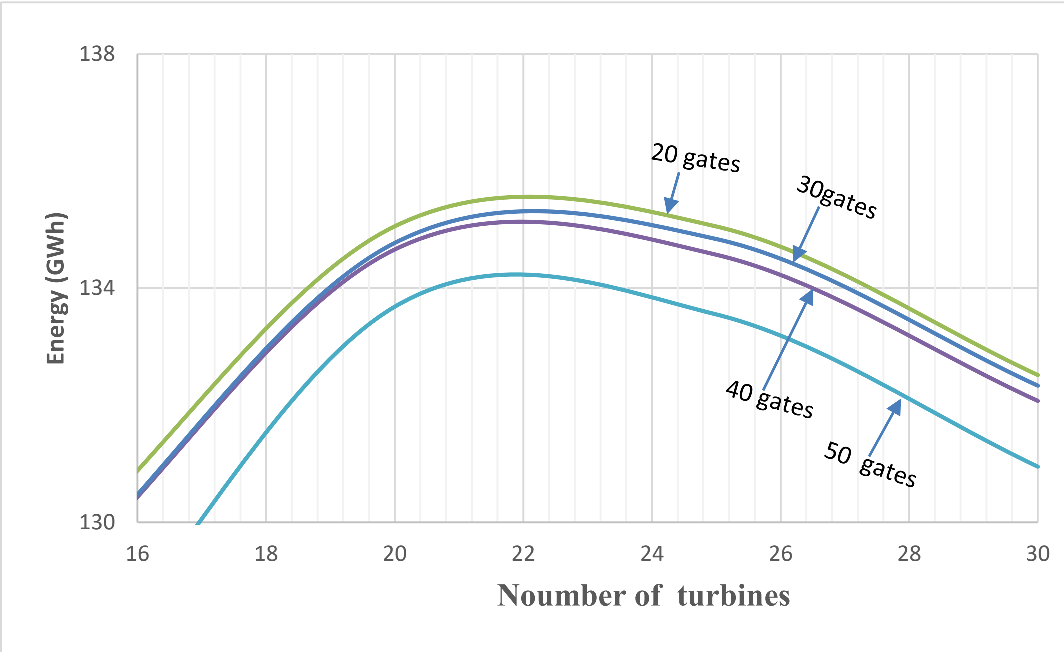

Figure 5.16: Energy generation from a vertical shape trapezoidal basin (slope s=2.0) as a function of turbines with different gates.

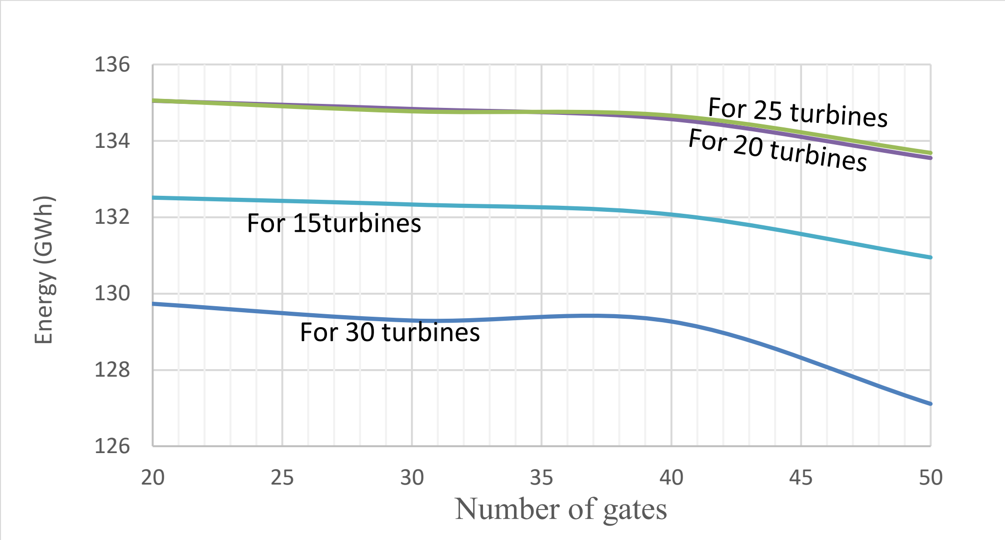

Figure 5. 17: Energy generation from a vertical shape trapezoidal basin (slope, s=2.0) as a function of gates with different turbines.

From Figure 5.16. and Figure 5.17, it is evident that 22 nos. turbines each 4 m dia. (2.25 MW) and 20 nos. sluice gates (each 12 m x12 m) will yield maximum annual energy output 135 GWh with a maximum capacity of 92 MW for the trapezoidal basin for s=2.0 with inputs mentioned in Article 5.4.2.1 and 5.4.2.2.

5.4.3 Power generation from a vertical shape parabolic basin considering horizontal water levels at the basin and sea

5.4.3.1 Parameters of a parabolic basin

Consider a parabolic basin having same volume as like as a rectangular basin within the same tidal range. Let, assume a parabolic basin with same tidal range R=2a.

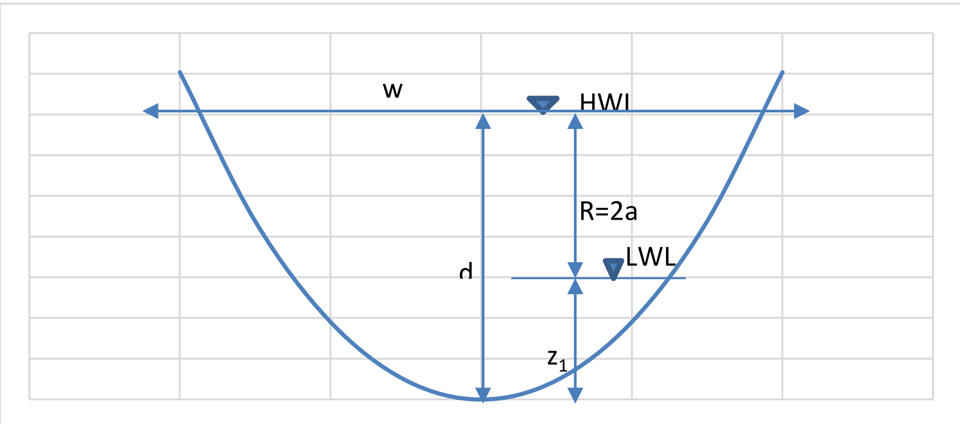

Figure 5. 18: Cross section of a parabolic basin.

If, cross sectional area of a parabolic basin is A_p, then,

$$A_p = \frac{2W}{3}d \tag{5.18}$$

Source: (Chow, 2013-2014)

where,

Ap= cross sectional area of a parabolic section;

w= width of the section; and

d= depth of the section.

Let, volume of the parabolic basin is Vp within the LWL and HWL, then

$$V_p = \frac{2Wd}{3}.L \tag{5.19}$$

where,

Vp= volume of the of the parabolic basin;

w= top width of the parabolic section; and

d= depth for which area of the cross section is A_P.

As tidal water varies between level Z_1 (LWL) to Z_2 (HWL)

$$\text{So, } Z_2 - Z_1 = R = 2a \tag{5.20}$$

From Table 5.1. and Table 5.4, we get.

$$Z_2 - Z_1 = R = 8.2 \text{ m} \tag{5.21}$$

where, Z_1= water level at LWH;

Z_2= water level at HWL;

a= tidal amplitude; and

R= tidal range.

If A_2 is the cross-sectional area of the parabolic section at level Z_2, A_1 is the cross-sectional area of the parabolic section at level Z_1 & w_2 and w_1 are water surface widths at level Z_2 and Z_1 , then According to Chow (2013-14)

$$A_2 = \frac{2w_2Z_2}{3} \tag{5.22}$$

$$A1 = \frac{2w_1Z_1}{3} \tag{5.23}$$

and

$$Z_2 = Z_1 + 8.2 \tag{5.24}$$

Subtracting Eqn. (5.16) and Eqn. (5.17) we can get cross-sectional area (A) of the parabolic section between level HWL and LWL. Then,

$$A = A_2 - A_1 = \frac{2}{3}[w_2 Z_2 - w_1 Z_1] \tag{5.25}$$

Volume of the tidal water enters into a parabolic basin in high tide or exit at low tide is Vw. Then,

$$Vw = A.\ L = [A_2 - A_1].\ L = \frac{2}{3}[w_2 Z_2 - w_1 Z_1].L \tag{5.26}$$

where, L= length of the parabolic basin.

Since the volume of the rectangular basin and volume of the parabolic basin between HWL and LWL are considered equal for comparison purpose, then from eqn. (5.3) and (5.19) we get:

$$bRL = \frac{2}{3}[w_2 Z_2 - w_1 Z_1].L \tag{5.27}$$

$$\text{So,} \quad bR = \frac{2}{3}[w_2 Z_2 - w_1 Z_1]. \tag{5.28}$$

where,

b= width of the rectangular basin;

L= length of the basin; and

W_1 anW$_2$ are the width of the parabolic basin at level Z_1 (LWL) and Z_2 (HWL).

5.4.3.2 Input tidal data for parabolic basin

Let assume same input tidal data taken for a rectangular basin shown in Table 5.13.

Table 5. 13: Input tidal data for trapezoidal basin.

Sl. No.	Parameters	Semi-diurnal Lunar Tide	Semi-diurnal Solar Tide
1.	Symbol	M_2	S_2
2.	Tidal Period, T	12.42	12.00
3.	Speed (rad/hr)	0.5059	0.5236
4.	Amplitude, a (m)	3.15	0.95
5.	Phase angle, δ (degree)	0	0
6.	Datum shift from MSL, a_o (m)	0	0

5.4.3.3 Calculation of parameters for a vertical shape parabolic basin

R= tidal range= HWL-LWL= Z_2-Z_1= 8.2 m

In Article **5.4.1**, we have assumed, b=1 km= 1000 m, L=5 km =5000 m for the rectangular basin. So, from Equation (5.28) we get:

$$\frac{2}{3}[w_2 Z_2 - w_1 Z_1] = b.R = 1000x8.2 = 8200 \quad (5.29)$$

From Eqn. (5.24) and (5.25), we can write

$$\frac{2}{3}[w_2(z_1 + 8.2) - w_1 Z_1] = 8200 \quad (5.30)$$

In Equation. (5.26) W_1, W_2, Z_1 are three unknown variable parameters which combinedly results such a cross-section of a parabolic basin of 8200m^2. From Eqn. (5.23) we can write:

$$\therefore w_2 = (12300 + w_1 Z_1)/(z_1 + 8.2) \quad (5.31)$$

Assuming a value for Z_1 (at LWL), we can get different sets of value for w_2 and w_1. Let assume an initial value of Z_1= 10.0 (LWL), then from Eqn. (5.31) we get:

$$\therefore w_2 = (12300 + 10w_1)/18.2 \quad (5.32)$$

For different values of Z_1 (LWL) with tidal range (Z_2-Z_1) of 8.2m, we can get a set of top widths of the parabolic section which are shown in the Table 5.14

Table 5. 14: Parameters of a parabolic section having equal area of a rectangular section and same tidal range.

Water level	Z (m)	w width (m)	Area of parabolic section, A (m^2) from bottom.	Eqn. for width at different levels for (Z_1=10m)	Remarks
Z_0	0	0	0	For W_1=400m W= 1.123 Z^2 + 28.77 Z - 9E-13 **Equation (5.33)**	Shown in Figure 5.19
Z_1 (LWL	10.0	400.0	2667		
Z_2 (HWL)	18.2	895.6	10867		
Z_0	0	0	0	For W1 =600m W= -0.5796 Z^2 + 65.796 Z - 2E-12 **Equation (5.34)**	-
Z_1 (LWL	10.0	600.0	4000		
Z_2 (HWL)	18.2	1005.5	12200		

Parameters of a vertical shape parabolic shape basin having equal area of a rectangular basin within same tidal range whose parameters mentioned in Table 5.14 are presented in Figure 5.19 and Figure 5.120.

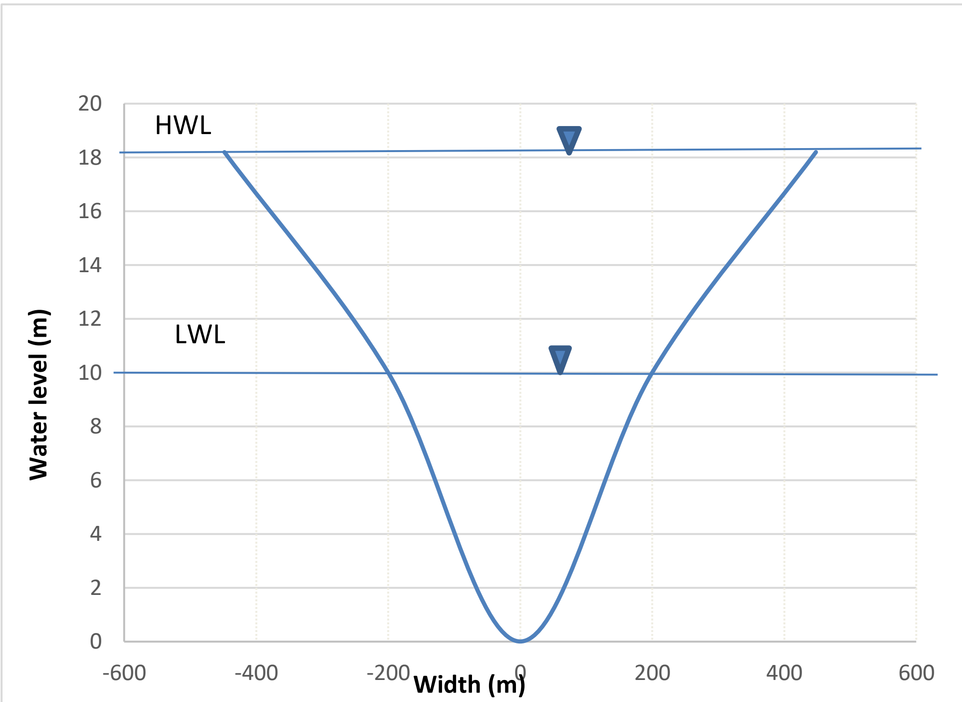

Figure 5. 19: Cross section of a vertical shape parabolic basin from equation (5.33).

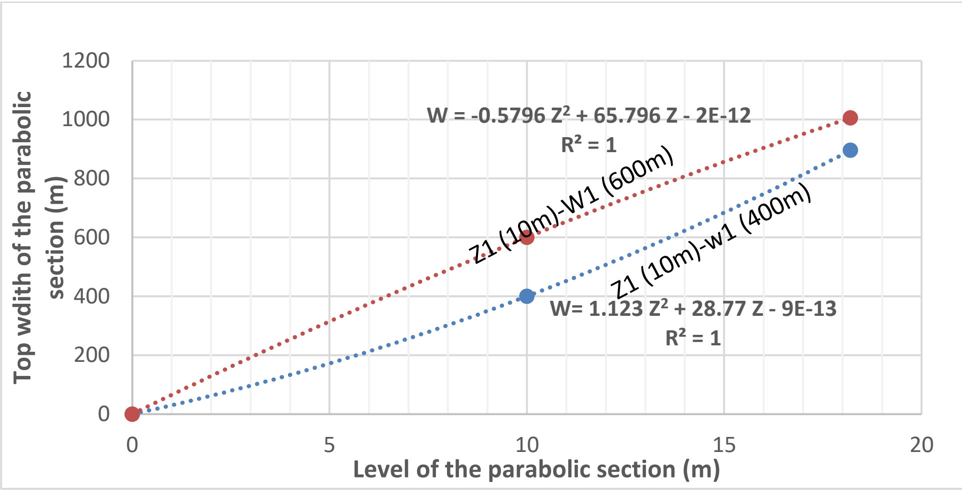

Figure 5. 20: Top width at different levels of a parabolic section from equations (5.33) and (5.34).

5.4.3.4 Power generation from a vertical shape parabolic basin

Results for a parabolic section having Z_1 =10m and w_1 =600m is shown in Table 5.15.

The input tidal data and basin parameters are taken as input data in the RTA model and the results are shown in the Table 5.15. The turbine diameter is taken each 4m (2.25 MW) and sluice gates each 12 m x12 m and other parameters similar that taken for the rectangular basin.

Table 5. 15: Energy from a vertical shape parabolic basin for Z_1 =10 m and w_1 =600 m (ebb generation).

Sl. No.	Nos. Turbine	No. Sluice	Energy (GWh)	Capacity (MW)	Nos. Turbine	No. Sluice	Energy (GWh)	Capacity (MW)
1	5	5	70.84	34.64	15	20	93.50	56.70
2	5	10	73.87	34.69	15	25	93.41	56.71
3	5	15	73.84	34.79	20	5	80.40	56.70
4	5	20	73.75	34.67	20	10	85.04	56.98
5	5	25	73.62	34.64	20	15	84.96	57.17
6	10	5	89.75	50.85	20	20	84.98	56.98
7	10	10	94.82	50.93	20	25	84.91	56.98
8	10	15	94.78	51.14	25	5	72.83	54.40
9	10	20	94.78	50.95	25	10	76.60	54.81
10	10	25	94.53	50.95	25	15	76.55	54.97
11	12	11	95.91	54.27	25	20	76.57	54.81
12	15	10	93.54	56.70	25	25	76.49	54.82
13	15	15	93.48	56.93	25	25	76.49	54.82

The results are plotted in Figure 5.21 and Figure 5.22.

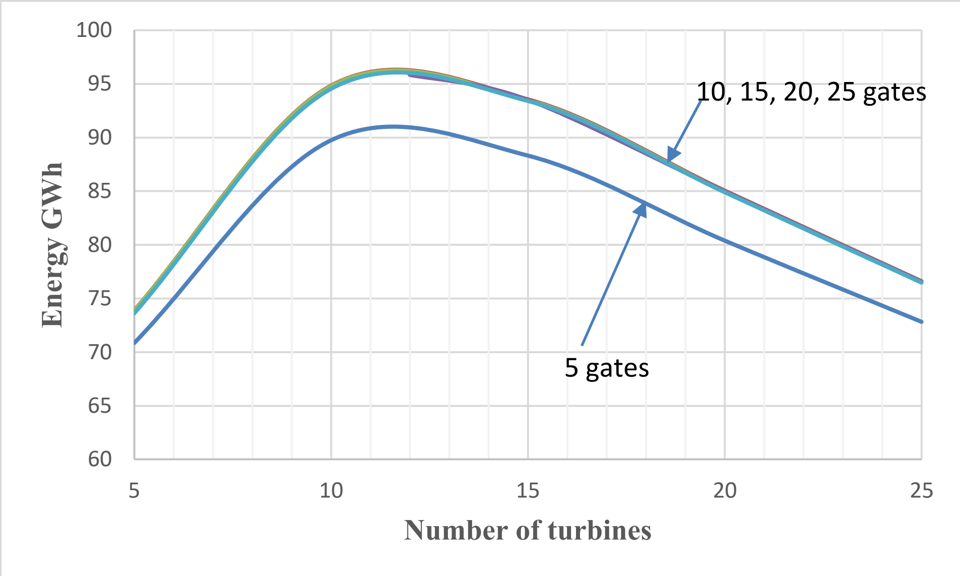

Figure 5. 21: Energy generation from a vertical shape parabolic basin (Top with 600 m) as a function of turbines with different gates.

.

From Figure 5.21, it is clear that energy increases up to 12 turbines and after that energy decreases irrespective of turbine number or gate number. It is also clear that for a particular turbine number energy generation for 11 to 25 gates do not varies so much rather more-less same.

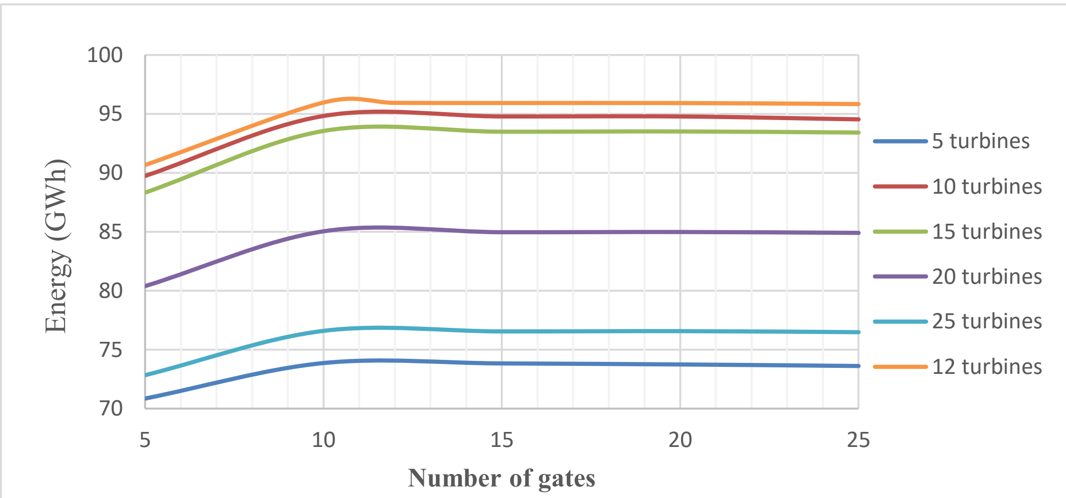

Figure 5. 22: Energy generation as a function of gates with different number of turbines (top width 600 m).

From Figure 5.21 and Figure 5.22, it is reveals that for 12 turbines 4 m dia. each (2.25 MW) and 11 nos. sluice gates (12 m x12 m each) will yield maximum annual energy output 96 GWh with a maximum capacity of 54.25 MW for a parabolic basin. After 12 turbines and 11 gates cost will increase but energy generation is steady or decreases which is not desirable.

Results for a parabolic section having Z_1 =10 m and w_1 =400 m.

Results for a parabolic section having Z_1 =10 m and w_1 =400 m is shown in Table 5.16

Table 5. 16: Results for a parabolic section having Z_1 =10m and w_1 =400 m.

Nos. of turbines	Nos. of gates	Annual energy (GWh)	Capacity (MW)	Nos. of turbines	Nos. of gates	Annual energy (GWh)	Capacity (MW)
5	5	66.32	33.04	12	5	75.35	47.72
5	10	67.81	33.10	12	10	77.44	47.92
5	15	67.76	33.07	12	12	77.40	48.00
5	20	67.74	33.08	12	15	77.40	47.80
10	5	77.20	45.89	12	20	77.37	47.86
10	10	79.28	46.02	15	5	77.37	47.86
10	15	79.24	45.94	15	10	72.35	48.92
10	20	79.23	45.98	15	15	61.89	46.85
12	5	75.35	47.72	15	20	63.47	47.30

The results are plotted in Figure 5.23 and Figure 5.24.

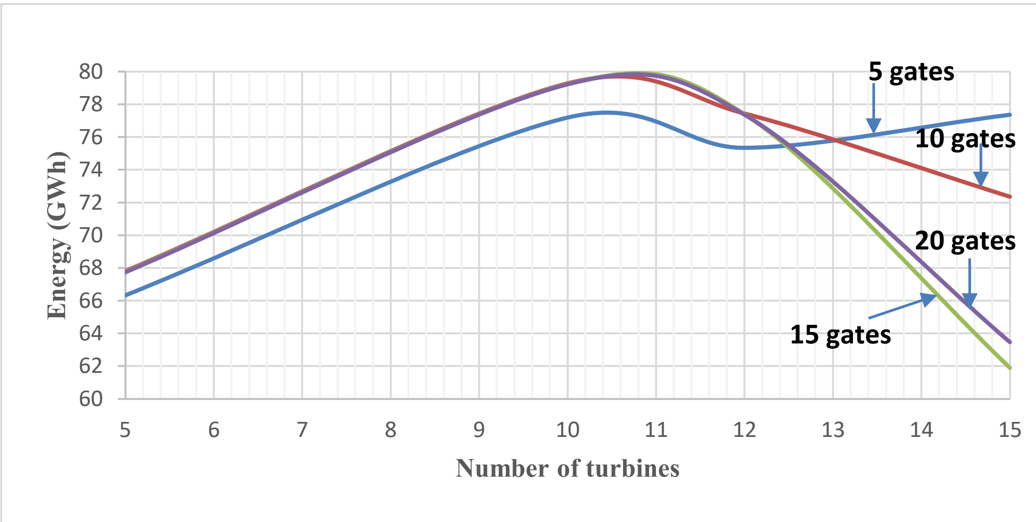

Figure 5. 23: Energy generation from a vertical shape parabolic basin as a function of turbines with different no. of gates (top width 400 m).

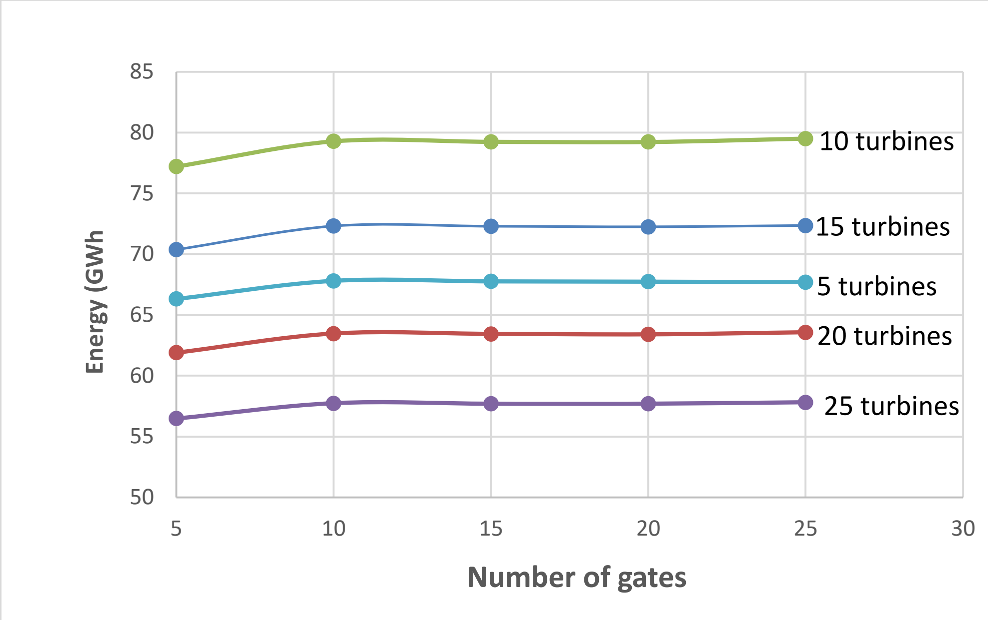

Figure 5. 24: Energy generation from a vertical shape parabolic basin as a function of gates with different no. of turbines (top width 400 m).

From Figure 5.23 it clear that energy increases up to 10.5 ≈10 turbines and after that energy decreases irrespective of turbine number or gate number. It also clear that energy increases up to 10 gates and after that energy decreases.

From Figure 5.23 and Figure 5.24 it is observed that 10 nos. turbines each 4m dia. (2.25 MW) and 10 nos. sluice gates (each 12m x12m) will yield maximum annual energy output 79.25 GWh with a maximum capacity of 46 MW for the parabolic basin. After 10 turbines and 10 gates cost will increase but energy generation is steady or decreases which is not desirable.

5.4.4 Comparison of results having different vertical shape tidal basin considering horizontal water levels at the basin and sea

From above discussion the comparison of results due to variation of vertical shapes are shown in Table 5.17.

Table 5. 17: Comparison of energy generation from different vertical shape tidal basins having same cross-sectional area within HWL and LWL and same basin length.

Parameters	Rectangular Basin (side slope s=0.0)	Trapezoidal Basin (Side slope s=0.5)	Trapezoidal Basin (Side slope s=2.0)	Parabolic Basin (ω_1=600m; Z_1=10m)	Parabolic Basin (ω_1=400m; Z_1=10m)
Cross sectional area of the basin (m^2) along the length	8200	8200	8200	8200	8200
Length of the basin (m)	5000	5000	5000	5000	5000
Tidal range	8.2	8.2	8.2	8.2	8.2
Maximum annual energy output (GWh)	166	170	135	96	79
As a % of rectangular basin	100%	102%	81%	58%	48%
Maximum power (MW)	87	87	92	54	46
Nos. turbine (4m dia.)	20	20	22	12	10
Nos. of sluice gate	30	40	20	11	10

From Table 5.17, it is observed that for different vertical shapes tidal basins having same tidal range (8.2 m), same cross-sectional area (8200 m^2) within the same tidal range (HWL-LWL) and same basin length (5000 m) energy production varies. Trapezoidal basin with side slope z=0.5 yields more energy (170 GWh) than that of (135 GWh) a trapezoidal basin with side slope z=2.0. Even it is more than that (166 GWh) of a rectangular basin (side slope z=0.0). Both trapezoidal basin and rectangular basin yield more energy than a parabolic basin. So, it is concluded that, if other parameters remain same, a vertical shape (i) trapezoidal basin having side slope, s=0.5 and (ii) rectangular basin yield more energy than other shapes.

Based on those findings, the hierarchy of vertical shape basins in respect of energy output can be expressed in Figure 5.25.

Trapezoidal basin (s=0.5) > Rectangular basin > Trapezoidal basin (s=2.0) > Parabolic basin

Figure 5. 25: The hierarchy of shapes of the basin in respect of energy output.

5.5 Summary

Chapter 5 provides idea about the impact of size and shape of a tidal basin on energy generation. Variation of energy generation for different sizes are assessed considering (i) different aspect ratio (ratio of width and length) with same basin area and tidal range and variation of energy generation for different vertical shapes (such as rectangular, trapezoidal and parabolic basin etc.) basins with same vertical cross-sectional area between HWL and LWL and with same basin length are assessed using RTA model.

In the RTA model it is assumed that tide levels at the sea and the basin are horizontal irrespective of length. But in practical it is not horizontal; it varies gradually with respect to aspect ratio and time.

To assess the impact of basin size on power generation, hypothetical basins having same area of 90 km^2 with different aspect ratios are taken and water levels inside and outside of the barrage are computed using the NAO.99b model (Matsumoto, et al., 2000). In calculating water levels at the basin and sea, normally, it is assumed that water level at both sides of the barrage is horizontal. But from NAO.99b model, it is observed that water level is not horizontal. It varies with aspect ratios. RTA model is run using the water levels inside and outside the barrage computed using NAO.99b model, and it is observed that mean power and energy reduces with decrease of aspect ratio.

Considering horizontal water levels at sea and basin, annual energy output is 32.603 GWh, whereas, it decreases to 14.816 GWh (45%), 13.251GWh (41%) and 10.720 GWh (33%) for aspect ratio of 0.9, 0.625 and 0.40 respectively considering non-horizontal shallow water levels.

One thing should be clear that water levels computed using NAO.99b model where flow is continuous, openings are vertically open and water opening heights are variable with changing water levels, whereas water levels computed from RTA model where turbines are kept submerged, turbine position is fixed, effective area is fixed and minimum head requirements are opted to protect the turbines- which is not exactly similar condition for water flow considered in the NAO.99b model. It would be better if NAO.99b model is applied for a barrage system to see the water level variations. If it would have done then we could get the clear idea about water level variations at sea and the basin for a tidal barrage system which is absent and is not considered in this study.

So, running the RTA model taking the water levels from the NAO.99b model for different aspect rations, the results we get, might be, to some extent, indicative and qualitative. Actual variation will be lesser than what we get from NAO.99b model as water flowing condition in the NAO.99b model and water flowing system in a tidal barrage system is different.

But, it could be concluded that water levels at sea and the basin are not exactly horizontal, it varies with aspect ratios. Higher the aspect ratio, higher is the water head for power generation. So, in selecting a tidal basin or a tidal barrage it is always important to remember that basin with higher aspect ratio will yield higher energy output.

Again, to assess the impact of different vertical shape tidal basin on power generation, hypothetical shape basins, such as rectangular, trapezoidal and parabolic shape, having same vertical cross-sectional area 8200 m^2 within the same tidal range (HWL- LWL= 8.2 m) and same basin length (5 km) are taken to run the RTA model. It is observed that a vertical shape (i) rectangular basin yields 166 GWh (100%), (ii) trapezoidal basin having slope, s=0.5 yields 170 GWh (102%), (iii) trapezoidal basin having slope, s=2.0 yields 135 GWh (81%), (iv) parabolic basin having top width 600 m yields 96 GWh (58%) and (v) parabolic basin having top width 400 m yields 79 GWh (58%) energy annually respectively.

So, in selecting a tidal basin or a tidal barrage it is always important to remember that basin size of higher aspect ratio yields higher energy and vertical shape trapezoidal basin with slope, s=0.5 or vertical shape rectangular basin also yields higher energy in compare to other vertical shapes.

.

CHAPTER 6
APPLICATION OF THE MODEL

6.1 Introduction

6.1.1 General

Application of any new model is very important. The RTA model (described in Chapter 3) is tested and verified in Chapter 4 and found the model is useful, flexible and more accurate than other methods. In this chapter the RTA model is applied for Sandwip Channel, one of the promising sites having higher tidal range (7.05m) than that of other channels in the coastal areas of Bangladesh considering dynamic water head and basin characteristics to see whether tidal barrage power could be generated in the channel and what would be the capacity and energy generation.

6.1.2 Flow-chart /procedure to assess tidal barrage power of Sandwip channel.

(1) **Collect observed tidal data**

For this study purpose 20 years observed data (1996-2015) for Sandwip was taken from Bangladesh Inland Water Transport Authority (BIWTA).

(2) **Sort, verify and rectify tidal data**

(i) Data were sorted and verified as per historical memory.

(ii) Avoid/delete unrealistic tide data.

(3) **Analyze observed tide data to find the tidal constituents**

(i) Sorted and rectified data used to find out tidal constituents with amplitudes and phase angles using GeoTide Analyzer 3.0 X 2015 of Payra Port Authority, Ministry of Shipping, Bangladesh.

(ii) Collected standard tidal speeds from scientific report (Simon & John, 2017).

(4) **Form an equation to find the water level of the sea with respect to time**.

Form an equation using identified tidal constituents having different amplitudes, phase angles and speeds to compute water level at sea.

$$Y(t) = a_0 + \sum_{i=1}^{n} a_i \cos(\frac{2\pi t}{T} - \emptyset_i) \quad (6.1)$$

where,

Y(t) = water level at sea due to tidal effect;

a_0 =mean sea level above chart datum;

n= number of tidal constituents;

a_i= amplitude of i^{th} tidal constituent;

T_i= tidal period of i^{th} tidal constituents; and

$\emptyset_i$= is the phase angle of i^{th} tidal constituent.

(5) **Collect bathymetric data**

Bathymetric data of Sandwip Channel having longitude, latitude and bed level hg (using GPS and single bean echo sounder) (data taken from BIWTA, CEGIS, Bangladesh Navy and Goggle Earth Pro) (see **Appendix C5**).

(6) **Prepare contour map of the tidal basin**.

Contour map developed using HYPACK ® Windows ® based Software is used with the help of BIWTA and CEGIS officials.

(7) **Analyze bathymetric data**

HYPACK ® Windows ® based Software is used with the help of BIWTA and CEGIS. The intention was to develop a relation between water surface area and level of the basin. The relation is like Equation. 6.2:

$$A_b = a_n Z^n + a_{n-1} Z^{n-1} + a_{n-2} Z^{n-2} + a_{n-3} Z^{n-3} + \cdots \ldots\ldots\ldots\ldots + a_1 Z^1 + a_0 \quad (6.2)$$

where,

A_b= surface area (m^2) of the basin at level Z;

Z(t)= level of the basin in (m) at any time, t; and

n= polynomial order.

a_n, a_{n-1} a_{n-2} etc…are the coefficient and can be get from trend analysis.

(8) **Plot a curve having relation between water surface area and corresponding water level.**

Putting data in excel sheet we got a graph and a trend-line with equation.

(9) **Calculate dynamic water head, h**

Calculate dynamic water head, h. Take absolute value at any time (t).

h (t) = ABS[Y(t)-Z(t)] (6.3)

(10) **Define nature of tide (either flood tide or ebb tide) of sea**.

If $Y_{t+1} > Y_t$; consider flood tide and expressed (+ 1) sign in the model; and

If $Y_{t+1} \leq Y_t$; consider ebb tide and expressed (-1) sign in the model.

(11) **Define nature of tide (either flood tide or ebb tide) for the basin**.

If $Y_{t+1} > Z_t$; consider flood tide and expressed (+ 1) sign in the model; and

If $Y_{t+1} \leq Z_t$; consider ebb tide and expressed (- 1) sign in the model.

(12) Fix minimum head for turbine operation

Minimum head for turbine opening is $h(t)_{min}$= 2.0 m is taken and once the turbine started it will not be closed until h(t) ≤ 1.8 m.

(13) Turbine and gate operation: either closed or opened.

(a) For two-way generation

(i) If turbine is opened, it is expressed in the model as (1) sign.

(ii) If turbine is closed, it is expressed in the model as (0) sign.

(iii) If gate is opened, it is expressed in the model as (1) sign.

(iv) If gate is closed, it is expressed in the model as (0) sign.

(v) When tides are similar in nature (either flood or ebb) at both sides of the barrage and head difference is zero (0) both turbines and gates are closed. It will remain continue until head reaches to a minimum head (in this case 2 m). When h reached to ≥2 m, turbines will be opened but gates will remain closed. Turbines will remain opened and gates will be remained closed until h falls to 1.8 m. When h=1.8 m turbine will be closed but gates will be opened until h=0.

(vi) Again, turbine will not be opened until head reaches to h≥2.0 m.

(b) Ebb generation

(i) During flood tide at the basin, turbines will remain closed but gates are opened.

(ii) During ebb tide at the basin, gates remain closed, but turbines will be opened when h≥ 2.0m and it will continue until h>1.8. When h reaches to ≤1.8m turbines will be closed.

(c) Flood generation

(i) During flood tide at the basin, gates will remain closed, but turbines will be opened when water head difference reaches to h≥2 m and will continue until head h falls to 1.8 m.

(ii) During ebb tide at the basin, turbines will be closed but gates will remain opened.

(14) Calculate Velocity of water through turbine

From Equation (3.42), we get velocity of water through turbine will be equals to:

$$V_T = \theta_T\, C_{DT} \sqrt{2gh} \tag{6.4}$$

where,

V_T= Water velocity through turbine

θ_T= zero when turbine is closed;

θ_T=1 when turbine is opened;

C_{DT} =Coefficient of discharge through turbine;

g=acceleration due to gravity; and

h= Water head.

(15) Calculate velocity of water through gate

From Equation. (3.43) we get, velocity of water through gate

$$V_G = \theta_G\, C_{DG} \sqrt{2gh} \tag{6.5}$$

Where,

V_G= Water velocity through gate;

θ_G= zero when gate is closed;

θ_G=1 when gate is opened;

C_{DG} =Coefficient of discharge through gate;

g=acceleration due to gravity; and

h= Water head.

(16) Calculate discharge through turbines

$$Q_T = N_T V_T A_T \quad (6.6)$$

where

Q_T= discharge passed through turbines;

N_T = Number of turbines;

V_T = Velocity of water through turbines;

A_T= Area of turbines = $\frac{\pi D^2}{4}$; and

D= Diameter of turbine.

(17) Calculate discharge through gates

$$Q_G = N_G \, \theta \, C_{DG} \sqrt{2gh} \, B_G H_G \quad (6.7)$$

Where

Q_G= discharge passed through gates;

N_G = Number of gates;

V_G= Velocity of water through gates;

B_G= Horizontal width of the gate; and

H_G= Height of the submerged gate opening.

(18) Calculate total discharge through turbines and gates,

$$Q = Q_T + Q_G \quad (6.8)$$

where,

Q= volume of discharge passed through turbines and/or gates.

Q_T= volume of discharge passed through turbines; ang

Q_G= volume of discharge passed through gates

(19) Water volume inflows/outflows

Inflow in the basin could be occurred from rivers, tributaries or through rainfall precipitation and also by pumping. Similarly, water outflow could be happened through spillway or by pumping other than sluice gates.

$V_{i/o}=\theta \, .Q_{i/o} . \, \Delta t$ (6.9)

where,

$V_{i/o}$ = volume of water inflow/outflow to the basin, m^3

$Q_{i/o}$= discharge inflow or outflow to the basin, m^3/s

Δt = duration of inflow or outflow, seconds.

θ= ±1, for inflow (+) sign and for outflow (-) sign.

(20) **Calculate incremental increase/decrease water level in the basin**.

Incremental increase/decrease of basin water level between time t_1 and t_2 can be calculated using following equations:

$$\begin{bmatrix} V_1 = \sqrt{2gh_1} \\ Q_1 = V_1 . A_1 \\ V_2 = \sqrt{2gh_2} \\ Q_2 = V_2 . A_2 \\ V_w = \frac{(Q_1+Q_2)}{2}(t_2 - t_1) \pm V_{i/o} \\ \partial Z_2 = \frac{V_w}{(A_{b1}+A_{b2})/2} \end{bmatrix} \quad (6.10)$$

(21) Power (kW) Calculation

Electrical Power:

$P\ (kW) = \eta \rho g Q_T h/1000$ (6.11)

g=acceleration due to gravity in m/s^2; and

Q_T= discharge passed through turbines m^3/s

h= Water head.

ρ = density of sea water in kg/m^3

η = efficiency of turbine system.

(22) Energy (kWh) Calculation

$$\text{Energy, E(kWh)} = \frac{(P_1+P_2)/2}{(t_1-t_2).3600} \qquad (6.12)$$

where,

E =Electrical energy $in\ kWh$;

P_1 and P_2 are the electrical power at time t_1 and t_2; and t in hours.

6.2 Tidal Characteristics in the Study Area of Bangladesh

6.2.1 General

Bangladesh has about 710 km long coast line along the Bay of Bengal with the continental shelf up to 50 m depth with an area of about 37,000 km^2 (Quader, 2010) in which tidal height varies from 2 to 8 m rise and fall (Mahbubuzzaman, et al., 2010). Bangladesh, an emerging economy of South Asia, needs electricity growth rate of at least 10% each year to maintain the yearly economic growth more than 7% (CPD, 2011). Power sector of Bangladesh has the installed power generation capacity of 22,787 MW as of 30 January, 2020 including captive and renewable energy (Power Cell, 2020). At present, 96% of the people of Bangladesh have access to electricity (Power Cell, 2020) with per capita generation is 510 kWh including captive and renewable energy (BPDB, 2020). In the year 2018-2019, per unit cost of electricity in Bangladesh was BDT 5.95/kWh (BPDB, 2020).

In our country most of the power stations are run by natural gas (11025 MW) accounting for 56.34% of the total installed capacity 19570 MW as of November 2019 (BPDB, 2019). In order to come out from this problem a quick solution envisaged by the government has started to use rental power plants which were temporary and quick and also thought out to be advantageous for the government. Bangladesh has many available spots that are suitable for constructing medium to large tidal power plants at coastal areas such as Hiron Points, Mongla, Char Changa, Cox's Bazar, Golachipa, Patuakhali, Sandwip, Barisal etc. Table 6.1 shows the tidal data for Bangladesh coasts where Sandwip, has higher tidal range, is an island along the south-eastern coast of

Bangladesh and among which Sandwip is the most emerging area for a tidal barrage. Sandwip is a Upazila (Sub-division) of Chittagong district located at 22^0 49′51.30" N and 91^0 42′11.85" E which is situated at the Meghna estuary on the Bay of Bengal and separated from the Chittagong coast by the Sandwip Channel (Roy, et al., 2015).

6.2.2 Tides at some locations of Bangladesh

Bangladesh Inland Water Transport Authority (BIWTA) through its department of Hydrography has been maintaining 53 Nos. water level recording stations to monitor water levels in the inland and coastal areas.

Table 6. 1: Tides in some locations of Bangladesh.

Station	Hiron Point	Mongla	Khal No.10	Sadar Ghat	Sandwip	Khepupara	Chandpur
LAT	-0.256	-0.261	-0.444	-0.423	-0.583	-0.323	+0.019
MLWS	0.225	0.325	0.261	0.239	0.238	0.195	0.256
MLWN	0.905	1.194	1.231	1.1	1.634	1.025	0.493
ML	1.7	2.31	2.664	2.481	3.243	2.06	2.172
MHWN	2.495	3.427	4.097	3.861	4.851	3.096	3.852
MHWS	3.175	4.296	5.067	4.722	6.248	3.925	4.088
HAT	3.656	5.772	5.772	5.385	7.070	4.445	4.326
Tidal Range	**3.912**	**6.033**	**6.216**	**5.808**	**7.653**	**4.768**	**4.307**

Source: (BIWTA, 2019).

From Table 6.1, it is clear that maximum tidal range is located at Sandwip and it is 7.653 m which is the highest among the mentioned coastal areas. Based on tidal range Sandwip, Khal No. 10, Mongla and Sadar Ghat, Chittagong etc. are some locations where tidal barrage power could be established. In this study, RTA model is applied for Sandwip Channel to assess tidal power potential.

6.2.3 Tidal data for Sandwip

6.2.3.1 Sources of tidal data

20 (Twenty) years' tidal data from 1996 to 2015 is taken from BIWTA for Sandwip location.

6.2.3.2 Data analysis technique

Data were sorted and unusual data are deleted and rest data are taken for analysis using Excel sheet. Sorted data were taken for analysis (**Appendix C1**). GeoTide Analyzer

3.x.2015 is used for tidal analysis with the help of Payra Port Authority (PPA) working under Ministry of Shipping of Bangladesh.

6.2.3.3 Software used.

GeoTide Analyser 3.0.15 is used to analyse the tidal data of Sandwip channel.

6.2.3.4 Tidal constituents

By running the Software "GeoTide Analyser 3.x,2015" for Sandwip gauge location with the sorted data shown in **Appendix C1**, 214 tidal constituents are identified with phase angles and amplitudes. The tidal analysis report generated from the software is attached in **Appendix C2**. Standard tidal speeds of each constituents are taken from the standard list of Tidal Constituents which was prepared by Mr Bernard Simon of SHOM and Cdr John Page of the UKHO on behalf of the IHO Tidal Committee, now the Tide, Water Level and Current Working Group (TWCWG). (Simon & Page, 2017). The name of constituents, phase angles, tidal speeds and amplitudes are shown in **(see Appendix C3).**

6.2.3.5 Resultant constituent

The resultant constituent is a summation of 214 tidal constituents **(Appndix-C3)** each with individual tidal amplitudes (a), phase angles ($\emptyset$)and speeds (σ). Predicted tide can be calculated using Equation (6.13) which is time variable:

$$Y(t) = a_0 + \sum_{i=1}^{n} a_i \cos(\sigma t - \emptyset_i) \qquad (6.13)$$

Equation (6.13) is used in the RTA model to calculate time series predicted tidal data for sea.

6.3 Basin Characteristics of the Study Area

6.3.1 Identification of a basin and its area

A tidal barrage utilizes the potential energy of the tide, built across a bay or estuary that experiences a tidal range in excess of 5 m. The tidal range of Sandwip channel is 7.5m which is the most promising site for Bangladesh in terms of tidal range and water surface area. From Equation (2.6), it clear that the tidal power is the product of square of tidal range, i.e. $P \infty R^2$ and also product of impounded area, i.e. higher the impounded area higher the tidal energy. As the tidal range of the channel is more or less same, so energy will be higher as the impounded area is higher. Based on these, the impounded area is selected as shown in the Figure 6.1.

Figure 6. 1: Google Earth Photo of Sandwip Channel.

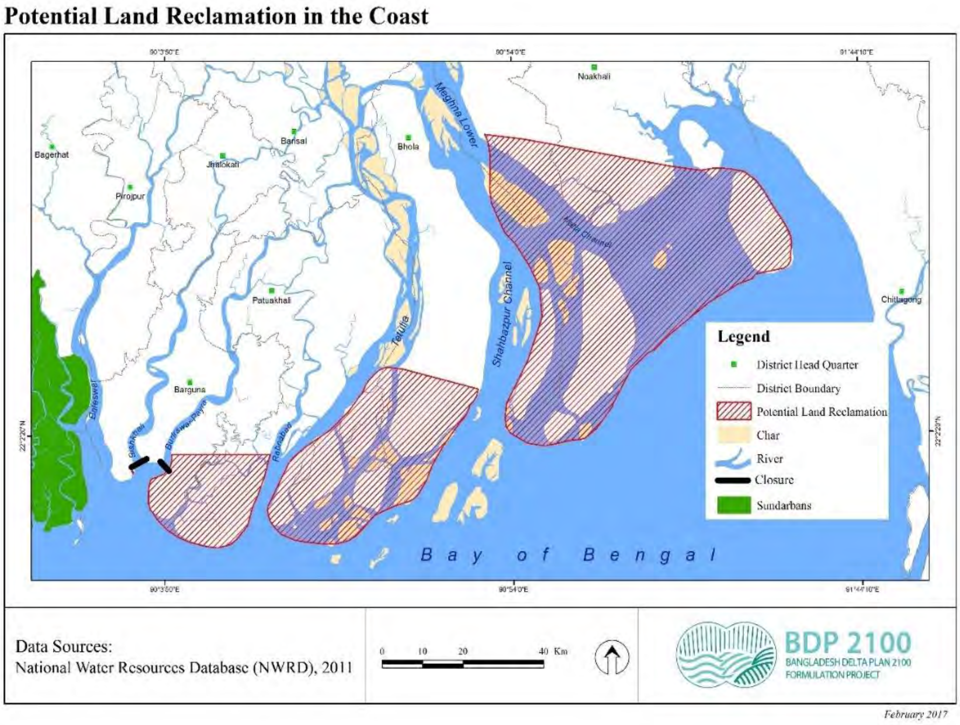

Figure 6. 2: Potential land reclamation in the coast (NWRD, 2011).

Bed profile of Sandwip Channel from Sandwip point to Hathazari point along the barrage alignment is shown in Figure 6.3 and **Appendix C4**. Bed profile is taken from google map from the point (22°26′27.14″ N, 91°31′59.60″ E) to (22°29′34.72″ N, 91°42′31.06″ E). Water level at Highest Astronomical Tide HAT is 7.07 m. If the top level of the barrage is considered 10 m, then the barrage length will be at least 18.9 m.

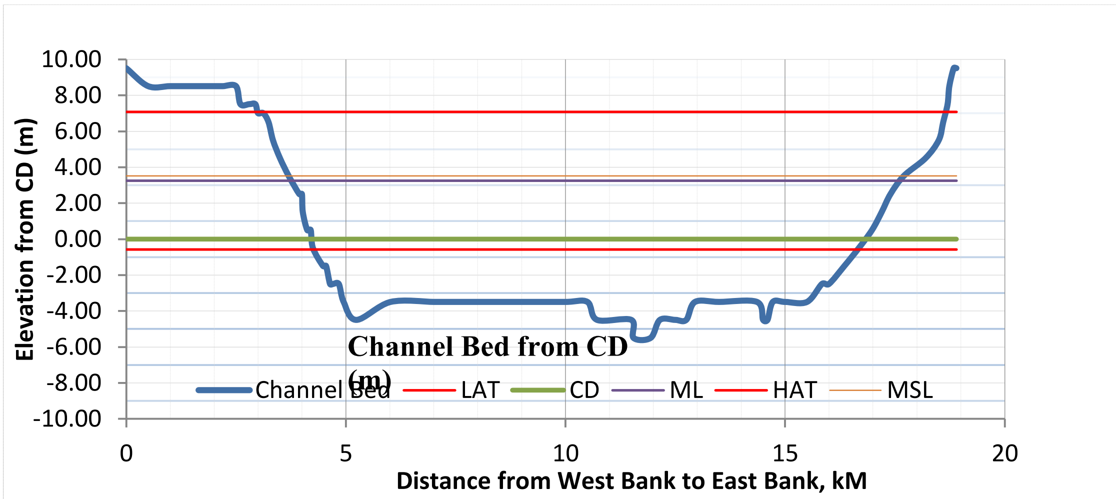

Figure 6. 3: Cross section of Sandwip Channel.

From Figure 6.1, it is clear that, if we would like to impound the water of the basin, we will require to construct another 2 embankments between point 1 (22°35′18.83″ N, 91°25′35.28″ E) to point 2 (22°37′09.06″ N, 91°23′24.99″ E) and between point 3

(22°40′59.45″ N, 91°18′53.05″ E) to point 4 (22°43′02.60″ N, 91°16′27.20″ E). The length of the first embankment will be 5.05 km and the length of the second embankment is 4.91km. The vertical cross-section of the first embankment and second embankment are shown in Figure 6.4 and Figure 6.5 respectively.

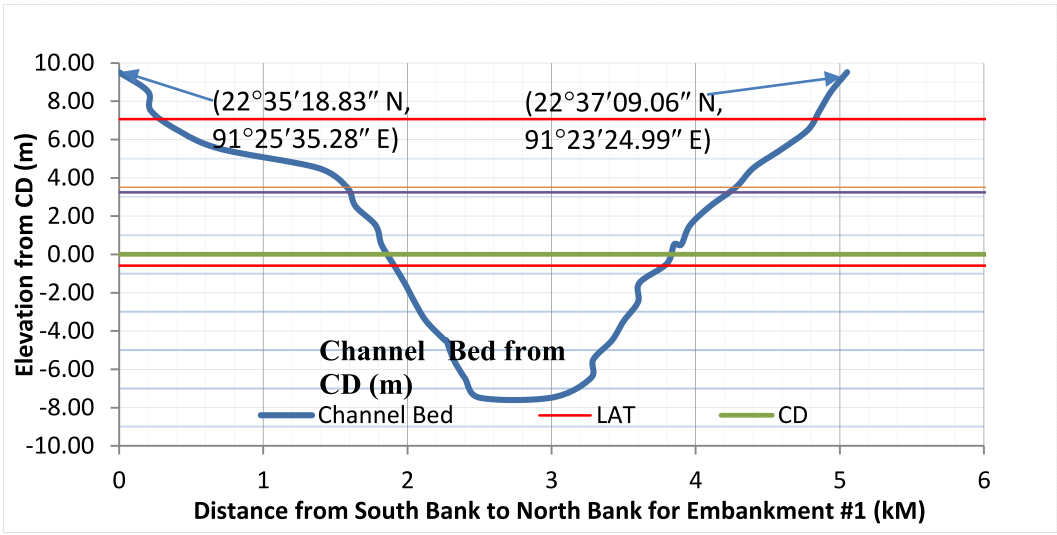

Figure 6. 4: Vertical cross-section of the first embankment (point 1 to point 2).

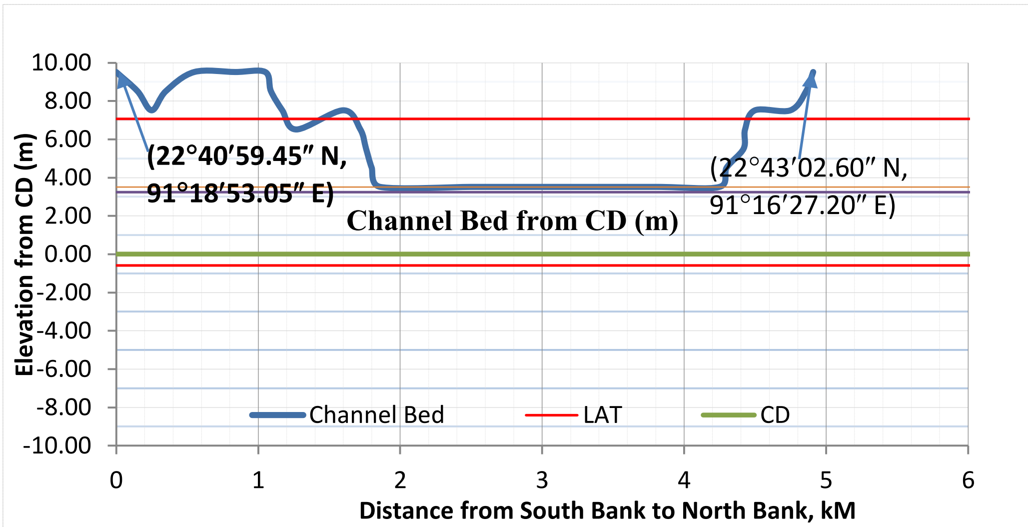

Figure 6. 5: Vertical cross-section of the second embankment (point 3 to point 4).

6.3.2 Sources of data collection

To assess tidal power potential at Sandwip, the most important task was to collect bathymetric data (both water & land part's) elevation data. In this connection water part's bathymetry was collected from BIWTA (surveyed in 2018) and land part's data was collected from USGS (SRTM) (collected through CEGIS). Both data were measured from Chart Datum (CD) reference in meters. Tidal data of 20 years of Sandwip Gauge station was collected from BIWTA hydrography department.

6.3.3 Data analysis technique

Land & water part's data available was not covering full area. Some gaps were found in between water & land part. For batter computation these gaps were filled up by TIN (Triangulated Irregular Network) modeling & also made a general surface with 300 meters x 300 meters gridded soundings with respect to CD (Chart Datum). In this study one of the most challenging parts was area-volume calculation for the desired area. Since study area is looks like a reservoir, contour has been generated for 1(one) m interval at that area. Area and volume were calculated with the help of TIN model using HYPACK 4.0 Software used by BIWTA for hydrographic survey solution shown in **Appendix C5.**

6.3.4 Area elevation relation of the impounded basin

Then area and volume of the basin impounded is shown in Table 6.2.

Table 6. 2: Wetted area and volume of the impounded Sandwip basin.

Level from CD (m) (above +ve)	Volume Above (Mm3)	Volume Below (Mm3)	Total Volume (Mm3)	Area Above (Mm^2)	Area Below (Mm^2)	Total area (Mm^2)
15	0.00	9062.90	9062.90	0.00	782.55	782.55
14	0.52	8280.87	8281.40	1.56	781.00	782.55
13	4.98	7502.78	7507.75	12.38	770.17	782.55
12	38.63	6753.88	6792.52	69.82	712.73	782.55
11	153.21	6085.91	6239.12	144.29	638.26	782.55
10	320.69	5470.84	5791.53	195.74	586.81	782.55
9	542.66	4910.25	5452.91	242.41	540.14	782.55
8	798.59	4383.63	5182.22	266.71	515.84	782.55
7	1073.93	3876.42	4950.36	283.71	498.84	782.55
6	1364.49	3384.44	4748.93	297.05	485.50	782.55
5	1668.23	2905.62	4573.84	310.28	472.27	782.55
4	1984.75	2439.59	4424.34	322.92	459.63	782.55
3	2314.71	1987.01	4301.72	337.90	444.65	782.55
2	2663.30	1553.04	4216.34	360.71	421.84	782.55
1	3037.27	1144.46	4181.72	386.77	395.78	782.55
0	3436.80	761.43	4198.23	412.43	370.16	782.60
-1	3866.06	408.14	4274.20	447.86	334.69	782.55
-2	4360.32	119.86	4480.17	577.78	204.77	782.55
-3	5043.54	20.53	5064.08	743.54	39.01	782.55
-4	5807.75	2.18	5809.93	776.12	6.43	782.55
-5	6588.17	0.06	6588.23	782.36	0.19	782.55
-6	7370.67	0.00	7370.67	782.55	0.00	782.55

The area of the impounded basin between -2 mCD to 10 mCD is plotted shown in Figure 6.6.

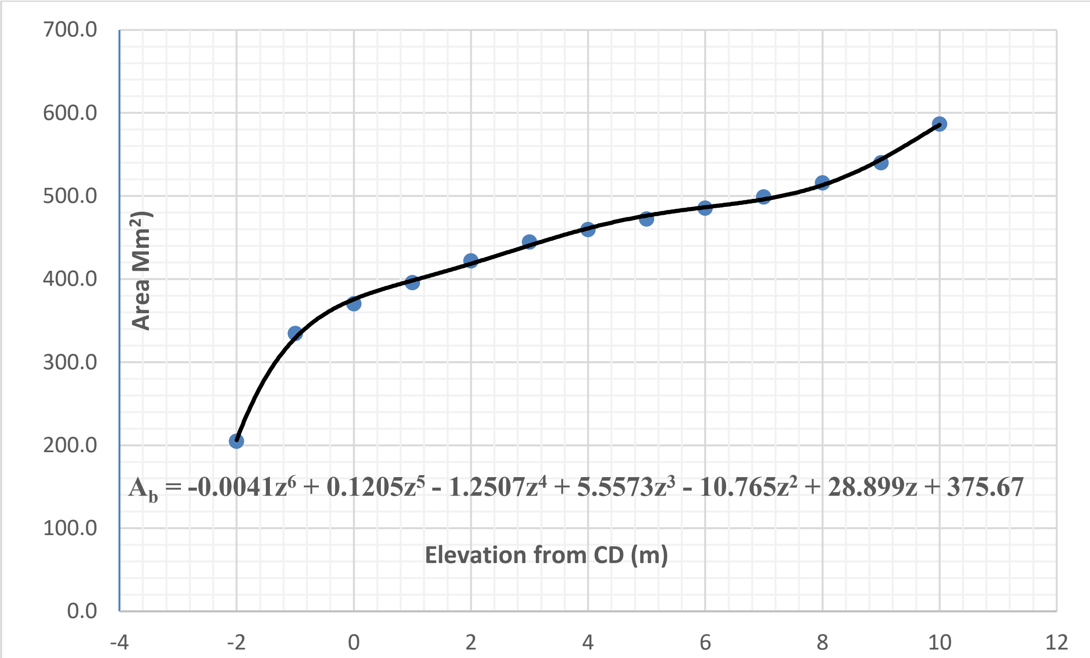

Figure 6. 6: Area-elevation curve for proposed Sandwip tidal basin (above CD +ve and below CD is -ve).

The area of the impounded basin which could be expressed in terms of elevation between (-2 m) to (10 m) from CD as Equation (6.14):

$$A_b = -0.0041Z^6 + 0.1205Z^5 - 1.2507Z^4 + 5.5573Z^3 - 10.765Z^2 + 28.899Z + 375.67 \qquad (6.14)$$

where,

A_b= Area of the impounded basin in $Mm^{2;}$ and

Z= water level elevation of the basin (in m) from Chart- Datum (CD).

6.4 Power Generation Assessment

6.4.1 Data input in the model

The following data are used in the RTA model for power assessment for Sandwip channel. These input data are changeable and model has the flexibility to use different values of the parameters.

Table 6. 3: Different parameters for power generation for Sandwip channel.

Sl. No.	Different parameters	Value	Unit
1	Area of basin, A_b from	Equation. (6.14)	km2
2	Acceleration due to gravity, g	9.807	m/s2
3	Density of sea water, ρ	1025	kg/m3
4	Threshold h to start turbine, h_1	2.0	m
5	Threshold h to stop turbine, h_2	1.8	m
6	Turbine tunnel diameter, D	6.0	m
7	Turbine discharge coefficient, Cd	0.90	
8	No. of turbines	200	
9	Turbine efficiency, η	0.40	
10	Width of single gate, B_g	12.0	m
11	Gate discharge coefficient	0.65	
13	Number of gates	500	
14	Gate Opening	6.0	m

Some authors mentioned that minimum 5 m tidal range is required for tidal power generation (Haque & Khatun, 2017), (www.iclei, 2016). Actually, a minimum head (h_S) is required for turbine starting and at a certain head (h_C) turbine should be closed. Angeloudis (2015) used value 1.5 m for h_S (Angeloudis, et al., 2015) to improve the performance for two way generation. Angeloudis (2016) used value 4.0 m for h_S and 1.0 m for (h_C) for ebb-only generation and value 2.5 m for h_S and 1.0 m for (h_C) for two way operation (Angeloudis & Falconer, 2016). Actually, minimum turbine starting and closing head is required for the protection of turbine, minimum tidal range is not a requirement. For the study purpose, value 2.0 m for h_S and 1.8 m for (h_C) is taken.

6.4.2 Results from Sandwip channel

The input of 214 tidal constituents with phase angles, speeds and amplitudes **Appendix C3** and also area elevation relation of the impounded basin **Appendix C5** is put in the RTA Model. Power and energy calculation is shown in **Appendix C6.** The results are shown in Table 6.4.

Table 6. 4 : Capacity and energy variation of Sandwip channel as a function of gates.

Turbine	Gates	Capacity			Energy
(Dia. 6m)	(12mx6m)	Max. (MW)	Avg. (MW)	Min. (MW)	(GWh)
200	500	1440	454	219	1361
200	600	1469	460	219	1432
200	700	1496	465	219	1486
200	800	1514	469	219	1529
200	900	1534	472	219	1564
200	1000	1532	475	219	1591
300	500	2051	647	328	1697
300	600	2102	656	328	1791
300	700	2142	662	328	1865
300	800	2168	668	328	1925
300	900	2197	672	328	1971
300	1000	2194	676	328	2008
400	500	2588	827	438	1928
400	600	2664	838	438	2044
400	700	2722	846	438	2131
400	800	2757	854	438	2203
400	900	2795	859	438	2257
400	1000	2792	863	438	2301
500	500	3062	994	547	2091
500	600	3165	1007	547	2221
500	700	3240	1017	547	2321
500	800	3284	1027	547	2402
500	900	3331	1032	547	2464
500	1000	3327	1038	547	2513

From Table 6.4, it is observed that 500 turbines and 1000 gates can produce maximum annual energy (2513 GWh) and average & maximum capacity will be 1038 MW and 3327 MW respectively. Similarly, 400 turbines and 1000 gates can produce maximum annual energy (2301 GWh) and average & maximum capacity will be 863 MW and 2792 MW respectively. From Table 6.4, it is also clear that as the number of gates increases for a particular number of turbines, energy generation is also increases.

6.5 Optimization of Sandwip Tidal Barrage Power Plant

6.5.1 Optimization based of energy generation

From Table 6.4, it is also clear that as the number of gates increases for a particular number of turbines, energy generation is also increases. Cost of turbines, generators, sluice gates, barrage and embankments for Sandwip channel is shown in **Appendix-C7.** Energy generation variation as a function of gates for different number of turbines is shown in Figure 6.7.

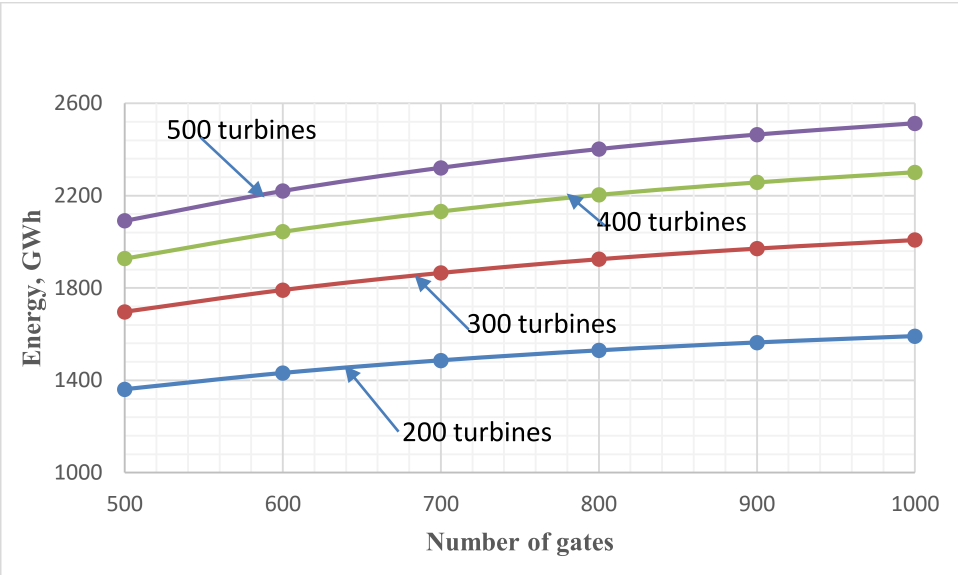

Figure 6. 7: Energy generation as a function of gates with different number of turbines for Sandwip channel.

From Figure 6.7, it is also evident that energy generation increases, as the gate number increases and theoretically, the maximum energy can be generated with 500 turbines and 1000 gates. But, the number of turbines and the number of gates should be considered in such a way so that all turbines and gates should be housed within the barrage length and tidal prism.

6.5.2 Optimization based on duration of supply

Tidal power is not continuous, rather it is intermittent. In most of the cases many authors assumed generation period is 1/3rd period of the day. From RTA model it is observed that it depends on basin area, effective areas of turbines and gates. Taking Sandwip tide and bathymetric data as input for the RTA model, four sets of turbines and gates namely; (200, 1000), (300, 900), (400, 800 and (500, 700) are taken and the results are shown in the Table 6.5.

Table 6. 5: Results (Ebb-generation) for Sandwip Basin for four sets of turbines and gates.

Elements	Turbines	200	300	400	500
	Gates	1000	900	800	700
Energy	(GWh)	1591	1971	2203	2321
Power output (MW)	Max	1532	2197	2757	3240
	Avg.	475	672	854	1017
	Min (>0)	219	328	438	547
Basin WL (m CD)	Max	5.89	5.86	5.80	5.74
	Min	2.98	2.74	2.45	2.15
Head (m)	Max	6.59	6.39	6.14	5.89
	Min	0.00	0.00	0.00	0.00
	Avg.	1.63	1.48	1.37	1.29
Tidal range basin (m)	Max	2.91	3.12	3.35	3.59
Tidal range sea (m)	Max	7.43	7.43	7.43	7.43
Production period		38%	33%	29%	26%
Non-production period		62%	67%	71%	74%

From Table 6.5 it is also clear if turbine numbers increases generation period decreases. Generation period is 38% of a year for 200 turbines and 1000 gates. On the other hand, generation period is 26% of a year for 500 turbines and 700 gates.

6.5.3 Optimization based on levelized cost of energy

Another way to optimize the capacity of a power plant is to calculate levelized cost of energy. Levelized cost of energy (see **Appendix C8)** for the economic life time (say, 50 years) of the plant, considering 5% maintenance cost of the plant cost with 2% growth and 4% discount factor for different turbines and gates is shown in Table 6.6.

Table 6. 6: Levelized cost of energy for Sandwip tidal barrage power plant.

Sl No.	Turbines	Gates	Plant Cost (BDT Crore)	Energy (GWh)	LCOE (BDT/kWh)
1	200	500	8483	1361	7.41
2	200	600	8526	1432	7.08
3	200	700	8568	1486	6.85
4	200	800	8610	1529	6.69
5	200	900	8652	1564	6.58
6	200	1000	8694	1591	6.49
7	300	500	11560	1697	8.10
8	300	600	11602	1791	7.70
9	300	700	11644	1865	7.42
10	300	800	11686	1925	7.22
11	300	900	11728	1971	7.07
12	300	1000	11770	2008	6.97
13	400	500	14636	1928	9.02
14	400	600	14678	2044	8.54
15	400	700	14721	2131	8.21
16	400	800	14763	2203	7.96
17	400	900	14805	2257	7.80
18	400	1000	14847	2301	7.67
19	500	500	17713	2091	10.07
20	500	600	17755	2221	9.50
21	500	700	17797	2321	9.11
22	500	800	17839	2402	8.83
23	500	900	17881	2464	8.62
24	500	1000	17923	2513	8.48

Plotting levelized cost of energy (LCOE) in excel sheet, we get the Figure 6.8.

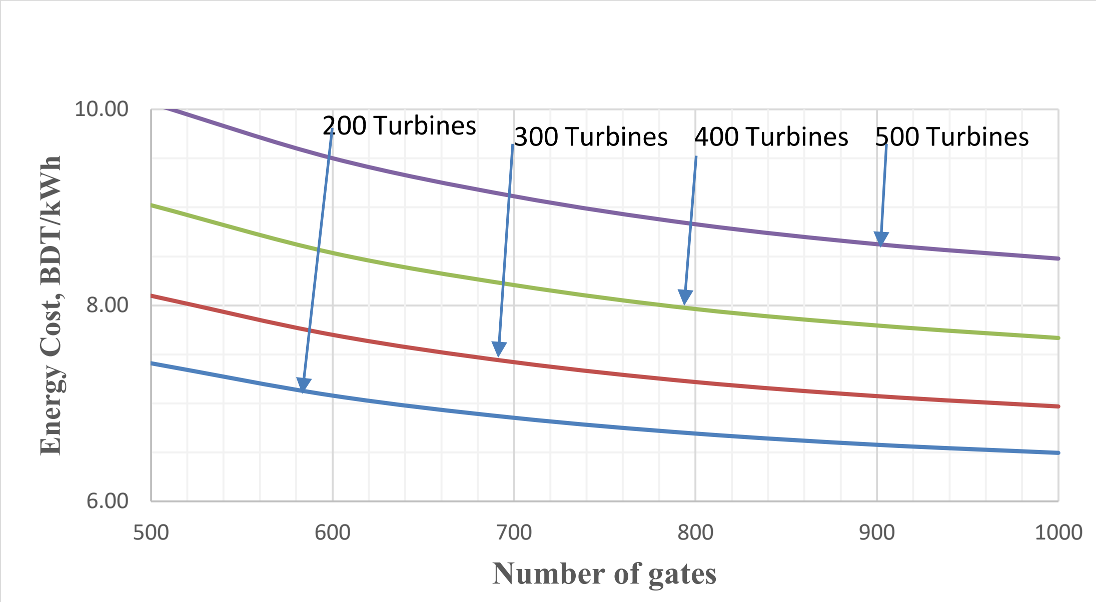

Figure 6. 8: Energy generation cost as a function of gates.

From Figure 6.7 it is already observed that, for Sandwip basin, as the number of turbines and gates increases, energy generation is also increases. But from Figure 6.8, it is also clear that as the number of turbines increases for a particular number of gates, energy generation cost increases. It should be kept in mind to select a set of turbines and gates.

From Figure 6.8, it is seen that LCOE is BDT 9.11/kWh for 500 turbines & 700 gates to produce 2311 GWh, BDT 7.96/kWh for 400 turbines & 800 gates to produce 2203 GWh, BDT 7.07/kWh for 300 turbines and 900 gates to produce 1971 GWh and BDT 6.49/kWh for 200 turbines and 1000 gates to produce 1591 GWh annually. If we base only on LCOE, then BDT 6.49/kWh is acceptable than other sets of turbines and gates. But, if install 400 turbines (each 6 m dia.) and 800 gates (12 m x 8 m), levelized cost will be BDT 7.96/kWh. If we compare this price (BDT 7.96/kWh) with other sources, it is evident that BDT 7.96/kWh is acceptable which is shown in the Table 6.7.

Table 6. 7: Cost comparison of energy generation from different energy systems.

Energy System		Fuel cost for each kWh (BDT)	Investment and OMC cost (BDT)	Total cost for each kWh (BDT)
Gas		1.11	1.95	3.06
Oil		17.89	2.75	20.64
Coal		7.00	2.50	8.50
Bio-gas [according to IDCOL]		0.50	3.50	4.00
Wind		-	7.66	7.66
Solar PV (seems to be high)		-	80.86	80.68
Tidal Barrage power at Sandwip	200 turbines + 1000 gates	-	6.49	6.49
	300 turbines + 900 gates	-	7.07	7.07
	400 turbines + 800 gates	-	7.96	7.96
	500 turbines + 700 gates	-	9.11	9.11

Source: (Samrat, et al., 2014)

If we compare energy generation cost of tidal power with other sources, BDT 7.96/kWh is acceptable in compare to oil and coal power. So, 400 turbines and 800 gates can be installed which will generate 2203 GWh annually and average power and maximum power will be 854 MW and 2757 MW respectively and will supply 29% time of a day.

6.5.4 Optimization based on housing of turbines and gates

Plant capacity can be optimized based on the minimum length requires for housing of proposed set of turbines and gates. Proposed barrage having 18 km can house 400 turbines and 800 gates easily.

6.6 Time Series Power Generation

RTA model calculates real time power and energy over the period. Energy is the product of power and time interval.

6.6.1 Time series power from observed tide data

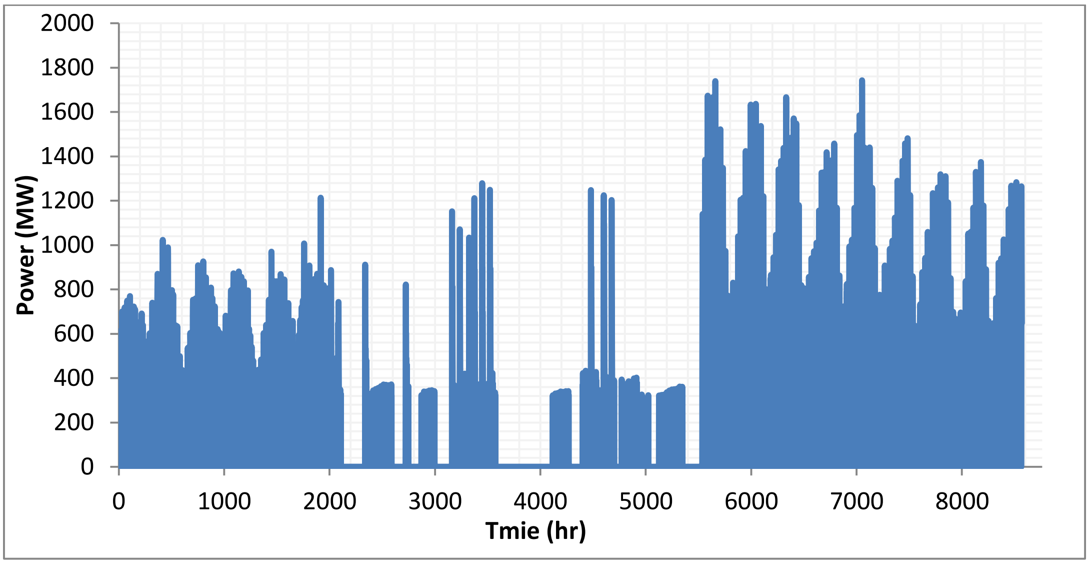

Figure 6. 9: Time series power generation (ebb mode) from observed data for the year 1996 using RTA model.

The data collected from BIWTA for the year 1996-2015 after 1-hour interval. It is observed that for each year data is discontinuous and night time data was not collected. Comparing with other years, it is observed that data for the year 1996 is better, though it is also discontinuous. From Figure 6.9, it is seen that power is variable and dynamic with respect to time, though it is discontinuous due to non-availability of tide data. Considering turbine minimum starting head (h_s) 2.0 m and turbine closing head (h_C) 1.8 m, duration of power generation is 29% of the year. Model can calculate power and energy for any time interval. The average power, minimum power (>0) and maximum power for Sandwip Channel (identified basin) are 854 MW, 438 MW and 2757 MW respectively for 400 turbines (each 6 m dia.) and 800 gates (each 12 m x 8 m). From the model, it is also observed that annual energy output 2203 GWh.

6.6.2 Time series predicted power

Observed tide data was analyzed to get harmonic constants (discussed earlier, also see Appendix C2). Putting the harmonic constants (of Sandwip area) in the RTA model as input, time series predicted tide data for the year 2010 is generated, based on which time series power is calculated which is shown in Figure 6.10.

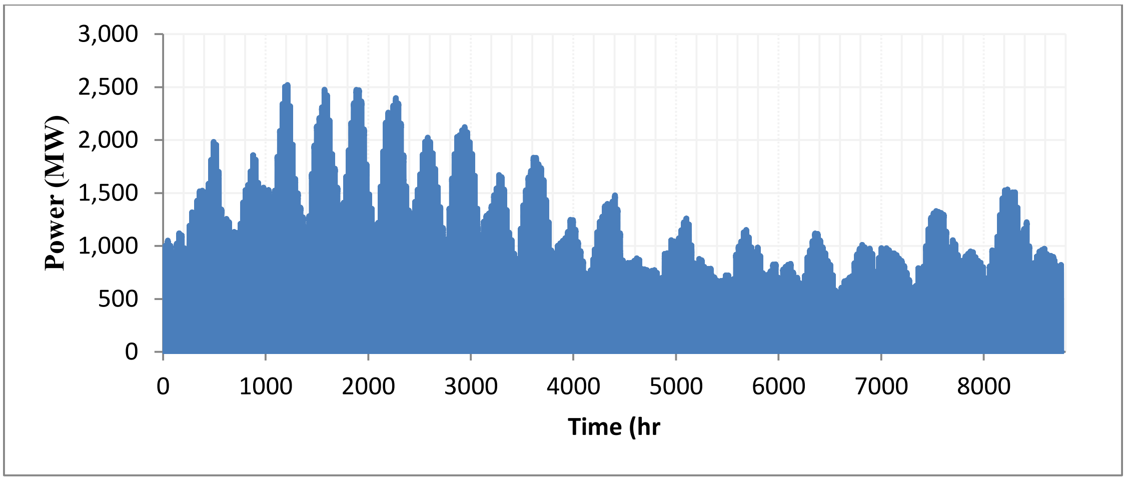

Figure 6. 10: Time series annual predicted power (ebb mode) from RTA model for Sandwip Channel for the year 2010.

From Figure 6.10, it is seen than power is variable with respect to time. Power is not static, rather it is dynamic. The average power, minimum power (>0) and maximum power for Sandwip channel (for the identified basin) are 854 MW, 438 MW and 2757 MW respectively. Considering turbine minimum starting head (h_s) 2.0 m and turbine closing head (h_C) 1.8 m, from the model, it is also observed that annual energy output 2203 GWh and duration of power generation is 29% of the year.

6.6.3 Discussions

It could be mentioned here that for prediction purpose, 6 minutes (0.1 hrs.) time interval was taken for running the RTA model, but observed data were taken after 1 hour interval. However, model can predict data for any time interval. Results will be more accurate, if time interval is smaller and if other things are remain same such as basin area vs, elevation relation, turbine and gate's efficiency etc.

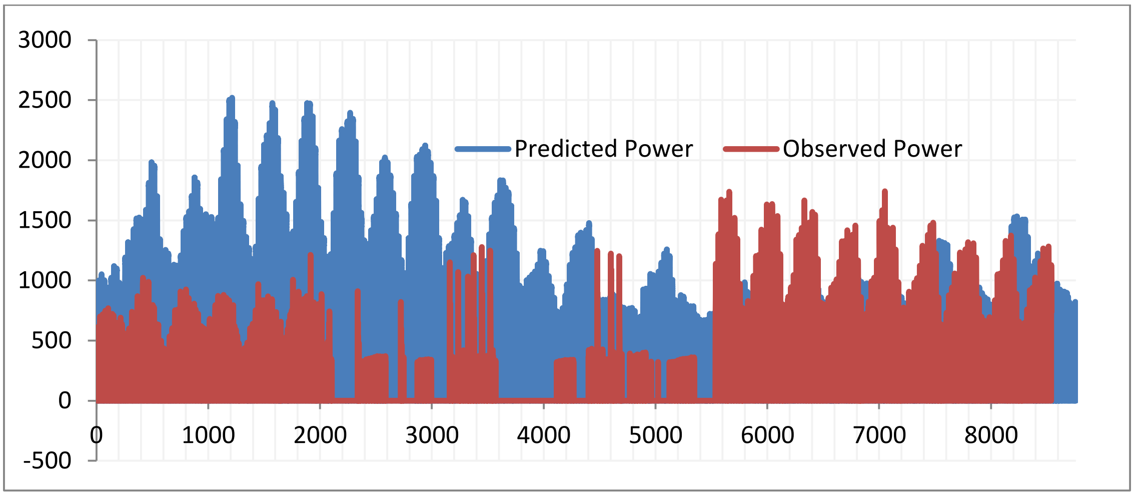

Figure 6. 11: Time series power (Predicted for 2010 and observed 1996).

Power from predicted data and power from observed data are not similar. There may be many reasons such as (i) observed data may not be collected with due care and cautions; (2) data collection interval was 1 hour and it was manual. So, if it is collected within the interval but put the value at the interval, then whole thing would be jeopardized; (3) gauge station was at a remote area.

On the other hand, RTA model predicts tide data using harmonic constants. Once the harmonic constants are assessed properly using (i) observed data and (ii) the Software (GeoTide Analyser 3.0.15), then RTA model can predict more accurate time series data. These data are calculated taking small time interval which gives more accurate water level vis-a vis, dynamic head, power and energy.

Actually, accuracy of the result depends on accuracy of the observed data, accuracy of the bathymetric data, efficiency of the turbine, gate and generator efficiency.

So, before implementing any tidal power plant, a detailed feasibility study should be conducted.

6.7 Summary

Bangladesh has been awarded the rights of 118,813 km^2 of territorial sea (Prothom-Alo, 2014). With an exclusive economic zone of 200 nautical miles and access to open sea, Bangladesh has about 710 km long coast line along the Bay of Bengal and a continental shelf (depth down to 50 m) with an area of about 37,000 km^2 (Quader, 2010), in where the tidal range varies from 2 to 8 m (Mahbubuzzaman, et al., 2010).

Bangladesh has some potentials sites for tidal barrage power generation. A tidal barrage power plant can be established at Sandwip Channel having more than 7 m of tidal range. From previous discussions, it was concluded that the RTA Model can be used to assess tidal power generation. In this chapter, the RTA model is applied for Sandwip Channel using necessary inputs from Figure 6.3. It is seen that energy generation increases with the increase of turbines and gates. It is also seen that energy generation increases with the increase of gates for a particular number of turbines. Again, it is also clear (from Figure 6.8) that, for a particular number of gates, energy generation cost increases as the number of turbines increases. Theoretically, 500 turbines and 1000 gates can generate the maximum energy (2513 GWh). But the number of turbines and the number of gates should be selected in such a way that all turbines and gates could be housed within the barrage length and within the tidal range. Considering all these factors and the Sandwip tide and bathymetric data as input to the RTA model, four sets of turbines and gates (200, 1000), (300, 900), (400, 800) and (500, 700) are selected and the results are shown in Table 6.5. It is observed that the lower the turbine capacity the higher the generation period. For example, for a combination of 200 turbines and 1000 gates, the generation period is 37% whereas for a combination of 400 turbines and 800 gates the generation period is 29%.

Figure 6.8 shows that the energy generation cost (LCOE) per unit (kWh) for the economic life time (say, 50 years) of the plant, considering 5% maintenance cost with 2% growth and 4% discount factor, is: (i) BDT 9.01/kWh for 500 turbines and 700 gates to produce 2321 GWh, (ii) BDT 7.96/kWh for 400 turbines and 800 gates to produce 2203 GWh, (iii) BDT 7.96/kWh for 300 turbines and 900 gates to produce 1971 GWh, and (iv) BDT 6.85/kWh for 200 turbines and 1000 gates to produce 1591 GWh annually. If 400 turbines and 800 gates are installed, the levelized cost will be

BDT 7.96/kWh. This cost is more economical than power generation from other sources such as oil (BDT 20.64/kWh) and coal (BDT 8.50/kWh). Therefore, 400 turbines and 800 gates can be installed to generate 2203 GWh annually with an average power and maximum power of 854 MW and 2757 MW, respectively, and a supply of 29% time of a day. The approximate total cost of the plant is BDT 14763 crore or 1678 mUSD (BDT 88 = 1 USD).

A tidal barrage power plant may thus be constructed at Sandwip Channel to produce large scale power to fulfil the country's electricity demand and to fulfil the target of 10% renewable energy. The barrage will not only produce electricity, but also establish road communication to the island which will create a huge opportunity for the tourism industry.

In this study the social, environmental and ecological impacts of the power plant have not been explored. However, in general a tidal power plant is pollution free unlike coal, gas and diesel power plants. Unlike hydropower plants, tidal power plants allow water to go back to the basin during high tides which reduces the impacts on ecology, wildlife, migratory birds, fish habitats, etc. The effect of the plant on marine life would not be extreme because of the aquatic expanse of the Bay of Bengal with alternative connectivity. Compared to coal power, tidal power generation of 2203 GWh per year will reduce 1.9 million tonnes of carbon emission per year. However, detailed studies on the environmental and social impacts with appropriate mitigating measures should be undertaken during the feasibility and detailed design phases to minimize the threats and adverse impacts.

CHAPTER 7
CONCLUSION AND RECOMMENDATION

7. 1 General Discussion

In order to achieve the global carbon emission reduction commitments, scientist have emphasised on green energy or renewable energy such as hydropower, wind power, solar power and tidal power as an attempt to lessen the climate change impacts (Owusu & Asumadu-Sarkodie, 2016). Tidal power is a reliable, predictable, pollution free, green, renewable and inexhaustible source of energy. Tidal power can be harnessed either using water velocity of tides called stream power or using potential energy called range power or barrage power. In general, barrage power can contribute more energy than stream power.

Tides create water mass movement which is the resultants of a series of harmonic motions with different tidal amplitudes and velocities from which tidal power can be generated. Tidal barrage power directly depends on square of the tidal head or range. The current approaches and practices for the assessment of tidal barrage power generation do not consider the continuous changes in the head differences between the sea and basin, rather a static overall estimate using an arbitrary reduction in efficiency and head difference is used. This study considered the real-time changes in water levels inside and outside the basin to compute the actual power generation potential based on dynamic water head, and developed a new analytical model to represent the water level variations and basin configuration.

A major outcome of this study is a Real Time Analytical (RTA) model developed for computing real-time water head, power and energy potential in a tidal barrage. The model is useful in assessing time series tidal power potential more accurately and to optimize the plant capacity. As the Sandwip Channel has higher tidal range compared to other coastal locations in Bangladesh, the RTA model is applied for Sandwip Channel to assess the tidal barrage power potential. It is found that the Sandwip Channel has a high potential for tidal barrage power generation.

7. 2 **Conclusion**

Now-a-days, tidal power is considered to be an important source of renewable energy. Tidal barrage power depends on tidal head difference between the inside and outside of the basin. However, water levels at these two sides vary with respect to time due to tidal fluctuations and barrage operation. The current approaches and practices for the assessment of tidal barrage power generation do not consider this continuous changes in the head difference between the sea and basin. In most cases, the tidal range, tidal amplitude, average range, average head, etc., are used instead of the dynamic head which represents the actual and real-time water level difference between the basin and sea. The RTA model developed under this study would provide more accurate time series results than previous approaches to calculate power and energy based on dynamic heads.

In the simplified base case considered for model development, the minimum head requirements for turbine operation to avoid cavitation were not considered. The base case considered continuous generation irrespective of water heads and also did not consider provision of gates. Since the theoretical base model was developed for continuous generation, it is not applicable for (i) flood-ebb generation with gate; (ii) flood generation with gate; or (iii) ebb generation with gate. These simplifications were upgraded in the RTA model by modifying and improving equations to assess these more practical modes of operation. The base case considered a very simple case with a single tidal constituent and a simple relation of the basin's area vs. elevation. These simplification were also upgraded in the RTA application where the observed tide is a superimposition of a series of tidal constituents having different tidal amplitudes, speeds and phase angles. Also, in the real cases the basin water surface is not always in a linear relation with elevation. This relation is represented by higher order polynomial equations.

The tide and basin data for the original base model is also used for the RTA model to test and verify its accuracy and suitability. The results have been found to be reasonably close. The maximum peak power found after running the original model was 980kW, whereas the maximum peak power was 983kW after running the RTA model. The RTA model with real-time operation shows 0.31% higher power than that of the original base model. Similarly, the average peak power found after running the original model was 408kW whereas it was 403 kW after running the RTA model.

The RTA model yields 1.23% higher power than that of the base case using the same inputs. The RTA model is also validated using the actual data of Severn barrage, UK. For the Severn barrage, from UKAEA (1980, 1984) study, the annual energy output was assessed to be 15.09 TWh. This was further assessed to be 11.12 TWh using "Turgency and Generation" 2006-2008: MATLAB based routines (0D approach) model. Using the RTA model (ebb generation), the annual energy output was assessed to be 10.77 TWh, which is only 3.15% less than the results from "Turgency and Generation" model. It was about 28.62% less than the results from the original UKAEA (1980,1984) study. These comparisons and validations show that the RTA model can reasonably assess the power generation potential for tidal barrage power plants.

Although this study assumes horizontal water level variation in the RTA model, it is discussed (in Chapter 5) that the water levels at the sea and the basin do not remain exactly horizontal during tidal fluctuation, rather they varies non-linearly. This non-linearity depends on the aspect ratio (width/length ratio) of the basin. It is observed that the mean power and energy decrease with a decrease of the aspect ratio. This conclusion was made based on two dimensional nao.99b model (Matsumoto, et al. 2000) experiments which employs non-linear shallow water equations. The structure and configuration used for the nao.99b model, however, is not exactly suitable for a tidal barrage. A tidal barrage has turbines, gates (submerged or open flow) and generation is intermittent. But the nao.99b model assumes gate operation and water flow to be continuous. Vertical cross-section shape of the tidal basin has influence on power and energy generation. Different types of vertical shape tidal basins having the same cross-sectional areas within the same tidal range and the same length would produce different amounts of energy. It is observed that a trapezoidal basin having a side slope s = 0.5 would yield more energy than a trapezoidal basin having s = 2.0, or a rectangular basin or a parabolic basin with similar tide data (same tidal range) and the same area of cross sections (within high tide and low tide) irrespective of the shape.

By analyzing the tidal data from 'Tide Table 2020' published by BIWTA, it is observed that the HAT (highest astronomical tide) and the LAT (lowest astronomical tide), MHWS, MLWS, MHWN and MLWN are different at different places of the coastal area of Bangladesh. These variations suggest different plant capacity at different places along the coast. Many authors suggest that a tidal range of at least 5.0 m is required for tidal barrage power generation. In reality, however, the minimum heads for turbine starting (h_s) and closing (h_c) are the prerequisites for turbine operation and protection. In this study, $h_s = 2.0$ m and $h_c = 1.8$ m were assumed. Turbine starting head (h_s) and closing head (h_c) depend on several factors such as turbine configuration, quality, strength, tidal fluctuations, volume of the basin, etc.

This study identifies some areas such as the Sandwip Channel, Chattogram (Khal No. 10 area), Mongla and Chattogram (Sadar Ghat area) are promising sites for tidal barrage power development with different plant capacities. This study presents an application of the RTA model for the most promising site at Sandwip Channel (having a tidal range more than 7 m) to assess the potentials for power generation. Using the past 20 years' tidal data, 214 tidal constituents (each of which is considered as a simple harmonic motion with different amplitude, speed and phase) were generated using the 'GeoTide Analyzer 3.0.x, 2015' software. GeoTide Analyzer converts observed tide gauge data directly into tidal harmonic constants which can then be used to make tidal predictions for any future date. Water level at the sea side was determined by summing up all constituents of simple harmonic motion. On the other hand, water level at the basin side at any particular time depends on basin configuration, area of the basin, water volume in the basin, water passed though turbines, etc. In the study a generalized equation is developed to calculate water surface area/volume in terms of water level. By calculating the difference in water levels, the dynamic water head is calculated at a particular time. Real-time power and energy are calculated using the dynamic water head. On the basis of these calculations, the analytical (RTA) model is developed to assess real-time water head, power and energy. The RTA model is flexible in introducing turbines and gates as well as their dimensions (diameter and size). The optimum capacity of the plant is assessed by calculating the least levelized cost of energy (LCOE).

Based on the analysis and discussions, it is concluded that the RTA Model can be used with reasonable reliability to assess tidal power generation. It is seen that energy generation increases with the increase of turbines and gates. It is also seen that energy generation increases with increase of gates for a particular number of turbines. For a particular number of gates, energy generation cost increases as the number of turbines increases. Theoretically, 500 turbines and 1000 gates can generate the maximum energy (2364 GWh). But the number of turbines and the number of gates should be considered in such a way that all turbines and gates are housed within the barrage length and tidal range. Considering the Sandwip tide and bathymetric data as input in the RTA model, four sets of turbines and gates (200,1000), (300, 900), (400, 800) and (500, 700) are selected. It is observed that the lower the turbine capacity the higher the generation period. For a combination of 200 turbines and 1000 gates, the generation period is 38% whereas for 400 turbines and 800 gates the generation period is 29%.

The per unit (kWh) energy generation cost for the economic life time (say, 50 years) of the plant (see Figure 6.8), considering 5% maintenance cost with 2% growth and 4% discount factor is BDT 6.49/kWh for 200 turbines and 1000 gates to produce 1591 GWh. The energy cost is BDT 7.07/kWh for 300 turbines and 900 gates to produce 1971 GWh, BDT 7.96/kWh for 400 turbines and 800 gates to produce 2203 GWh and BDT 9.11/kWh for 500 turbines and 700 gates to produce 2321 GWh annually. If 400 turbines and 800 gates are installed, the levelized cost will be BDT 7.96/kWh. A barrage system having a perimeter of 18 km for Sandwip Channel can house 400 turbines and 800 gates. The corresponding energy price will be BDT 7.96/kWh. If we compare tidal energy generation costs at Sandwip Channel (i.e. BDT 7.96/kWh) with the same from other sources, it is better in comparison to oil (BDT 20.64/kWh) and coal power (BDT 8.50/kWh). Therefore, a combination of 400 turbines and 800 gates can be installed which will generate 2203 GWh annually with an average and maximum power of 854 MW and 2757 MW, respectively, and will supply 29% time of a day. This plant will cost BDT 14763 crore equivalent to 1678 million USD (BDT 88 = 1 USD).

In this study the social, environmental and ecological impacts of the plant are not considered. However, in general a tidal power plant is pollution free, unlike coal, gas and diesel power plants. Also, unlike hydropower plants, tidal power plants allow water to go back to the basin during high tides which reduces the impacts on ecology, wildlife, migratory birds, fish habitats, etc. The effect on marine life would not be extreme since the Bay of Bengal is wide. Compared to coal power, 2203 GWh per year tidal power will reduce 1.98 million tonnes of carbon emission per year. Proper mitigating measures during feasibility study and detailed design phases should be considered to reduce the threat and negative impacts.

7. 3 Recommendations

The following specific recommendations are made based on this study:

1) This real time analytical model can be used for tidal barrage power assessment;
2) The real-time analytical model is developed based on some assumptions such as water levels at sea and the basins are considered as horizontal, but it is in reality non-linear. So, a further study could be taken up to quantify the reduction of power generation due to non-linearity of water levels;
3) Tidal barrage can be established at the southern coastal part of Bangladesh having a 5-m tidal range;
4) The Sandwip channel could be developed for tidal barrage power generation as a promising site; and
5) Further a detailed feasibility study could be taken up for the development of a tidal barrage for power generation.

A tidal barrage may be constructed in the Sandwip Channel to produce large scale power to fulfil the country's electricity demand and to fulfil the target of 10% renewable energy. The barrage will not only produce electricity, but also establish road communication to the island which will contribute to local economy and support the tourism industry. Power Division of Bangladesh declared a target of 10% electricity generation from renewable resources by 2020. GOB is also eager to develop infrastructure on a Public-Private Partnership (PPP) basis. Government has already enacted the Bangladesh Public-Private Partnership Act, 2015, formulated Rules for Viability Gap Financing (VGF) for Public-Private Partnership Projects, 2018 to fill the gap of viability of a PPP project and Rules for Public-Private Partnership Technical Assistance Financing (PPPTAF), 2018 for the financing for feasibility studies. GOB can establish a tidal barrage at Sandwip from self-financing and/or taking project aid from development partners or even under PPP basis with viability gap financing.

RFERENCES

Ahmad, M., Hasan, G. M. J., Billah, H. & Mahenoor, G. M. M., 2018. *Renewable Energy Potentials along the Bay of Bengal due to Tidal Water Level Variation.* Dhaka, MATEC Web of Conferences.

Alam, M. T., Ahamed, T., Tareq, Y., Wahid, A., Hossain, S., 2012. *Prospect of Tidal Power Generation in Bangladesh Through Tidal Barrage Using Low Head Water Turbine.* Dhaka, IEEE, pp. 750-753.

Alternative Energy, 2020. *Alternative Energy Tutorials: Tidal Barrage.* [Online] Available at: http://www.alternative-energy-tutorials.com/ [Accessed 07 March 2020].

Angeloudis, A., Ahmadian, R., Falconer, R. & Evans, B. B., 2015. Numerical model simulations for optimisation of tidal lagoon schemes. *ScienceDirect Applied Energy,* 165(2016), p. 535.

Angeloudis, A. & Falconer, R. A., 2016. Sensitivity of tidal lagoons and barrage hydrodynamic impacts and energy outputs to operational characteristics.. *ScienceDirect Renewable Energy,* 144(2017), pp. 337-351.

Angeloudis, A., Kramer, S., Avdis, A. & Matthew, P. D., 2018. Optimizing Tidal Range Power Plant Operation. *Applied Energy,* Volume 212, pp. 680-690.

Bahaj, A., Myers, L., Thompson, M. & Jorge, N., 2007 . *Characterising the wake of horizontal axis marine current turbines.* Porto Portugal, University of Southampton Porto, Portugal, p. 7th European wave and tidal energy conference .

Baker, A., 1991. *Tidal Power.* Energy Series 6 ed. London: Peter Perigrinus Ltd..

Batten, W., Bahaj, A., Molland, A. & Chaplin, J., 2007. Experimentally validatednumerical method for the hydrodynamic design of horizontal axis tidal turbines. *Ocean Eng.,* 34(7), pp. 1013-1020.

BIWTA, 2019. *Bangladesh Tide Table 2020,* Dhaka: BIWTA.

BIWTA, 2019. *Bangladesh Tide Table 2020,* Dhaka: Hydrographic Department, BIWTA.

Bowditch, N., 2002. Tides and Tidal Currents. In: 2. B. Edition, ed. *The American Practical Navigator.* Bethesda, Maryland: National Imagery and Mapping Agency, p. 129.

BPDB, 2019. *BPDB.* [Online].

BPDB, 2020. *Progressive Information of Power Sector.* [Online] Available at: https://bpdb.gov.bd/bpdb_new/d3pbs_uploads/files/Key%20Information%20of%20Power%20Sector%20Development%20Program%20_%20October.pdf

Bryden, I. G., Grinsted, T. & Melville, G., 2004. Assessing the potential of a simple tidal channel todeliver useful energy. *Journal of Applied Ocean Research,* Volume 26, pp. 198-204.

Burrows, R., Walkington, I., Yates, N., Hedges, T., Chen, D., Li, M., Zhou, J., Wolf, J., Proctor, R., Holt, J., 2009. *Tapping the Tidal Potential of the Eastern Irish Sea,* Liverpool: Proudman Oceanographic Laboratory.

Burstyn, H., 1962. Galileo's attempt to prove that the earth moves. *ISIS,* 53(2), pp. 161-185.

Callaghan, J., 2006. Future marine energy: results of the marine energy challenge: costcompetitiveness and growth of wave and tidal stream energy. *Carbon Trust.*

Power Cell., 2020. *Renewable Energy Master Database.* [Online] [Accessed 09 March 2020].

Chow, V., 2013-2014. *Open Channel Hydraulics.* International Student Edition ed. Tokyo: McGraw-Hill Kogakusha, Ltd..

CIRIA, 1996. *Beach management manual.* First ed. London: University of California.

CPD, 2011. *State of the Bangladesh Economy in FY 2010-2011,* Dhaka: CPD.

Dean, R., 1966. 4: Tides and Harmonic Analysis. In: T. I. Arthur, ed. *Estuary and Coastline Hydrodynamics.* Florida: McGRAW-HILL BOOK COMPANY, INC., pp. 209-210.

Department of Indian Energy and US Department of Energy, 2013. *Levlized Cost of Energy,* Delhi: https://www.energy.gov/sites/prod/files/2015/08/f25/LCOE.pdf.

Desmukh, T. & Amitkumar, S. G., 2015. Tidal Current Energy: An Overview. *IJRET: International Journal of Research in Engineering and Technology (IJRET),* 04(07), pp. 147-151.

Etemadi, A., Emami, Y., AsefAfshar, O. & Emdadi, A., 2011. Electricity Generation by the Tidal Barrages. *ICSGCE:Energy Procedia,* 27-30 September, 12(2011), pp. 928-935.

Fraenkel, P., 2002. Power and Energy. In: *Power from marine currents. Proc Inst Mech Eng, Part A*., pp. 1-14.

GOB, 2008. *Renewable Energy Policy of Bangladesh, 2008,* Dhaka: Power Division, Ministry of Power Energy and Mineral Resources.

Hagerman, G., Polagye, B., Bedard, R. & Previsic, M., 2006. *Methology for Estimating Tidal Current Energy Resources and Power Production by Tidal In-Stream Energy Conversion (TISEC).* EPRI North American ed. North American: Tidal in-stream energy conversion (TISEC).

Halder, P. K., Paul, N., Joardder, M. U. H. & Sarker, M., 2015. Energy scarcity and potential of renewable energy in Bangladesh. *Renewable and Sustainable Energy Reviews,* Volume 51.

Haque, M. & Khatun, M., 2017. Tidal Energy:Perspective of Bangladesh. *J. Bangladesh Acad.sci,* 41(2), pp. 201-215.

ICCB, 2018. *ICCB laments power outages.* [Online] Available at: http://www. newagebd. net/article/35481/articlelist/323/article/35972 [Accessed 2019].

IEA, 2019. *Global Energy & CO2 Status Report 2019,* Paris: IEA.

Independent, 2018. *Sustainable energy major challenge for Bangladesh: ICCB.* [Online]
Available at: http://www.theindependentbd.com/post/138847 [Accessed 03 March 2020 2019].

Islam, R. M. & Ahmad, M., 2004. *Living in the Coast, Problems, Opportunity and Challenges,* Dhaka: PDO- ICZMP .

Jahan, N., Hasan, M.A., Hossain, M.T., Subaye, N., 2013. Present Status of Installed Solar Energy forGeneration of Electricity in Bangladesh. *International Joutnal of Scientific & Engineering Research,* October .4(10).

Khare, V., Khare, C., Nema, S. & Baredar, P., 2018. *Tidal Energy Systems: Design, Optimization and Control..* 1st Edition (October 30, 2018) ed.:Elsevier.

Knight, O. & Hill, K., 2007. *Turning the Tide-Tidal Power in the UK,* London: Sustaianle Development Commission, UK.

Lamb, H., 1994. Hydrodynamics. In: *Hydrodynamics.* 6 ed. London: Cambridge University Press, p. 768.

Lewis, M. J., Angeloudis, A., Robins, P. E., Evans, P. S., Neill, S. P., 2017. Influence of storm surge on tidal range energy. *ScienceDirect Energy,* 122(2017), pp. 25-36.

Looney, B., 2020. *BP Statistical Review of World Energy June 2020,* London: BP plc.

MacKay, D., 2007. Enhancing Electrical Supply by Pumped Storage in Tidal Lagoons.

Mahbubuzzaman, M., Islam, M. S. & Rahman, M. M., 2010. *Harnessing Tidal Power,* Dhaka: Daily Star.

Matsumoto, K., Takanezawa, T. & Masatsugu, O., 2000. TOPPEX/POSEIDON Altimeter data into Hydrodynamical Model. *Journal of Oceanography,* January, 56(5), pp. 567-581.

McCollum, D.L., Zhou, W., Bertram, C., DeBoer, H.S., Bosetti, V., Busch, S., Després, J., Drouet, L., Emmerling, J., Fay, M., Fricko, O., 2018. Energy Investment Needs for Fulfilling the Paris Agreement and Achieving the Sustainable Development Goals.. *Nature Energy,* 3(7), pp. 589-599.

McErlean, T., 2007. Harnessing the Tides- the Early Medieval Tide Mills at Nendrum Monastrery, Strangford Lough, Northern Ireland.. *Archaeological Monographs,* 7(TSO), p. 468.

McErlean, T., Eaewood, C., Moore, D. & Murphy, E., 2007. The sequence of early Christian period horizontal tide mills at nendrum monastery: An interim statement.. *Historical Archaeology,* 41(3), pp. 63-75.

Moazzem, K. & Ali, M., 2019. *Power and Energy Sector: Challenges of Moving beyond the Transition Stage.* Dhaka, CPD.

Moazzem, K. G., 2019. *The power and energy sector of Bangladesh: Challenges of moving beyond the transition stage.,* Dhaka: Centre for Policy Dialouge .

Nabi, M. S., 2019. *Can Bangladesh meet its 10% renewable energy target by 2020?.* [Online] Available at: https://www.dhakatribune.com/bangladesh/power-energy/2019/01/12/can-bangladesh-meet-its-10-renewable-energy-target-by-2020 [Accessed 2019].

Nathaniel Bowditch, L., 2002. *The American Practical Navigator.* 2002 Bicentennial Edition ed. Bethesda, Maryland: National Imagery and Mapping Agency.

,Neil, S.P., Angeloudis, A., Robins, P.E., Walkington, I., Ward, S. L., Masters, I., Lewis, M.J., Piano, M., Avdis, A., Piggott, M. D., Aggidis, G., Evans, P.; Adcock, T. A. A.; Zidonis, A.; Ahmadian, R.; Falconer, R.. Tidal range energy resource and optimization–Past perspectives and future challenges. *Renewable energy,* Volume 127, pp. 763-778.

Nicholls-Lee, R. & Turnock, S., 2008. Tidal energy extraction: renewable, sustainable andpredictable. *Science Progress,* 91(1), p. 81–111.

Owusu, P. A. & Asumadu-Sarkodie, S., 2016. A Review of Renewable Energy Sources, Sustainability Issues and Climate Change Mitigation. *Cogent Engineering,* 3(1).

Prothom Alo., 2014. *Second Victory at Sea,* Dhaka: Prohom Alo.

Parker, B., 2007. *Tidal analysis and prediction.* London: National Oceanic & Atmospheric Adminstration.

Power Cell, 2020. *Achievement of Power Sector at A Glance,* Dhaka:

Prandle, D., 1984. Simple theory for designing tidal power schemes. *Advances in Water Resources,* 7(1), pp. 21-27.

PSMP, 2016. *Power System Master Plan 2016,* Dhaka: Power Division, Ministry of Power, Energy and Mineral Resources.

Pugh, D. T., 1987. *Tides, Surges and Mean Sea-Level.* 1987 ed. London: John Willey & Sons.

Quader, O., 2010. Coastal and marine biodiversity of Bangladesh (Bay of Bengal). *Proc. of International Conference on Environmental Aspects of Bangladesh (ICEAB10), Japan, Sept. 2010,* September .

Rashid, F., Ashwaq, H. M. & Ahmed, H., 2012. Power Production using Tidal Energy. *British Journal of Science,* 3(2), pp. 112-115.

Rashid, F., Mohamad, A. & Hashim, A., 2012. Power Production using Tidal Energy. *British Journal of Science,* 3(2).

Roberts, A., Thomas, B., Sewell, P., Khan, Z., Balmain, S., Gillman, Jl., 2016. Current tidal power technologies and their suitability for applications in coastal and marine areas.. *J. Ocean Eng. Mar. Energy 2,,* p. 227–245 .

Ross, D., 1995. Introduction to Oceanography. In: *Introduction to Oceanography.* New York,: HarperCollins, pp. 236-242.

Roy, P., Das, R. & Topu, S., 2015. *Possibilities of Tidal Power in Bangladesh.* Dhaka, ICME.

Salequzzaman, M., 2014. *Prospects and Sustainability of Green Power: Case Study of Tidal Power.* Sweden, 10th international conference of the Greening of Industry Network.

Roberts, A.; Thomas, B.; Sewell, P; Khan, Z; Balmain, S; Gillman, J2014. *Wave Energy in Bangladesh.* Chittagong, Bangladesh, Department of EEE, IIUC, Chittagong, Bangladesh., p. 005.

Shaikh, M. R. T. & Shaiyek, M. B. T., 2011. Tidal Power: An Effective Methodof Generating Power, International Journal of Scientific & Engineering Research.. *Sodin H. Scotland's renewable resource, Edinburgh,* 2(5).

Shevkar, S. & Otari, K., 2015. Tidal Energy Harvesting. *International Journal of Science, Engineering and Technology Research (IJSETR),* 4(4), pp. 990-994.

Shevkar, S. & Otari, K., 2015. *Tidal Energy Harvesting..* 4 ed. London: Int. J. Sci. Eng. Technol. Res,.

Simeons, C., 1980. Chapter 4: Tidal Power. In: *Hydro-power- The use of water as an alternative source of energy(.* s.l.:Oxford, Pergamon Press, Ltd., pp. 81-107.

Simeons, C., 2019. Tidal Energy System 2019. *Sciencedirect.*

Simmons, R. A., Coyle, E. & Chapman, B., 2014. In: *Global Energy Policy Perspectives.* pp. 27-72.

Simon, B. & John, C., 2017. *Tidal Constituents,* s.l.: Tide, Water Level and Current Working Group (TWCWG).

Simon, B. & Page, J., 2017. *Tidal Constituents,* London: TWCWG.

SREDA, 2015. *Energy Efficiency and Conservation Master Plan up to 2030,* s.l.: SREDA and Power Division, Ministry of Power, Energy and Mineral Resources, Government of the People's Republic of Bangladesh.

Sumich, J. L., 1996. Introduction to the biology of marine life. Jones & Bartlett Learning.. In: Sixth ed. Dubuque: Wm. C. Brown, pp. 30-35.

Taylor, F. H. D., 2014. Encyclopedia of the Solar System (Third Edition). *Scienedirectcom,* pp. 305-322.

Tester, J.W., Drake, E.M., Driscoll, M. J., Golay, M. W.; Peters, W. A.; 2012. Sustainable energy: choosing among options. *MIT press.*

Thurman, H., 1994 . *Introductory Oceanography.* Seventh ed. New York, NY: Macmillan.

Tiwari, G. & Gupta, M., 2010. Renewable Energy. p. 474.

Tousif, S. M. R. & Taslim, S. M. B., 2011. Tidal Power: An Effective Method of Generating Power. *Scientific & Engineering Research,* 2(5).

Tousif, S. & Taslim, S., 2011. Tidal Power: An Effective Method of Generating Power. *International Journal of Science & Engineering Research,* May.2(5).

U.S. Department of Energy, 2013. *An Evaluation of the U.S. Department of Energy's Marine and Hydrokinetic Resource Assessments..* Washington, DC.: The National Academies Press.

UN, 2015. *Sustainable Development Goals. (*Online] Available at: https://www.un.org/

sustainabledevelopment/sustainable-development-goals/[Accessed 2019].

UNDESA, 2013. *World Population Projected to Reach 9.6 Billion by 2050.* [Online] Available at:https://www.un.org/en/development/desa/news/population/un-report-world-population-projected-to-reach-9-6-billion-by-2050.html [Accessed 5 June 2019].

University of Strathclyde, 2015. *Tidal Barrage as an Application for Flood Defence on the Isle of Whithorn.* [Online] Available at: http://www.esru.strath.ac.uk/EandE/Web_sites/14-15/Tidal_barrage/welcome.html
[Accessed 12 2019].

USGS, n.d. *How Much Water is There on Earth?*. [Online] Available at: https://www.usgs.gov/special-topic/water-science-school/science/how-much-water-there-earth?qt-science_center_objects=0#qt-science_center_objects [Accessed 2019].

www.iclei, 2016. *iclei.* [Online] Available at: http:// www.iclei.org

Xia, J., Falconer, R. A., Lin, B. & Tan, G., 2012. Estimation of annual energy output from a tidal barrage using two different methods. *Academia, Edu.*

Xue, J., Ahmadian, R. & Falconer, R. A., 2019. Optimising the Operation of Tidal Range Schemes. *MDPI Energies,* 12(15).

APPENDICES

Appendix A1: The Base Case of Isle of Whithorn Tidal Barrage

Appendix A2: Water level, head, power and energy variations at different modes

Isle of Whithorn Model: Tidal Barrage Calculation spread sheet

Barrage Model

With this model it is possible to estimate the optimum tunnel diameter to calculate the power output and the water level behaviour inside the basin. Values highlighted in green are site specific and should be adapted before calculation. A discharge coefficient Cd of 0.9 has been chosen for a optimized, stream lined duct without an operating turbine. Later the power output is multiplied by different efficiency rates for the turbine ηturb, the transmission ηtr and the generator ηgen --> ηtot

Site specific details		
Tidal Range		
MEAN	5	m
MAXIMUM	6	m
MINIMUM	1.75	m
Basin area		
Basin Area at MHWS	150082	m²
Basin Area at MLWS	51723	m²
MHWS	6.9	m
MLWS	0.7	m
Sea level		
Mean sea level Z	7	m
VARIABLE		
Amplitude range a	4	m
High Water level	11	m
Low Water level	3.00	m
Discharge coeff.	0.9	
Turbine tunnel diameter	2.6	m
Turbine tunnel area	5.31	m²

Coefficients		
w	0.00013956	rad/s
g	9.81	
ρ	1025	
ηtot	0.4	
Cd	0.9	

Basin area Calculation	
Linear functio y=mx+n	
m	15864.3548
n	40617.9516

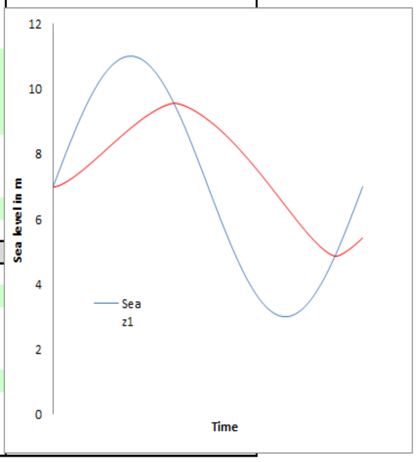

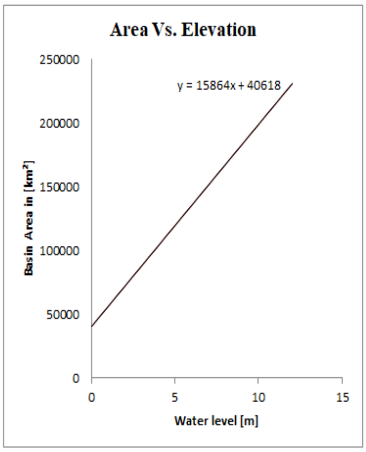

Time step	t in s	z1 in m	z2 in m	v m/s	Q in m³/s	B in m²	decide +/-	dz in m	Head in m	Power in kW
0	0	7	7	0	0	0		0	0	0
1	300	7.16741775	7	1.63114571	8.6602282	151668.435	1	0.01712992	0.167417748	5.831545862
2	600	7.33454209	7.017129922	2.24596919	11.9245053	151940.191	1	0.02354447	0.317412164	15.22358025
3	900	7.50108012	7.040674394	2.70496947	14.3614717	152313.709	1	0.02828663	0.460405724	26.59454251
4	1200	7.66673998	7.068961024	3.08221068	16.3643552	152762.458	1	0.03213687	0.597778952	39.34525658
5	1500	7.83123133	7.10109789	3.40638029	18.0854662	153272.288	1	0.0353987	0.730133442	53.11104098
6	1800	7.9942659	7.13649659	3.69213237	19.6026073	153833.866	1	0.03822814	0.857769313	67.6296609
7	2100	8.15555796	7.174724728	3.94811321	20.9616842	154440.331	1	0.04071803	0.980833234	82.69404031
8	2400	8.31482483	7.215442753	4.17990429	22.1923307	155086.296	1	0.042929	1.099382081	98.13059525
9	2700	8.47178739	7.258371751	4.39133739	23.3148907	155767.337	1	0.0449033	1.213415643	113.7878356
10	3000	8.62617056	7.303275049	4.58516303	24.3439675	156479.698	1	0.04667181	1.322895507	129.5298208
11	3300	8.77770375	7.349946856	4.76342295	25.2904014	157220.117	1	0.04825795	1.427756898	145.2321789
12	3600	8.92612142	7.398204805	4.92767251	26.1624502	157985.698	1	0.04968004	1.527916611	160.7795952
13	3900	9.07116343	7.44788484	5.07912079	26.9665333	158773.84	1	0.05095273	1.623278591	176.0641943
14	4200	9.2125756	7.498837567	5.2187228	27.707721	159582.172	1	0.052088	1.713738038	190.9844934
15	4500	9.3501101	7.550925568	5.34724232	28.3900687	160408.514	1	0.05309581	1.799184535	205.4447353
16	4800	9.48352589	7.604021382	5.46529611	29.0168506	161250.845	1	0.05398456	1.879504506	219.3544803
17	5100	9.61258914	7.658005937	5.57338561	29.5907293	162107.275	1	0.05476138	1.954583203	232.6283798
18	5400	9.73707367	7.712767321	5.67192043	30.1138794	162976.029	1	0.05543247	2.024306348	245.1860786
19	5700	9.85676131	7.768199791	5.76123575	30.5880805	163855.43	1	0.05600317	2.088561516	256.9522112
20	6000	9.97144229	7.824202965	5.84160568	31.0147879	164743.884	1	0.05647819	2.147239329	267.8564645
21	6300	10.0809156	7.880681155	5.91325347	31.3951869	165639.874	1	0.05686165	2.200234491	277.8336887
22	6600	10.1849895	7.937542802	5.97635946	31.730235	166541.947	1	0.05715719	2.2474467	286.8240432
23	6900	10.2834815	7.994699997	6.03106731	32.0206949	167448.709	1	0.05736807	2.28878147	294.7731658
24	7200	10.3762189	8.052068062	6.07748882	32.2671603	168358.817	1	0.05749713	2.324150867	301.6323558
25	7500	10.4630394	8.109565188	6.11570783	32.4700761	169270.971	1	0.05754692	2.35347417	307.3587679
26	7800	10.5437906	8.167112107	6.1457831	32.6297545	170183.916	1	0.05751969	2.37667849	311.9156071
27	8100	10.6183311	8.224631798	6.16775068	32.7463868	171096.429	1	0.05741742	2.393699325	315.2723243
28	8400	10.6865303	8.282049221	6.18162553	32.8200524	172007.319	1	0.05724184	2.404481081	317.4048063

RESULTS		
Power P		
Mean P	261.12	kW
Max P	654.44	kW
Min P	5.83	kW
Power per C	0.00	kW
Flow rate Q		
Mean Q	27.82	m3/s
Max Q	41.77	m3/s
Min Q	3.95	m3/s
Head H		
Mean H	1.96	m
Max H	3.90	m
Min H	0.03	m
Tidal range basin	4.74	m

Water level , head, power and energy at different modes for 24.8 hrs

Time	SEA	Basin at Flood-Ebb Mode				Basin at Ebb Mode				Basin at Flood Mode			
t (hr)	y (m CD)	z (m CD	H (m)	Pt (kW	Et (kW	z (m CD)	H (m)	Pt (kW)	Et (kW	z (m CI	H (m)	Pt (kV	Et (kWh)
-	7.00	7.00	-			7.00	-			7.00	-		
0.10	7.20	7.00	0.20	-	-	7.00	0.20	-	-	7.00	0.20	-	-
0.20	7.40	7.00	0.40	-	-	7.02	0.39	-	-	7.00	0.40	-	-
0.30	7.60	7.00	0.60	-	-	7.05	0.55	-	-	7.00	0.60	-	-
0.40	7.80	7.00	0.80	-	-	7.10	0.70	-	-	7.00	0.80	-	-
0.50	8.00	7.00	1.00	-	-	7.16	0.84	-	-	7.00	1.00	-	-
0.60	8.20	7.00	1.20	-	-	7.22	0.97	-	-	7.00	1.20	-	-
0.70	8.39	7.00	1.39	-	-	7.29	1.10	-	-	7.00	1.39	-	-
0.80	8.58	7.00	1.58	-	-	7.36	1.22	-	-	7.00	1.58	-	-
0.90	8.76	7.00	1.76	-	-	7.43	1.32	-	-	7.00	1.76	-	-
1.00	8.94	7.00	1.94	-	-	7.51	1.43	-	-	7.00	1.94	-	-
1.10	9.11	7.00	2.11	261	13	7.59	1.52	-	-	7.00	2.11	261	13
1.20	9.28	7.07	2.21	279	27	7.67	1.61	-	-	7.04	2.25	286	27
1.30	9.45	7.15	2.30	296	29	7.76	1.69	-	-	7.11	2.33	303	29
1.40	9.60	7.22	2.38	312	30	7.84	1.76	-	-	7.19	2.42	319	31
1.50	9.75	7.30	2.45	327	32	7.93	1.82	-	-	7.26	2.49	334	33
1.60	9.90	7.37	2.52	341	33	8.02	1.88	-	-	7.34	2.56	348	34
1.70	10.03	7.45	2.58	353	35	8.11	1.92	-	-	7.42	2.61	360	35
1.80	10.16	7.53	2.63	363	36	8.20	1.96	-	-	7.50	2.66	370	36
1.90	10.28	7.61	2.67	372	37	8.29	1.99	-	-	7.57	2.71	379	37
2.00	10.39	7.68	2.71	379	38	8.37	2.02	-	-	7.65	2.74	386	38
2.10	10.49	7.76	2.73	385	38	8.46	2.03	-	-	7.73	2.76	391	39
2.20	10.59	7.84	2.75	388	39	8.55	2.04	-	-	7.81	2.78	394	39
2.30	10.67	7.91	2.76	390	39	8.64	2.03	-	-	7.89	2.79	396	40
2.40	10.75	7.99	2.76	390	39	8.73	2.02	-	-	7.96	2.79	395	40
2.50	10.81	8.06	2.75	388	39	8.82	2.00	-	-	8.04	2.77	393	39
2.60	10.87	8.14	2.73	384	39	8.90	1.97	-	-	8.12	2.75	389	39
2.70	10.92	8.21	2.70	378	38	8.99	1.93	-	-	8.19	2.72	383	39
2.80	10.95	8.29	2.67	370	37	9.07	1.88	-	-	8.27	2.69	375	38
2.90	10.98	8.36	2.62	361	37	9.15	1.83	-	-	8.34	2.64	365	37
3.00	10.99	8.43	2.56	349	35	9.23	1.76	-	-	8.41	2.58	353	36
3.10	11.00	8.50	2.50	336	34	9.31	1.69	-	-	8.48	2.52	340	35
3.20	11.00	8.57	2.43	322	33	9.39	1.61	-	-	8.55	2.44	325	33
3.30	10.98	8.64	2.34	305	31	9.46	1.52	-	-	8.62	2.36	308	32
3.40	10.96	8.70	2.25	288	30	9.53	1.42	-	-	8.69	2.27	291	30
3.50	10.92	8.77	2.15	269	28	9.60	1.32	-	-	8.75	2.17	271	28
3.60	10.88	8.83	2.05	249	26	9.67	1.21	-	-	8.82	2.06	251	26
3.70	10.82	8.89	1.93	-	12	9.73	1.09	-	-	8.88	1.94	230	24
3.80	10.76	9.06	1.70	-	-	9.79	0.97	-	-	8.94	1.82	208	22
3.90	10.68	9.21	1.47	-	-	9.85	0.83	-	-	9.00	1.68	-	10
4.00	10.60	9.35	1.25	-	-	9.90	0.70	-	-	9.02	1.57	-	-
4.10	10.50	9.48	1.02	-	-	9.95	0.56	-	-	9.02	1.48	-	-
4.20	10.40	9.59	0.81	-	-	9.99	0.41	-	-	9.02	1.38	-	-
4.30	10.29	9.70	0.60	-	-	10.03	0.26	-	-	9.02	1.27	-	-
4.40	10.17	9.78	0.39	-	-	10.06	0.11	-	-	9.02	1.15	-	-
4.50	10.04	9.85	0.19	-	-	10.08	0.04	-	-	9.02	1.02	-	-
4.60	9.91	9.90	0.01	-	-	10.07	0.16	-	-	9.02	0.89	-	-
4.70	9.77	9.91	0.14	-	-	10.07	0.31	-	-	9.02	0.74	-	-
4.80	9.62	9.91	0.29	-	-	10.07	0.46	-	-	9.02	0.59	-	-
4.90	9.46	9.91	0.45	-	-	10.07	0.61	-	-	9.02	0.44	-	-
5.00	9.30	9.91	0.61	-	-	10.07	0.78	-	-	9.02	0.27	-	-
5.10	9.13	9.91	0.78	-	-	10.07	0.94	-	-	9.02	0.11	-	-
5.20	8.96	9.91	0.95	-	-	10.07	1.12	-	-	9.02	0.07	-	-
5.30	8.78	9.91	1.13	-	-	10.07	1.30	-	-	9.01	0.23	-	-
5.40	8.59	9.91	1.32	-	-	10.07	1.48	-	-	8.96	0.37	-	-
5.50	8.41	9.91	1.50	-	-	10.07	1.67	-	-	8.90	0.49	-	-
5.60	8.21	9.91	1.70	-	-	10.07	1.86	-	-	8.82	0.61	-	-
5.70	8.02	9.91	1.89	-	-	10.07	2.05	250	25	8.73	0.71	-	-
5.80	7.82	9.91	2.09	257	13	10.07	2.24	286	29	8.64	0.81	-	-
5.90	7.62	9.86	2.23	283	27	10.05	2.43	322	32	8.53	0.90	-	-
6.00	7.42	9.80	2.37	311	30	10.04	2.61	360	36	8.42	0.99	-	-
6.10	7.22	9.74	2.52	339	33	10.02	2.80	399	40	8.30	1.07	-	-
6.20	7.02	9.68	2.66	368	35	10.01	2.99	439	44	8.17	1.15	-	-
6.30	6.82	9.61	2.79	397	38	9.99	3.17	481	48	8.04	1.22	-	-
6.40	6.62	9.55	2.93	427	41	9.97	3.36	524	52	7.90	1.28	-	-

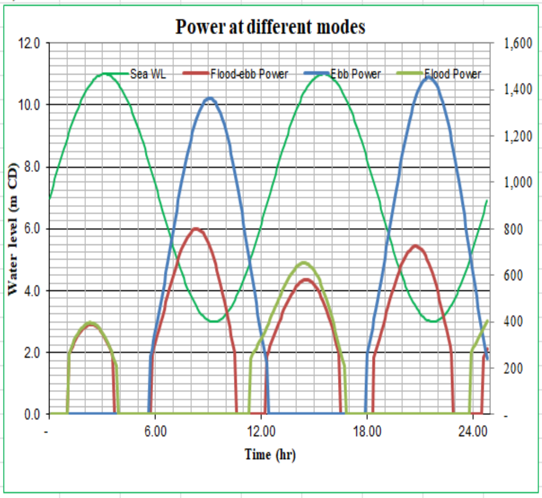

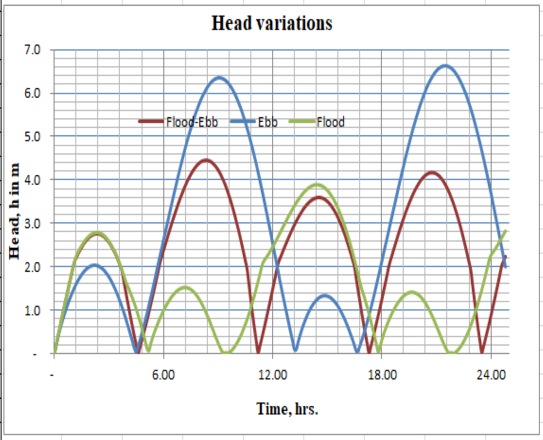

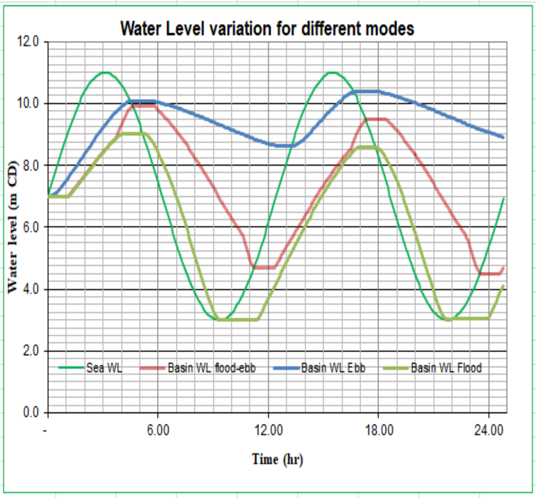

Appendix B1: Cost Calculation of Severn Barrage, UK.

Nos. Turbine	200	224	248	300	200	224
Nos. of caissons required to house turbines	50	56	62	75	50	56
Nos. Sluice gates	200	200	200	200	250	250
Nos of sluice Cassissons required for gates	50	50	50	50	62.5	62.5

Costs of Barrage Elements

Caissons construction	€M (1988)					
Construction yards	339	339	339	339	339	339
Turbine-generator Caissons (54 Nos. 4.3km)	1002	1122	1242	1503	1002	1122
Sluice Cassissons (46 Nos. 4.1 km)	355	355	355	355	443	443
Plain Cassions	270	270	270	270	270	270
Lock Caissons	81	81	81	81	81	81
Breakwater Caissons	86	86	86	86	86	86
Steelwork fabrication and installations	580	580	580	580	580	580
Dredging	380	380	380	380	380	380
Foundations	377	377	377	377	377	377
Caisson Installation	148	148	148	148	148	148
Embankments and breakwaters	382	382	382	382	382	382
Substations	65	65	65	65	65	65
Service roads	141	141	141	141	141	141
Contingencies	639	639	639	639	639	639
CIVIL WORKS TOTAL	**4845**	**4965**	**5085**	**5346**	**4933**	**5053**

54 Turbine -generator caissons would house 216 turbine-generator sets

Turbines,generator and ancilary plant	2131	2387	2642	3197	2131	2387
Contingencies (5% above cost)	107	119	132	160	107	119
TURBINE/GENERATORS TOTAL	**2238**	**2506**	**2775**	**3356**	**2238**	**2506**

Total cost of the Plant	**7082**	**7471**	**7860**	**8702**	**7171**	**7559**
TGh	10.517	11.206	11.757	12.562	11.029	11.753
Turbine	200	224	248	300	200.000	224.000
Gates	200	200	200	200	250	250
MW	7469	6000	6793	7444	5005	6000

Appendix B2: Levelized Cost of Energy (LCOE) for Severn Barrage

Year	Inititial Cost, €m	Maintenance cost, 5%	Fuel cost	Discount factor	Present value cost	Energy GWh/year	PV Energy (GWh)
	8008	5%		4%	8008	12.9460	
		2%					
1		408.00	-	0.96	392.31		12.45
2		408.00	-	0.92	377.22		11.97
3		408.00	-	0.89	362.71		11.51
4		408.00	-	0.85	348.76		11.07
5		408.00	-	0.82	335.35		10.64
6		408.00	-	0.79	322.45		10.23
7		408.00	-	0.76	310.05		9.84
8		408.00	-	0.73	298.12		9.46
9		408.00	-	0.70	286.65		9.10
10		408.00	-	0.68	275.63		8.75
11		408.00	-	0.65	265.03		8.41
12		408.00	-	0.62	254.84		8.09
13		408.00	-	0.60	245.03		7.78
14		408.00	-	0.58	235.61		7.48
15		408.00	-	0.56	226.55		7.19
16		408.00	-	0.53	217.83		6.91
17		408.00	-	0.51	209.46		6.65
18		408.00	-	0.49	201.40		6.39
19		408.00	-	0.47	193.65		6.14
20		408.00	-	0.46	186.21		5.91
21		408.00	-	0.44	179.04		5.68
22		408.00	-	0.42	172.16		5.46
23		408.00	-	0.41	165.54		5.25
24		408.00	-	0.39	159.17		5.05
25		408.00	-	0.38	153.05		4.86
26		408.00	-	0.36	147.16		4.67
27		408.00	-	0.35	141.50		4.49
28		408.00	-	0.33	136.06		4.32
29		408.00	-	0.32	130.83		4.15
30		408.00	-	0.31	125.79		3.99
31		408.00	-	0.30	120.96		3.84
32		408.00	-	0.29	116.30		3.69
33		408.00	-	0.27	111.83		3.55
34		408.00	-	0.26	107.53		3.41
35		408.00	-	0.25	103.39		3.28
36		408.00	-	0.24	99.42		3.15
37		408.00	-	0.23	95.59		3.03
38		408.00	-	0.23	91.92		2.92
39		408.00	-	0.22	88.38		2.80
40		408.00	-	0.21	84.98		2.70
41		408.00	-	0.20	81.71		2.59
42		408.00	-	0.19	78.57		2.49
43		408.00	-	0.19	75.55		2.40
44		408.00	-	0.18	72.64		2.30
45		408.00	-	0.17	69.85		2.22
46		408.00	-	0.16	67.16		2.13
47		408.00	-	0.16	64.58		2.05
48		408.00	-	0.15	62.10		1.97
49		408.00	-	0.15	59.71		1.89
50		408.00	-	0.14	57.41		1.82
					16772.72		278.11
				LCOE	0.06031	€/kWh	
					6.031	p/kWh	

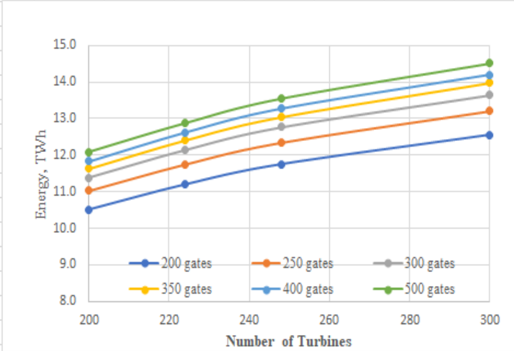

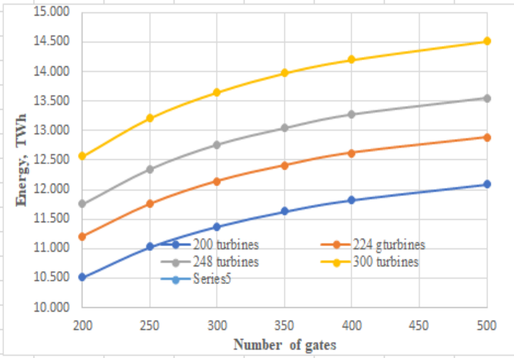

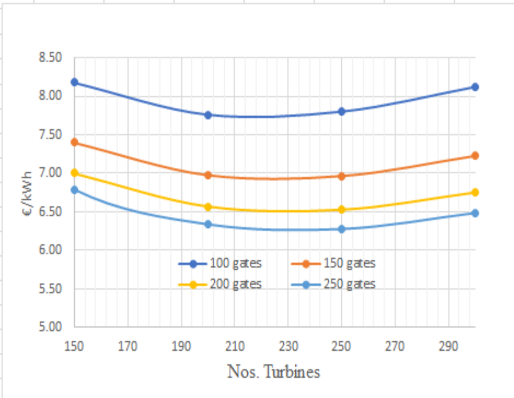

Appendix C1: 20 Years Tidal Data of Sandwip Channel (Sample)

	Tide Data from 2015 to 1996											
Date	Time	Height(cm)	Height (m)	Date	Time	Height(cm)	Height (m)	Date	Time	Height(cm)	Height (m)
01/01/1996	0:00	473	4.73	02/01/1996	18:00	107	1.07	05/01/1996	2:00	526	5.26
01/01/1996	23:00	472	4.72	03/01/1996	1:00	480	4.8	05/01/1996	3:00	505	5.05
01/01/1996	0:00	445	4.45	03/01/1996	13:00	444	4.44	05/01/1996	23:59	501	5.01
01/01/1996	22:00	421	4.21	03/01/1996	12:00	439	4.39	05/01/1996	13:59	484	4.84
01/01/1996	11:00	414	4.14	03/01/1996	14:00	405	4.05	05/01/1996	12:59	470	4.7
01/01/1996	12:00	405	4.05	03/01/1996	11:00	390	3.9	05/01/1996	14:59	405	4.05
01/01/1996	10:00	392	3.92	03/01/1996	2:00	385	3.85	05/01/1996	3:59	399	3.99
01/01/1996	1:00	388	3.88	03/01/1996	0:00	350	3.5	05/01/1996	11:59	390	3.9
01/01/1996	13:00	352	3.52	03/01/1996	15:00	321	3.21	05/01/1996	15:59	335	3.35
01/01/1996	21:00	350	3.5	03/01/1996	3:00	305	3.05	05/01/1996	10:59	320	3.2
01/01/1996	9:00	325	3.25	03/01/1996	10:00	301	3.01	05/01/1996	4:59	288	2.88
01/01/1996	14:00	287	2.87	03/01/1996	16:00	246	2.46	05/01/1996	22:59	270	2.7
01/01/1996	2:00	280	2.8	03/01/1996	23:00	245	2.45	05/01/1996	16:59	255	2.55
01/01/1996	8:00	259	2.59	03/01/1996	4:00	225	2.25	05/01/1996	5:59	220	2.2
01/01/1996	20:00	238	2.38	03/01/1996	22:00	186	1.86	05/01/1996	9:59	188	1.88
01/01/1996	15:00	215	2.15	03/01/1996	9:00	180	1.8	05/01/1996	17:59	168	1.68
01/01/1996	3:00	201	2.01	03/01/1996	5:00	172	1.72	05/01/1996	6:59	154	1.54
01/01/1996	19:00	192	1.92	03/01/1996	17:00	164	1.64	05/01/1996	8:59	125	1.25
01/01/1996	7:00	172	1.72	03/01/1996	21:00	140	1.4	05/01/1996	18:59	122	1.22
01/01/1996	16:00	167	1.67	03/01/1996	6:00	125	1.25	05/01/1996	21:59	120	1.2
01/01/1996	4:00	160	1.6	03/01/1996	18:00	122	1.22	05/01/1996	19:59	78	0.78
01/01/1996	5:00	132	1.32	03/01/1996	8:00	120	1.2	05/01/1996	7:59	74	0.74
01/01/1996	6:00	132	1.32	03/01/1996	7:00	103	1.03	05/01/1996	20:59	68	0.68
01/01/1996	18:00	129	1.29	03/01/1996	20:00	101	1.01	06/01/1996	0:59	530	5.3
01/01/1996	17:00	128	1.28	03/01/1996	19:00	96	0.96	06/01/1996	1:59	525	5.25
02/01/1996	0:00	486	4.86	04/01/1996	0:00	489	4.89	06/01/1996	13:59	500	5
02/01/1996	23:00	458	4.58	04/01/1996	1:00	470	4.7	06/01/1996	14:59	485	4.85
02/01/1996	12:00	432	4.32	04/01/1996	13:00	465	4.65	06/01/1996	12:59	480	4.8
02/01/1996	13:00	416	4.16	04/01/1996	14:00	456	4.56	06/01/1996	2:59	460	4.6
02/01/1996	1:00	415	4.15	04/01/1996	23:00	430	4.3	06/01/1996	15:59	391	3.91
02/01/1996	22:00	402	4.02	04/01/1996	12:00	425	4.25	06/01/1996	3:59	370	3.7
02/01/1996	11:00	380	3.8	04/01/1996	15:00	408	4.08	06/01/1996	23:59	362	3.62
02/01/1996	2:00	351	3.51	04/01/1996	2:00	395	3.95	06/01/1996	11:59	357	3.57
02/01/1996	14:00	347	3.47	04/01/1996	11:00	358	3.58	06/01/1996	4:59	315	3.15
02/01/1996	10:00	341	3.41	04/01/1996	3:00	348	3.48	06/01/1996	16:59	285	2.85
02/01/1996	21:00	321	3.21	04/01/1996	22:00	340	3.4	06/01/1996	10:59	275	2.75
02/01/1996	3:00	303	3.03	04/01/1996	16:00	291	2.91	06/01/1996	22:59	275	2.75
02/01/1996	15:00	287	2.87	04/01/1996	4:00	285	2.85	06/01/1996	17:59	208	2.08
02/01/1996	9:00	252	2.52	04/01/1996	10:00	250	2.5	06/01/1996	5:59	200	2
02/01/1996	4:00	250	2.5	04/01/1996	5:00	222	2.22	06/01/1996	18:59	149	1.49
02/01/1996	20:00	220	2.2	04/01/1996	17:00	205	2.05	06/01/1996	6:59	145	1.45
02/01/1996	16:00	202	2.02	04/01/1996	6:00	152	1.52	06/01/1996	9:59	128	1.28
02/01/1996	8:00	182	1.82	04/01/1996	21:00	145	1.45	06/01/1996	21:59	125	1.25
02/01/1996	5:00	180	1.8	04/01/1996	18:00	140	1.4	06/01/1996	19:59	100	1
02/01/1996	17:00	140	1.4	04/01/1996	9:00	128	1.28	06/01/1996	7:59	84	0.84
02/01/1996	7:00	138	1.38	04/01/1996	7:00	117	1.17	06/01/1996	8:59	62	0.62
02/01/1996	6:00	116	1.16	04/01/1996	8:00	84	0.84	06/01/1996	20:59	59	0.59
02/01/1996	19:00	115	1.15	04/01/1996	19:00	80	0.8	07/01/1996	1:59	520	5.2
02/01/1996	18:00	107	1.07	04/01/1996	20:00	75	0.75	07/01/1996	14:59	499	4.99
03/01/1996	1:00	480	4.8	05/01/1996	1:00	527	5.27	07/01/1996	2:59	490	4.9
03/01/1996	13:00	444	4.44	05/01/1996	2:00	526	5.26	07/01/1996	13:59	489	4.89

Appendix C2: Tidal Analysis Report on Sandwip Channel.

Tidal Analysis Report

Compare: C:\Users\Hp\Desktop\Rafiq Tide Test - 2\Sandip Tide 1996 to 2015.rec
With: C:\Users\Hp\Desktop\Rafiq Tide Test - 2\Sandip Tide 1996 to 2015_UKHOTotalTidePlus20191109162744.tc1
Duration of source points: 7299 Days
Number of source points in total: 33307
Number of Source points meeting DTG matching criteria: 33307
Number of Source points not meeting DTG matching criteria: 0
DTG Source: DateTime from A
DTG Match: Exact Match

Residual Statistics

Mean of Observed (A): 2.797m
Mean of Predicted (B): 2.797m
Mean Difference (A-B): :0.000m
Mean Absolute Difference |A-B|: :0.554m
RMS Difference (A,B): 0.862m
Maximum Positive Difference: 4.818m on Wednesday, October 1, 2003 11:59:00, Point 19649
Maximum Negative Difference: -6.126m on Monday, June 8, 2009 13:59:00, Point 21677

Analysing Tidal Predictions

Generated from Harmonic Constants File: C:\Users\Hp\Desktop\Rafiq Tide Test - 2\Sandip Tide 1996 to 2015_UKHOTotalTidePlus20191109162744.tc1
Number of harmonic components: 231 in 214 groups
Prediction Scan from Friday, January 1, 2010 to Friday, August 11, 2028

Tidal Statistics

Maximum: 6.802m at 13-Jul-10 14:54:00
Minimum: -0.846m at 21-Apr-19 22:12:00
Maximum Rise from Low Tide to High Tide: 5.989m at 06-Jul-27 12:30:00
Maximum Fall from High Tide to Low Tide: 6.887m at 08-May-12 18:45:00
Fastest Rate of Rise: 2.659m/hr at 29-Sep-19 13:09:00
Fastest Rate of Fall: -2.322m/hr at 26-Aug-25 1:51:00
Number of Spring Tides found. High Waters: 450 Low Waters: 452
Number of Neap Tides found. High Waters: 445 Low Waters: 460

Tidal Levels

HAT: 6.802m
MHWS: 4.736m
MHHW: 5.179m
MHW: 3.909m
MHWN: 3.514m
ML: 2.641m
MLWN: 2.692m
MLW: 1.297m
MLLW: 0.722m
MLWS: 0.588m
LAT: -0.846m

Listing of Harmonic Constants

Filename: C:\Users\Hp\Desktop\Rafiq Tide Test - 2\Sandip Tide 1996 to 2015_UKHOTotalTidePlus20191109162744.tc1

#ANALYZER 3.0.15
#FILENAME C:\Users\Hp\Desktop\Rafiq Tide Test - 2\Sandip Tide 1996 to 2015.rec
#IMP_FILE C:\Users\Hp\Desktop\Rafiq Tide Test - 2\Sandip Tide 1996 to 2015.txt|27 Aug 2019 12:10:33
#LOCATION Sanwdip
#GAUGE_ID Sanwdip
#TIMEZONE +0600
#POSITION 22°29.03`N,091°26.22`E
#SCHEMENAME UKHOTotalTidePlus.sch|14 Feb 2015 02:36:18
#MODE HEIGHT
'User:User:09-Nov-19 , 16:27:38
'Number of Input Points:33307
'Input Duration: 7299.6 Days
'Matrix Inversion
'RMS Error: 0.861847
#MEAN 2.638998

#GROUP Sa,057.703,0.06965	#GROUP SNK2,171.481,0.02417
#GROUP Ssa,264.323,0.19025	#GROUP NA2,331.131,0.07514
#GROUP Mnum,195.856,0.00767	#GROUP N2,034.403,0.21856
#GROUP Mm,189.181,0.05147	#GROUP NB2,066.617,0.05922
#GROUP Msf,247.476,0.16365	#GROUP nu2,034.320,0.08862
#GROUP Mf,342.096,0.02690	#GROUP 2KN2S2,151.875,0.00972
#GROUP 2Q1,251.215,0.00807	#GROUP MSK2,130.803,0.10697
#GROUP sig1,110.005,0.03172	#GROUP MPS2,107.875,0.19788
#GROUP Q1,256.164,0.01845	#GROUP M2,046.384,1.28770
#GROUP rho1,296.168,0.00729	#GROUP MSP2,310.846,0.31817
#GROUP O1,336.785,0.19084	#GROUP MKS2,238.627,0.08649
#GROUP MS1,357.527,0.27674	#GROUP M2(KS)2,183.158,0.02502
#GROUP MP1,125.634,0.09921	#GROUP lambda2,060.360,0.07740
#GROUP NO1,163.622,0.02984	#GROUP L2,056.968,0.15263
#GROUP chi1,242.664,0.01003	#GROUP 2SK2,117.356,0.05794
#GROUP pi1,282.812,0.14080	#GROUP T2,031.638,0.15551
#GROUP P1,357.197,0.29460	#GROUP S2,089.069,0.39198
#GROUP S1,244.914,0.70762	#GROUP R2,000.320,0.13775
#GROUP K1,104.617,0.24025	#GROUP K2,057.361,0.07145
#GROUP psi1,110.306,0.19294	#GROUP MSnu2,353.939,0.00564
#GROUP phi1,311.653,0.03974	#GROUP MSN2,253.798,0.03675
#GROUP th1,121.553,0.01909	#GROUP KJ2,101.413,0.01713
#GROUP J1,179.764,0.01328	#GROUP 2KM(SN)2,240.256,0.00427
#GROUP 2PO1,173.361,0.04237	#GROUP 2SM2,227.363,0.07499
#GROUP SO1,268.638,0.05952	#GROUP 2MS2N2,136.238,0.01455
#GROUP OO1,225.017,0.02593	#GROUP SKM2,277.289,0.03940
#GROUP KQ1,247.183,0.00783	#GROUP 3(SM)N2,184.101,0.00441
#GROUP 2MN2S2,133.781,0.00611	#GROUP SKN2,201.447,0.00709
#GROUP 3M(SK)2,289.222,0.00552	#GROUP NK3,207.025,0.01412
#GROUP 2NS2,129.140,0.01282	#GROUP MP3,038.941,0.24825
#GROUP 3M2S2,056.907,0.01992	#GROUP 2MP3,144.361,0.08637
#GROUP MNK2,142.692,0.02048	#GROUP M3,077.091,0.01806
#GROUP MNS2,136.001,0.05591	#GROUP MQ3,116.415,0.01959
#GROUP MnuS2,175.808,0.01843	#GROUP MO3,330.030,0.08953
#GROUP MNK2S2,188.180,0.00555	#GROUP 2NKM3,114.502,0.01142
#GROUP 2MK2,130.411,0.01956	#GROUP 2MS3,027.970,0.13663
#GROUP 2N2,021.678,0.05173	
#GROUP mu2,157.365,0.19056	

#GROUP MS3,102.614,0.40669	#GROUP MSN6,133.985,0.03619
#GROUP MK3,079.348,0.18919	#GROUP 4MN6,161.254,0.00360
#GROUP 2MQ3,243.500,0.01044	#GROUP MNK6,176.538,0.02329
#GROUP SP3,117.381,0.03267	#GROUP 2(MS)K6,092.761,0.00387
#GROUP S3,275.088,0.07035	#GROUP 2MT6,340.736,0.02583
#GROUP SK3,202.180,0.03589	#GROUP 2MS6,278.897,0.01373
#GROUP K3,132.627,0.01132	#GROUP 2MK6,219.962,0.03358
#GROUP 4MS4,147.698,0.00720	#GROUP 2SN6,282.016,0.02113
#GROUP 2MNS4,090.917,0.03494	#GROUP 3MSN6,225.844,0.00867
#GROUP 3MK4,126.921,0.01114	#GROUP MKL6,142.985,0.01030
#GROUP 2N4,082.579,0.01676	#GROUP 2SM6,238.314,0.05555
#GROUP 2NKS4,352.699,0.00869	#GROUP MSK6,301.181,0.00832
#GROUP MSNK4,181.371,0.01526	#GROUP S6,071.870,0.03055
#GROUP MN4,066.939,0.01474	#GROUP 2MNO7,101.028,0.00960
#GROUP Mnu4,359.811,0.01163	#GROUP 4MK7,066.362,0.01123
#GROUP MNKS4,144.790,0.01643	#GROUP 2NMK7,159.466,0.00229
#GROUP 2MSK4,167.915,0.05249	#GROUP M7,197.968,0.00459
#GROUP MA4,065.827,0.11614	#GROUP 2MNK7,294.878,0.02121
#GROUP M4,267.333,0.11507	#GROUP 2MSO7,086.028,0.05773
#GROUP 2MRS4,305.347,0.12449	#GROUP MSKO7,231.760,0.02125
#GROUP 2MKS4,224.419,0.02171	#GROUP 5MK8,052.368,0.00156
#GROUP SN4,142.855,0.03340	#GROUP 2(MN)8,134.349,0.00682
#GROUP 3MN4,194.844,0.03328	#GROUP 5MS8,230.767,0.00564
#GROUP NK4,237.521,0.01866	#GROUP 2(MN)KS8,323.130,0.00360
#GROUP M2SK4,180.256,0.00695	#GROUP 3MN8,011.471,0.00499
#GROUP MT4,058.183,0.05531	#GROUP 3Mnu8,359.048,0.00181
#GROUP MS4,040.948,0.14273	#GROUP 3MNKS8,122.127,0.01245
#GROUP MR4,001.158,0.10470	#GROUP 4MSK8,081.633,0.00239
#GROUP MK4,215.792,0.02332	#GROUP MA8,301.354,0.00133
#GROUP 2SNM4,284.303,0.02446	#GROUP M8,065.068,0.00807
#GROUP 2MSN4,255.824,0.03650	#GROUP 2MSN8,149.873,0.02385
#GROUP S4,171.574,0.12032	#GROUP 2MNK8,180.869,0.00899
#GROUP SK4,228.492,0.01423	#GROUP 3MS8,141.635,0.05637
#GROUP 3SM4,059.581,0.04204	#GROUP 3MK8,234.162,0.02117
#GROUP 2SKM4,117.234,0.01547	#GROUP 2SNM8,277.214,0.01493
#GROUP MNO5,090.508,0.01530	#GROUP MSNK8,159.306,0.01725
#GROUP 2NKMS5,105.531,0.00111	#GROUP 2(MS)8,149.497,0.00805
#GROUP 3MK5,056.580,0.05855	#GROUP 2MSK8,252.665,0.00856
#GROUP 2NK5,146.882,0.01332	#GROUP 3SM8,144.672,0.03767
#GROUP 3MS5,099.721,0.06356	#GROUP 2SMK8,254.433,0.00376
#GROUP 3MP5,224.290,0.00954	#GROUP S8,316.647,0.01339
#GROUP M5,351.496,0.00864	#GROUP 3MN09,139.505,0.00736
#GROUP MNK5,259.345,0.02460	#GROUP 2(MN)K9,209.451,0.00724
#GROUP MB5,144.962,0.01100	#GROUP MA9,039.935,0.00227
#GROUP MSO5,032.962,0.10134	#GROUP 3MNK9,295.151,0.01313
#GROUP 2MS5,109.075,0.20143	#GROUP 4MK9,264.689,0.00681
#GROUP 3MO5,177.693,0.09144	#GROUP 3MSK9,043.206,0.00825
#GROUP 3MQ5,064.348,0.00759	#GROUP 3M2N10,202.391,0.00910
#GROUP 2(MN)S6,354.577,0.00875	#GROUP 6MS10,318.937,0.01015
#GROUP 3MNS6,074.248,0.00426	#GROUP 3M2NKS10,358.412,0.00969
#GROUP 4MK6,281.457,0.00443	#GROUP 4MSNK10,150.341,0.00159
#GROUP M2N6,102.360,0.00639	#GROUP 4MN10,281.089,0.00928
#GROUP 4MS6,009.214,0.01201	#GROUP 4Mnu10,057.612,0.00121
#GROUP 2NMKS6,261.687,0.00502	#GROUP 5MSK10,049.466,0.00250
#GROUP 2MSNK6,169.434,0.01161	#GROUP M10,292.142,0.00556
#GROUP 2MN6,154.012,0.02542	#GROUP 3MSN10,202.400,0.00731
#GROUP 2Mnu6,242.861,0.00560	#GROUP 6MN10,327.232,0.00503
#GROUP MA6,138.726,0.04383	GROUP 3MNK10,076.009,0.01045
#GROUP M6,230.479,0.04245	#GROUP 4MK10,264.531,0.00491

#GROUP 2MNSK10,145.372,0.01034 #GROUP 3M2S10,004.316,0.02114 #GROUP 4MSK11,293.795,0.00864 #GROUP 4M2N12,187.963,0.00926 #GROUP 4M2NKS12,326.742,0.00751 #GROUP 5MSNK12,011.156,0.00476 #GROUP 5MN12,280.151,0.00763 #GROUP 5Mnu12,136.622,0.01127 #GROUP 6MSK12,047.915,0.00249 #GROUP MA12,298.584,0.00105	#GROUP M12,348.898,0.00203 #GROUP 4MSN12,221.535,0.01864 #GROUP 5MS12,223.226,0.01855 #GROUP 5MK12,288.160,0.00936 #GROUP 3MNKS12,162.636,0.00416 #GROUP 4M2S12,306.843,0.01142 #GROUP 5MSN14,239.466,0.01017 #GROUP 5MNK14,258.300,0.00493 #GROUP 6MS14,235.784,0.01019

Report created automatically by GeoTide Analyzer 3.0.15 on Saturday, November 9, 2019 16:30:12.

Appendix C3: 214 Tidal Constituents for Sandwip Channel Tide

Name of the constituents	*Name*	*Speed (Deg/hr)*	Tidal Peiod, T (hrs.)	Phase (degree)	Amplitude (m)
Long Term Constituents	Sa	0.041069	8765.8210896	57.703	0.06965
	Ssa	0.082137	4382.9052087	264.323	0.19025
	Mnum (Mνm)	0.471521	763.4865121	195.856	0.00767
	Mm	0.544375	661.3092049	189.181	0.05147
	MSf	1.015896	354.3670522	247.476	0.16365
	Mf	1.098033	327.8589988	342.096	0.0269
Diurnal Constituents	2Q1	12.85429	28.0062225	251.215	0.00807
	sig 1	12.92714	27.8483876	110.005	0.03172
	Q1	13.39866	26.8683567	256.164	0.01845
	(rho1)	13.47151	26.7230533	296.168	0.00729
	O1	13.94304	25.8193417	336.785	0.19084
	MS1	13.9841	25.7435153	357.527	0.27674
	MP1	14.02517	25.6681328	125.634	0.09921
	NO1	14.49669	24.8332484	163.622	0.02984
	(chi1)	14.56955	24.7090720	242.664	0.01003
	(pi1)	14.91786	24.1321400	282.812	0.1408
	P1	14.95893	24.0658902	357.197	0.2946
	S1	15	23.9999968	244.914	0.70762
	K1	15.04069	23.9350785	104.617	0.24025
	psi1	15.08214	23.8692992	110.306	0.19294
	phi1	15.12321	23.8044764	311.653	0.03974
	th1	15.51259	23.2069569	121.553	0.01909
	J1	15.58544	23.0984768	179.764	0.01328
	2PO1	15.97483	22.5354552	173.361	0.04237
	SO1	16.05696	22.4201780	268.638	0.05952
	OO1	16.1391	22.3060742	225.017	0.02593
	KQ1	16.68348	21.5782365	247.183	0.00783
Semi-Diurnal Constituents	2MN2S2	26.40794	13.6322647	133.781	0.00611
	3M(SK)2	26.87018	13.3977540	289.222	0.00552
	2NS2	26.87946	13.3931266	129.14	0.01282
	3M2S2	26.95231	13.3569241	56.907	0.01992
	MNK2	27.3417	13.1667031	142.692	0.02048
	MNS2	27.42383	13.1272674	136.001	0.05591
	MnuS2 (MνS2)	27.49669	13.0924862	175.808	0.01843
	MNK2S2	27.50597	13.0880673	188.18	0.00555
	2MS2K2	27.80393	12.9478081	331.315	0.01036
	2MK2	27.88607	12.9096708	130.411	0.01956
	2N2	27.89535	12.9053745	21.678	0.05173
	mu2 (μ2)	27.96821	12.8717576	157.365	0.19056
	SNK2	28.35759	12.6950129	171.481	0.02417
	NA2	28.39866	12.6766532	331.131	0.07514
	N2	28.43973	12.6583482	34.403	34.403
	NB2	28.4808	12.6400961	66.617	0.05922
	nu2 (ν2)	28.51258	12.6260044	34.32	0.08862
	2KN2S2	28.604	12.5856506	151.875	0.00972
	MSK2	28.90197	12.4558996	130.803	0.10697
	MPS2	28.94304	12.4382254	107.875	0.19788
	M2	28.9841	12.4206012	46.384	1.2877
	MSP2	29.02517	12.4030269	310.846	310.846
	MKS2	29.06624	12.3855023	238.627	0.08649
	M2(KS)2	29.14838	12.3506015	183.158	0.02502
	lambda2 (Z2)	29.45563	12.2217742	60.36	0.0774
	L2	29.52848	12.1916202	56.968	0.15263
	2SK2	29.91786	12.0329451	117.356	0.05794

Name of the constituents	*Name*	*Speed (Deg/hr)*	Tidal Peiod, T (hrs.)	Phase (degree)	Amplitude (m)
Semi-Diurnal Constituents	T2	29.95893	12.0164492	31.638	0.15551
	S2	30	12.0000000	89.069	0.39198
	R2	30.04107	11.9835958	0.13775	0.13775
	K2	30.08214	11.9672348	0.07145	0.07145
	MSnu2 (MSν2)	30.47152	11.8143101	353.939	0.00564
	MSN2	30.54437	11.7861309	253.798	0.03675
	KJ2	30.62651	11.7545217	101.413	0.01713
	2KM(SN)2	30.70865	11.7230815	240.256	0.00427
	2SM2	31.0159	11.6069516	227.363	0.07499
	2MS2N2	31.08875	11.5797517	136.238	0.01455
	SKM2	31.09803	11.5762949	277.289	0.0394
	3(SM)N2	31.48742	11.4331386	184.101	0.00441
	SKN2	31.64241	11.3771367	201.447	0.00709
Third-Diurnal Constituents	MQ3	42.38277	8.4940187	116.415	0.01959
	MO3	42.92714	8.3863030	330.03	0.08953
	2NKM3	42.93642	8.3844897	114.502	0.01142
	2MS3	42.96821	8.3782874	27.97	0.13663
	2MP3	43.00928	8.3702872	144.361	0.08637
	M3	43.476156	8.2804008	77.091	0.01806
	NK3	43.4808	8.2795168	207.025	0.01412
	MP3	43.94304	8.1924245	38.941	0.24825
	MS3	43.9841	8.1847751	102.614	0.40669
	MK3	44.02517	8.1771399	79.348	0.18919
	2MQ3	44.56955	8.0772639	243.5	0.01044
	SP3	44.95893	8.0073078	117.381	0.03267
	S3	45	8.0000000	275.088	0.07035
	SK3	45.04107	7.9927056	202.18	0.03589
	K3	45.12321	7.9781565	132.627	0.01132
Fouth-Diurnal Constituents	4MS4	55.93642	6.4358788	147.698	0.0072
	2MNS4	56.40794	6.3820805	90.917	0.03494
	3MK4	56.87018	6.3302073	126.921	0.01114
	2N4	56.87946	6.3291741	82.579	0.01676
	2NKS4	56.9616	6.3200476	352.699	0.00869
	MSNK4	57.3417	6.2781540	181.371	0.01526
	MN4	57.42383	6.2691739	66.939	0.01474
	Mnu4 (Mν4)	57.49669	6.2612303	359.811	0.01163
	MNKS4	57.50597	6.2602195	144.79	0.01643
	2MSK4	57.88607	6.2191127	167.915	0.05249
	MA4	57.92714	6.2147035	65.827	0.11614
	M4	57.96821	6.2103006	267.333	0.11507
	2MRS4	58.00928	6.2059041	305.347	0.12449
	2MKS4	58.05035	6.2015134	224.419	0.02171
	SN4	58.43973	6.1601928	142.855	0.0334
	3MN4	58.51258	6.1525228	194.844	0.03328
	NK4	58.52187	6.1515467	237.521	0.01866
	M2SK4	58.90197	6.1118502	180.256	0.00695
	MT4	58.94304	6.1075916	58.183	0.05531
	MS4	58.9841	6.1033393	40.948	0.14273
	MR4	59.02517	6.0990929	1.158	0.1047
	MK4	59.06624	6.0948520	215.792	0.02332
	2SNM4	59.45563	6.0549359	284.303	0.02446
	2MSN4	59.52848	6.0475255	255.824	0.0365
	S4	60	6.0000000	284.303	0.02446
	SK4	60.08137	5.9918737	255.824	0.0365

Name of the constituents	Name	Speed (Deg/hr)	Tidal Peiod, T (hrs.)	Phase (degree)	Amplitude (m)
Fourth-Diurnal	3SM4	61.0159	5.9001019	171.574	0.12032
	2SKM4	61.09803	5.8921700	228.492	0.01423
Fifth-Diurnal Constituents	MNO5	71.36687	5.0443575	59.581	0.04204
	2NKMS5	71.45365	5.0382312	117.234	0.01547
	3MK5	71.91124	5.0061712	90.508	0.0153
	2NK5	71.92053	5.0055250	105.531	0.00111
	3MS5	71.95231	5.0033138	56.58	0.05855
	3MP5	71.99338	5.0004597	146.882	0.01332
	M5	72.46026	4.9682405	99.721	0.06356
	MNK5	72.4649	4.9679222	224.29	0.00954
	MB5	72.50133	4.9654262	351.496	0.00864
	MSO5	72.92714	4.9364338	259.345	0.0246
	2MS5	72.96821	4.9336555	144.962	0.011
	3MO5	73.00928	4.9308802	32.962	0.10134
	3MQ5	73.55365	4.8943865	109.075	0.20143
Sixth-Diurnal Constituents	2(MN)S6	84.84767	4.2428980	177.693	0.09144
	3MNS6	85.39204	4.2158495	64.348	0.00759
	4MK6	85.85428	4.1931515	354.577	0.00875
	M2N6	85.86356	4.1926981	74.248	0.00426
	4MS6	85.93642	4.1891437	281.457	0.00443
	2NMKS6	85.9457006	#VALUE!	102.36	0.00639
	2MSNK6	86.3258007	#VALUE!	9.214	0.01201
	2MN6	86.40794	4.1662839	261.687	0.00502
	2Mnu6 (2Mv6)	86.48079	4.1627741	169.434	0.01161
	2MNKS6	86.49008	4.1623273	154.012	0.02542
	3MSK6	86.87018	4.1441150	242.861	0.0056
	MA6	86.91124	4.1421568	139.501	0.01313
	M6	86.95231	4.1402004	238.515	0.01753
	MSN6	87.42383	4.1178702	138.726	0.04383
	4MN6	87.49669	4.1144415	230.479	0.04245
	MKN6	87.50597	4.1140050	133.985	0.03619
	2(MS)K6	87.88607	4.0962122	161.254	0.0036
	2MT6	87.92714	4.0942989	176.538	0.02329
	2MS6	87.96821	4.0923875	92.761	0.00387
	2MK6	88.05035	4.0885700	340.736	0.02583
	2SN6	88.43973	4.0705688	282.016	0.02113
	3MSN6	88.51258	4.0672183	225.844	0.00867
	MKL6	88.59472	4.0634476	142.985	0.0103
	2SM6	88.9841	4.0456664	238.314	0.05555
	SKM6	89.06624	4.0419354	301.181	0.00832
	S6	90	4.0000000	71.87	0.03055
Seventh-Diurnal Constituents	2MNO7	100.351	3.5874091	101.028	0.0096
	4MK7	100.8953	3.5680535	66.362	0.01123
	2NMK7	100.9046	3.5677252	159.46	0.00229
	M7	101.4444	3.5487431	197.968	0.00459
	2MNK7	101.449	3.5485808	294.878	0.02121
	2MSO7	101.9112	3.5324856	86.028	0.05773
	MSKO7	103.0093	3.4948309	231.76	0.02125
Seventh-Diurnal Constituents	5MK8	114.8384	3.1348404	52.368	0.00156
	2(MN)8	114.8477	3.1345869	134.349	0.00682
	5MS8	114.9205	3.1325998	230.767	0.00564
	2(MN)KS8	114.9298	3.1323467	323.13	0.0036
	3MN8	115.392	3.1197992	11.471	0.00499

Name of the constituents	Name	Speed (Deg/hr)	Tidal Peiod, T (hrs.)	Phase (degree)	Amplitude (m)
Eighth-Diurnal Constituents	3Mnu8 (3Mv8)	115.4649	3.1178307	359.048	0.00181
	3MNKS8	115.4742	3.1175801	122.127	0.01245
	4MSK8	115.8543	3.1073518	81.633	0.00239
	MA8	115.8953	3.1062506	301.354	0.00133
	M8	115.9364	3.1051503	65.068	0.00807
	2MSN8	116.4079	3.0925726	149.873	0.02385
	2MNK8	116.4901	3.0903920	180.869	0.00899
	3MS8	116.9523	3.0781777	141.635	0.05637
	3MK8	117.0345	3.0760174	234.162	0.02117
	2SNM8	117.4238	3.0658171	277.214	0.01493
	MSNK8	117.506	3.0636741	159.306	0.01725
	2(MS)8	117.9682	3.0516696	149.497	0.00805
	2MSK8	118.0503	3.0495463	252.665	0.00856
	3SM8	118.9841	3.0256142	144.672	0.03767
	2SMK8	119.0662	3.0235270	254.433	0.00376
	S8	120	3.0000000	316.647	0.01339
Nineth-Diurnal Constituents	3MNO9	129.3351	2.7834676	139.505	0.00736
	2(MN)K9	129.8887	2.7716029	209.451	0.00724
	MA9	130.3874	2.7610030	39.935	0.00227
	3MNK9	130.4331	2.7600354	295.151	0.01313
	4MK9	130.9775	2.7485640	264.689	0.00681
	3MSK9	131.9934	2.7274095	43.206	0.00825
Tenth-Diurnal Constituents	3M2N10	143.8318	2.5029240	202.391	0.0091
	6MS10	143.9046	2.5016569	318.937	0.01015
	3M2NKS10	143.9139	2.5014955	358.412	0.00969
	4MSNK10	144.294	2.4949061	150.341	0.00159
	4MN10	144.3761	2.4934867	281.089	0.00928
	4Mnu10 (4Mv10)	144.449	2.4922291	57.612	0.00121
	5MSK10	144.8384	2.4855290	49.466	0.0025
	M10	144.9205	2.4841202	292.142	0.00556
	3MSN10	145.392	2.4760640	202.4	0.00731
	6MN10	145.4649	2.4748239	327.232	0.00503
	3MNK10	145.4742	2.4746660	76.009	0.01045
	4MK10	146.0185	2.4654403	264.531	0.00491
	2MNSK10	146.4901	2.4575044	145.372	0.01034
	3M2S10	146.9523	2.4497743	4.316	0.02114
Eleventh-Diu	4MSK11	160.9775	2.2363376	293.795	0.00864
Twelveth-Diurnal Constituents	4M2N12	172.8159	2.0831419	187.963	0.00926
	4M2NKS12	172.898	2.0821523	326.742	0.00751
	5MSNK12	173.2781	2.0775849	11.156	0.00476
	5MN12	173.3603	2.0766006	280.151	0.00763
	5Mnu12 (5Mv12)	173.4331	2.0757283	136.622	0.01127
	6MSK12	173.8225	2.0710784	47.915	0.00249
	MA12	173.8636	2.0705892	298.584	0.00105
	M12	173.9046	2.0701002	348.898	0.00203
	4MSN12	174.3761	2.0645026	221.535	0.01864
	5MS12	174.9205	2.0580776	223.226	0.01855
	5MK12	175.0027	2.0571116	288.16	0.00936
	3MNKS12	175.4742	2.0515839	162.636	0.00416
	4M2S12	175.9364	2.0461938	306.843	0.01142
Fourteenth-Diurnal Constituents	5MSN14	203.3603	1.7702575	239.466	0.01017
	5MNK14	203.4424	1.7695427	258.3	0.00493
	6MS14	203.9046	1.7655313	235.784	0.01019

Appendix C4: Location of Sandwip Channel.

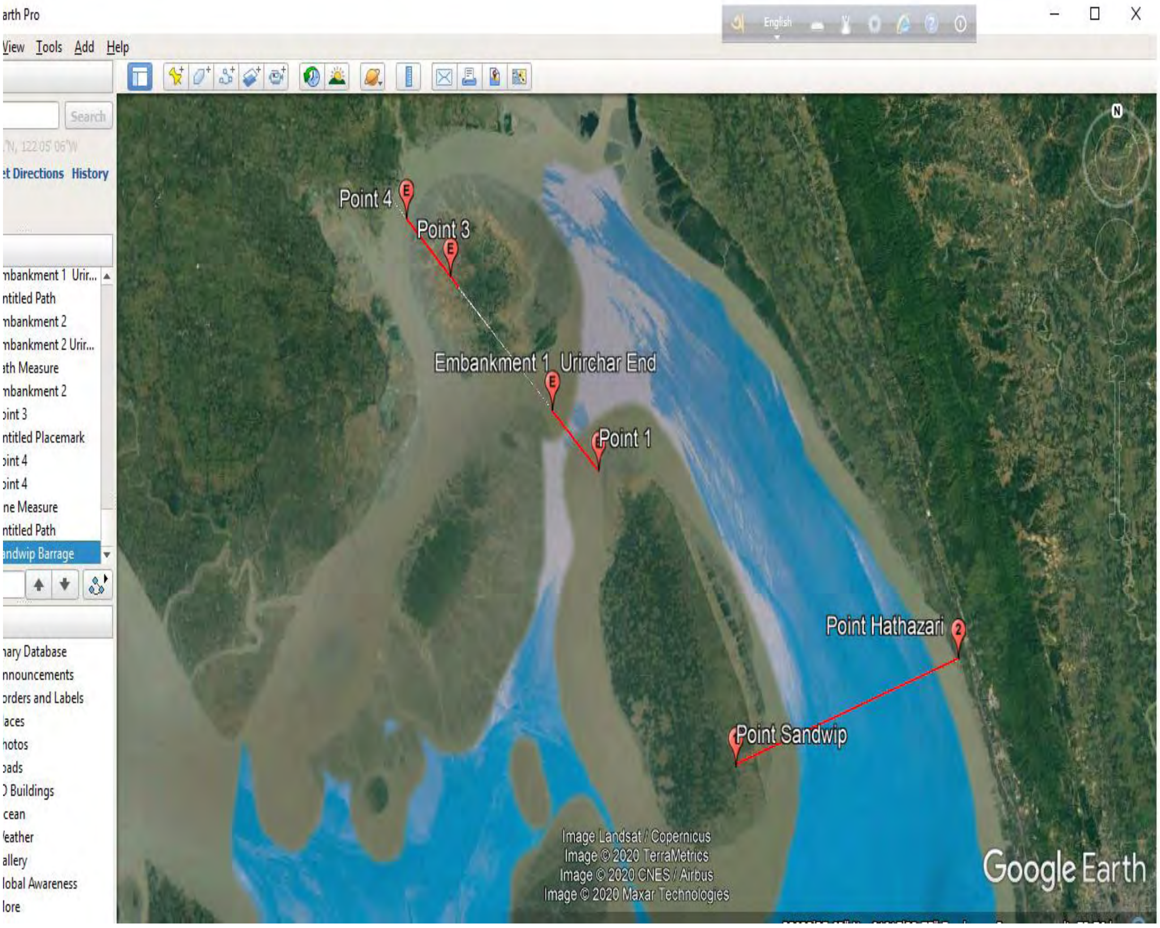

Appendix C5: Bathymetric Data of Sandwip Channel.

Bathymertic Data of Sandwip Channel for the Impounded Area						
Elevation from CD, Up (+ve)	Volume Above	Volume Below	Total Volume	Area Above	Area Below	Total area
(m)	(Million m^3)	(Million m^3)	(Million m^3)	(Million m^2)	(Million m^2)	(Million m^2)
15	0.00	9062.90	9062.90	0.00	782.55	782.55
14	0.52	8280.87	8281.40	1.56	781.00	782.55
13	4.98	7502.78	7507.75	12.38	770.17	782.55
12	38.63	6753.88	6792.52	69.82	712.73	782.55
11	153.21	6085.91	6239.12	144.29	638.26	782.55
10	320.69	5470.84	5791.53	195.74	586.81	782.55
9	542.66	4910.25	5452.91	242.41	540.14	782.55
8	798.59	4383.63	5182.22	266.71	515.84	782.55
7	1073.93	3876.42	4950.36	283.71	498.84	782.55
6	1364.49	3384.44	4748.93	297.05	485.50	782.55
5	1668.23	2905.62	4573.84	310.28	472.27	782.55
4	1984.75	2439.59	4424.34	322.92	459.63	782.55
3	2314.71	1987.01	4301.72	337.90	444.65	782.55
2	2663.30	1553.04	4216.34	360.71	421.84	782.55
1	3037.27	1144.46	4181.72	386.77	395.78	782.55
0	3436.80	761.43	4198.23	412.43	370.16	782.60
-1	3866.06	408.14	4274.20	447.86	334.69	782.55
-2	4360.32	119.86	4480.17	577.78	204.77	782.55
-3	5043.54	20.53	5064.08	743.54	39.01	782.55
-4	5807.75	2.18	5809.93	776.12	6.43	782.55
-5	6588.17	0.06	6588.23	782.36	0.19	782.55
-6	7370.67	0.00	7370.67	782.55	0.00	782.55

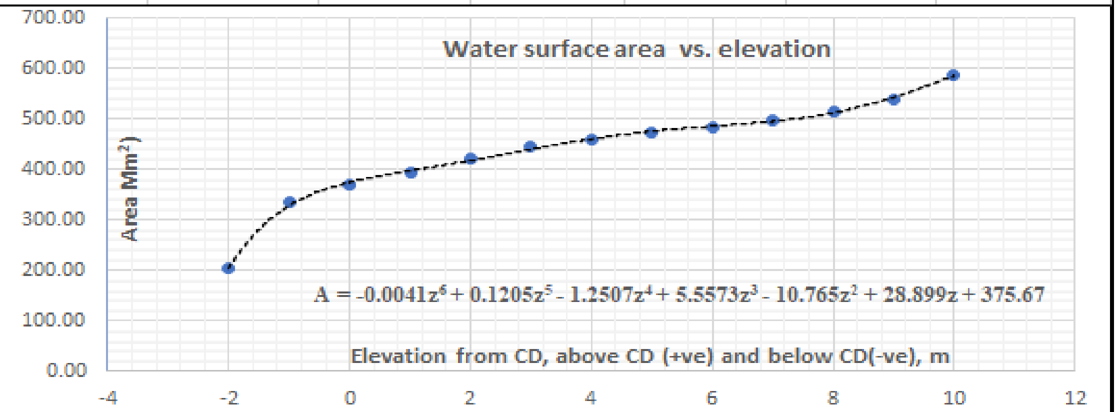

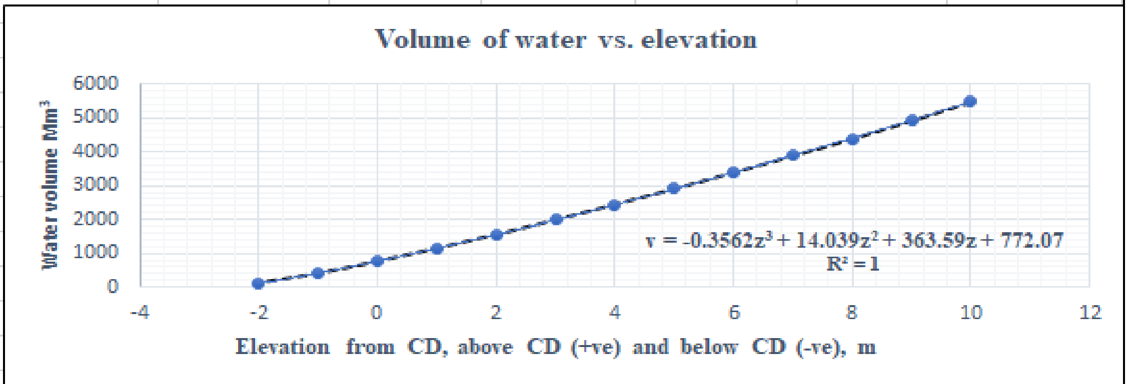

Appendix C6: Energy Calculation for Sandwip Power Plant using the RTA Model.

Real-Time Analytical Model

Elements		200	300	400	500
Elements	Turbines	200	300	400	500
	Gates	1000	900	800	700
Energy (GWh)	Annual	1591	1971	2203	2321
Power output (MW)	Max.	1532	2197	2757	3240
	Average	475	672	854	1017
	Min (>0)	219	328	438	547
Basin WL (m CD)	Max.	5.89	5.86	5.80	5.74
	Min.	2.98	2.74	2.45	2.15
Head (m)	Max.	6.59	6.39	6.14	5.89
	Min.	0.00	0.00	0.00	0.00
	Average	1.63	1.48	1.37	1.29
Tidal range basin (m)	Max.	2.91	3.12	3.35	3.59
Tidal range sea (m)	Max.	7.43	7.43	7.43	7.43
Production period	23128	38%	33%	29%	26%
Non-production period	64472	62%	67%	71%	74%
Total time steps	87600				

Area of basin (mean), Ab =		km2
Accl. of gravity, g =	9.807	m/s2
Mean tidal range basin, Dhb =		m
Density sea water, r =	1025	kg/m3
Threshold H to start turbine, H1 =	2	m
Threshold H to stop turbine, H2 =	1.8	m
Turbine dia	6	m
Turbine Cd =	0.9	
No. of turbines =	400	
Turbine efficiency, h =	0.4	
Width of single gate, bg =	12	m
Invert elevation of gate, zg =	1	m CD
Gate discharge coeff. =	0.65	
Number of gates =	800	
Gate Opening=	6	m

Amplitude (m)	0.0697
Speed (Deg/hr)	0.0411
Tidal Peiod, T (hrs.)	8765.8211
Phase (degree)	57.7030

	Ebb Generation with gates			Sea Tide	Basin Tide	Turbine	Gates	Velocity through single turbine	Velocity through single gate	Discharge through all turbines	Discharge through all gates	Discharge through all turbines and gates	Water surface area of the basin	Change of water level	Capacity of the plant	Generation of energy, MWh	Water level from CD, ML+2.641 (from GeoTide)			
	Sea water	Basin water	Head	Flood: 1 Ebb: -1	Flood: 1 Ebb: -1	Open: 1 Closed: 0	Open: 1 Closed: 0													
t (hr)	y (m CD)	z (m CD)	H (m)	Flood/Ebb	Flood/Ebb	Turbine	Gate	vt (m/s)	vt (m/s)	Q (m3/s)	Q (m3/s)	Q (m3/s)	Ab (10^6 m2)	dz (m)	Pt (MW)	Et(MWh)	GeoTide)	t (hrs)	ηtotal (ML)	η1
0.0	4.080	4.080	0.000	-1	-1	0	0	0.00	0.00	0.00	0.00	0.00	462.56				4.080	0.00	1.4387	0.0372
0.1	3.944	4.080	0.136	-1	-1	0	0	0.00	0.00	0.00	0.00	0.00	462.56	0.00	0.00	0.00	3.944	0.10	1.3027	0.0372
0.2	3.812	4.080	0.268	-1	-1	0	0	0.00	0.00	0.00	0.00	0.00	462.56	0.00	0.00	0.00	3.812	0.20	1.1708	0.0372
0.3	3.682	4.080	0.398	-1	-1	0	0	0.00	0.00	0.00	0.00	0.00	462.56	0.00	0.00	0.00	3.682	0.30	1.0408	0.0372
0.4	3.552	4.080	0.528	-1	-1	0	0	0.00	0.00	0.00	0.00	0.00	462.56	0.00	0.00	0.00	3.552	0.40	0.9110	0.0372
0.5	3.421	4.080	0.659	-1	-1	0	0	0.00	0.00	0.00	0.00	0.00	462.56	0.00	0.00	0.00	3.421	0.50	0.7795	0.0372
0.6	3.286	4.080	0.793	-1	-1	0	0	0.00	0.00	0.00	0.00	0.00	462.56	0.00	0.00	0.00	3.286	0.60	0.6452	0.0372
0.7	3.149	4.080	0.931	-1	-1	0	0	0.00	0.00	0.00	0.00	0.00	462.56	0.00	0.00	0.00	3.149	0.70	0.5076	0.0372
0.8	3.008	4.080	1.072	-1	-1	0	0	0.00	0.00	0.00	0.00	0.00	462.56	0.00	0.00	0.00	3.008	0.80	0.3666	0.0372
0.9	2.864	4.080	1.216	-1	-1	0	0	0.00	0.00	0.00	0.00	0.00	462.56	0.00	0.00	0.00	2.864	0.90	0.2232	0.0372
1.0	2.720	4.080	1.360	-1	-1	0	0	0.00	0.00	0.00	0.00	0.00	462.56	0.00	0.00	0.00	2.720	1.00	0.0786	0.0372
1.1	2.576	4.080	1.504	-1	-1	0	0	0.00	0.00	0.00	0.00	0.00	462.56	0.00	0.00	0.00	2.576	1.10	-0.0653	0.0372
1.2	2.434	4.080	1.645	-1	-1	0	0	0.0000	0.0000	0.00	0.00	0.00	462.56	0.00	0.00	0.00	2.434	1.20	-0.2067	0.0372
1.3	2.297	4.080	1.782	-1	-1	0	0	0.0000	0.0000	0.00	0.00	0.00	462.56	0.00	0.00	0.00	2.297	1.30	-0.3435	0.0372
1.4	2.167	4.080	1.913	-1	-1	0	0	0.0000	0.0000	0.00	0.00	0.00	462.56	0.00	0.00	0.00	2.167	1.40	-0.4743	0.0372
1.5	2.043	4.080	2.037	-1	-1	1	0	5.6882	0.0000	80415.11	0.00	80415.11	462.56	-0.0313	658.5019	32.9251	2.043	1.50	-0.5979	0.0372
1.6	1.927	4.048	2.121	-1	-1	1	0	5.8052	0.0000	82069.36	0.00	82069.36	462.00	-0.0633	699.9826	67.9242	1.927	1.60	-0.7138	0.0371
1.7	1.819	4.048	2.230	-1	-1	1	0	5.9519	0.0000	84142.53	0.00	84142.53	462.00	-0.0648	754.3810	72.7182	1.819	1.70	-0.8223	0.0371
1.8	1.717	3.984	2.267	-1	-1	1	0	6.0014	0.0000	84842.5	0.00	84842.5	460.81	-0.0659	773.3649	76.3873	1.717	1.80	-0.9244	0.0371
1.9	1.620	3.984	2.364	-1	-1	1	0	6.1284	0.0000	86638.41	0.00	86638.41	460.81	-0.0670	823.5225	79.8444	1.620	1.90	-1.0213	0.0371
2.0	1.526	3.917	2.391	-1	-1	1	0	6.1632	0.0000	87129.64	0.00	87129.64	459.56	-0.0680	837.6099	83.0566	1.526	2.00	-1.1152	0.0371

Appendix C7: Cost Calculation of Sandwip Tidal Barrage Power Plant

	Turbine			200	200	200	300	300	300	400	400	400	500	500	500
	Gates			800	900	1000	800	900	1000	800	900	1000	700	800	900
	GWh			1529	1564	1591	1925	1971	2008	2203	2257	2301	2321	2402	2464
	Nos. Turbine			200	200	200	300	300	300	400	400	400	500	500	500
	Nos. of caissons required to house turbines			50	50	50	75	75	75	100	100	100	125	125	125
	Nos. Sluice gates			800	900	1000	800	900	1000	800	900	1000	700	800	900
	Nos. of sluice Cassissons required for			200	225	250	200	225	250	200	225	250	175	200	225
A. Costs of Barrage Elements	Barrage length, km	20													
	Embankment,km	8													
Caissons construction	Total Length, km	28	Crore												
	From 1988 UKAEA	Used	BDT												
Turbine Gate Cassison, 4 turbines in one caisson length, for 6m dia turbine one caisson length is 35m	€0.33 million for 12mX12m turbine gate[1]	8m X 8m turbine gate[3]	1.377	275	275	275	413	413	413	551	551	551	689	689	689
Sluice Gate Cassisson, 4 sluice gates in one caisson length, for 12mX6m sluice gate, sluice caisson length is 64.5m	€0.33 million for 12mX12m sluice gate[1]	12mX6m [3]	1.55	1240	1395	1550	1240	1395	1550	1240	1395	1550	1085	1240	1395
[2] Plain Cassion cost		Crore/km	70	375	262	149	313	200	88	252	139	26	304	191	78
[2] Steelwork fabrication and installations, 20 km			200	200	200	200	200	200	200	200	200	200	200	200	200
[2] Foundations, 20 km			200	200	200	200	200	200	200	200	200	200	200	200	200
[2] Embankment, 8 km	BDT Crore/km		40	320	320	320	320	320	320	320	320	320	320	320	320
CIVIL WORKS TOTAL				2610	2652	2694	2686	2728	2770	2763	2805	2847	2797	2839	2881
TURBINE , GENERATOR AND ANCILIARY PLANTS	€ 5million for 9m dia individual turbine caisson	6m dia turbine	30.00	6000	6000	6000	9000	9000	9000	12000	12000	12000	15000	15000	15000
Total cost of the Plant				**8610**	**8652**	**8694**	**11686**	**11728**	**11770**	**14763**	**14805**	**14847**	**17797**	**17839**	**17881**
GWh				**1529**	**1564**	**1591**	**1925**	**1971**	**2008**	**2203**	**2257**	**2301**	**2321**	**2402**	**2464**

Appendix C8: Calculation of Levelized Cost of Energy for Sandwip Tidal Barrage Power Plant.

Calculation of Levelized Cost of Energy

Year	Maintenance cost 5% of total cost with growth 2%	Fuel cost	Discount Factor 4%	Present value of cost, BDT Crore	Year	Energy Output /year, GWh	Discount Factor 0.04	Present Value of Energy, GWh
0	14763	-	1.00	14763	0	2203	1.00	-
1	738.13	-	0.96	709.74	1	2203	0.96	2118.60
2	752.90	-	0.92	696.09	2	2203	0.92	2037.12
3	767.95	-	0.89	682.71	3	2203	0.89	1958.77
4	783.31	-	0.85	669.58	4	2203	0.85	1883.43
5	798.98	-	0.82	656.70	5	2203	0.82	1810.99
6	814.96	-	0.79	644.07	6	2203	0.79	1741.34
7	831.26	-	0.76	631.69	7	2203	0.76	1674.36
8	847.88	-	0.73	619.54	8	2203	0.73	1609.97
9	864.84	-	0.70	607.63	9	2203	0.70	1548.04
10	882.14	-	0.68	595.94	10	2203	0.68	1488.50
11	899.78	-	0.65	584.48	11	2203	0.65	1431.25
12	917.78	-	0.62	573.24	12	2203	0.62	1376.20
13	936.13	-	0.60	562.22	13	2203	0.60	1323.27
14	954.85	-	0.58	551.40	14	2203	0.58	1272.38
15	973.95	-	0.56	540.80	15	2203	0.56	1223.44
16	993.43	-	0.53	530.40	16	2203	0.53	1176.39
17	1013.30	-	0.51	520.20	17	2203	0.51	1131.14
18	1033.57	-	0.49	510.20	18	2203	0.49	1087.63
19	1054.24	-	0.47	500.39	19	2203	0.47	1045.80
20	1075.32	-	0.46	490.76	20	2203	0.46	1005.58
21	1096.83	-	0.44	481.32	21	2203	0.44	966.90
22	1118.76	-	0.42	472.07	22	2203	0.42	929.71
23	1141.14	-	0.41	462.99	23	2203	0.41	893.96
24	1163.96	-	0.39	454.09	24	2203	0.39	859.57
25	1187.24	-	0.38	445.35	25	2203	0.38	826.51
26	1210.99	-	0.36	436.79	26	2203	0.36	794.72
27	1235.21	-	0.35	428.39	27	2203	0.35	764.16
28	1259.91	-	0.33	420.15	28	2203	0.33	734.77
29	1285.11	-	0.32	412.07	29	2203	0.32	706.51
30	1310.81	-	0.31	404.15	30	2203	0.31	679.33
31	1337.03	-	0.30	396.38	31	2203	0.30	653.21
32	1363.77	-	0.29	388.75	32	2203	0.29	628.08
33	1391.04		0.27	381.28	33	2203	0.27	603.92
34	1418.86	-	0.26	373.94	34	2203	0.26	580.70
35	1447.24	-	0.25	366.75	35	2203	0.25	558.36
36	1476.19		0.24	359.70	36	2203	0.24	536.89
37	1505.71	-	0.23	352.78	37	2203	0.23	516.24
38	1535.82	-	0.23	346.00	38	2203	0.23	496.38
39	1566.54		0.22	339.34	39	2203	0.22	477.29
40	1597.87	-	0.21	332.82	40	2203	0.21	458.93
41	1629.83	-	0.20	326.42	41	2203	0.20	441.28
42	1662.42		0.19	320.14	42	2203	0.19	424.31
43	1695.67	-	0.19	313.98	43	2203	0.19	407.99
44	1729.59	-	0.18	307.95	44	2203	0.18	392.30
45	1764.18		0.17	302.02	45	2203	0.17	377.21
46	1799.46	-	0.16	296.22	46	2203	0.16	362.70
47	1835.45	-	0.16	290.52	47	2203	0.16	348.75
48	1872.16		0.15	284.93	48	2203	0.15	335.34
49	1909.60	-	0.15	279.45	49	2203	0.15	322.44
50	1947.80	-	0.14	274.08	50	2203	0.14	310.04
	PV Cost, BDT Crore			37691		PV Energy, GWh		47333

Levelized cost of Energy 7.96 BDT/kWh

Nos. of Turbine	Nos. of Gates	Initial Cost of Investment	Energy output/year, GWh	LCOE, BDT/kWh
200	500	8483	1361	7.41
200	600	8526	1432	7.08
200	700	8568	1486	6.85
200	800	8610	1529	6.69
200	900	8652	1564	6.58
200	1000	8694	1591	6.49
300	500	11560	1697	8.10
300	600	11602	1791	7.70
300	700	11644	1865	7.42
300	800	11686	1925	7.22
300	900	11728	1971	7.07
300	1000	11770	2008	6.97
400	500	14636	1928	9.02
400	600	14678	2044	8.54
400	700	14721	2131	8.21
400	800	14763	2203	7.96
400	900	14805	2257	7.80
400	1000	14847	2301	7.67
500	500	17713	2091	10.07
500	600	17755	2221	9.50
500	700	17797	2321	9.11
500	800	17839	2402	8.83
500	900	17881	2464	8.62
500	1000	17923	2513	8.48

Appendix D: Thesis Proposal Approval by CASR, BUET.

BANGLADESH UNIVERSITY OF ENGINEERING AND TECHNOLOGY, DHAKA.
OFFICE OF THE MEMBER SECRETARY OF THE COMMITTEE FOR ADVANCE STUDIES AND RESEARCH, BUET, DHAKA.

Application for the Approval of Ph.D. Thesis Proposal

Date: 04 July 2019

1. **Name of the student:** MD. RAFIQUL ISLAM KHAN **Status:** Part-Time
   Roll No.: 1009284001P **Session:** October 2009
2. **Present Address and Cell Phone:** Joint Secretary, Ministry of Shipping, Bangladesh Secretariat, Dhaka-1000, +880-1715 295995
3. **Name of the Department:** Institute of Water and Flood Management (IWFM)
   Program: PhD (WRD)
4. **Name of the Supervisor:** Dr. M. Shah Alam Khan **Designation:** Professor
5. **Name of the Co-Supervisor:** Not applicable **Designation:** Not applicable
6. **Date of the First Enrolment in the Program:** 5 December 2009

7. **Tentative Title:** DEVELOPMENT OF AN ANALYTICAL MODEL FOR REAL-TIME ASSESSMENT OF TIDAL BARRAGE POWER GENERATION.

8. Background and present state of the problem

Tidal power is considered to be an important source of renewable energy [1, 2, 3, 4]. Although the government of Bangladesh emphasizes the need for renewable energy [5] an assessment of the potential for tidal power generation in Bangladesh is yet to be initiated. Tidal power can be generated either by converting potential energy or by utilizing the in-stream kinetic energy into electrical energy [6]. Tidal barrage power plants harness the potential energy contained in an impounding basin where a relatively large tidal range exists [2]. Although tidal power is reasonably predictable, its magnitude changes periodically at different temporal scales because of the variations in tide-producing gravitational forces caused by the sun and the moon [7, 8, 9].

Energy has been extracted from tides for centuries [10]. At present there are five *tidal range* power plants in operation around the world [9] *La Rance* tidal power (240 MW) in France and the *Sihwa Lake* tidal power plant (254 MW) in South Korea are two larger tidal power plants. Other three tidal range power plants, relatively small in size, are: *Kislaya Guba* (1.7 MW) in Russia, *Annapolis Royal* (20 MW) in Canada and *Jiangxia* (3.9 MW) in China. In the assessment of tidal power generation, the basic equation relates the mass of water and water head difference with the theoretical potential energy while the energy available from a barrage depends on water surface impounded by the barrage and the corresponding tidal range [9, 10]. However, a minimum water head difference between the sea and the basin is required for tidal power generation [11]. In the current practice for assessing the tidal power potential for a plant, primarily the duration of power generation and hydraulic efficiency are considered. Power generation duration is assumed to be one-third time of the day and the efficiency of the system is assumed to be 90%. Based on these, the design extractable power is 30% of potential energy [12, 13].

Several methods and numerical approaches have been developed to assess tidal power and energy. Prandle [9] used tidal amplitude instead of tidal range to assess the maximum tidal power. The actual extractable energy per tidal cycle equals to 0.27 E_{max} (for ebb only) and 0.37 E_{max} (for two way generation). Lamb [12] used mean tidal range instead of maximum tidal range whereas Rashid et al. [14] used tidal range and 60% conversion factor to calculate power. Tester et al. used an average power conversion efficiency of 33% [15] and Xia at el. [13] used the mean tidal range for tidal power assessment. Neil et al. [3] suggested theoretical and zero dimensional (0D) models with more detailed depth-averaged (2D) equations and hydro-environmental tools for the

Approved in CASR

DAERS

1

assessment of tidal power. Alam et al. [16] developed a method to calculate the required number of turbines based on the impounded water volume and the water flow passing through the turbines.

In a tidal barrage, tidal water level on the sea side is a superimposition of a number of periodically-varying tidal constituents, while the water level in the basin depends on the geometric configuration of the basin and operational control of the turbines. All previous methods for the assessment of tidal power are based on fixed assumed variables such as duration of power generation, and ignore the actual real-time variability in these variables. Assessment of power generation potential based on real-time water head differences, long-term tidal data and basin configuration will yield a more accurate estimation of power generation. An analytical model based on a set of equations that describe this real-time variability will be instrumental in designing tidal barrage power plants.

9. Objectives with specific aim and possible outcome

The goal of this study is to achieve a better estimation of tidal power generation by establishing a real-time functional relation (i) between water level and basin volume, which in turn will relate to turbine discharge and water level changes in the basin, and (ii) among the tidal constituents having different phases and amplitudes in the sea side, expressed as a superimposed function with respect to time. This approach will require formulation of an analytical model employing equations to compute the dynamic water head, power and energy considering water level variations in a tidal barrage.

The main objectives of the study are to:

1) develop an analytical model with equations to compute dynamic water head, power and energy for a tidal barrage with variable water levels at the sea and the basin,
2) determine the optimum basin configuration that yields the maximum tidal power, and
3) assess the tidal power generation potential from a tidal barrage in the coastal area of Bangladesh.

Possible Outcome

A major outcome of this study will be an analytical model for computing real-time water head, power and energy potential in a tidal barrage. The model will be useful in assessing tidal power potential more accurately.

Original contribution

The current approaches and practices for the assessment of tidal barrage power generation do not consider the continuous changes in the head differences between the sea and basin. Rather a static overall estimate using an arbitrary reduction in efficiency and head difference is used. The proposed study will consider the real-time changes in water levels inside and outside the basin to compute the actual power generation potential based on dynamic water head, and develop a new analytical model to represent the water level variations and basin configuration.

10. Outline of Methodology

The following steps will be followed in conducting the study:

(i) Review of literature on tidal barrage power generation and assessment

Literature on tidal barrage power will be reviewed to compile different analytical and empirical approaches, understand the tidal power generation processes, and gather information on the tidal characteristics in the coastal area of Bangladesh.

Approved by CASR
DAERS

(ii) Develop a model to compute real-time water head, energy and power for a tidal barrage

A set of new equations will be developed to compute real-time water head, power and energy from an enclosed basin at any time considering the variations in water levels at both sides of the barrage. For this purpose, an equation will be also developed considering different tidal constituents at the sea side to represent the real-time tide levels. Long-term observed data will be used to validate the equations. A relationship between the stage and volume of water in the impounded basin will be developed considering the basin configuration and contour maps. During high tide (for ebb generation) a higher water level or during low tide (for flood generation) a lower water level at the basin will be fixed to start energy production with or without pumping. Then, the real-time water head between water levels of the two sides will be computed. After a small time interval, the new water level at the basin side will be computed based on the amount of water passed through the turbines during this time period. This will be also related to the relation developed between the stage and volume of the basin. At the same time interval, the new tide level at the sea side will be computed using the equations developed to represent the tidal constituents. Then a new dynamic head will be calculated based on which power and energy will be calculated. Similarly, after every time step water head, power and energy will be computed based on which maximum, minimum and average power and potential energy for a particular time period will be computed.

(iii) Determine the optimum basin configuration for tidal power generation

Using hypothetical tidal data, different basin configurations will be considered to observe power generation variations and determine the optimum configuration which yields the maximum power and energy by solving the newly developed equations.

(iv) Application of the model to assess power potential

The model will be applied to assess the power generation potential in a case study site in the coast of Bangladesh. A barrage site will be selected based on tidal range, basin area, volume of the impounded water, basin configuration, etc. A relation between the stage and volume will be established from the contour map of the tidal basin. Then the dynamic water head, power and energy will be calculated for a particular tidal period. In the same way, the maximum, minimum and average power and energy will be computed to test the model and to get an idea of power generation potential in Bangladesh.

11. References

[1]) Tethys 2018. "Tidal energy advantages and disadvantages: key points to consider." Pacific Northwest National Laboratory (PNNL)(2018).

[2] Angeloudis A., Kramer, S.C., Avdis A., & Matthew D. P. "Optimizing tidal range power plant operation." Department of Earth Science and Engineering, Imperial College, London, UK. Elsevier: Applied Energy (212) 680-690 (2018).

[3] Neil, S.P., Angeloudis, A., Robins, P.E., Walkington, I., Ward, S. L., Masters, I., Lewis, M.J., Piano, M., Avdis, A., Piggott, M. D., Aggidis, G., Evans, P., Adcock, T. A.A., Zidonis, A., Ahmadian, R., Falconer, R., "Tidal range energy resource and optimization-Past perspective and future challenges." ELSEVIER: Renewable Energy (127) 763-778 (2018).

[4] Alternative Energy Tutorials. "Tidal Energy." [Internet]. [accessed on June 22, 2019].

[5] GOB *National Energy Policy, 1996*. Government of Bangladesh, Ministry of Power, Energy and Mineral Resources, Dhaka (1996).

[6] Wikipedia the free encyclopaedia. "Tidal Power." [Internet]. [accessed on June 23, 2019].

[7] American Energy Independence. "Renewable Energy from the Ocean." [Internet]. [cited June 23, 2019].

Approved by CASR

DAERS

[8] ScienceDirectTopics."Tides- an overview." [Internet]. [accessed on June 23, 2019].

[9] Prandle, D., "Simple theory for designing tidal power schemes." Adv. Water Resource. (71) 21-27 (1984).

[10] Shevkar, S.S., & Otari, K.A., "Tidal Energy Harvesting." International Journal of Science, Engineering and Technology Research (IJSETR), April 2015, Vol. 4 (4) (2015).

[11] McErlean, T., "Harnessing the Tides- the Early Medieval Tide Mills at Nendrum Monastrery, Strangford Lough, Northern Ireland." Archaeological Monographs No.7, TSO (2007).

[12] Lamb, H. (1994). Hydrodynamics (6th edition). Cambridge University Press, London. 768pp.

[13] Xia, J. , Roger A., Falconer, L. B., and Tan, G., "Estimation of annual energy output from a tidal barrage using two different methods." (2012). Academia. Edu (2012). [Internet]. [accessed on 27 Jun 2019] Available from: https://www.academia.edu/ 1484837/ Estimation_of_annual_energy_output_from_a_tidal_barrage_using_two_different methods.

[14] Rashid F. L., Ashwaq. H. M., and Ahmed, H., "Power Production using Tidal Energy". British Journal of Science, 112 February 2012, Vol. 3 (2). 112-115pp. Babylon University, Ministry of Science and Technology, Baghdad- Iraq Ministry of Higher Education & Scientific Research. (2012).

[15] Tester, J.W., Drake, E.M., Discoll, M.J., Golay, M.W., Peters, W.A., "Sustainable energy: Choosing among options". MIT Press. 870 pp. (2005).

[16] Alam, M. T., Ahamed, T., Tareq, Y., Wahid, A., and Hossain, S., "Prospect of Tidal Power Generation in Bangladesh Trough Tidal Barrage Using Low Head Water Turbine." in 7th International Conference on Electrical and computer Engineering. Published by IEEE, March 2012, (2012).

Approved by CASR

DAERS

12. **List of the courses so far taken**

Course no.	Course name	Credit	Grade	Grade point	G.P.A
WFM 6305	Coastal Zone Management	3	A+	4.0	3.67
WFM 6209	Interdisciplinary Field Research Methodology in Water Management	3	A	3.5	
WFM 6201	Hazards and Risk Analysis	3	A	3.5	
WFM 6000	Thesis	45	-	-	

Signature of the tabulator: _Snowman_

13. Tentative Cost Estimate

Items and Quantity	Rate	Cost (Taka)
A)Cost of Materials i) Photocopy of books, reports, articles etc. ii) Purchase of secondary data: Rainfall data 3 stations daily data for last 20 years. iii) Purchase contour maps for different coastal areas.	--	5,000 9,000 5,000
	Sub-Total (A)	19,000
B) Field visits i) Field visits (2 Nos.) with roundtrip fares ii) Living cost (6 days) iii) Local transport (4 days)	Tk. 4000x2 Tk. 1000x6 Tk. 3000x4	8,000 6,000 12,000
	Sub-Total (B)	26,000
C. Typing, Drafting, Binding & Paper etc.	Sub-Total (C)	4,000
Total cost (Taka Forty Nine thousand only)	---	49,000

14. **Approximate time (in hour) for BUET workshop facilities:** Not applicable

15. **Justification of having Co-Supervisor:** Not applicable

16. **Doctoral Committee/BPGS/RAC reference:**
Meeting No. 06, Resolution No. 01, Date: 04-07-2019

17. **Appointment of Supervisor & Co-supervisor Approved by the CASR:**
Meeting No. 222, Resolution No.139, Date: 14-07-2010

18. **Appointment of Doctoral Committee Approved by the CASR:**
Meeting No. 223, Resolution No. 92, Date: 03-10-2010

19. **Result of the comprehensive examination for PhD:**
Date: 15-06-2019 Satisfactory

Approved by CASR*

DAERS

5

20. Number of post-graduate student(s) working with the Supervisor at present: 6 (Six)

	Names and signatures of the members of the Doctoral Committee	
Signature of the Student	1.	Dr. M. Shah Alam Khan Professor, IWFM, BUET, Dhaka (Supervisor)
Signature of the Supervisor	2.	Dr. Sujit Kumar Bala Professor and Director IWFM, BUET, Dhaka.
Signature of the Director Director IWFM BUET, Dhaka	3.	Dr. Mohammad Anisul Haque Professor, IWFM, BUET, Dhaka
	4.	Dr. Mohammad Asad Hussain Associate Professor, IWFM, BUET, Dhaka
	5.	Dr. Aminul Hoque Professor (Retd.), Department of EEE, BUET, Dhaka and Vice Chancellor (designate), Eastern University.
	6.	Dr. Umme Kulsum Navera Professor Department of WRE, BUET, Dhaka

Approved by CASR

DAERS